

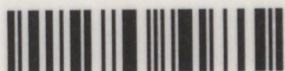
Investigation of factors effecting Yield Stress
Determinations using the Slump Test

ICHEGBO MAXWELL NYEKWE

CAPE PENINSULA
UNIVERSITY OF TECHNOLOGY
Library and Information Services

Dewey No. ARC 620.106 NYE

CAPE PENINSULA
UNIVERSITY OF TECHNOLOGY



20116281

CPT ARC 620.106 NYE



**Cape Peninsula
University of Technology**

**INVESTIGATION OF FACTORS EFFECTING YIELD STRESS DETERMINATIONS USING
THE SLUMP TEST.**

by

ICHEGBO MAXWELL NYEKWE

B. Eng (Hons): Chemical Engineering

**A Dissertation submitted in fulfilment of requirements for the degree
Master Technology: Chemical Engineering**

in the Faculty of Engineering

at the Cape Peninsula University of Technology

Supervisor: Prof. R. Haldenwang

Co-supervisor: Prof. I Masalova

Cape Town

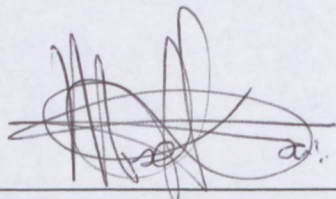
November, 2008

CPUT Copyright Information

**The dissertation may not be published either in part (in scholarly, scientific or
technical journals), or as a whole (as a monograph), unless permission has been
obtained from the university**

DECLARATION

I, Maxwell Nyekwe Ichebgo, hereby declare that the contents of this thesis represent my own unaided work, and that it has not previously been submitted for academic examination towards any qualification. Further, it represents my own opinions and not necessarily those of the Cape Peninsula University of Technology

A handwritten signature in dark ink, consisting of several loops and a long horizontal stroke, positioned above a horizontal line.

Maxwell Nyekwe Ichebgo

November, 2008

ABSTRACT

Certain non-Newtonian fluids exhibit a yield stress which can be measured with a variety of instruments varying from very sophisticated rotary and tube viscometers to hand-held slump cones and cylinders of various sizes. Accurate yield stress measurement is significant for process design and disposal operations for thickened tailings. The slump value was first related to the yield stress by Murata (1984). Later, that work was corrected by Christensen (1991) for an error in the mathematical analysis. Slump, based on a circular cylindrical geometry was first investigated by Chandler (1986). These concepts led to the study by Pashias et al., (1996) that formed the basis for the current research.

The Flow Process Research Centre (FPRC) at the Cape Peninsula University of Technology developed a slump meter designed to lift the cone or cylinder vertically at controlled lifting speeds. In addition the simple hand-held cylinder which is an adaptation of slump cones which were originally developed by the concrete industry to determine the flowability of fresh concrete was also used. The vane technique was used as a control. Cones and cylinders made of stainless steel and PVC were fitted to the slump meter. The yield stresses of four non-Newtonian fluids at different concentrations were tested in four different configurations at different lift speeds to ascertain whether the measuring position, lift speed, slip, geometry, wall surface material, and stability has an effect on the value of yield stress measured. The effect of different predictive models was also ascertained. The cylinder, lump and cone models relating slump to yield stress was used in the dimensional analysis of the results. The objective of this work was to determine if the slump tests (cone, cylinder and the hand-held cylinder) would generate yield stress values comparable to those found using the vane technique.

It was established that there was no significant effect of lift speed, stability, geometry and wall surface material on the value of yield stress. The effect of measuring position on the value of yield stress calculated gave a difference of 25%. Using dimensional analysis, the lump model (Hallbom, 2005) more accurately predicts the material yield stress when using the hand-held cylinder as well as all the cone results (due to its specific geometry), and cylinder configurations, thus affirming the work of Clayton et al., 2003.

It is concluded that, although the materials and concentrations tested induced errors within 40%, the hand-held cylinder shows promise as a reliable, quick and simple way of measuring the yield stress.

ACKNOWLEDGEMENTS

During the course of my graduate studies I have learnt more than I have learnt in my entire life. This process was continuously supported by many and I am glad to have this opportunity to express my gratitude.

I wish to thank:

Prof. Rainer Haldenwang, firstly, though I cannot thank him enough, for believing in me more than I believed in myself. I am grateful to him for entrusting me with such an exciting project and for standing by me throughout the process. I truly appreciate the immense amount of patience he showed during my transition from an undergraduate student to a graduate researcher. It is a blessing from God to have been guided by such a hardworking and understanding professor.

I would also like to thank the following persons and organisations:

Marco Almeida, from Angola, who assisted me in all the experimental work.

While at the Cape Peninsula University of Technology (CPUT), I enjoyed a number of very good friendships.

To the Rheology group, Slurry group and Flume group of the Flow Process Research Centre (FPRC) and everyone else, thanks for making my stay a memorable one.

I would like to express my gratitude to my family, especially my mother (Madam Sarah T.N. Ichebgo) and my lover (Ogonda Ihunwo) for making me what I am. Their constant support (prayers) through these years, from thousands of miles away, was highly inspiring. I cannot imagine doing anything without them. I would also like to thank Hon Sir Freddy Ichebgo, Barr. Promise Ichebgo, Dr. Amakalanwo Ichebgo and Justice Ogunka for their encouragement and moral supports.

The financial assistance of the National Research Foundation (NRF) towards this research is acknowledged. Opinions expressed in this thesis and the conclusions arrived at are those of the author, and are not necessarily to be attributed to the National Research Foundation (NRF).

The Cape Peninsula University of Technology (CPUT) also provided funding for this project, for which I am indebted.

Maxwell Nyekwe Ichebgo

November, 2008

DEDICATION

I would like to dedicate the slump test: Validation of yield stress models, effect of measuring position, slip, lift of speed and stability on determining yield stress to my mother Madam Sarah T.N Ichebo and my late father Chief Tobiah N. Ichebo. I would also like to dedicate it to Ogonda Ihunwo (the love of my life), my senior brother Samuel C. Ichebo and my late Aunt Fannie Wogbo.

Be careful for nothing; but in everything by prayer and supplication with thanksgiving let your requests be made known unto God. And the peace of God, which passeth all understanding, shall keep your hearts and minds through Christ Jesus.

Philippians 4:6-7

THANK YOU JESUS

TABLE OF CONTENTS

DECLARATION	II
ABSTRACT	III
ACKNOWLEDGEMENTS	IV
DEDICATION	V
TABLE OF CONTENTS	VI
LIST OF FIGURES	XVIII
CLARIFICATION OF BASIC TERMS AND CONCEPTS	XX
NOMENCLATURE	XXI
CHAPTER 1	1.1
INTRODUCTION	1.1
1.1 BACKGROUND	1.1
1.2 STATEMENT OF THE RESEARCH PROBLEM	1.2
1.3 OBJECTIVE OF THE RESEARCH	1.2
1.4 RESEARCH DESIGN AND METHODOLOGY	1.2
1.4.1 Literature review (Chapter 2)	1.3
1.4.2 The experimental procedures (Chapter 3)	1.3
1.4.3 Results and discussion (Chapter 4)	1.4
1.4.4 Summary, conclusion and recommendation (Chapter 5)	1.4
1.5 DELINEATION OF THE RESEARCH	1.4
1.6 SIGNIFICANCE OF THE RESEARCH	1.4
1.7 SUMMARY	1.5
CHAPTER 2	2.1
THEORY AND LITERATURE REVIEW	2.1
2.1 INTRODUCTION	2.1
2.2 RHEOLOGY	2.1
2.3 SHEAR STRESS AND SHEAR STRAIN	2.2
2.4 CLASSIFICATION OF FLUIDS	2.3
2.4.1 Newtonian fluids	2.4
2.4.2 Non-Newtonian fluids	2.4

TABLE OF CONTENTS

DECLARATION.....	II
ABSTRACT	III
ACKNOWLEDGEMENTS.....	IV
DEDICATION	V
TABLE OF CONTENTS.....	VI
LIST OF FIGURES.....	XVIII
CLARIFICATION OF BASIC TERMS AND CONCEPTS	XX
NOMENCLATURE	XXI
CHAPTER 1	1.1
INTRODUCTION.....	1.1
1.1 BACKGROUND	1.1
1.2 STATEMENT OF THE RESEARCH PROBLEM	1.2
1.3 OBJECTIVE OF THE RESEARCH.....	1.2
1.4 RESEARCH DESIGN AND METHODOLOGY.....	1.2
1.4.1 Literature review (Chapter 2).....	1.3
1.4.2 The experimental procedures (Chapter 3).....	1.3
1.4.3 Results and discussion (Chapter 4).....	1.4
1.4.4 Summary, conclusion and recommendation (Chapter 5).....	1.4
1.5 DELINEATION OF THE RESEARCH	1.4
1.6 SIGNIFICANCE OF THE RESEARCH.....	1.4
1.7 SUMMARY.....	1.5
CHAPTER 2	2.1
THEORY AND LITERATURE REVIEW	2.1
2.1 INTRODUCTION.....	2.1
2.2 RHEOLOGY.....	2.1
2.3 SHEAR STRESS AND SHEAR STRAIN.....	2.2
2.4 CLASSIFICATION OF FLUIDS.....	2.3
2.4.1 Newtonian fluids	2.4
2.4.2 Non-Newtonian fluids	2.4

2.4.3	Classification of non-Newtonian fluids	2.4
2.4.4	Time-independent non-Newtonian fluids.....	2.5
2.4.4.1	Pseudoplastic fluids.....	2.5
2.4.4.2	Dilatant or shear thickening fluids.....	2.5
2.4.4.3	Viscoplastic fluids.....	2.5
2.4.5	Time-dependent fluid behaviour	2.6
2.5	CHOICE OF RHEOLOGICAL MODEL.....	2.8
2.6	RHEOLOGICAL CHARACTERISATION	2.10
2.6.1	Viscometry	2.10
2.6.1.1	Rotational viscometer.....	2.11
2.7	MIXTURES	2.11
2.7.1	Homogeneous mixtures.....	2.11
2.7.2	Non-homogeneous (or settling) mixtures	2.11
2.8	FACTORS AFFECTING RHEOLOGICAL PROPERTIES	2.11
2.8.1	Temperature.....	2.12
2.8.2	Shear rate	2.12
	Particle Size Distribution	2.13
2.9	YIELD STRESS THEORY	2.13
2.9.1	General definitions and applications of yield stress.....	2.13
2.9.2	Existence of yield stress	2.15
2.9.3	Classification of yield stress.....	2.17
2.10	YIELD STRESS MEASUREMENT TECHNIQUES	2.18
2.11	DIFFICULTIES IN MEASURING YIELD STRESS	2.19
2.12	THE VANE AND VANE RHEOMETRY	2.20
2.12.1	History of the vane.....	2.20
2.12.2	Principle of the vane	2.21
2.12.3	Merits and limitations on the use of vane geometry	2.23
2.12.3.1	Merits	2.23
2.12.3.2	Limitations.....	2.25
2.12.4	Assumptions for the vane technique.....	2.25
2.12.5	Experimental studies validating the vane technique.....	2.26
2.12.6	Numerical studies on vane technique	2.27
2.12.6.1	Rigid cylinder concept	2.27
2.12.6.2	Deformation zone concepts.....	2.28
2.12.6.3	Yielding and formation of deformation zone	2.29
2.12.7	VANE RHEOMETRY CALCULATIONS.....	2.32

2.13	THE SLUMP TECHNIQUE AND MODELS	2.35
2.13.1	Relationship between slump height and yield stress	2.40
2.13.2	The slump models	2.41
2.13.2.1	The cone model	2.41
2.13.2.2	The cylinder model	2.43
2.13.2.3	Lump model	2.44
2.13.3	Merits of using the cylinder over the cone slump test	2.45
2.13.4	Yield criterion	2.46
2.13.5	Behaviour at the interface	2.47
2.13.6	Effect of inertia	2.47
2.14	SLIP	2.48
2.14.1	Definition of slip	2.48
2.14.2	Slip correction techniques	2.49
2.14.3	Slip assessment	2.49
2.15	SHEAR HISTORY	2.50
2.16	EFFECT OF SAMPLE PREPARATION	2.51
2.17	SUMMARY	2.51
CHAPTER 3		3.1
EXPERIMENTAL WORK		3.1
3.1	INTRODUCTION	3.1
3.2	EXPERIMENTAL APPARATUS	3.1
3.2.1	THE VANE TECHNIQUE	3.2
3.2.1.1	Calibration and testing	3.2
3.2.1.2	Analysis of margin of error	3.5
3.2.1.3	Mode of operation and theory	3.7
3.2.1.4	The equipment for measurement	3.8
3.2.2	THE SLUMP METER	3.9
3.2.2.1	Calibration and testing	3.10
3.2.2.2	The geometries	3.13
3.2.3	THE HAND-HELD CYLINDER	3.13
3.2.4	THE SHEAR MIXER	3.14
3.2.5	THE HALOGEN MOISTURE ANALYSER	3.16
3.3	EXPERIMENTAL PROCEDURES	3.16
3.3.1	Yield stress measurement using the slump meter	3.16
3.3.2	Yield stress measurement using the vane techniques	3.17

3.3.3	Yield stress measurement using the hand-held cylinder	3.19
3.3.4	Shearing of the kaolinite tailings and sand.....	3.19
3.4	MATERIALS.....	3.20
3.4.1	Preparation of kaolin.....	3.20
3.4.2	Kaolinite tailings and preparation.....	3.21
3.4.2.1	Preparation of kaolinite tailings.....	3.21
3.4.3	Preparation of sand	3.21
3.4.4	Mixture of kaolinite tailings and sand	3.22
3.4.5	Laponite	3.24
3.4.5.1	Preparation of laponite	3.25
3.5	OTHER MEASURED VARIABLES	3.25
3.5.1	Determination of relative density.....	3.25
3.5.2	Determination of moisture content.....	3.27
3.5.3	Determination of quantities of a mixture.....	3.27
3.6	NON-NEWTONIAN FLUID TEMPERATURE.....	3.29
3.7	SUMMARY OF THE RANGE OF MATERIALS TESTED.....	3.30
3.8	EXPERIMENTAL ERRORS	3.32
3.8.1	Error theory	3.33
3.8.2	Gross error	3.33
3.8.3	Systematic error or cumulative error.....	3.33
3.8.4	Random error	3.34
3.9	SUMMARY.....	3.37
CHAPTER 4	4.1
RESULTS AND DISCUSSION	4.1
4.1	INTRODUCTION.....	4.1
4.2	EFFECT OF POSITION OF SLUMP MEASUREMENT ON THE YIELD STRESS.....	4.2
4.3	VALIDATION OF LUMP MODEL ON YIELD STRESS	4.8
4.4	EFFECT OF LIFT SPEED ON YIELD STRESS	4.14
4.5	EFFECT OF STABILITY ON YIELD STRESS.....	4.18
4.6	EFFECT OF WALL SURFACE MATERIALS ON YIELD STRESS	4.21
4.7	EFFECT OF THE GEOMETRY ON YIELD STRESS	4.24
4.8	EFFECT OF SLIP ON YIELD STRESS.....	4.26
4.9	SUMMARY	4.30
CHAPTER 5	5.1

CONCLUSIONS AND RECOMMENDATIONS	5.1
5.1 INTRODUCTION.....	5.1
5.2 SUMMARY.....	5.2
5.3 CONTRIBUTIONS	5.3
5.4 CONCLUSIONS.....	5.3
5.5 RECOMMENDATIONS.....	5.5
REFERENCES.....	1
APPENDIX A – SLUMP DATA	1
TABLE A.1: SLUMP TEST FOR 14 % KAOLIN (WITHOUT SPRAY) USING THE SLUMP METER.....	1
TABLE A.2 SLUMP TEST FOR 14 % KAOLIN (WITH SPRAY) USING THE SLUMP METER	1
TABLE A.3 SLUMP TEST FOR 16 % KAOLIN (WITHOUT SPRAY) USING THE SLUMP METER	2
TABLE A.4 SLUMP TEST FOR 16 % KAOLIN (WITH SPRAY) USING THE SLUMP METER	3
TABLE A.5 SLUMP TEST FOR 18 % KAOLIN (WITHOUT SPRAY) USING THE SLUMP METER	4
TABLE A.6 SLUMP TEST FOR 18 % KAOLIN (WITH SPRAY) USING THE SLUMP METER	5
TABLE A.7 SLUMP TEST FOR 20 % KAOLIN (WITHOUT SPRAY) USING THE SLUMP METER	6
TABLE A.8 SLUMP TEST FOR 20 % KAOLIN (WITH SPRAY) USING THE SLUMP METER	7
TABLE A.9 SLUMP TEST FOR 14 % KAOLINITE TAILING (WITHOUT SPRAY) USING THE SLUMP METER.....	8
TABLE A.10 SLUMP TEST FOR 14 % KAOLINITE TAILING (WITH SPRAY) USING THE SLUMP METER.....	9
TABLE A.11 SLUMP TEST FOR 16 % KAOLINITE TAILING (WITHOUT SPRAY) USING THE SLUMP METER.....	10
TABLE A.12 SLUMP TEST FOR 16 % KAOLINITE TAILING (WITH SPRAY) USING THE SLUMP METER.....	11
TABLE A.13 SLUMP TEST FOR 18 % KAOLINITE TAILING (WITHOUT SPRAY) USING THE SLUMP METER.....	12

TABLE A.14 SLUMP TEST FOR 18 % KAOLINITE TAILING (WITH SPRAY) USING THE SLUMP METER.....	13
TABLE A.15 SLUMP TEST FOR 20 % KAOLINITE TAILING (WITHOUT SPRAY) USING THE SLUMP METE	14
TABLE A.16 SLUMP TEST FOR 20 % KAOLINITE TAILING (WITH SPRAY) USING THE SLUMP METER.....	15
TABLE A.17 SLUMP TEST FOR 4 % LAPONITE (WITHOUT SPRAY) USING THE SLUMP METER.....	16
TABLE A.18 SLUMP TEST FOR 4 % LAPONITE (WITH SPRAY) USING THE SLUMP METER	17
TABLE A.19 SLUMP TEST FOR 5 % LAPONITE (WITHOUT SPRAY) USING THE SLUMP METER.....	18
TABLE A.20 SLUMP TEST FOR 5 % LAPONITE (WITH SPRAY) USING THE SLUMP METER	19
TABLE A.21 SLUMP TEST FOR 6 % LAPONITE (WITHOUT SPRAY) USING THE SLUMP METER.....	20
TABLE A.22 SLUMP TEST FOR 6 % LAPONITE (WITH SPRAY) USING THE SLUMP METER	21
TABLE A.23 SLUMP TEST FOR 7 % LAPONITE (WITHOUT SPRAY) USING THE SLUMP METER.....	22
TABLE A.24 SLUMP TEST FOR 7 % LAPONITE (WITH SPRAY) USING THE SLUMP METER	23
TABLE A.25 SLUMP TEST FOR 5 MINS 90:10 AT RELATIVE DENSITY OF 1.75 KAOLINITE TAILINGS AND SAND USING THE SLUMP METER	24
TABLE A.26 SLUMP TEST FOR 10 MINS 90:10 AT RELATIVE DENSITY OF 1.75 KAOLINITE TAILINGS PLUS USING THE SLUMP METER	25
TABLE A.27 SLUMP TEST FOR 20 MINS 90:10 AT RELATIVE DENSITY OF 1.75 KAOLINITE TAILINGS AND SAND USING THE SLUMP METER	26
TABLE A.28 SLUMP TEST FOR 5 MINS 90:10 AT RELATIVE DENSITY OF 1.8 KAOLINITE TAILINGS AND SAND USING THE SLUMP METER	27

TABLE A.29 SLUMP TEST FOR 10 MINS 90:10 AT RELATIVE DENSITY OF 1.8 KAOLINITE
TAILINGS AND SAND USING THE SLUMP METER28

TABLE A.30 SLUMP TEST FOR 20 MINS 90:10 AT RELATIVE DENSITY OF 1.8 KAOLINITE
TAILINGS AND SAND USING THE SLUMP METER29

TABLE A.31 SLUMP TEST FOR 5 MINS 80:20 AT RELATIVE DENSITY OF 1.6 KAOLINITE
TAILINGS AND SAND USING THE SLUMP METER30

TABLE A.32 SLUMP TEST FOR 10 MINS 80:20 AT RELATIVE DENSITY OF 1.6 KAOLINITE
TAILINGS AND SAND USING THE SLUMP METER31

TABLE A.33 SLUMP TEST FOR 20 MINS 80:20 AT RELATIVE DENSITY OF 1.6 KAOLINITE
TAILINGS AND SAND USING THE SLUMP METER32

TABLE A.34 SLUMP TEST FOR 5 MINS 90:10 AT RELATIVE DENSITY OF 1.75 KAOLINITE
TAILINGS AND SAND USING THE SLUMP METER33

TABLE A.35 SLUMP TEST FOR 10 MINS 80:20 AT RELATIVE DENSITY OF 1.7 KAOLINITE
TAILINGS AND SAND USING THE SLUMP METER34

TABLE A.36 SLUMP TEST FOR 20 MINS 80:20 AT RELATIVE DENSITY OF 1.7 KAOLINITE
TAILINGS AND SAND USING THE SLUMP METER35

TABLE A.37 SLUMP TEST FOR 5 MINS 80:20 AT RELATIVE DENSITY OF 1.8 KAOLINITE
TAILINGS AND SAND USING THE SLUMP METER36

TABLE A.38 SLUMP TEST FOR 10 MINS 80:20 AT RELATIVE DENSITY OF 1.8 KAOLINITE
TAILINGS AND SAND USING THE SLUMP METER37

TABLE A. 39 SLUMP TEST FOR 20 MINS 80:20 AT RELATIVE DENSITY OF 1.8 KAOLINITE
TAILINGS AND SAND USING THE SLUMP METER38

TABLE A. 40 SLUMP TEST FOR 5 MINS 70:30 AT RELATIVE DENSITY OF 1.4 KAOLINITE
TAILINGS AND SAND USING THE SLUMP METER39

TABLE A. 41 SLUMP TEST FOR 10 MINS 70:30 AT RELATIVE DENSITY OF 1.4 KAOLINITE
TAILINGS AND SAND USING THE SLUMP METER40

TABLE A. 42 SLUMP TEST FOR 20 MINS 70:30 AT RELATIVE DENSITY OF 1.4 KAOLINITE
TAILINGS AND SAND USING THE SLUMP METER41

TABLE A. 43 SLUMP TEST FOR 5 MINS 70:30 AT RELATIVE DENSITY OF 1.5 KAOLINITE
TAILINGS AND SAND USING THE SLUMP METER42

TABLE A. 44 SLUMP TEST FOR 10 MINS 70:30 AT RELATIVE DENSITY OF 1.5 KAOLINITE TAILINGS AND SAND USING THE SLUMP METER43

TABLE A. 45 SLUMP TEST FOR 20 MINS 70:30 AT RELATIVE DENSITY OF 1.5 KAOLINITE TAILINGS AND SAND USING THE SLUMP METER44

TABLE A. 46 SLUMP TEST FOR 5 MINS 70:30 AT RELATIVE DENSITY OF 1.6 KAOLINITE TAILINGS AND SAND USING THE SLUMP METER45

TABLE A. 47 SLUMP TEST FOR 10 MINS 70:30 AT RELATIVE DENSITY OF 1.6 KAOLINITE TAILINGS AND SAND USING THE SLUMP METER46

TABLE A. 48 SLUMP TEST FOR 20 MINS 70:30 AT RELATIVE DENSITY OF 1.6 KAOLINITE TAILINGS AND SAND USING THE SLUMP METER47

APPENDIX B – HAND – HELD CYLINDER (DATA)1

TABLE B. 1 SLUMP TEST FOR 14 % AND 16 % KAOLIN USING THE HAND-HELD CYLINDER1

TABLE B. 2 SLUMP TEST FOR 18 % AND 20 % KAOLIN USING THE HAND-HELD CYLINDER2

TABLE B. 3 SLUMP TEST FOR 14 % AND 16 % KAOLINITE TAILINGS USING THE HAND-HELD CYLINDER.....2

TABLE B. 4 SLUMP TEST FOR 18 % AND 20 % KAOLINITE TAILINGS USING THE HAND-HELD CYLINDER.....3

TABLE B. 5 SLUMP TEST FOR 4 % AND 5 % LAPONITE USING THE HAND-HELD CYLINDER4

TABLE B. 6 SLUMP TEST FOR 6 % AND 7 % LAPONITE USING THE HAND-HELD CYLINDER5

TABLE B. 7 SLUMP TEST FOR 5 MINS 90:10 RELATIVE DENSITY AT 1.75 KAOLINITE TAILINGS AND SAND USING THE HAND-HELD CYLINDER6

TABLE B.8 SLUMP TEST FOR 10 MINS 90:10 RELATIVE DENSITY AT 1.75 KAOLINITE TAILINGS AND SAND USING THE HAND-HELD CYLINDER.....7

TABLE B. 9 SLUMP TEST FOR 5 MINS 90:10 RELATIVE DENSITY AT 1.75 KAOLINITE TAILINGS AND SAND USING THE HAND-HELD CYLINDER7

TABLE B.8 SLUMP TEST FOR 10 MINS 90:10 RELATIVE DENSITY AT 1.75 KAOLINITE TAILINGS AND SAND USING THE HAND-HELD CYLINDER8

TABLE B. 9 SLUMP TEST FOR 10 MINS 90:10 RELATIVE DENSITY AT 1.8 KAOLINITE TAILINGS AND SAND USING THE HAND-HELD CYLINDER	8
TABLE B. 10 SLUMP TEST FOR 20 MINS 90:10 RELATIVE DENSITY AT 1.8 KAOLINITE TAILINGS AND SAND USING THE HAND-HELD CYLINDER	9
TABLE B. 11 SLUMP TEST FOR 5 MINS 80:20 RELATIVE DENSITY AT 1.6 KAOLINITE TAILINGS AND SAND USING THE HAND-HELD CYLINDER	9
TABLE B. 12 SLUMP TEST FOR 10 MINS 80:20 RELATIVE DENSITY AT 1.6 KAOLINITE TAILINGS AND SAND USING THE HAND-HELD CYLINDER	10
TABLE B. 13 SLUMP TEST FOR 20 MINS 80:20 RELATIVE DENSITY AT 1.6 KAOLINITE TAILINGS AND SAND USING THE HAND-HELD CYLINDER	10
TABLE B. 14 SLUMP TEST FOR 5 MINS 80:20 RELATIVE DENSITY AT 1.7 KAOLINITE TAILINGS AND SAND USING THE HAND-HELD CYLINDER	11
TABLE B. 15 SLUMP TEST FOR 10 MINS 80:20 RELATIVE DENSITY AT 1.7 KAOLINITE TAILINGS AND SAND USING THE HAND-HELD CYLINDER	11
TABLE B. 16 SLUMP TEST FOR 20 MINS 80:20 RELATIVE DENSITY AT 1.7 KAOLINITE TAILINGS AND SAND USING THE HAND-HELD CYLINDER	12
TABLE B. 17 SLUMP TEST FOR 5 MINS 80:20 RELATIVE DENSITY AT 1.8 KAOLINITE TAILINGS AND SAND USING THE HAND-HELD CYLINDER	12
TABLE B. 18 SLUMP TEST FOR 10 MINS 80:20 RELATIVE DENSITY AT 1.8 KAOLINITE TAILINGS AND SAND USING THE HAND-HELD CYLINDER	13
TABLE B. 19 SLUMP TEST FOR 20 MINS 80:20 RELATIVE DENSITY AT 1.8 KAOLINITE TAILINGS AND SAND USING THE HAND-HELD CYLINDER	13
TABLE B. 20 SLUMP TEST FOR 5 MINS 70:30 RELATIVE DENSITY AT 1.4 KAOLINITE TAILINGS AND SAND USING THE HAND-HELD CYLINDER	14
TABLE B. 21 SLUMP TEST FOR 10 MINS 70:30 RELATIVE DENSITY AT 1.4 KAOLINITE TAILINGS AND SAND USING THE HAND-HELD CYLINDER	14
TABLE B. 22 SLUMP TEST FOR 20 MINS 70:30 RELATIVE DENSITY AT 1.4 KAOLINITE TAILINGS AND SAND USING THE HAND-HELD CYLINDER	15
TABLE B. 23 SLUMP TEST FOR 5 MINS 70:30 RELATIVE DENSITY AT 1.5 KAOLINITE TAILINGS AND SAND USING THE HAND-HELD CYLINDER	15

TABLE B. 25 SLUMP TEST FOR 10 MINS 70:30 RELATIVE DENSITY AT 1.5 KAOLINITE TAILINGS AND SAND USING THE HAND-HELD CYLINDER	16
TABLE B. 26 SLUMP TEST FOR 20 MINS 70:30 RELATIVE DENSITY AT 1.5 KAOLINITE TAILING AND SAND USING THE HAND-HELD CYLINDER	16
TABLE B. 27 SLUMP TEST FOR 5 MINS 70:30 RELATIVE DENSITY AT 1.6 KAOLINITE TAILINGS AND SAND USING THE HAND-HELD CYLINDER	17
TABLE B. 28 SLUMP TEST FOR 10 MINS 70:30 RELATIVE DENSITY AT 1.6 KAOLINITE TAILINGS AND SAND USING THE HAND-HELD CYLINDER	17
TABLE B. 29 SLUMP TEST FOR 20 MINS 70:30 RELATIVE DENSITY AT 1.6 KAOLINITE TAILINGS AND SAND USING THE HAND-HELD CYLINDER	18
APPENDIX C – VANE DATA.....	1
TABLE C. 1 TORQUE AS A FUNCTION OF TIME FOR KAOLINITE TAILINGS	1
TABLE C. 2 TORQUE AS A FUNCTION OF TIME FOR KAOLIN TAILINGS	1
TABLE C. 3 TORQUE AS A FUNCTION OF TIME FOR 90:10 KAOLINITE TAILINGS AND SAND FOR EACH RELATIVE DENSITY AND SHEAR PERIOD.....	2
TABLE C. 4 TORQUE AS A FUNCTION OF TIME FOR 80:20 KAOLINITE TAILINGS AND SAND FOR EACH RELATIVE DENSITY AND SHEAR PERIOD.....	3
APPENDIX D – ANALYSIS OF RESULTS	1
TABLE D: 1 VALIDATION OF YIELD STRESS MODELSS ON YIELD STRESS.....	1
TABLE D: 2 VALIDATION OF YIELD STRESS MODELS ON YIELD STRESS	2
TABLE D: 3 SUMMARY FOR VALIDATION OF YIELD STRESS MODELS	2
TABLE D: 4 EFFECT OF SLIP ON YIELD STRESS FOR MATERIALS WITH APPROXIMATE MODEL	3
TABLE D: 5 EFFECT OF SLIP ON YIELD STRESS FOR MATERIALS WITH LUMP MODEL	4
TABLE D: 6 EFFECT OF SLIP ON YIELD STRESS FOR MATERIALS WITH CYLINDER MODEL	5
TABLE D: 7 EFFECT OF SLIP ON YIELD STRESS FOR MATERIALS WITH LUMP MODEL	6
TABLE D: 8 EFFECT OF SLIP ON YIELD STRESS FOR MATERIALS WITH LUMP MODEL	8
TABLE D: 9 EFFECT OF SLIP ON YIELD STRESS FOR MATERIALS WITH LUMP MODEL	8

TABLE D: 10 EFFECT OF LIFT SPEED ON YIELD STRESS FOR MATERIALS WITH APPROXIMATE MODEL9

TABLE D: 11 EFFECT OF LIFT SPEED ON YIELD STRESS FOR MATERIALS WITH LUMP MODEL10

TABLE D: 12 EFFECT OF LIFT SPEED ON YIELD STRESS FOR MATERIALS WITH CYLINDER MODEL.....11

TABLE D: 13 EFFECT OF LIFT SPEED ON YIELD STRESS FOR MATERIALS WITH APPROXIMATE MODEL12

TABLE D: 14 EFFECT OF LIFT SPEED ON YIELD STRESS FOR MATERIALS WITH LUMP MODEL13

TABLE D: 15 EFFECT OF LIFT SPEED ON YIELD STRESS FOR MATERIALS WITH CYLINDER MODEL.....14

TABLE D: 16A EFFECT OF STABILITY ON YIELD STRESS FOR THREE MATERIALS.15

TABLE D: 16B EFFECT OF STABILITY ON YIELD STRESS FOR THREE MATERIALS.16

TABLE D: 17 EFFECT OF STABILITY ON YIELD STRESS FOR THREE MATERIALS.17

TABLE D: 18 EFFECT OF STABILITY ON YIELD STRESS FOR MATERIALS.18

TABLE D: 19 EFFECT OF STABILITY ON YIELD STRESS FOR MATERIALS.19

TABLE D: 20 EFFECT OF GEOMETRY SURFACE MATERIALS ON YIELD STRESS FOR THREE MATERIALS.20

TABLE D: 21 EFFECT OF GEOMETRY SURFACE MATERIALS ON YIELD STRESS FOR THREE MATERIALS.21

TABLE D: 22 EFFECT OF GEOMETRY ON YIELD STRESS FOR THREE MATERIALS.23

TABLE D: 22B EFFECT OF GEOMETRY ON YIELD STRESS FOR THREE MATERIALS.24

TABLE D: 23A EFFECT OF GEOMETRY ON YIELD STRESS FOR THREE MATERIALS.25

TABLE D: 23B EFFECT OF GEOMETRY ON YIELD STRESS FOR THREE MATERIALS.26

APPENDIX E - PHOTOS.....1

TABLE E: 1 SLUMP HEIGHT OF KAOLINITE TAILINGS MATERIAL USING CONE (STAINLESS STEEL AND PVC) FOR ALL CONCENTRATIONS.....1

TABLE E: 2 SLUMP HEIGHT OF KAOLINITE TAILINGS MATERIAL USING HAND-HELD CYLINDER2

TABLE E: 3 GEOMETRIES (CONE AND CYLINDER) AND HAND-HELD CYLINDER USED
FOR THE TEST WORK.....2

TABLE E: 4 EQUIPMENTS USED FOR THE TEST WORK3

LIST OF FIGURES

FIGURE 2.1: MOVEMENT OF LAYERS OF FLUID ON APPLICATION OF FORCE (ADAPTED FROM NIELSEN, 1998)..... 2.2

FIGURE 2.2: DEFORMATION OF A SOLID ON APPLICATION OF FORCE, (ADAPTED FROM NIELSEN, 1998) 2.2

FIGURE 2.3: GENERALISED FLOW CURVES SHOWING RHEOLOGICAL CHARACTERISTICS OF NEWTONIAN FLOW..... 2.4

FIGURE 2.4: NON-NEWTONIAN FLUIDS FLOW CURVES (PATERSON & COOKE, 1999) 2.7

FIGURE 2.5: TYPICAL FLOW CURVES FOR YIELD STRESS FLUIDS (ADOPTED FROM BOGER, SCALES, & SOFRA, 2008)..... 2.9

FIGURE 2.6: BEHAVIOUR OF NEWTONIAN AND YIELD STRESS FLUIDS (ADAPTED FROM MC CABE, SMITH & HARIOTT, 1993 & DEEPTI, 2005)..... 2.14

FIGURE 2.7: YIELD STRESS DETERMINATION AT DIFFERENT SHEAR RATES (ADAPTED FROM DODGE & METZNER 1959) 2.16

FIGURE 2.8: CLASSIFICATION OF YIELD STRESS (ADAPTED FROM LIDELL AND BOGER, 196). 2.17

FIGURE 2.9: SCHEMATIC DIAGRAM OF CYLINDRICAL PENETROMETER (ADAPTED FROM UHLHERR ET AL., 2001)..... 2.19

FIGURE 2.10: FOUR-BLADED VANES (ADAPTED FROM DEEPTI, 2005)..... 2.21

FIGURE 2.11: VANE IN A CUP (ADAPTED FROM DEEPTI, 2005) 2.21

FIGURE 2.12: TYPICAL TORQUE-TIME RESPONSE (ADAPTED FROM ALDERMAN ET AL., 1991)2.23

FIGURE 2.13: DEFORMATION ZONE 2.28

FIGURE 2.14: FLOW IN GAP (ADAPTED FROM DEEPTI TANJORE 2005) 2.30

FIGURE 2.15: TORQUE – TIME RESPONSE (ADAPTED FROM YAN & JAMES, 1997)..... 2.31

FIGURE 2.16: SLUMP MEASUREMENT 2.38

FIGURE 2.17: SCHEMATIC DIAGRAM OF THE CONE SLUMP TEST (ADAPTED FROM CLAYTON ET AL., 2003). 2.38

FIGURE 2.18: SLUMP OF A MATERIAL AFTER THE CONE IS LIFTED AND ASSOCIATED STRESS DISTRIBUTION (ADAPTED FROM CLAYTON ET AL., 2003; AND SAAK ET AL., 2004). 2.42

FIGURE 2.19: SAMPLE BEFORE (A) AND AFTER (B) SLUMP TEST (ADAPTED FROM OMURA & STEFFE, 2001) 2.44

LIST OF TABLES

TABLE 3. 1: SUMMARY OF YIELD STRESS	3.4
TABLE 3. 2: CALIBRATION OF THE SLUMP METER	3.12
TABLE 3. 3: EXAMPLE OF MIXTURE KAOLINITE TAILINGS AND SAND	3.22
TABLE 3. 4: YIELD STRESS RESULTS FOR ALL THE MATERIALS AND CONCENTRATION USING THE VANE TECHNIQUE	3.30
TABLE 3. 5: YIELD STRESS RESULTS FOR ALL THE MATERIALS AND CONCENTRATION USING THE VANE TECHNIQUE	3.31
TABLE 4. 1: EFFECT OF POSITION OF SLUMP MEASUREMENT ON YIELD STRESS	4.5
TABLE 4. 2: THE REPEATABILITY OF SLUMP HEIGHT AND YIELD STRESS VALUES USING THE HAND- HELD CYLINDER FOR KAOLIN, KAOLINITE TAILINGS AND LAPONITE MATERIALS.	4.6
TABLE 4. 3: SUMMARY OF VALIDATION OF LUMP MODEL USING HAND-HELD CYLINDER	4.13
TABLE 4. 4: PERCENTAGE VARIANCE.....	4.20

CLARIFICATION OF BASIC TERMS AND CONCEPTS

<u>Term</u>	<u>Definitions</u>
Flow curve	Curve relating shear stress to the true rate of shear of a fluid.
Kaolin	A fine white clay powder used for porcelain and paper making which exhibits rheological characteristics similar to many mineral tailings.
Model	An idealised relationship of rheological behaviour expressible in mathematical, mechanical or electrical terms.
Newtonian fluids	Any fluid that has a simple proportional relationship between shear stress and shear rate.
Non-Newtonian fluids	Any fluid that does not obey Newton's law, which states that stress that is linearly related to strain or viscosity is stress or shear rate dependent.
Rheology	The science of the deformation and flow of material, which deals with the deformation of materials as a result of an applied stress.
Rheometer	An instrument used for measuring rheological properties such as viscosity and yield stress.
Slump meter	A mechanical slump meter designed to lift the cone or cylinder vertically at controlled lifting speeds.
Slump test	Tests conducted with cones and cylinders filled with a flowable material. The slumped amount is measured and this slump height is then related to the yield stress of the material.
Slip	Slip occurs in the flow of a two-phase system because of the displacement of the dispersed phase away from a solid boundary

NOMENCLATURE

SYMBOL	DESCRIPTION	UNITS
A	Area of a section	m^2
A_c	Area of the base cone	m^2
A_u/A_b	Base area ratio	m^2
a	Centrifugal acceleration	m/s^2
C_v	Volumetric concentration	
D	Diameter of the container	m
d_f	Fracture diameter	m
d_v	Vane diameter	m
f'	Dimensionless slump flow area	
f_a	Slump flow area of the hardened paste	m^2
G	Hooken shear modulus	m^2/s
g	Gravitational acceleration	m/s^2
H	Height	m
h	Slump height	mm
H_i	Initial Slump height	mm
H_f	Final Slump height	mm
h'_i	Dimensionless height of deformed region	
h'_o	Dimensionless height of undeformed region	
h_v	Height of the vane	m
L	Length of the vane	mm
L	Final height of the lump	m
L/H	Height ratio	
L'	Dimensionless lump height	
ΔL	Change in length	m
I	Typical inertia stress	Pa
M	Mass	kg
M_h	Torque required for the upper and lower horizontal surfaces of the vane	N m
M_0	Maximum torque	Nm
N	Number of measurement	
N	Rotational speed	rpm
R	Radical distance from axis of rotation	m

RD	Relative density	m
R_c	Cup radius	
R_v	Vane radius	
r_x	Radius of cross section	m
S	Standard deviation	
S	Slump height	m
Sk	Skewness	
S'	Dimensionless slump	
S^2	Variance	
$S_{\bar{X}}$	Standard error	
S_{ξ}	Horizontal resistance	
t	Time	s
τ_e	Stress on vane ends	
$t_{s\bar{X}}$	Confidence level standard error	
V	Velocity	m/s
W_x	Dead weight acting on cross section	N
\bar{X}	Arithmetic mean	
X_1	The measurement	
z_1	Depth of the vane surface from the surface of the material	m
z_2	Height of the vane from bottom of cup	m
τ_y	Yield stress	Pa
τ_{yHB}	Herschel-Bulkley's yield stress	Pa
τ'_y	Dimensionless yield stress	
Ω	Angular velocity of the vane	s^{-1}
α	Confidence limit	
α_1^2	Reciprocal of the square corresponding confidence limit	
η	Viscosity	Pa.s
η_{pl}	Characteristic viscosity	Pa.s
θ	Vane rotation angle	
μ	Newtonian viscosity	Pa s
μ_c	Critical value	

ξ	Normal strain	
ρ	Density of the sample	kg/m ³
σ	Average compressive stress	Pa
σ_{cy}	Stress required to produce yielding	Pa
τ	Shear stress	Pa
τ_B	Bingham yield stress	Pa
γ	Shear strain	
$\dot{\gamma}$	Strain rate	s ⁻¹
γ_0	Yield strain	s ⁻¹

CHAPTER 1

CHAPTER 1

INTRODUCTION

1.1 BACKGROUND

The yield stress debate has been going on for a long time. For practical engineering design it is however accepted as a reality that has to be dealt with. Most of the techniques used in measurement of yield stress are sophisticated, tedious and require highly skilled personnel to perform and interpret the results. The simple hand-held cylinder which was adapted from the concrete cone used to measure the flowability of concrete has been used to measure the yield stress of mining tailings and pastes.

Since Pashias, Boger, Summer and Glenister in 1996 first published the use of the hand-held cylinder for the measurement of yield stress, a number of researchers and engineers have continued with their work. Pashias et al., (1996) used the hand-held cylinder to measure the yield stress of three different mineral suspensions namely: titania, zirconia and bauxite residue and compared it to the vane technique as a control. Pashias et al, (1996) concluded that the cylinder model predicted the yield stress value better than the cone model both at low to high dimensionless slump.

Clayton, Grice and Boger, 2003 investigated the yield stress by using the cylinder slump tests and cone slump tests. The vane technique was used as a reference and related models were compared to yield stress values determined by using the vane technique and they found that the cylinder technique is the better technique. Their analysis also shows that the cylinder model accurately predicted the material yield stress than the cone model.

Saak, Jennings, and Shah in 2004 used Portland cement, paste, clay, ceramic and deionized water for all experiments at water to cement ratios (w/c) ranging from 0.30 to 0.45 . Various amounts of fly ash, silica fume, and superplasticizers were added to the paste to give a wide range of yield stress values. A PVC cylinder and brass cone were used to conduct slump tests. The cylinder model and cone model relating slump to yield stress was used in the dimensional analysis of their results. The results indicate that the model fits the experimental data for cylinder slump test over a wide range of yield stress values for a variety of materials, including cement paste, clays, and ceramic suspensions.

One of the contradictions found in the literature is the point of measurement to determine the slump height. In the traditional concrete slump test, the measurement is taken at the highest point. The slump position was measured at the midpoint in the test conducted by Pashias et al., (1996). However, Gawu and Fourie (2004) used an average of three lowest values but there was not enough evidence in the literature to support their rationale for using the three lowest points.

In addition to the cone and cylinder models, Hallbom presented the lump model in 2005. Haldenwang, Slatter & Masalova, (2007) validated the lump model only over a limited range of dimensionless yield stress values of 0.1 – 0.3.

These two issues will therefore be addressed in this work, in addition to the effect of lift speed, slip, stability, wall surface materials and geometry on the yield stress.

1.2 STATEMENT OF THE RESEARCH PROBLEM

The effect of the slump height measuring point on the calculated yield stress has not been studied in detail. Furthermore, additional experimental data for validation of yield stress models will be beneficial to the industry.

1.3 OBJECTIVE OF THE RESEARCH

The objectives of the research were as follows:

- To evaluate the effect of position of slump measurement on the yield stress;
- To compare yield stress values obtained with the vane test and the slump measurements using four theoretical predictive models.
- To evaluate the effect of stability and lift speed on the measurement of the yield stress;
- To evaluate the effect of wall surface materials on the yield stress measurements;
- To evaluate the effect of geometry on the yield stress;
- To experimentally investigate and evaluate the effect of slip.

1.4 RESEARCH DESIGN AND METHODOLOGY

The following steps were taken in order to achieve the objectives:

1.4.1 Literature review (Chapter 2)

A comprehensive literature review was undertaken on yield stress measurement using the slump technique and vane technique. A review of methodology used by researchers to measure yield stress was also done. Work by Nguyen and Boger (1983 & 1985), Pashias, Boger, Summers & Glenister (1996), Clayton, Grice & Boger (2003), Saak, Jennings & Shah (2003), Gawu & Fourie, (2004), Hallbom, (2005) and Haldenwang, Slatter & Masalova (2007) were found to be relevant.

1.4.2 The experimental procedures (Chapter 3)

As was expected, this work involved much experimental work. Laboratory experiments for this project were conducted in the Flow Process Research Centre (FPRC) at the Cape Peninsula University of Technology, Cape Town, South Africa. A mechanical slump meter developed at (FPRC) was used for the tests. The mechanical slump meter was designed to lift the cone or cylinder vertically at controlled lifting speeds, in comparison with hand-held cylinder. One major feature of the slump meter is that the lifting motion is perfectly vertical, and lateral movement is eliminated.

Slump tests at different concentrations of kaolin, kaolinite tailings, laponite and kaolinite tailings and sand (kaolinite mine tailings) at mix ratios of 90/10, 80/20 and 70/30 were tested to determine their yield stresses. The highest and lowest points of the slumped materials was taken as the slump height and was measured with digital depth gauge to an accuracy of 0.5 mm. The effect of the speed of lifting of the slump meter and the lift by hand was conducted to establish whether there is a critical lifting speed. The parameter was also evaluated by operating the slump meter at different lifting speed and different lift by hand. The effect of slip on the sides of hand-held cylinder, cones and cylinders was also evaluated for each kaolin, kaolinite tailings, laponite and kaolinite tailings and sand (kaolinite mine tailings). This was done by spraying silicone spray on the sides of the cones (stainless steel

and PVC) and the hand-held cylinder. The different techniques and models were used to determine what the effects of the different parameters were on the value of the yield stress.

Different cones and cylinders were inserted in the main frame made from stainless steel and PVC. Stainless steel and PVC materials were used to perform the slump testing. A hand-held cylinder consisting of a stainless steel cylinder of 75 mm diameter and 75 mm height was used to carry out slump tests. A shear mixer with rotation speed of 510 rpm was used for pre-shearing test samples. A Paar Physica MC1 rheometer fitted with a vane was used to measure the static yield stress.

1.4.3 Results and discussion (Chapter 4)

The data obtained experimentally was used to evaluate the effect of lift speed, slip, position of slump measurement, wall surface materials, geometry and was compared to the lump, cylinder and approximate cylinder models. The results are discussed in Chapter 4.

1.4.4 Summary, conclusion and recommendation (Chapter 5)

The effect of slip, lift speed, position of slump measurement, wall surface materials, geometry and comparison of models is evaluated and presented to assist design engineers and operators in obtaining accurate information using the hand-held cylinder. The significant recommendations made for future work are presented in the summary and recommendations in Chapter 5.

1.5 DELINEATION OF THE RESEARCH

This research project did not investigate the effect that ageing has on the yield stress measurement.

1.6 SIGNIFICANCE OF THE RESEARCH

The hand-held cylinder has the potential to become a simple qualitative test to establish the yield stress of industrial materials. To be able to confidently use this instrument, variables effecting the measurement need to be quantified. Yield stress is an important parameter for predicting pressure loss in pipelines and stacking angles in backfill operations (Sofra & Boger, 2001b) as well as product quality. This becomes even more relevant as engineers design more environmentally superior thickened tailings discharged techniques for backfilling and pumping operations (Pashias et al, 1996 and Sofra & Boger, 2001b).

1.7 SUMMARY

An introduction, the aims, an overview and the methodology of this thesis are presented in this chapter. The next chapter (Chapter 2) will present the literature review.

CHAPTER 2

CHAPTER 2

THEORY AND LITERATURE REVIEW

2.1 INTRODUCTION

This chapter presents the relevant fundamental rheological theory and literature review pertaining to yield stress measurements. The relevant rheological fundamentals are discussed, with more emphasis on the most generally used and applicable yield stress models. This is followed by a discussion of theory on vane rheometry and slump measurements. The application of yield stress is also presented: including the inherent problems associated with experimental tests, as well as their corrections.

2.2 RHEOLOGY

Rheology is the science of the deformation and flow of material, which deals with the deformation of materials as a result of an applied stress. The emphasis on flow means that it is concerned with the relationships between stress, strain, strain rate and time (Malkin, 1994 and De Larrard, Sztikar, Hu & Joly, 1994).

Rheological properties describe flow characteristics of substances and principles of rheology are used by industries for process design and quality control (Stokes, Telford & Williamson, 2005). Food scientists, for instance, use rheology when creating or re-designing food products by associating changes in texture and mouth feel with variations in rheological properties (Barnes & Nguyen, 2001; De Krester, Scales, Boger, 1997 and Zhu, Sun, Papadopoulos, & De Kee 2001). Thus, rheology can be used as a vital tool for assessing product performance and consumer acceptance. To assess these physical properties, rheological relationships known as constitutive equations are established. The most essential parameters defining the constitutive equations are stress and strain.

Rheology has provided invaluable information on the structure and dynamics of complex fluids such as polymer and surfactant solutions, gels, and colloidal suspensions. Traditional rheological techniques generally involve measuring the mechanical response of a sample under an externally applied stress.

2.3 SHEAR STRESS AND SHEAR STRAIN

When a material is subjected to a force (F), the sample responds by deforming, see Figures 2.1 and 2.2. Shear stress (τ) is defined as the amount of force applied on the material per unit area (A) of the application surface with units of Pascal (Pa).

$$\tau = \frac{F}{A}$$

2.1

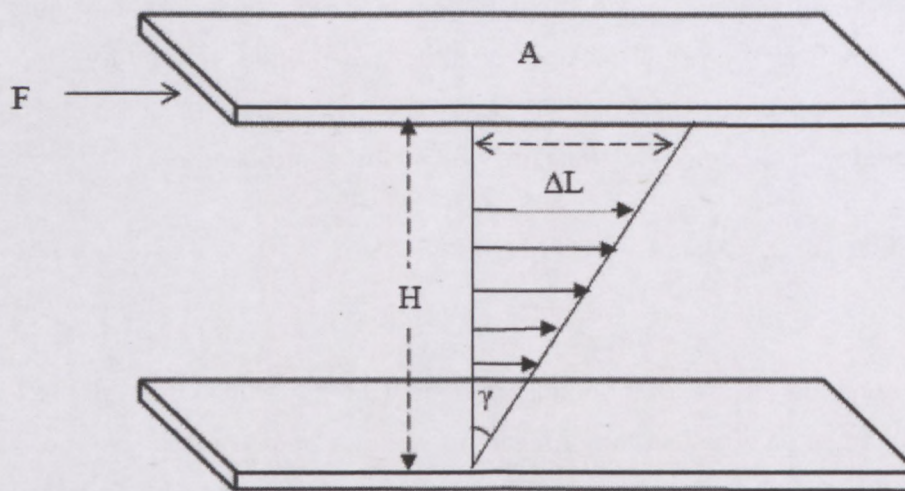


Figure 2. 1: Movement of layers of fluid on application of force (Adapted from Nielsen, 1998)

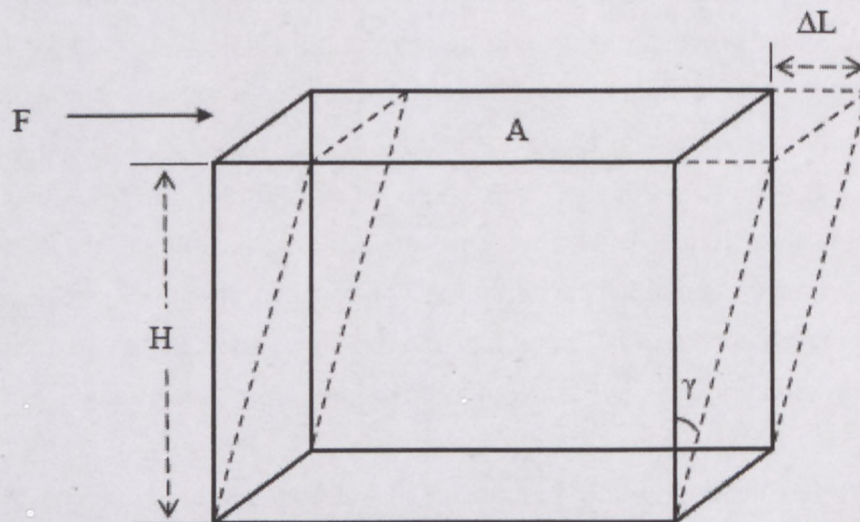


Figure 2. 2: Deformation of a solid on application of force, (Adapted from Nielsen, 1998)

The resulting deformation is measured as strain (γ), computed as the relative displacement in the material. Accordingly, strain, a dimensionless quantity, is the ratio of the change in length (ΔL) to the original length (H).

$$\gamma = \tan^{-1} \left(\frac{\Delta L}{H} \right) \quad 2.2$$

Normal and shear are two classifications of stress categorised depending on the direction of force application. When a force is applied perpendicular to the material surface (Figure 2.1), normal stress is observed which induces a normal strain (γ). Similarly, a force applied parallel to the material surface (Figure 2.2) causes a shear stress and consequently a shear strain (γ) (Hadley & Weber, 1975; Baker, 1998 and Hackley & Ferraris, 2001).

Shear strain rate $\dot{\gamma}$ is the time rate of change of strain occurring in the material and can be defined as the rate at which adjacent layers of a material move with respect to each other (Baker, 1998; Nielsen, 1998 and Hackley & Ferraris, 2001). Shear rate is a velocity-related parameter and is usually expressed in reciprocal seconds (1/s).

$$\dot{\gamma} = \frac{d\gamma}{dt} \quad 2.3$$

Apparent viscosity (η) of fluids is described as the resistance to flow offered by fluid layers during the application of a shearing force and is measured according to the following equation (McCabe, Smith & Harriott, 1993).

$$\eta = \frac{\tau}{\dot{\gamma}} \quad 2.4$$

Viscosity is one of many such parameters, describing stress-strain and stress-strain rate relationships, used to characterise materials.

2.4 CLASSIFICATION OF FLUIDS

Generally fluids can be described as either Newtonian or non-Newtonian.

2.4.1 Newtonian fluids

Any fluids that have a simple proportional relationship between shear stress and shear rate are known as a Newtonian fluid, as shown in Figure 2.3. Newtonian fluids start to flow when a stress is applied, and deformation stops instantly when the stress is removed (Chhabra & Richardson, 1999). Basically, the viscosity of a Newtonian fluid will remain constant at a given temperature irrespective of which speed and spindle are used to measure it. Typical examples of Newtonian fluids are water, glycerine and motor oils. Physically, the shear rate is the rate of angular deformation of the fluid (Liu, 2003).

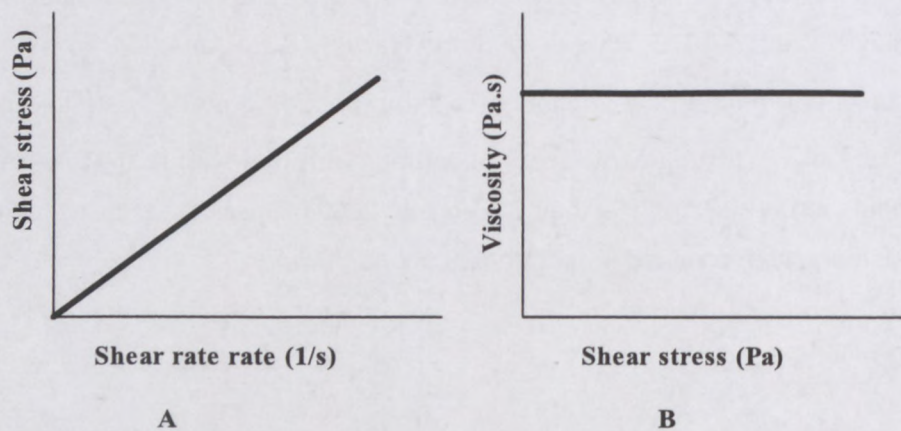


Figure 2. 3: Generalised flow curves showing rheological characteristics of Newtonian flow.

2.4.2 Non-Newtonian fluids

The fluids which do not obey Newton's law of fluid flow are called non-Newtonian fluids. Plots of shear stress versus shear rate are typically used to characterise non-Newtonian fluids. The relationship between shear stress and shear rate is not linear.

Figure 2.4 below is non-Newtonian fluid flow curves overview.

2.4.3 Classification of non-Newtonian fluids

There are numerous types of non-Newtonian flow behaviour, characterised by the way a fluid's viscosity changes in response to variations in shear rate (Chhabra & Richardson,

1999). In most real materials, they often exhibit a combination of two or even all the three types of non-Newtonian features (Chhabra & Richardson, 1999). It is, however, possible to identify the dominant non-Newtonian characteristic and to take this as the basis for the subsequent process calculation (Chhabra & Richardson, 1999). The most common types of non-Newtonian fluids are time-independent non-Newtonian fluids, time dependent non-Newtonian fluids and viscoelastic fluids.

2.4.4 Time-independent non-Newtonian fluids

Time-independent non-Newtonian fluids are fluids of which the rate of shear at any point is determined only by the value of the shear stress at that point at that instant. These fluids may be further subdivided into three types:

2.4.4.1 Pseudoplastic fluids

This type of fluid will display a decreasing viscosity with an increasing shear rate. This type of flow behaviour is also called as “shear-thinning” flow behaviour. This common type of fluid behaviour observed is pseudoplasticity or shear-thinning (Chhabra & Richardson, 1999).

2.4.4.2 Dilatant or shear thickening fluids

This type of time-independence fluid will display an increasing viscosity with an increase in shear rate characterises the dilatant fluid. Dilatancy is also referred as “shear-thickening” flow behaviour. Dilatant fluids are similar to pseudoplastic fluids in that they exhibit no yield stress, but their shear rate increases with increasing apparent viscosity; thus these fluids are also called shear-thickening (Chhabra & Richardson, 1999). This phenomenon is due to the fact that at high shear rates, the material expands or dilates slightly so that there is no longer sufficient liquid to fill the increased void space and facilitate direct solid-solid contacts which result in increased friction and higher shear stress. This mechanism causes the apparent viscosity to rise rapidly with increasing shear rate (Chhabra & Richardson, 1999).

2.4.4.3 Viscoplastic fluids

This type of fluid behaves as a solid under static conditions. A certain amount of force must be applied to the fluid before any flow is induced and this force is called the yield value. Below the yield value, the material behaves essentially as an elastic solid (Skelland, 1967). Once the yield value is exceeded and flow begins, plastic fluids may display Newtonian, pseudoplastic or dilatant flow characteristics. Example of this type of fluid is a clay suspension. Two types of these fluids encountered in the industry are:

- (a) Bingham plastic fluids: This is a fluid which is characterised by a constant plastic viscosity and a yield stress (Malkin, 1984 and Chhabra & Richardson, 1999).
- (b) Another type is a yield pseudoplastic fluids which possesses a yield stress as well as non-linear curvature (Chhabra & Richardson, 1999)

2.4.5 Time-dependent fluid behaviour

Thixotropic and rheopectic fluids are of a non-Newtonian type where time dependency has to be considered.

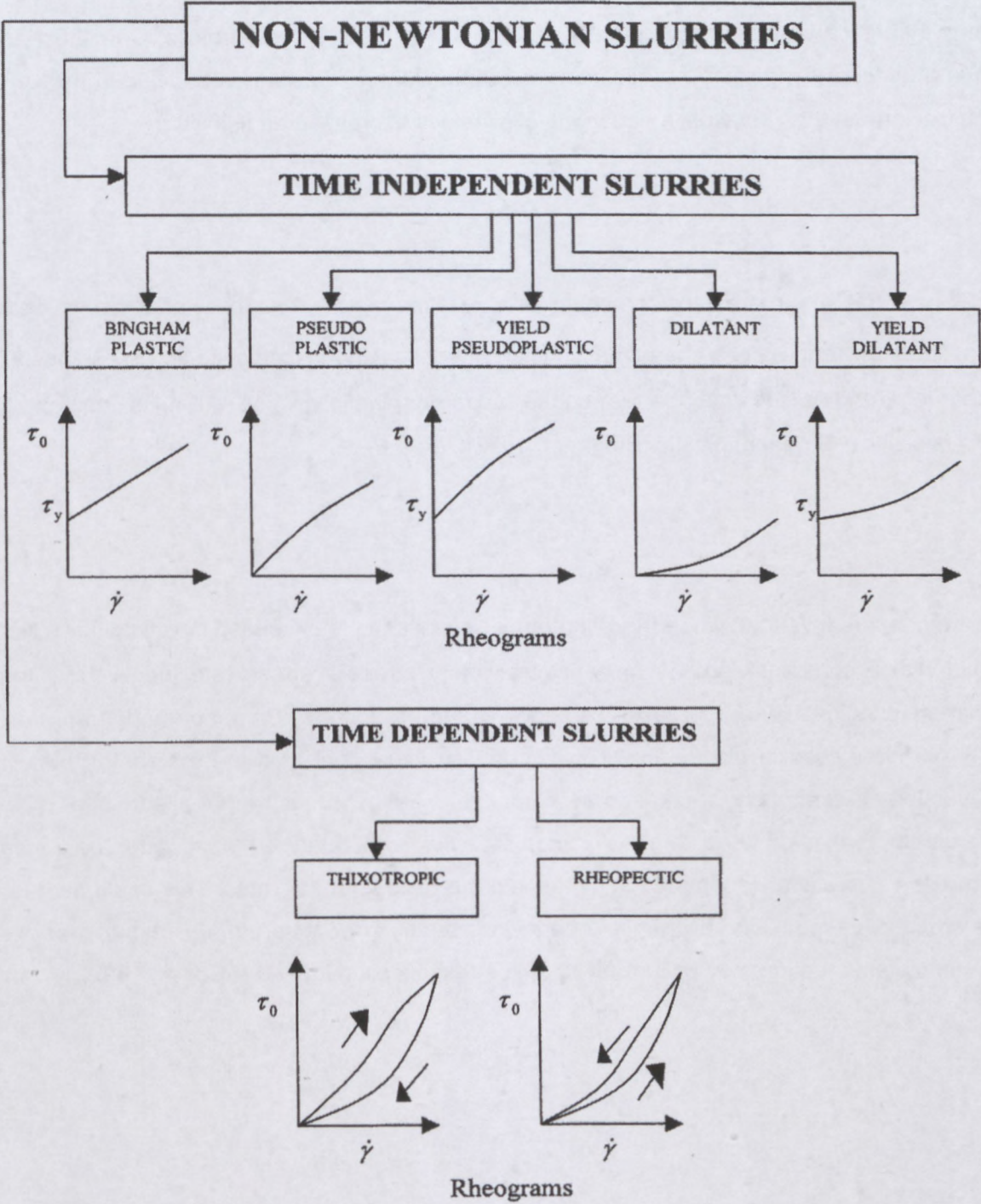


Figure 2. 4: Non-Newtonian fluids flow curves (Paterson & Cooke, 1999)

2.5 CHOICE OF RHEOLOGICAL MODEL

Many theoretical and empirical models have been reported in the literature. Only those that have a direct and significant implication for suspensions and pastes are included here. The general form of the constitutive equations available is expressed as follows:

$$\tau = \tau_y + \eta_{pl} \dot{\gamma} \quad \tau \geq \tau_y \quad \dot{\gamma} = 0, \quad \tau < \tau_y \quad 2.5$$

where τ is the shear stress, $\dot{\gamma}$ the shear rate, τ_y is the yield stress that has to be exceeded to initiate flow, and η_{pl} is a characteristic viscosity describing viscoplastic flow. η_{pl} varies with shear rate, and as such may be termed the "apparent plastic viscosity". If η_{pl} is constant, the fluid is called a Bingham plastic (Bingham, 1922):

$$\tau = \tau_B + \eta_{pl} \dot{\gamma}, \quad \tau \geq \tau_B \quad 2.6$$

This model predicts that, when the Bingham yield stress τ_B is exceeded, the fluid flows like a liquid with a constant viscosity η_{pl} . A typical shear stress – stress rate (flow) curve for a Bingham plastic is linear (curve B), as shown in Figure 2.5. The Bingham model represents only the ideal case of plastic flow in which the structure that aids the material in resisting irreversible deformation breaks down completely as soon as the applied shear stress overcomes the yield values. In most viscoplastic fluids encountered in practice, the linearity of the flow curve is only obtained at high shear stresses or shear rates. This could be due to the structure responsible for the yield behaviour breaking down gradually during shear and its complete disruption may occur only at high stress levels (Nguyen & Boger, 1992).

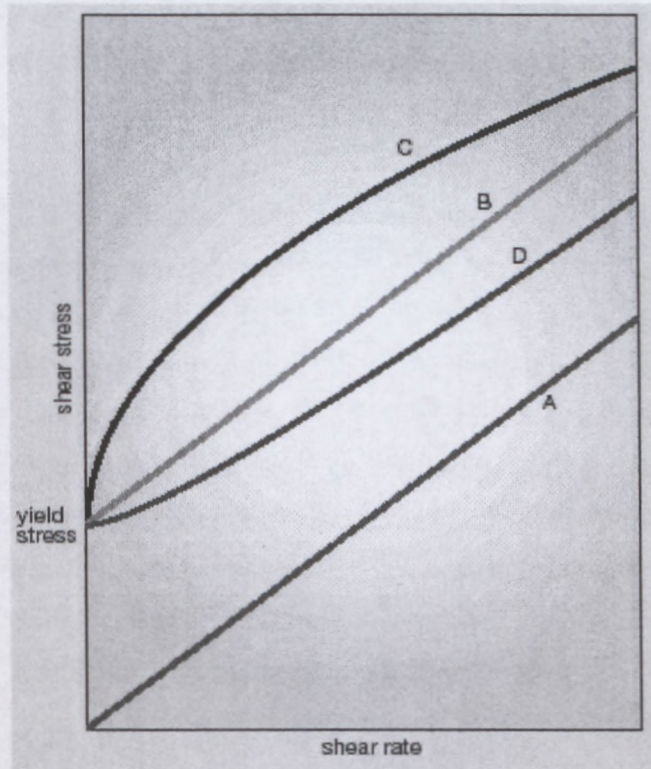


Figure 2. 5: Typical flow curves for yield stress fluids (Adopted from Boger, Scales, & Sofra, 2008)

Generally, viscoplastic fluids that are not Bingham plastics may exhibit either type of nonlinear flow behaviour, as shown in Figure 2.5. Similar to nonlinear viscous behaviour, curve C is for yield-pseudo plastic fluids with the apparent plastic viscosity (η_{pl}) decreasing with shear rate, and curve D describes yield-dilatant fluids with η_{pl} increasing with shear rate. Nonlinear viscoplastic flow behaviour may be described by the following empirical model, which is a modified form of Equation 2.5:

$$\tau = \tau_{HB} + k\dot{\gamma}^n, \quad \tau \geq \tau_{HB} \quad 2.7$$

Here τ_{HB} is the yield stress and k and n is constants equivalent to the power law parameters commonly used for approximating the behaviour of many viscous fluids. For $n < 1$ the fluid is a yield-pseudo plastic; and $n > 1$ corresponds to yield-dilatant behaviour. If $n = 1$, Equation 2.7 reduces to the Bingham model (Equation 2.5), and if $\tau_{HB} = 0$, the power law model is obtained. The three-parameter Herschel-Bulkley model has been found applicable to a variety of viscoplastic systems (Bird, Grance & Yorusso, 1983). It is useful for correlating experimental data for a given type of fluid in which a spectrum of rheological behaviour may

exist under different conditions. The main drawback, however, is the hard procedure required for determining the stress model parameters (Blair, 1966; Heywood & Cheng, 1984).

The selection of a particular model for a given system depends on a number of factors, for example the goodness of the model fit, the simplicity of the constitutive equation involved, personal tastes and the intended application. It has been shown by many workers that, over a restricted range of shear rates – typically from low to high – more than one of the models described above can be used for correlating data for a given yield stress fluid (Charm, 1963; Thomas, 1963 and Darby & Cheremisoff, 1986). This is for a typically industrial suspension (Nguyen, 1983). On the other hand, it is possible that no single model would be sufficient for describing the observed flow behaviour over a wider range of shear rates (Umeya, Isoda, Ishii & Sawamura, 1969). It is thus recommended that, whatever the model used, great care must be exercised if the resulting empirical equation is to be used beyond the range of the experimental data obtained.

2.6 RHEOLOGICAL CHARACTERISATION

The rheological characterisation of non-Newtonian fluids is not easy (Chhabra & Richardson, 1999). Rheological characterisation of non-Newtonian fluids is useful in several slurry handling design applications. Some aspects of this, for instance, involves predicting performance, behaviour, pump selection and sizing (Heywood & Brown, 1991).

2.6.1 Viscometry

The science of measuring the Newtonian and non-Newtonian properties of slurries is called viscometry. Viscometry includes the collection of physical data from tests on a sample of the fluid under investigation; the establishment of the relationship between shear stress and shear rate (Kochler & Fowler, 2003); the identification of the applicable rheological model; and, finally, the determination of actual values of constants in the model, e.g. yield stress, k and n (Slatter, 1994). The instruments for measuring rheological properties can be classified into two categories, namely rotational viscometry and tube viscometry. For the aim of this thesis, only the rotational type will be used and therefore reviewed. The rotational type can also be used to investigate the time-dependent behaviour of a material as opposed to tube viscometry, in which the passage of a material is allowed through the pipe.

2.6.1.1 Rotational viscometer

The rotational viscometer consists of a concentric bob and cup, one of which can rotate to produce shear in the fluid placed in the annular space between the stationary and the rotary cylinder. The measurements of the torque of the elements allow the determination of the shear stress (Chhabra & Richardson, 1999). The shear stress is determined by measuring the applied torque on one of the elements. The rheometer is a very sophisticated instrument and capable of measuring the full range of rheological phenomena. The rheometers can be found using one of the many geometries, among others: concentric cylinders, cone and plate and parallel disks. The main measurements are angular velocity and applied torque. The software connected to these instruments converts these signals into shear rate and shear stress (Chhabra & Richardson, 1999).

Rotational rheometers are most typically used at industrial sites. Rheometers have been used to quantify both the yield stress and the viscosity of materials.

2.7 MIXTURES

2.7.1 Homogeneous mixtures

Homogeneous mixtures are characterised by a uniform concentration of particles and its flow as a single-phase fluid (Thomas, 1961). The term homogenous is used to imply a uniform spatial distribution of the solid particles and a uniform concentration of solids (Wilson, Pugh, Addie, Visintainer & Clift, 1993). Homogenous can be defined as a limiting form of behaviour that is approached by non-Newtonian fluids (Shook & Roco, 1991).

2.7.2 Non-homogeneous (or settling) mixtures

In contrast to homogenous mixtures, mixtures of this type show a finite tendency to settle and the fluids do not display single-phase behaviour.

2.8 FACTORS AFFECTING RHEOLOGICAL PROPERTIES

The various parameters that strongly influence the rheological properties of materials are given below:

2.8.1 Temperature

"One of the most obvious factors that can have an effect on the rheological behaviour of a material is temperature" (Yetkin et al., 2000). Temperature control is the single most important parameter for obtaining accurate and precise kinematic viscosity measurements.

Some fluids are quite sensitive to temperature, and a relatively small variation will result in significant changes in the viscosity of that fluid. Others are relatively insensitive to temperature. Consideration of the effect of temperature on viscosity is essential in the evaluation of materials that will be subjected to temperature variations in processing or in use. Thickening with Aculyn 22 undergoes a modest decrease as the temperature rises from 20° C to 75° C (Rohm & Haag, 2002).

2.8.2 Shear rate

Non-Newtonian fluids tend to be the rule rather than the exception in the real world, making an appreciation of the effects of shear rate a necessity for anyone engaged in the practical application of rheological data. It would, for example, be disastrous to try to pump a dilatant fluid through a system, only to have it go solid inside the pump, bringing the whole process to an abrupt halt. While this is an extreme example, the importance of shear rate effects should not be underestimated. "When a material is subjected to a variety of shear rates in processing or use, it is essential to know its viscosity at the projected shear rates. "If these are not known, an estimate should be made" (Traxler, 1961 and Yetkin et al., 2000). Viscosity measurements should be taken at shear rates as close as possible to the estimated values. "It is frequently impossible to approximate projected shear rate values during measurement due to these values falling outside the shear rate range of the viscometer" (Yetkin et al., 2000). In this case, it is necessary to make measurements at

several shear rates and extrapolate the data to the projected values. Yelkin et al., (2000) pointed out that “, this is not the most accurate technique for acquiring this information, but it is often the only alternative available, especially when the projected shear rates are very high”. In fact, it is always advisable to make viscosity measurements at several shear rates to detect rheological behaviour that may have an effect on processing or use.

Particle Size Distribution

A number of factors influence the rheology of a suspension, including particle size, particle size distribution, and the volume fraction of solids present. The procedure of determining the proportion of mineral particles in each of these classes is known as Particle size analysis (Chong, Christiansen & Baer, 1971).

Particle size analysis and shape, particularly at the sub 10 micrometer level is an important tool that can be used to distinguish between various clay components that can affect the rheological performance of non-Newtonian fluid. Among the factors that determine the viscosity of the non-Newtonian fluid are the fineness of the clay particles in the natural state and the degree to which the particles and aggregates are cleaved or dispersed during the hydration process (Coussot & Piau, 1994)

2.9 YIELD STRESS THEORY

2.9.1 General definitions and applications of yield stress

Most fluids do not display Newtonian behaviour and are therefore referred to as non-Newtonian materials. Certain non-Newtonian materials (clay, candy compounds, corn starch in water, and sand/water mixtures) exhibit a property known as yield stress: see Figure 2.6. The idea of a yield stress was initially attributed to Schwedoff in connection with experiments conducted on gelatine solutions. In the previous century, Professor Eugene Bingham proved that a substance possesses a yield stress below which plastic deformation ceases. He also developed the Bingham equation for a non-Newtonian fluid with a yield stress (Barnes, 1999).

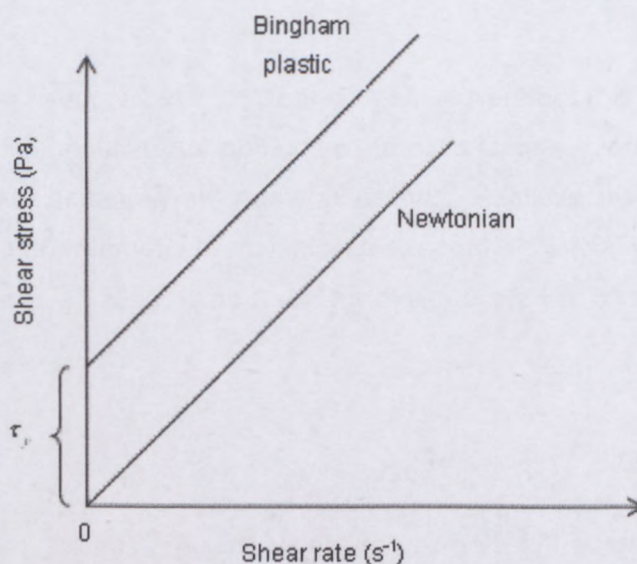


Figure 2. 6: Behaviour of Newtonian and yield stress fluids (Adapted from Mc Cabe, Smith & Hariott, 1993 & Deepti, 2005)

As a critical rheological property, different researchers from various disciplines of science have studied yield stress extensively; the outcome has been same versions of the yield stress definition. Among many of them, yield stress has been defined by Blair, 1949; Keentok, 1982; Yan & James, 1997; Barnes, 1999; Sofra & Boger, 2001a and De Kee, Christopher, Max & Kyle, 2004 as the minimum stress required to initiate a flow.

According to Nguyen and Boger (1983), the yield stress is defined as “the strength of the coherent network structure as the force per unit area required to break down the structure, followed by a rupture of the network bonds or linkages connecting the flow units”.

Accordingly, these non-Newtonian materials (clay, candy compounds, corn starch in water, and sand/water mixtures) are expected to be a viscoelastic solid prior to yielding and a viscoelastic liquid post yielding (Malkin, 1994 and Guo, Tiu, Uhlherr & Fang, 2003). Yield stress is often a desirable property and is accountable for functional performance of many suspensions (Nguyen & Boger, 1983 & 1985; Yoshimura et al, 1987; Nguyen & Boger, 1992, and Coussot, Proust & Ancey, 1996). For example, paints are required to be suitably thin for application purposes. At the same time, paints are also required to exhibit a yield stress to supply sufficient resistance to avoid sagging or flow after application. Numerous food products, including ketchup, mayonnaise and salad dressings, are specifically designed to impart a yield stress.

For example, a salad dressing is expected to be thick and not flow freely from a container, but simultaneously should not require high stresses to initiate flow. Thus, the application and intensity of yield stress are significant components for product quality (Zhang & Nguyen, 1996 and Christopher & Helene, 2006).

Another practical application of the yield stress is found in the mineral industry in thickened tailings disposals. Yield stress plays an important role in such activities. The thickened tailings are piled up at the disposal site. The design of a dry disposal system requires prediction of the angle of repose formed by the deposited tailings; if the relationship between tailings rheology, operating conditions and the depositional behaviour is known, the desired slope can be achieved.

Yield stress is practically useful in engineering design and operation of processes where handling and transport of industrial suspensions are involved" (Nguyen & Boger, 1983 and 1985).

2.9.2 Existence of yield stress

Recently, there has been much debate over the existence of the yield stress. Barnes and Walters (1985) have argued that, given the correct measurements in which the low shear rate regions are made; the yield stress does not exist. They further argued "that the apparent observed yield stress is a direct function of limitations imposed by the low shear stress due to with the rheometers used in the experiments"(Barnes & Walter, 1985 and Gardiner, Dlugogorski, Jamesson & Chhabra, 1998). They concluded that, for shear rates which are satisfactorily low, all fluids will demonstrate Newtonian behaviour, but enough time must be allowed for the yield stress to occur. The practical definition of static yield stress or dynamic yield stress is then determined by whether or not yield occurs in the time scale of the application or process (Gardiner et al., 1998).

From this viewpoint, the conception of a yield stress is a useful idealisation. Yet, regardless of earlier concerns, there is strong experimental and theoretical support for the proposition that a time yield stress exists for fluids with an internal structure, such as suspensions, mining tailings, fresh concrete and pastes (Kraynik & Hansen, 1987; and Gardiner et al., 1998). Finally, Barnes and Walters (1985) stated that experimental verification of true yield

stress would involve an infinite amount of time, and therefore be impossible to perform (Evans, 1992).

The concept proposed by Barnes and Walters (1985) received criticism (Astarita, 1990 and Kee & Fong, 1993) from Hartnett and Hu (1989), who identified yield stress as an 'engineering reality' (Hartnett & Hu, 1989, Yan & James, 1997; and Tatsumi, Ishioka & Matsumoto, 2002). In their approach, Hartnett and Hu (1989) used a falling ball technique and observed no change in the position of a nylon ball after several months as it was allowed to drop through a solution of high viscosity. Thus, the solution used for the experiment exhibited a significant yield stress. Barnes (1999), defending their position on yield stress, suggested the use of a microscope to observe the change in position. Astarita (1990) and Evans (1992) built a bridge between the divergent theories stating that the entire concept revolves around the order of distance measured and experimental time scale. Accordingly, the existence of yield stress depends on the nature of the experiment being conducted. Schurz (1992) and Cheng (1986), similar to Evan's theory, affirmed that an "apparent yield stress", which would be distinguished according to a significant measurable time and lowest possible shear rate, is more meaningful. Therefore, yield stress is believed to be a time-dependent property varying inversely with the time period employed for the test. A longer measurement time (lower rate) will generate a smaller yield stress value (Nguyen & Boger, 1992). Accordingly, a higher strain rate would produce a higher yield stress and vice versa, as shown in Figure 2.7 (Nguyen & Boger, 1992; Guo et al., 2003; and Uhlherr et al., 2005).

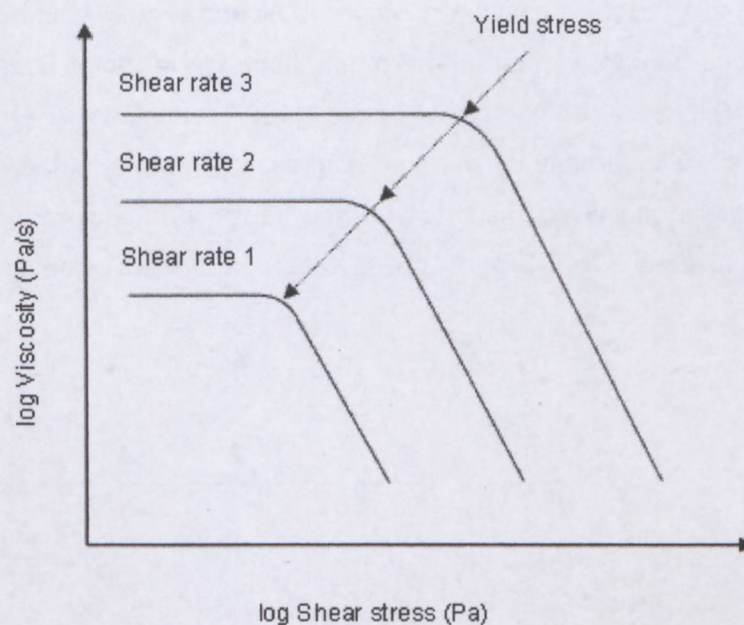


Figure 2. 7: Yield stress determination at different shear rates (Adapted from Dodge & Metzner 1959)

Uhlherr et al. (2005) believed that the material yielding is determined by a critical strain, the yield strain (γ_0), rather than by a critical stress or critical shear rate. The yield stress concept might be in debate, but the application of the theory and models developed based on the rheological behaviour of several materials that do not exhibit free flow in small ranges of stress values is significant in many practical engineering applications (Barnes, 1997; and Uhlherr et al., 2005).

2.9.3 Classification of yield stress

Traditionally, yield stress is categorised into two types: static and dynamic yield stress (Guo et al., 2003). Lidell and Boger (1996) classified yield stresses on the basis of the transition of the torque-time profile from one region to the other (see Figure 2.8). In Figure 2.8, the static yield stress is defined as the stress corresponding to the transition between fully elastic and viscoelastic behaviour of the material, that is, the stress observed at point C. Prior to point C, the vane is static and hence no movement is observed in the material.

The dynamic yield stress is defined as the difference between the static yield stress and the peak stress corresponding to the transition observed between viscoelastic behaviour of the material to fully viscous behaviour, that is, the stress observed at point D, the peak stress (James, Williams & Williams, (1987); Yan & James, (1997) and Guo et al., 2003). Thus, dynamic yield stress is the difference between peak stress and static yield stress. Beyond C, the vane starts rotating in the viscoelastic region and hence is in a dynamic position. The speed of vane rotation equals that of the applied rotational speed when the fully viscous region is reached.

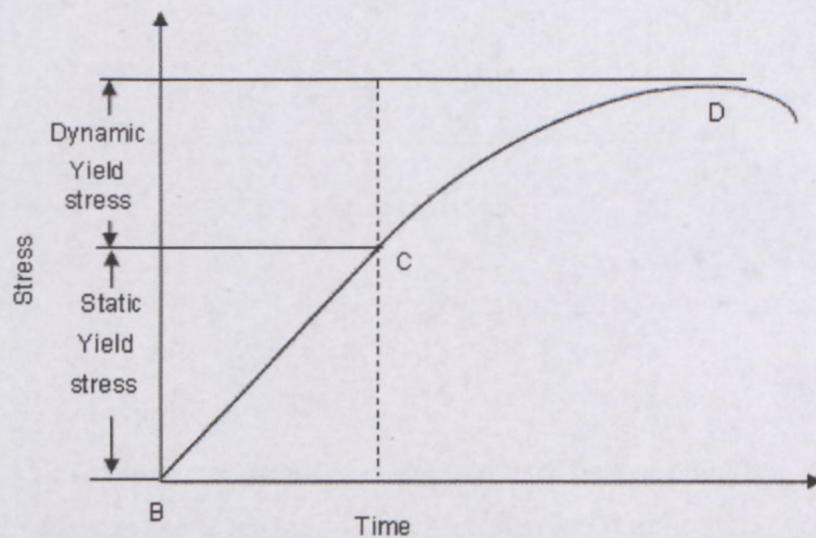


Figure 2. 8: Classification of yield stress (Adapted from Lidell and Boger, 1996)

2.10 YIELD STRESS MEASUREMENT TECHNIQUES

In principle, the technique and instrument employed for measuring flow properties of non-Newtonian suspensions is valid for measuring yield stress. In practice, however, the presence of the yield value imposes certain limitations on the type of instrument that can be used and the type of technique to be used for analysing the experimental data (Nguyen & Boger, 1992). A strong interest in yield stress fluids for decades has led to the development of many experimental methods and techniques for measuring the yield stress property (Nguyen et al., 2005). While each technique has its own merits, and though some techniques may be more popular than the others, no single technique has been universally accepted as the standard for measuring yield stress.

The most common technique used to measure yield stress involves extrapolating the stress-strain rate flow curve to zero strain rate through the use of an appropriate model. The other good technique requires measuring the stress application at a constant rotational rate and observing stress as a function of time (Liddell & Boger, 1996).

Uhlherr et al., (2001) used a simple static technique using a penetrometer for measuring yield stress of a viscoplastic fluid. They observed that there is no reason to believe that the penetrometer results are less reliable than those from the other techniques. No simple explanation can be offered for the discrepancies observed. Thus, this technique provides a relatively quick and low cost technique of obtaining a realistic value of yield stress without the need for costly stress controlled or speed-controlled rheometers (Uhlherr et al., 2001). The principle of this technique is based on the measurement of the static equilibrium of a falling penetrometer in a yield stress fluid.

When the penetrometer is gently released in a fluid with yield stress, it quickly falls under gravity toward an equilibrium position, as shown in Figure 2.9. The resistance forces due to the yield stress on the surface of the penetrometer and buoyancy simultaneously apply to limit the motion. The penetrometer reaches static equilibrium when the force due to gravity is balanced by the resistance forces.

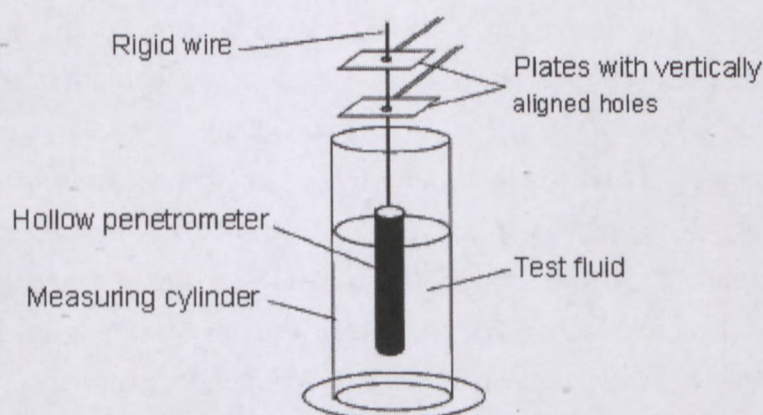


Figure 2. 9: Schematic diagram of cylindrical penetrometer (Adapted from Uhlherr et al., 2001)

Quite a number of techniques have been developed to gauge yield stress, notably the vane technique (Nguyen & Boger, 1983 and 1985) and the modified slump technique widely known as “hand-held cylinder” (Pashias et al., 1996). The vane and flow curve technique

relies on advanced electronic equipment such as the rotary viscometer fitted with various geometries, whereas the slump technique is a very simple technique. However, in all these cases, the focus is to obtain an accurate and reproducible estimate of the yield stress. For the purpose of this work, the vane technique and the slump technique will be discussed in details in this work.

2.11 DIFFICULTIES IN MEASURING YIELD STRESS

One fundamental problem with the concept of yield stress fluids is the difficulty in determining the yield stress (Boger & Nguyen, 1992). Depending on the experimental procedure quite different values of the yield stress can be obtained (Barnes, 1999). Indeed, it has been demonstrated that a variation of the yield stress of more than one order of magnitude can be obtained depending on the way it is measured (James, Williams & Williams, 1987). The usual interpretation is that the structure and/or properties of the yield stress fluids are not probed in the same way, depending on the measurement technique. The huge variation in yield stress cannot be attributed to the difficulty of distinguishing between a finite and an infinite viscosity, but hinges on more fundamental problems with this 'ideal' concept of yield stress fluids. This, of course, is well known to rheologists, but since no reasonable and easy way of introducing a variable yield stress is generally accepted, researchers and engineers often choose to work with the yield stress nonetheless and often treat it as if it is a material constant which is just tricky to determine. The second problem with the yield stress is shear localisation; all related models suggest that all shear rates are possible in a material (Peder, Moller, Mewis & Bonn, 2006). However, as soon as one makes an attempt to create a homogeneous flow in practice, this generally fails; only a small region of the material actually moves, and the rest remains "solid". The reasons for this: is shear banding (localisation). Shear localisation is a basic property of yield stress fluids that always manifests itself at low enough shear rates. The manifestation in this respect is independent of the precise experimental protocol or measurement geometry.

The third potential problems while testing for the yield stress is the possibility of slip at the surfaces. Magnin and Piau (1990) used strain field observations to study the effect of slip on the measurement of yield stress of an aqueous gel, and found that slip played an important role when using smooth surfaces. When the surface roughness was sufficiently high, slip was found to be negligible. Patton (1964) performed cold spot testing on model wax-oil

systems and found that failure was cohesive (yielding) when using roughened surfaces. He also observed that there was no correlation between the amount of deposit and the surface roughness.

2.12 THE VANE AND VANE RHEOMETRY

2.12.1 History of the vane

The historical use of the vane may be traced back to as early as 1939 when Russell worked with a “small glass vane” to study the coagulation of sodium clay gels (Russell, 1939). His main aim in using the vane geometry was to eliminate the possibility of slipping. Then a vane geometry known as the FL rotor (see Figure 2.10), where the FL nomenclature was derived from the German word “flügel”, which can be translated as wings or vane, was introduced. This six-bladed vane introduced by a Germany company (Gerbrueder Haake, Karlsruhe) was used to overcome slip problems and to measure yield stress. Thus, Nguyen and Boger (1983 and 1985), further developed the vane technique and it has grown in popularity as a simple and effective technique for direct measurement of the yield stress property.

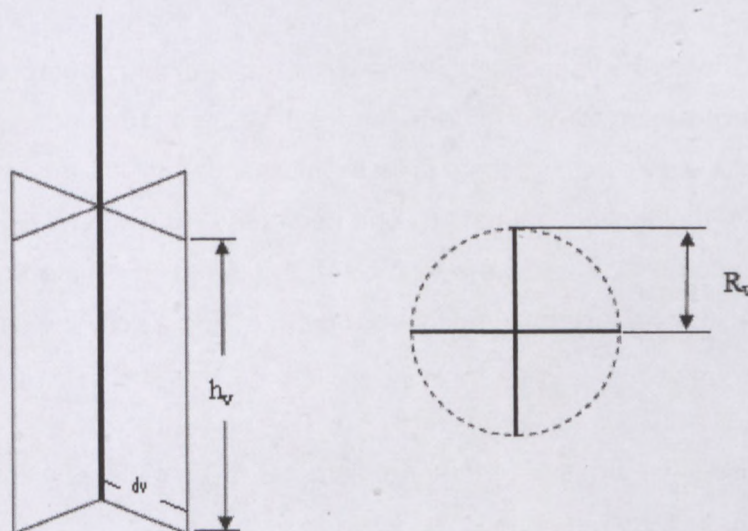


Figure 2. 10: Four-bladed vanes (Adapted from Deepti, 2005)

2.12.2 Principle of the vane

The depth of the suspension and the diameter of the container should be at least twice as large as the length and diameter of the vane to minimise any effects caused by the rigid boundaries, as shown on Figure 2.11 below

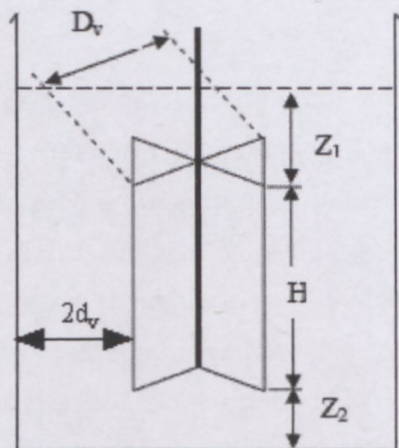


Figure 2. 11: Vane in a cup (Adapted from Deepti, 2005)

During the vane shear test, the vane is immersed in the material that undergoes yielding; the material yields within the body of the material and not as a solid boundary, and therefore overcomes slip. A vane works best as there is less disturbance of the sample when inserting the vane, compared to the conventional measuring geometry. Nguyen and Boger (1985) and Barnes (1995) mentioned that, in the vane technique, the stress to initiate flow from a vane immersed in the sample to be tested is measured. Steffe (1996) specify the limits of the vane and vessel dimensions as:

- Ratio of the vane length (h_v) to vane diameter (d_v) should lie within 1.5 and 4.0, i.e. $1.5 \geq h_v/d_v \geq 4.0$
- Depth of the vane surface from the surface of material (Z_1) can be 0, or the ratio of Z_1 to the diameter should be greater than 1.0, i.e. $Z_1 = 0$ or $Z_1/d_v \geq 1.0$ (the yield stress computation would differ accordingly).

- Ratio of the height of vane from bottom of cup (Z_2) to vane diameter (d_v) should be greater than 0.5, i.e. $Z_2/d_v \geq 0.5$. The ratio ensures that the end effects at the top and bottom of the vane are negligible.
- The vane blades are assumed to be infinitely thin to avoid complications in yield stress computations (Nguyen & Boger, 1992; Atkinson & Sherwood, 1992; and Barnes & Nguyen, 2001).

If the vane is completely immersed in the sample, $D/d_v > 2.0$, where D is the diameter of the container. "The vane is then rotated very slowly at a constant low speed (1.0 rpm) as low as possible, and the torsional moment required in maintaining the constant motion of the vane is measured as a function of time (or angle of rotation)" (De Kee et al., 2004). For materials having yield stress with a typical torque-time curve (See Figure 2.12), as the vane rotates from rest, the region of the suspension close to the edges of the vane blades would deform elastically, as shown by the linear part of the torque-time response. The material between the blades moves along with the vane. Such linear behaviour may be attributed to the mere stretching of the "network bonds" interconnecting the structural elements. Since more bonds would be stretched and the resistance to more deformation increase as the vane's rotation continues, the torque required to keep the motion constant must also rise.

Breaking of the already stretched bonds would eventually occur, even though in a gradual manner, as shown by the curved part following the linear region in the torque-time response (Nguyen & Boger, 1983).

Finally, when the majority of the network bonds have been broken, the network would collapse and the material may be said to yield microscopically.

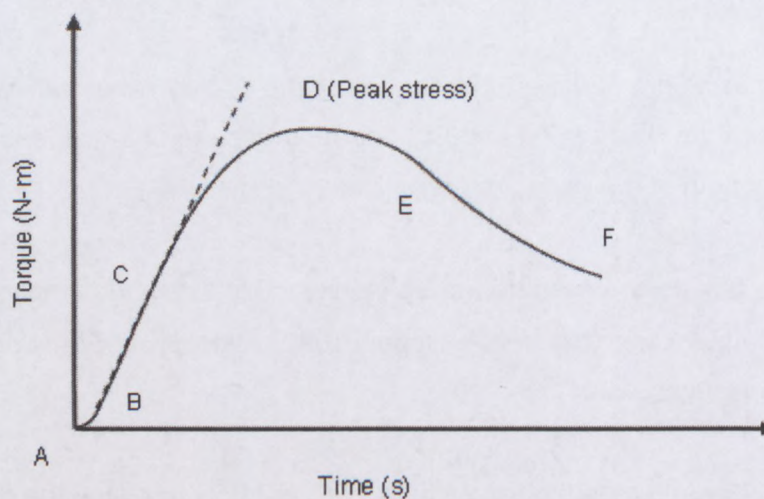


Figure 2. 12: Typical torque-time response (Adapted from Alderman et al., 1991)

Nguyen and Boger (1985) used vanes with four blades (see Figure 2.11 and Figure 2.12) and Qui and Rao (1988) used vanes with six and eight blades and they all produced similar results.

2.12.3 Merits and limitations on the use of vane geometry

Barnes and Nguyen (2001) emphasised the increasing popularity of the vane technique in their review paper on rotating vane rheometry. Some of the merits of using the vane rheometer have been discussed elaborately with emphasis on various fields, where the vane technique has been adopted due to these advantages (Barnes & Nguyen, 2001).

2.12.3.1 Merits

- Elimination of wall-slip effects. (Nguyen & Boger, 1983; Yoshimura et al, 1987; James et al., 1987; Nguyen & Boger, 1992; and Barnes & Nguyen, 2001).
- Yielding surface or the shear surface is present within the material, which eliminates wall depletion (slip).
- Minimum disturbance to the sample. Thin blades of the sensitive network developed in a material, which is significant when testing weak gels, thixotropic materials, or foam-like materials (Tran & Glumac, 2002; Banfill, 2003; Stokes et al., 2005; and Bagdassarov & Pinkerton, 2004).

- Larger gaps provide fewer problems occurring due to particulate material and reduces viscous heating greatly compared to bob and cup (Barnes, 1999; Barnes & Nguyen, 2001; Ancy, 2003; Krulis & Rohm, 2004; and Stokes & Telford, 2004 & 2005).
- Quick single-point determination of yield stress (Nguyen & Boger, 1983; Nguyen & Boger, 1992; and Barnes & Nguyen, 2001)
- Higher shear rates can be obtained than with cone and plate and coquette geometry due to minimum slip and larger surface area (Garrido et al., 2003).
- Larger surface area – The technique of matching viscosities provides less error for geometries with larger surface areas and thus can be used with vane geometry with higher numbers of blades (Rao & Cooley, 1984).
- Can perform in situ yield stress measurements (Nguyen & Boger, 1983 and Carozza et al., 2000).
- Simple attachment, easily fixed to an existing rheometer (Barnes & Nguyen, 2001).
- Simple sample preparation (Truong et al., 2002).
- Simplicity of fabrication (Barnes, 1995; and Nguyen, 2001)
- Simple to clean (Barnes, 1995 and Barnes & Nguyen, 2001).

2.12.3.2 Limitations

- At high rotational speeds there is the possibility of the development of secondary flow behind the vane and slip (Barnes & Carnali, 1989; Barnes, 1995; Barnes, 1999; and Zhu et al., 2001).

- With low viscosity fluids as the inertial effects become more prominent this will create vortices (Macosko, 1994). -The dissipation of energy associated with the vortices would indicate a higher viscosity (Barnes & Nguyen, 2001 and Barnes & Bell, 2003).
- When the end effects are prominent – End effects in couette geometry are avoided by modifying the bob's contour which cannot be used with the vane due to the constraints of vane geometry (Barnes & Carnali, 1989).
- When materials containing a high measure of particulate matter – The vane is not very reliable when assessing non-Newtonian high measures of solids even at very low shear rates (Nguyen and Boger, 1983).
- With expensive samples – Larger gaps require higher amounts of sample which is not preferable with expensive materials (Deepti, 2005).

2.12.4 Assumptions for the vane technique

A summary of the assumptions for the vane technique follows (Yan & James, 1997; Stokes & Telford, 2004; Nguyen & Boger, 1983 & 1985; and Nguyen & Boger, 1992).

- The vane forms a rigid cylinder with the material trapped within the blades.
- The material trapped within the blades rotates along with the vane during rotation, and hence no secondary flow occurs between the blades.
- The yield surface has a cylindrical shape.
- The stress distribution is uniform over the surface of the vane cylinder.
- The vane geometry is considered to be two-dimensional since the vane length is assumed to be infinitely long.

2.12.5 Experimental studies validating the vane technique

The observation of slip effects in yield stress measurement with rotating cylinder viscometers led several researchers to investigate the use of the vane geometry. As seen in Figure 2.10, the four thin-bladed vanes arranged at equal angles around a small cylindrical shaft is used as a relative measurement of the yield stress value with the stress relaxation method by Russell (1939) and Hobson (1940) in the constant shear rate experiment. They suggested that there was no direct relationship between the quantity measured and the true rheological yield stress. Keentok (1982), following his work on the measurement of yield stress using an instrol 3250 rheometer, affirmed the ideal that a vane device can be used for yield stress measurement.

Nguyen and Boger (1983) used four established techniques for determining the yield stress of red mud and established that the quantity measured with the vane technique is a true material property that is independent of the vane dimensions and rotational speeds. The indirect measurements of the yield stress were found to suffer certain drawbacks since the accuracy involved was largely dependent on the availability and accuracy of the rheological data at low shear rates. The results obtained also demonstrated that the quantity measured with the vane technique is identifiable with the true yield stress, especially in highly concentrated systems.

From the work of Yoo, Rao & Steffe, (1995) the vane technique was used to measure yield stresses of 15 commercial food dispersions under controlled shear stress and controlled shear rate operating conditions. Magnitudes of yield stress at controlled shear stress were higher than those of yield stresses at controlled shear rates for tomato products and baby foods. There were good linear correlations ($R^2 = 0.96, 0.86$) for food dispersions with undisturbed structure (UDS) and with broken down structure (BDS) (Yoo, Rao & Steffe, 1995).

Yoshimura et al., (1987) presented yield stress measurements on a series of model oil-in-water emulsions using three different techniques and obtained reasonable agreement among the three techniques, with no one technique consistently giving higher or lower values for the yield stress than when compared to the other techniques.

Sherwood and Meeten (1991) used a complex variable technique to calculate torque on an infinitely long two-bladed vane. They then computed the torque on a series of N-bladed vanes of finite length by means of a boundary integral technique. They predicted the effect of the ends of the vane on the torque. Their prediction worked very well.

Nguyen et al. (2005) evaluated the reliability and reproducibility of several common yield stress measuring techniques employed at six different laboratories and with different instruments, and suggested that the measured yield stress varies with both the technique and the operator.

However, when their results were properly analysed, certain consistent trends emerged and helped to identify the factors that affect practical yield stress measurements. Among the different techniques employed, direct techniques were found to produce more reliable and repeated results than indirect results which rely on extrapolation from shear viscosity data. Of the direct techniques, the techniques specially designed to determine the yield stress under static conditions and independent of conventional rheological measurements gave the most consistent yield stress values with lowest deviations among different laboratories.

2.12.6 Numerical studies on vane technique

2.12.6.1 Rigid cylinder concept

The vane and material held within the blades develop into a cylindrical body upon rotation. The cylindrical body is called a "rigid cylinder" with the yielding surface equivalent to the cylindrical surface of the vane (Keentok, 1982; Liddel & Boger, 1996; Gardiner et al., 1998; Barnes, 1999; and Stokes & Telford, 2004). The rigid cylinder behaves similarly to that of a bob in the coquette geometry (see Figure 2.13). Nguyen & Boger (1992); Maia & Covas (1998) and Keentok, Milthorpe & Donovan (1985) used the finite element technique to analyse the stress distribution of vane rotation in a Bingham Plastic model fluid for three different vanes with two, three and four blades. The results for the two- and three-bladed vanes were slightly irregular, but the yield surface for a four-bladed vane was approximately cylindrical. Photographs of a transparent Bingham liquid confirmed the occurrence of a cylindrical yielding surface, strengthening the rigid cylinder assumption (Keentok, Milthorpe and Donovan, 1985). Yan and James (1997) also conducted finite element analysis on Herschel-Bulkley and Casson materials. A mesh that was considerably finer than that used

by Keentok, Milthorpe & Donovan, (1985) was used to analyse the yielding surface. The strain in the fluid occurred only at the edges of the vane and nowhere inside the rigid cylinder (Yan & James, 1997). The rigid cylinder is a valid concept and has been accepted by numerous researchers (Barnes & Carnali, 1989; Liddell & Boger, 1996; Yan & James, 1997; and Barnes, 1999).

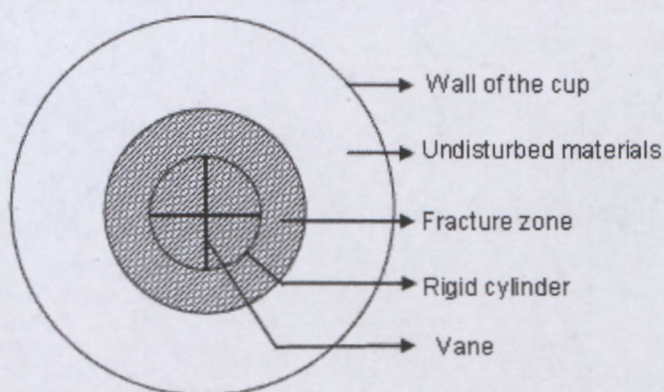


Figure 2. 13: Deformation Zone

2.12.6.2 Deformation zone concepts

The flow behaviour when using a vane has been studied by researchers considering materials of different behaviours (Barnes & Carnali, 1989; Keentok, Milthorpe & Donovan, 1985; Glenn III, Keener & Daubert, 2000; and Sherwood & Meeten, 1991). The studies proved the validity of the "rigid cylinder concept", but also brought into light the fact that a finite area beyond the rigid cylinder observes some movement due to the vane rotation. Hence the concept of a deformation zone was developed which indicated that the diameter of the affected area due to vane rotation is larger than the rigid cylinder (vane) diameter. The implementation of the vane diameter in the computations of the shear strength in such cases would lead to a magnified value (Oslen, 1999). The shaded area in Figure 2.12 represents the deformation area.

Keentok, Milthorpe and Donovan (1985) demonstrated the presence of a deformation zone using viscoelastic greases and gelatine gels which exhibited the Herschel-Bulkley behaviour.

Keentok, Milthorpe and Donovan (1985) and many other researchers refer to the deformation zone as the “fracture zone”. This zone is the affected area surrounding the vane when the vane is rotated in the material until fracture. The ratio of the fracture zone diameter to the vane diameter $\left(\frac{d_f}{d_v}\right)$ was estimated to be approximately 1.05 for greases, while, for gelatine gels, the ratio was approximately 2. The shear surfaces of gelatine gels were found to be approximately cylindrical. An attempt was made to establish a relation between the ratio of yield stress and

viscosity of the fluids $\left(\frac{\tau_y}{\eta}\right)$ and the ratio $\left(\frac{d_f}{d_v}\right)$; however, no conclusive results could be obtained. Numerical simulations were also performed as an analytical support to the observed behaviour and the $\left(\frac{d_f}{d_v}\right)$ value thus obtained was 1.025 for greases (Keentok, Milthorpe & Donovan, 1985).

Yan and James (2000) conducted a study on the stress distribution in a vane-in-cup geometry with a power law fluid which confirmed that the material around the circular circumference of the vane participated in the movement due to vane rotation (Yan & James, 1997; and Barnes & Carnali, 1989). An enhanced numerical approach to the stress profile of the region around the vane blades agreed with the fracture zone concept (Yan & James, 1997). The concept of a fracture zone is believed to exist, thus knowledge of the fracture zone is necessary in order to determine the actual strain in the material (Carozza, Servias & Roberts, 2000).

Olsen (1999) saw the fracture zone diameter as the effective cutting diameter of the vane, and the cutting diameter for clay was observed to be much larger than the vane cylinder (Olsen, 1999). Troung and Daubert (2001) observed a distinct fracture zone area when testing tofu and gellan gums with the vane rheometer. The extent of the fracture zone depends upon the material being tested and the rotational speed. A more solid-like material or a higher rotational speed would cause a larger fracture zone (Ancy, 2003 and Keentok, Milthorpe & Donovan, 1985).

Thus, the vane technique is not a very appropriate fundamental technique due to the ambiguity in computing the actual strain (Troung & Daubert, 2001). Therefore, to overcome

the uncertainty caused by the fracture zone, the implementation of a correction factor involving the extent of fracture zone in the stress computations has been suggested (Keentok, 1982; Keentok, Milthorpe & Donovan 1985; Glenn III et al., 2000; and Troung & Daubert, 2001 & Troung et al., 2002).

2.12.6.3 Yielding and formation of deformation zone

The following discussion gives a brief description of yielding and formation of the deformation zone within a vane-in-cup rheometer. The area between the vane cylinder and cup wall is generally referred to as a gap, as illustrated in Figure 2.14. The flow of material observed in the gap when the vane is subjected to rotation, is more complicated and the stress distribution is more non-uniform than in simple bob-in-cup geometry (Nguyen & Boger, 1985; Yan & James, 1997 and Stokes & Telford, 2004).

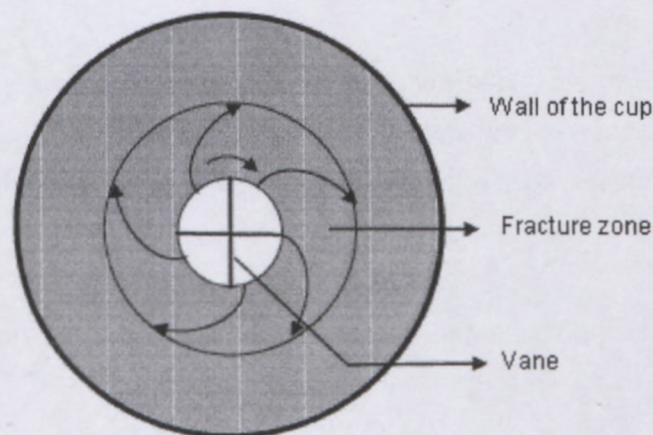


Figure 2. 14: Flow in gap (Adapted from Deepti, 2005)

The shear stress decreases with distance from the vane cylinder, but the stress within the cylinder increases from the centre of the vane to the vane edge, as shown in Figure 2.15. Accordingly, the maximum value of stress is observed at the cylindrical surface of the vane. The finite element analysis of the stress distribution for the present scenario determined that the stress peaks at the tips of the vane (Nguyen & Boger, 1985; Yan & James, 1997 and Stokes & Telford, 2004).

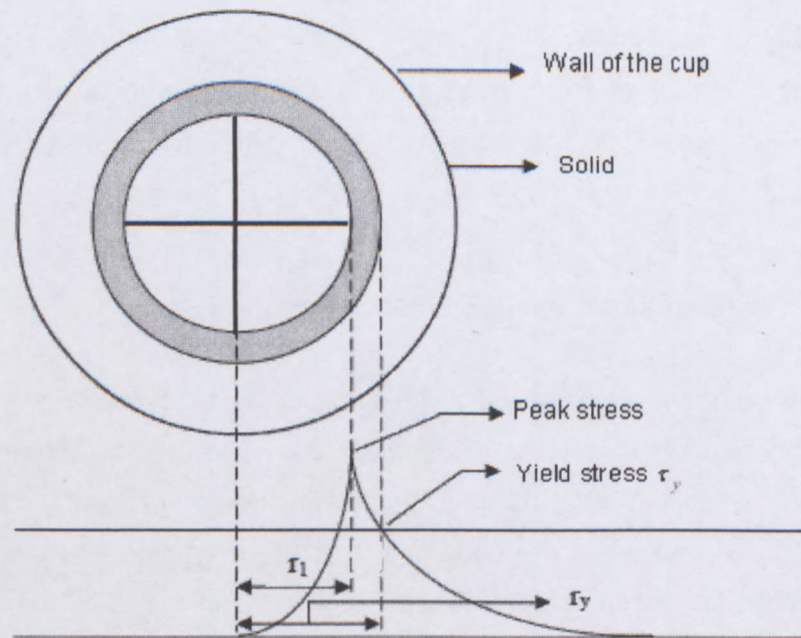


Figure 2. 15: Torque – time response (Adapted from Yan & James, 1997)

Until the stress at the vane tips is lesser than the yield stress, no flow is observed in the gap. When the peak stress exceeds the yield stress, yielding of material is observed at the tips of the vane. Yielding is observed throughout the vane cylinder only on further rotation of the vane.

Thus, at complete yielding, the peak stress observed will be the yield stress. As stated earlier, the stress decreases radically from the vane cylinder.

Consequently, the yield stress of the material is observed at complete yielding within the gap, at a point closer to the vane. A layer of material entrapped between the vane cylinder and the point of yield stress observation experiences a stress greater than the yield stress. This layer is the deformation zone and terminates at a point where stress lower than the yield stress occurs (Zhang & Nguyen, 1996; and Yan & James, 1997). Thus the yielding layer of the cylinder is a layer of fluid trapped between two solid layers of material between the blades and the material past the fracture zone. The width of the yielding layer depends on the shear rate and the material (Gebhard, 1994 and Yan & James, 1997).

Though the concept of stress peaking at the vane tips has been proven, the yield stress computations are based on the assumption that the stress observed throughout the entire

vane cylinder is uniform. Materials become non-linear at the tips of the vane but the total torque measured is affected only when the non-linearity is considerable (Alderman, Meeten & Sherwood, 1991). Yan and James (1997) used numerical approximations to prove that the assumption of a cylindrical yielding surface is applicable to various types of fluids, while Nguyen and Boger stated that the assumption is valid only at the moment of yielding (Nguyen & Boger, 1983 & 1985; Yan & James, 1997; Pernell, Foegeding & Daubert, 2000 and Glenn III, Keener & Daubert 2000). After yielding, the material fractures and hence the assumption does not prevail. Furthermore, for shear-thinning liquids, the flow in the gap is found to be similar to that observed in concentric-cylinder geometry (Barnes, 1997). Therefore, most vane rheometry computations exclude the concepts of stress distribution and the fracture zone of the vane rheometer in spite of the prominence of the theories (Sherwood & Meeten, 1991, and Barnes & Nguyen, 2001).

2.12.7 VANE RHEOMETRY CALCULATIONS

The computation of yield stress using the vane rheometer is based on the geometry of the vane. The following specifications have been established for the positioning of the vane during experimentation. (Nguyen & Boger, 1983 & 1985; Liddell & Boger, 1996; and Steffe, 1996). See page 2.21, Figure 2.10 and Figure 2.11.

The total torque (M_o) required to surmount the yield stress of the fluid can be broken down into two parts:

- (1) the torque (M_C) required for the vane's cylindrical surface,

$$M_C = \left[(\pi d_v h_v) (\tau_y) \right] \left[\frac{d_v}{2} \right] = \frac{\pi h_v d_v^2}{2} \tau_y \quad 2.8$$

In the expression above, $(\pi d_v h_v)$ represents the area of stress application (cylindrical surface area), and $\frac{d_v}{2}$ is the distance from the point of force application to the vane's cylindrical surface (radius of the vane, R_v).

- (2) the torque (M_h) required for the upper and lower horizontal surfaces of the vane:

$$M_h = 2 \int_0^{\frac{D_v}{2}} 2\pi r^2 dr \tau_e \quad 2.9$$

where τ_e is the shear stress on the vanes. The area of stress application (upper and lower horizontal surfaces of the vane) is represented by $2\pi r^2$.

Assuming τ_e varies with the radius (r) according to a power-law relationship,

$$\tau_e = \left(\frac{2r}{d_v} \right)^m \tau_y \quad 2.10$$

Substituting the vane of τ_e in Equation 2.9:

$$M_h = 4\pi r \int_0^{\frac{d_v}{2}} 2 \left(\frac{2r}{d_v} \right)^m \tau_y dr \quad 2.11$$

$$= \frac{2^m (4\pi \tau_y)}{d_v^m} \int_0^{\frac{d_v}{2}} r^{2+m} dr \quad 2.12$$

Substituting $r = d_v/2$:

$$M_h = \frac{2m + 2\pi \tau_y}{d_v^m} \frac{\left(\frac{d_v}{2} \right)^{3+m}}{3+m} \quad 2.13$$

$$= \frac{\pi \tau_y d_v^3}{2(3+m)}$$

Hence, the total torque can be determined as

$$M_o = M_c + M_h \quad 2.14$$

$$M_o = \frac{\pi h d_v^2}{2} \tau_y + \frac{\pi \tau_y d_v^3}{2(3+m)} \quad 2.15$$

$$= \frac{\pi \tau_y d_v^2}{2} \left(h_v + \frac{d_v}{3+m} \right) \quad 2.16$$

$$= \frac{\pi \tau_y d_v^3}{2} \left(\frac{h}{d_v} + \frac{1}{m+3} \right)$$

Re-writing the above expression, the yield stress of the material (τ_y) can be determined as

$$\tau_y = \frac{2M_o}{\pi d_v^3} \left(\frac{h_v}{d_v} + \frac{1}{m+3} \right)^{-1} \quad 2.17$$

Substituting “m” as zero is usually satisfactory and errors in using Equation 2.17 for $m > 1$ decreases with larger values of $\left(\frac{h_v}{d_v} \right)$. If $m = 1$, errors $\leq 3.7\%$ may be obtained with $\left(\frac{h_v}{d_v} \right) > 2$ (Barnes, 1999). Conventionally, “m” is assumed to be zero.

Equation 2.17 is valid when $\frac{Z_1}{d_v} \geq 1.0$, while, when $Z_1 = 0$ the yield stress computation is

$$\tau_y = \frac{2 M_o}{\pi d_v^3} \left(\frac{h_v}{d_v} + \frac{1}{6} \right)^{-1} \quad 2.18$$

Various researchers used Equation 2.17 in different forms (Nguyen & Barnes, 1983; Yoshimura et al, 1987; Nguyen & Boger, 1992; Lidell & Boger, 1996; Troung, Daubert, Drake & Baxter, 2002 and Stokes & Telford, 2004). For example, Barnes and Nguyen (2001) also calculated the stress from the peak torque observed. The total torque (M_o) was computed as the sum of the torque on the cylindrical surfaces (M_c) and the horizontal edges (M_h) of the cylinder. However, M_c and M_h were defined as follows:

$$M_c = 2\pi \tau_y h_v R_v^2 \quad 2.19$$

$$M_h = \frac{4\pi \tau_y R_v^3}{3} \quad 2.20$$

The total torque according to Equation 2.14 would be

$$M_o = (2\pi h_v R_v^2) \tau_y + \left(\frac{4\pi h_v^3}{3} \right) \tau_y \quad 2.21$$

$$= 2\pi R_v^3 \tau_y \left(\frac{h_v}{R_v} + \frac{2}{3} \right) \quad 2.22$$

Re-arranging the above equation, the yield stress would be calculated as

$$\tau_y = \frac{M_o}{2\pi R_v^3} \left(\frac{h_v}{R_v} + \frac{2}{3} \right)^{-1} \quad 2.23$$

Sherwood and Meeten (1991) calculated the torque for a two-bladed vane to be

$$M = 2\pi d_v^3 \mu \Omega (I + 0.66), \quad 2.24$$

where μ is the viscosity of sample, Ω is the vane's angular velocity. i.e. $d\theta/dt$, and $I = \frac{h_v}{R_v}$

The torque per unit length on an n-bladed vane of infinite length is indicated as

$$M = 2\pi d_v^2 \mu \Omega (2 \cdot 2^{n-1}) \quad 2.25$$

A vane with an infinite number of blades is equivalent to a solid cylinder (Sherwood & Meeten, 1991; and Atkinson & Sherwood, 1992).

Equation 2.18 has been used in this work.

2.13 THE SLUMP TECHNIQUE AND MODELS

One of the simpler techniques for the single-point measurement of the yield stress is to use slump. The civil engineering community has used a conical device for measuring the slump and workability of concrete for many years (Boger et al., 2008). It is believed that it was first used by

Chapman (Bartos, Sonebi & Tamini, 2002). However, such a single value workability test has been criticised on the basis that the same value may be produced by two concretes with quite different rheological characteristics (Tattersall & Bloomer, 1979; Tattersall & Banfill, 1983 and Tattersall, 1991).

In the concrete industry the dimensions of the cone geometry are 300 mm in height, with top and base diameter of 100 mm and 200 mm respectively (ASTM C 143 and SABS, 1994 etc). The Australian standard dimensions are 150 mm in height, with top diameter of 50 mm and base diameter of 100 mm (AS2701.5). There is no standard for the cylinder geometry. Yield stress measurements using the cylinder geometries are used in addition to the ASTM standard cone slump test.

Pashias et al., in 1996 published their paper on the hand-held cylinder. The hand-held cylinder is a stainless steel pipe of size 73 mm diameter by 75 mm high. Using the cylinder, they successfully measured the yield stress of three different mineral suspensions (titanium dioxide zirconia dioxide and bauxite residue). In addition Hallbom, 2005 and Haldenwang et al., 2007 used the same geometry (cylinder). Hallbom, 2005 tested tailings and Haldenwang, et al., 2007 tested kaolin suspension, laponite solution and kaolinite tailings.

In the tests conducted by Clayton et al., in (2003), using the Australian Standard (AS 2701.5) the yield stresses of numerous mineral tailing pastes were measured. The cone geometry dimensions used were 150 mm in height, with top diameter of 50 mm and base diameter of 200 mm. The cylinder geometry dimensions used were 102 mm in height and 102 mm diameter. As there was no standard for the cylinder test, the cone test methodology was adapted for the cylinder test. The vane technique was used as a reference and related models (cone and cylinder) were compared to yield stress values determined by using the vane technique. Their analysis shows that the cylinder model more accurately predicted the material yield stress than the cone model. They also made a strong case for the replacement

of the generally used cone test with the “simpler and cheap” as well as more accurate cylinder test.

Saak et al., 2004, measured the slump test of cement paste, ceramic suspension and clay using the cone and cylinder. The dimensions of the cone and cylinder used were 50 mm and 75 mm in height with diameter of 26 mm and 45 mm respectively. The results from the cone slump tests were plotted using the cone and the cylinder model. They included the Pashias et al., 1996 data in the results. All the data did not fit the cone model. The cylinder model and cone model relating slump to yield stress were used in the dimensional analysis of their results. The results indicate that the cylinder model fits the experimental data for cylinder slump test over a wide range of yield stress values for a variety of materials, including cement paste, clays, and ceramic suspensions (Saak et al., 2004).

Roussel et al., in 2005 investigated the flow induced by a smaller cone test for cement pastes and grouts. The dimensions of the cone geometry used were 50 mm in height and with a diameter of 50 mm. The experimental results of several cement pastes validate the obtained relation but also show the necessity to take into account the surface tension effects for low yield stress materials. The modified relation allows the prediction of the plastic yield stress value from the measured spread (Roussel et al., 2005).

Rheologists have adopted the slump test technique in order to measure the flow property of a highly flocculated fluid. This indirect test (slump test) removes the usage of complex equipment that is used to measure the yield stress (Sofra & Boger, 2000). The yield stress increases exponentially with solids concentration (Boger, 2006), so a small change in concentration can result in a large change in the yield stress. As the slump test estimates the workability of fresh concrete, which determines how the final strength of concrete will be, Ritcey (1989) compared this with the flow properties of tailings in a waste disposal scheme, which needed to be tailored for the angle of repose. Therefore, the slump test finds extensive industrial application for monitoring material consistency in flocculated suspensions (Pashias et al., 1996), used in surface and underground tailings disposal operations in which the dilute tailings produced in processing are concentrated into a high solids concentration for disposal (Clayton et al., 2003). A result of the highly concentrated nature of the tailings is the presence of an appreciable yield stress, which is the minimum shear stress for irreversible deformation and flow to occur.

Figure 2.16, illustrates the traditional technique of measuring the slump height.

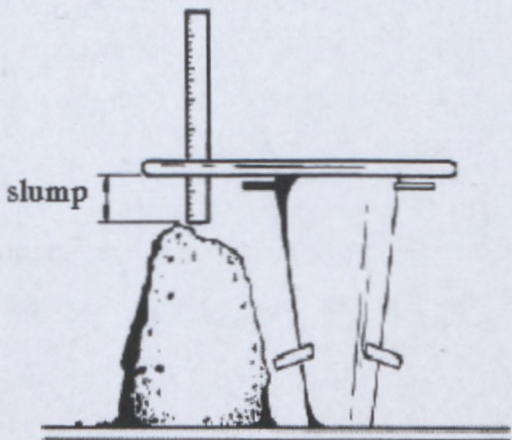


Figure 2.16: Slump measurement

When performing a slump test, a frustum is filled with the material to be tested. It is then lifted, allowing the material to collapse.

The removal process should be performed 5 s to 10 s by a steady up-ward lift being careful not to twist the cone or remove it in a lateral direction (SABS 862-1, 1994). For a 300 mm cone this amounts to a 30 - 60 mm/s test. The entire test, from moulding to demoulding, should be carried out within 150 s.

The slump test process using the cone geometry is explained as shown in Figure 2.17 (Clayton et al., 2003).

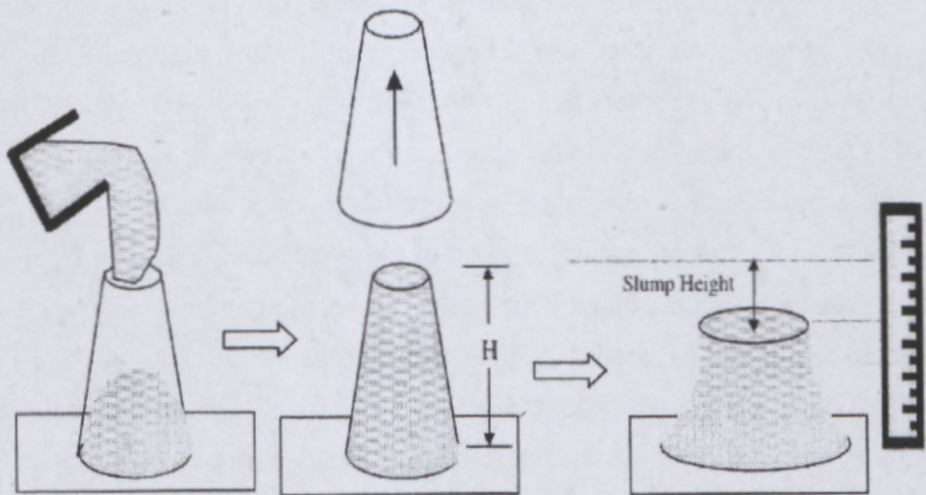


Figure 2.17: Schematic diagram of the cone slump test (Adapted from Clayton et al., 2003).

Tanigawa and Mori, (1989) and Tanigawa, Mori & Watanabe (1991) performed measurements of the slump as a function of time. They found that the slump-time curve could be simulated by finite element analysis of the fresh concrete assuming it to be a Bingham material. "The slump-time curve depends on both the yield stress and the plastic viscosity" (Ferraris & Francois, 1998).

Since the final slump is related directly to the yield stress, it is reasonable to assume that the time-dependence of slump is likely to be controlled by the plastic viscosity (Ferraris & Francois, 1998).

The slump is the difference between the height of the mould at the beginning of the test and after flow stoppage, with the spread being the final diameter of the collapsed sample (Schowalter & Christensen, 1987). The point where the slump is measured is important because the top of the slumped materials is not an even surface. Concrete slump measurements are taken at the highest point of the slump cone (SABS, 1994; ASTM C-143, 1996; etc). In the tests conducted by Pashias et al., (1996), the middle point of the slump height was measured. Height is measured to the nearest 0.5 mm. The heights were measured at various intervals over a one-hour period. No measurable difference was detected. Various surfaces were used; these ranged from rubber, smooth wood, rough wood and stainless steel. Little discrepancy was found. They argued that the measurement is insensitive to the type of suspension being tested. Density and concentrations are also measured at the time of testing.

Gawu and Fourie in 2004 investigated the yield stress using tailings (zinc, gold and mineral sand tailings). Yield stress at varying solids concentrations were determined using three different techniques, i.e, the modified slump test with an open-ended cylinder having an aspect ratio of 1.2, the vane technique and controlled stress rheometer. In the test conducted by Gawu and Fourie in (2004), an average of the three lowest points of the slump was used to determine the accuracy and precision of the position of slump. The results were graphically compared with those obtained using the vane technique. They found that the observed relations appeared to predict better yield stress results up to 200 Pa when compared with the vane technique and the rheometer results. From the work of Gawu and Fourie in 2004, they showed that, the tailings tested induced errors as much as $\pm 30\%$ for some samples. Yield stress versus solids concentration results for the zinc and gold tailings were obtained. Zinc tailings showed excellent correlation between the range of 53% and

62% solids concentration, beyond which there is more divergence of the results. They argued that the major difference in the vane results at higher solid concentrations compared with both the controlled stress and slump test results were due to shear history, even if slip was obvious with the controlled stress test results. For the gold tailings, good agreement exists up to approximately 350 Pa yield stress (Gawu and Fourie, 2004).

In the tests conducted by Pashias et al., in (1996), the cylinder frustum was lifted at various speeds with the support of a variable speed motor and pulley system. Velocities from 0.1 to 30 m/s were tested. They found that, the velocity with which the cylinder frustum is lifted has no effect on the final slump height. It is not clear how stable the lifting device was.

Except for Pashias et al., 1996, most of the cones and cylinders used were lifted by hand. The aim of this work is to verify within a certain range, the effect of lift speed in a stabilised lifting device on the value of yield stress.

2.13.1 Relationship between slump height and yield stress

Several attempts to relate slump to yield stress can be found in the literature. Murata (1984) and Schowalter and Christensen (1998) recorded a relationship between slump and yield stress by assuming that the cone could be divided into two parts. In the upper part, the shear stress does not reach the yield stress and no flow occurs. In the lower part of the cone, the shear stress induced by the self-weight of the material is higher than the yield stress and flow occurs. The height of the flowing lower part decreases until the shear stress in this zone becomes equal to the yield stress, after which the flow stops. Schowalter and Christensen (1998) indicated a relation between the final total height of the cone and the yield stress that did not depend on the mould geometry or cylindrical geometry (Pashias et al., 1996) from similar assumptions. This relation or similar ones were successfully validated by Clayton et al. (2003) and Saak et al., (2004) in the case of cylindrical moulds. However, in the case of conical moulds, a discrepancy between predicted and measured slumps was consistently obtained (Roussel, Stefani & Lery, 2005).

The above advance relationship relating slump to yield stress most likely does not apply since, in general, there apparently is no undeformed region for the large slumps and the spread seems to be a more important parameter for estimating the material yield stress (Coussot et al., 2002b and Domone, 1998). Extending a two-dimensional solution, Liu and

Mei (1989) wrote a solution for this spreading problem for a yield stress fluid. Their approach was based on the assumption that the depth of the fluid layer is everywhere much smaller than the characteristic length of the solid-liquid interface (Russel, 2006).

2.13.2 The slump models

The model used for measuring the yield stress from a conical slump was first undertaken by Murata in 1984 and was later corrected by Schowalter and Christensen (1998) to evaluate the workability and consistency of fresh concrete. It was adopted by Pashias et al. (1996) for a cylindrical geometry because of its simplicity. The cylinder model is generalised for cylinders of any size, whereas the cone model is detailed for a cone with a base diameter twice that of the top diameter.

The reliability of different models adapted by Pashias et al. (1996) and Haldenwang et al. (2007) using more established techniques, like the vane technique as a control (Haldenwang et al., 2007) observed greater effect of the model used.

2.13.2.1 The cone model

The slump test is the measurement of the amount of final deformation of the sample due to its own weight as shown in Figure 2.18. In most comparisons found in the literatures, the results are expressed in terms of dimensionless variables to enable generalisation of the slump model for sized geometries and different yield stress materials. The dimensionless variables are defined as follows:

$$\tau'_y = \frac{\tau_y}{\rho g H} \quad 2.27$$

$$s' = \frac{s}{H} \quad 2.28$$

$$h'_o = \frac{h_o}{H} \quad 2.29$$

$$h'_1 = \frac{h_1}{H} \quad 2.30$$

where s' dimensionless slump height

τ'_y dimensionless yield stress

h'_0 dimensionless height of undeformed region

h'_1 dimensionless height of deformed region

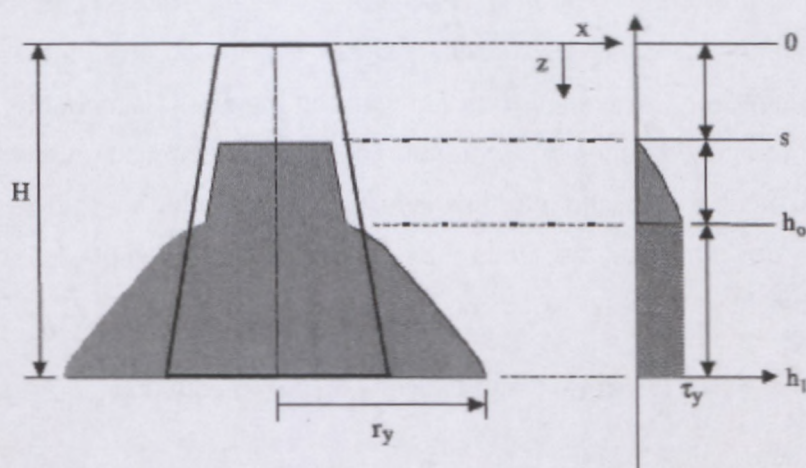


Figure 2. 18: Slump of a material after the cone is lifted and associated stress distribution
(Adapted from Clayton et al., 2003; and Saak et al., 2004).

Figure 2.18 illustrates that, at some point h'_0 along the height of the undeformed cone, the material experiences a stress that is larger than the dimensionless yield stress and the material slumps until the stress is reduced to the dimensionless yield stress. In Figure 2.18 above the vertical stress does not exceed the yield stress and the region remains yielded. In the slumping process, it is assumed that the interface layer between the yielded and unyielded material is a horizontal surface that moves down as the material beneath it slumps (Clayton et al., 2003; Saak et al., 2004; and Fourie & Dunn, 2007). Therefore, the final height consists of an unyielded region and a yielded region (Clayton et al., 2003).

In the tests conducted by Saak et al., 2004, they showed that results from the cone tests do not fit the cone model but instead follow the cylinder slump model at low yield stress values. At high yield stresses, the data deviated from the cone model as filling the slump cone becomes difficult and large air voids are present (Saak et al., 2004). They finally concluded that the yield stress of cement paste measured with a vane and cylinder model displayed an

excellent agreement. Their results agreed with Pashias et al's, 1996 findings using the cylinder model.

2.13.2.2 The cylinder model

The cylinder model basically has been adapted from the cone model. The analysis of the cone model by Schowalter and Christensen (1998) was used to develop this model. Pashias et al. (1996) used the cone model to develop a simple relationship between the dimensionless slump and the dimensionless yield stress; their theoretical models are derived from a relationship between the pressure distribution and the stress distribution in a vertical cylinder composed of an incompressible material. The model assumes that all the horizontal planes remain horizontal, that is, the interface layer between yielded and unyielded material remains flat. In this development, the amount by which a cylinder sample height is reduced from the original height is referred to as the slump height h (Figure 2.19). Dimensionless

slump height $\left(\frac{h}{H}\right)$ is related to the yield stress by the following equation:

$$\frac{h}{H} = 1 - \left(\frac{2\tau_y}{\rho g H}\right) \left[1 - \ln\left(\frac{2\tau_y}{\rho g H}\right)\right], \quad 2.34$$

where: h = slump height (m)

H = original height of the sample (m)

τ_y = Yield stress (Pa)

ρ = Density of the sample (Kg/m^3)

g = gravitational acceleration (m/s^2)

So, for simplicity, a dimensionless yield stress may be defined as

$$\tau'_y = \frac{\tau_y}{\rho g H} \quad 2.35$$

Using this definition, equation 2.34 becomes

$$\frac{h}{H} = 1 - 2\tau_y \left[1 - \ln(2\tau_y)\right] \quad 2.36$$

The $\ln(2\tau'_y)$ term may be expressed as an infinite series, for $0 \leq \tau_y \leq 1$, as,

$$\ln(2\tau'_y) = (2\tau'_y - 1) - \frac{1}{2}(2\tau'_y - 1)^2 + \frac{1}{3}(2\tau'_y - 1)^3 - \dots$$

Using the first two terms of the above series, a simplified form of equation 2.36 may be written as

$$\frac{h}{H} = 1 - 4(\tau'_y)^3 + 8(\tau'_y)^2 - 5\tau'_y \quad 2.37$$

Equation 2.36 will be used to evaluate the data generated in this study.

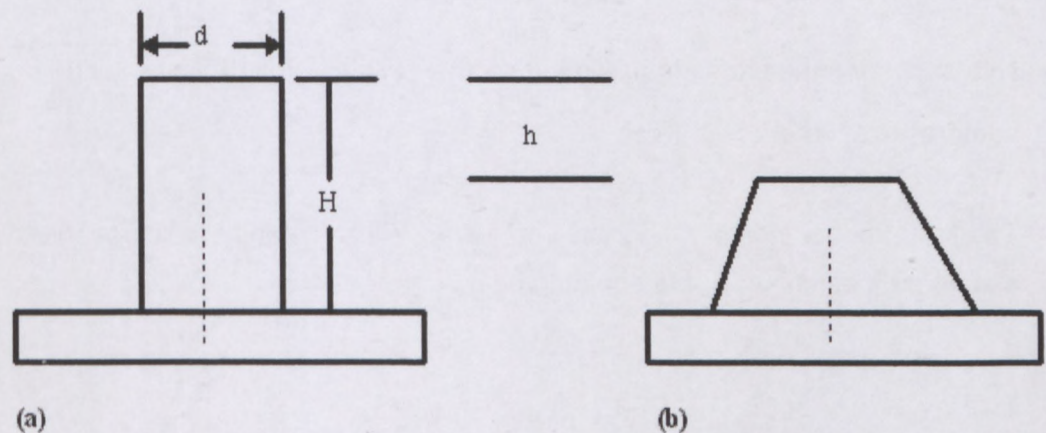


Figure 2. 19: Sample before (a) and after (b) slump test (Adapted from Omura & Steffe, 2001)

The model for calculating the yield stress from the conical slump was devised by Murata (1984). Despite problems with the physical model, the cylinder model work as a semi-empirical model and provides reasonable predictions for the yield stress at medium to high slumps (Hallbom, 2005).

2.13.2.3 Lump model

The lump model (Hallbom, 2005) has been derived from the lump of the final shape by the collapsing cylinder. From this definition, it can be said that this allows the height ratio (L/H)

and the base area ratio (A_u/A_b) to be estimated. The yield stress is made dimensionless using the lump height (L) rather than the initial cylinder height (H) (Hallbom, 2005). The reasoning for using lump height is that 'it is conceptually easier because it trends in the same direction as most of the variables of interest' (Haldenwang et al., 2007). That is, both shear and compressive yield stress increase with increase of lump. Hallbom also mentions the fact that it simplifies the non-dimensionalisation when the container height is not used. The author investigates the modification of the cylinder model by including the Von Mises failure criterion. The Von Mises criterion tends to be more accurate and is often the preferred choice for analysis of the mechanics of metal forming operations (Talbert & Avitzur, 1996). The lump model incorporating the Von Mises failure criterion is represented in terms of the slump form, as shown in the equation below.

$$\frac{\tau_y}{\sigma_{cy}} = \frac{1}{\sqrt{3}}, \quad 2.31$$

with σ_{cy} being the stress required to produce yielding along a shear plane due to an applied compressive force.

The lump model incorporating the Von Mises failure criterion is represented in terms of the slump form, as shown in the equation below

$$\tau'_y = \frac{1}{2} L' \sqrt{3} (L - 1) \quad 2.32$$

where L' is the dimensionless lump height (L/H).

The lump model in dimensionless slump form in a similar form to the cylinder model is

$$S' = \frac{1}{\sqrt{3}} \ln \left(\frac{2\tau'_y}{1 - S'} \right) \quad 2.33$$

Hallbom (2005) evaluated the yield stress using the lump model and it was found to correlate with the yield stress predictions from the cylinder model, especially at low slumps but at high slumps the cylinder model underpredicted the yield stress.

2.13.3 Merits of using the cylinder over the cone slump test

The ultimate use of the slump test is for where a simple, accurate, robust and cheap measurement technique is desired. For general application, the cylinder slump test has many advantages over the cone slump test:

Cylinder slump measurements can be completed with a section of pipe or even a beer can, whereas cone measurement must be completed with a cone manufactured to certain specifications.

Due to the more complex cone geometry, the cone is more difficult to fill, leading to the likely presence of air bubbles which can adversely affect the results.

The position of the slumped material is less consistent for the cone test, especially at high yield stress values.

2.13.4 Yield criterion

It should be noted that all the analytical approaches above involve a uni-dimensional expression of the yield criterion and behaviour law: flow occurs or stops when the shear stress becomes lower or higher than the yield stress. The other components of the stress tensor are not taken into account when writing a scalar yield criterion. This greatly simplifies the analysis of the flow, but is valid only if the flow is dominated by shear stresses (that is, the diagonal terms of the deviatoric stress tensor can be neglected compared to the shear stress). In fact, this assumption is true only in the ideal two-dimensional case studied by Coussot et al. (2002b) (very high slumps). This simplification is similar to the use of the lubrication theory in the squeezing flow (Covey & Stanmore, 1981). The squeezing flow test is a simple compression test carried out on cylindrical samples with reduced slenderness. By using the lubrication theory, only the shear stress is considered and the flow can be studied easily, but this theory generates what is called the "squeezing flow paradox". On the plane of symmetry between the two plates, the shear stress equals zero. The uni-dimensional yield criterion is, of course, not fulfilled and the material should flow as a solid body (i.e. "plug flow"). But Lipscomb and Denn (1984) demonstrated that plug regions cannot exist in the squeezing flow of yield stress fluids. Clearly a solid body cannot move radially outward with

a velocity that increases with the radial coordinate as the conservation equations demand. Wilson (1993) has pointed out that this paradoxical “yielded/unyielded” region is due to the neglect of the extensional stresses close to the centre plane where they are of a higher order than the shear stress. A proper three-dimensional criterion is thereafter needed to avoid this paradox and Adams et al. (1997) quoted “a comprehensive yield criterion as one which is based upon a combination of all the acting components of the stress”.

2.13.5 Behaviour at the interface

Most analyses in the literature are carried out assuming sticky flow at the base of the deposit. If we go into further details, the following distinction could be made. In the case of fluid concretes (i.e. low yield stress, high slumps), this assumption is probably valid as these concretes behave just like suspensions but, in the case of high yield stresses, this assumption should be questioned. A concrete with high yield stress may be obtained by two different trends in the mix proportioning. On one hand, the amount of cement or fine particles may be high. The colloidal force network that can be built between these fine particles increases the yield stress of the mixture (Raynaud, Moucheron, Baudez, Berrand, Guibaud & Coussot (2002). The concrete is similar to a dense fine suspension and, in this case, the assumption of a sticking flow is also valid, as experimentally obtained by Pashias et al. (1996). On the other hand, the amount of coarse particles may be high. The behaviour of the obtained concrete becomes closer to the behaviour of a cohesive granular material. In this case, as for a granular material, the behaviour at the interface may be frictional. Because of the uncertainty in the behaviour at the interface, the results obtained with a sticky flow assumption should be considered with care in the case of high yield stress concretes as the validity of the assumption of a sticking flow depends on the tested material aspect and mix proportioning. More recently, Chamberlain, Clayton, Landman and Sader (2003) considered the influence of plate roughness on the critical yield stress, assuming a coulomb type friction law at the interface involving a friction coefficient μ equal to zero for a perfect slip case. They showed that there was no influence of the friction parameter on the height of incipient failure (or critical yield stress) above a critical value μ_c depending on the cylinder radius, and that the interface could then be considered as perfectly rough. They also showed that the difference between height of incipient failure predicted for the perfect slip ($\mu_c = 0$) cases increased from zero for small radii to 18 % for a radius equal to $2\tau_o/\rho g$. In the case of typical concrete, this reference radius becomes 0.16 m (yield stress of the order of a magnitude of 2000 Pa and density around 2500 kg/m³). The radius of the ASTM Abrams cone (ASTM, 1996) being equal to 0.1 m, the error made while neglecting the friction at the

interface in the case of concrete should be lower than 18 % for low slumps and high yield stresses (Russel, 2006).

2.13.6 Effect of inertia

In all the analytical studies above, inertia (or dynamic) effects are neglected. Because of the simplifying assumption, the influence of the lifting speed of the mould (which depends on the operator) on the measured slump has been studied: the velocity of the flow and its kinetic energy are not taken into account and the final shape is calculated as a quasi static state, assuming it is reached slowly enough. In other words, what happens before the stoppage of the flow does not influence the shape at stoppage. Tattersall and Banfill (1983) experimentally concluded that the slump of fresh concrete is indeed highly correlated with yield stress but is not significantly affected by the plastic viscosity. This conclusion was also reached by Murata (1984). Let us check here that neglecting inertia effects is a correct assumption on a theoretical point of view: let us roughly compare the typical inertia stress ($I = \rho V^2$) to the material yield stress. For a small slump, the flow duration is of the order of magnitude of 1 s for a slump of the order of 10 cm. We thus have $I \approx 20$ Pa, a value much smaller than the material yield stress in such a case (typically larger than several hundreds of Pa). For a large slump, the flow duration is of the order of magnitude of 2–3 s for a slump of the order of 20 cm. We thus again have $I \approx 20$ Pa, a value once again much smaller than the material yield stress in such a case (typically larger than several tens of Pascals). This confirms the experimental deductions of Tattersall and Banfill (1983) and Murata (1984).

Conclusively, the final shape only depends on the yield stress.

2.14 SLIP

2.14.1 Definition of slip

Substances that exhibit a yield stress are typically multiphase systems which, due to the formation of a three-dimensional network, resist instant flow (Nguyen & Boger, 1983; Barnes & Carnali, 1989; Alderman et al., 1991; Roberts & Barnes, 2001; and Coussot & Nguyen, 2002). Such multiphase systems typically exhibit the problem of slip when tested at low shear rates with smooth surfaces geometries (Savarmand, 2002; Walls, Caines, Sanchez & Khan, 2003; and Dobbie, Fleming & Busby, 1998).

Maxwell Nyekwe Ichegbo: Investigation of factors effecting yield stress determinations using the slump test.

While determining the yield stress, wall slip can have a noteworthy consequence for the measurement of yield stress. Using different techniques can yield different results, for instance, a slip can be encountered when a smooth-walled cup is used, and less slip when a rough one is used.

During yield stress measurement using a controlled stress rheometer with smooth-walled coaxial cylinders, slip is defined as the result of both static and dynamic forces that develop during testing (Saak et al., 2004).

2.14.2 Slip correction techniques

As the extreme of profiling, the vane geometry has the merit of being easy to make and clean. The vane technique has been used successfully by a number of groups to overcome the effect of slip, see for instance the work of Sherwood and Meeten (1991) following that of Nguyen and Boger (1983).

Yoshimura et al., (1987) presented a slip alteration methodology for parallel plate systems, based on a comparison of shear stress versus shear rate at different gap settings. For slip to be corrected, it first has to be checked whether it is present and this can be done by checking results from data collected, using tubes of different radii. In the absence of slip, plots of torque (M) versus the apparent shear rate at the rim, determined by using a single plate (constant radius) but different gap heights, will yield identical curves.

2.14.3 Slip assessment

Cheng and Parker (1976) presented a technique of determining wall-slip based on the use of a smooth and a rough bob. Cheng (1984) suggested that the idea of a static and dynamic yield stress could be explained by assuming that there are two types of structure in a thixotropic fluid.

One structure is insensitive to shear rate and serves to define the dynamic yield stress associated with the equilibrium flow curve. A second structure is the weak structure. When the two structures are combined, they offer resistance to flow, which determines the static yield stress.

Qiu and Rao (1989) used the Mooney viscometer technique to evaluate slip in applesauce. According to the investigations done, it was found that the wall slip correction did not influence the flow behaviour index significantly, but it increased the consistency coefficient. If slip is a serious problem, mixer viscometry should be evaluated as an alternate experimental technique.

Recent investigations suggest that, for pasty materials exhibiting a yield stress (such as concentrated suspensions) heterogeneous flows may occur. Persello and Agassant, (1994) observed wall slip in concentrated silica suspensions; however, the use of roughened surfaces to suppress slip resulted in fracture of the bulk rather than homogenous flows. The effect of wall slip on apparent yield stress of sediments was shown in a corresponding publication, where a smooth-walled rheometer yielded the following values: 23, 27 and 32 Pa. Contrarily, the vane geometry gave values of 62, 105 and 111 Pa. Both yield stress measurements were taken on volume concentrations (mud) of 8.8 %, 15.6 % and 16.8 % respectively (Williams et al., 1994).

Yoo et al. (1995) defined a new dimensionless number, the yield number, defined as the static yield stress divided by the dynamic yield stress, to differentiate yield stresses.

Barnes (1995) mentioned how numerous workers have described the role of wall slip effects on measurements made with conventional smooth-walled geometries. Slip can occur and can involve fluctuating torque in a rotational viscometer under steady rotation (Cheng, 1986).

During a slump test performed by Pashias et al. (1996) oil was applied on the hand-held cylinder to determine the effect of slip. They found that the yield stress of mineral suspensions (titania, zirconia and bauxite residue) with and without is insignificant.

Meeker, Bonnetaze, & Cloitre (2004) investigated the slip and flow of highly concentrated suspensions of soft particles by directly observing the sample flow in a rheometer using video macrosopy and tracer particles to visualise the paste flow with and without wall slip. They observed that the magnitude of slip depends on the applied stress. Well above the yield stress, slip is negligible compared to the bulk flow. Just above the yield stress, slip becomes significant and the total deformation results from a combination of bulk flow and slip. At and below the yield stress, the bulk flow is negligible.

2.15 SHEAR HISTORY

The amount and type of shear that a sample receives prior to testing for rheology is referred to as “shear history”. The measurement protocols must be identical to ensure repeatability. The amount of mixing prior to measurement and the time the sample has been left standing all need to be considered. The low shear viscosity of many mineral types of non-Newtonian fluid is highly time dependent and exhibits a high level of hysteresis dependent on the direction from which it has been measured. Many types of non-Newtonian fluid develop a strong gel structure with time. This has a major impact on yield stress measurements.

The simplest technique for assessing the effect of shear history is to measure the yield stress (or torque) as a function of shearing time at a fixed shear rate. Many concentrated suspensions, particularly flocculated or coagulated suspensions, possess a networked structure which may be broken down as they are subjected to shear (Gladman, Usher & Scales, 2006)

The yield stress measured in a previously sheared sample will increase steadily with time of rest due to a recovery of the broken down structure in the static state. Thus a sample left undisturbed after being completely mixed would possess a yield stress that is higher than that tested immediately after mixing without rest. Furthermore, yield stress measurements on samples with a partially recovered (thixotropic) structure are more likely to be affected by the experimental time scales and techniques employed than the measurements with the materials at the equilibrium structural state (Cheng, 1986). A recent work by Coussot et al. (2002b) has showed a complex interaction between yielding and thixotropic behaviour of suspensions that makes yield stress measurements without a carefully controlled shear history very hard to interpret.

2.16 EFFECT OF SAMPLE PREPARATION

One feature which may affect viscosity measurements is the sample preparation and conditioning. “It is desirable to have a homogeneous sample so that more consistent results may be obtained” (Sofra & Boger, 2001b and Boger et al., 2008). One of the biggest problems in mixing substances is the tendency of a material to split into non-homogeneous layers. The most likely contributing factor may come from the characteristics and condition of

the suspension of samples. Hand stirring and mechanical agitation employed to disperse solid particles in liquid could affect the final state of the suspension samples.

2.17 SUMMARY

The arguments given for the non-existence of yield stress are not new; most engineers have accepted yield stress as a useful parameter that is of key importance and which influences the pump start-up pressure, pipeline pressure losses, thickener underflow density and slope angle deposition. Given this, different techniques have been used in an effort to obtain an accurate measurement of yield stress. The review above focused on the fact that different authors have clearly stated that the vane technique has been by far the best technique for measuring yield stress; hence it was used as a benchmark for all the other techniques. Many other techniques were used to measure yield stress, coupled with different effects that came with each technique.

The ASTM as well as SABS 143-86 describe the slump cone test for concrete. The cone size is 300 mm in height, with top and base diameter of 100 mm and 200 mm respectively. An Australian standard (AS2701.5) is available for slump measurement of concrete with a cone size of 150 mm in height, with top diameter of 50 mm and base diameter of 100 mm. No dimensional standards for the cylinder geometry are available. The literature also shows that various researchers have measured yield stress of various mineral tailings using cone and cylinder geometries with different dimensions. The sizes of cones and cylinders used in this work are smaller than that used for concrete, but within the size range used by other researchers who have investigated similar non-Newtonian fluids.

The hand-held cylinder originally developed by Pashias et al., (1996) is disposed to human error because it is manually controlled. The hand-held cylinder was used primarily to measure the yield stress. A hand-held cylinder is by far the most convenient and cost effective way of measuring yield stress, thus this technique is used widely in the industry. Modelling the relationship between yield stress and slump has been one of the greatest challenges with regard to getting an accurate yield stress measurement. The dimensionless slump model originally developed by Murata is generalized, making it applicable for any cone and cylinder geometry.

The effect of measuring position on yield stress could have a major consequence on the yield stress value measured with the slump meter (cone and cylinder) as well as hand-held cylinder. It was therefore intended to study the effect of this parameter on yield stress in this thesis.

The literature shows evidence that the lift speed, slip, position of slump measurement and geometry has been studied and has limited effect on the value of the yield stress. This will be evaluated in this work for different non-Newtonian fluids to verify. As far as can be ascertained the effect of stability of lift has not been studied and therefore will be included in this work by fixing the cones and cylinders in a mechanical lifting device.

The literature review has been presented in detail in this chapter on the definition of and the different measurement techniques to determine the yield stress. In the next chapter (Chapter 3) the experimental procedures that were involved will be presented.

CHAPTER 3

CHAPTER 3

EXPERIMENTAL WORK

3.1 INTRODUCTION

This chapter provides a comprehensive description of the experimental methodology adopted for this study. A description of the apparatus and instrumentation used for both the slump measurement and the vane technique is addressed, including the technique used for the determination and analysis of the effect of position of slump measurement, wall surface materials, geometry, stability and speed of lift

The focus of this chapter is the measurement of yield stress when using the slump technique and the vane shear technique. The slump technique experiments were conducted with a mechanical slump meter cone geometry (PVC and stainless steel) and cylinder geometry (PVC and stainless steel) as well as the hand-held cylinder, using materials such as kaolinite tailings, kaolinite mine tailings (kaolinite tailings and sand), laponite and kaolin. The vane technique was used to measure yield stress independently.

The experimental work was done with the following question in mind:

What is the effect of the measuring position on yield stress, effect of lift speed, stability, slip, wall surface materials, geometry and validation of yield stress models on the value of the yield stress measured with the hand-held cylinder as well as all the other cone and cylinder configurations?.

3.2 EXPERIMENTAL APPARATUS

The experimental work for this project was conducted in the Flow Process Research Centre (FPRC) at the Cape Peninsula University of Technology (CPUT). A mechanical slump meter with lift speed control, developed at FPRC, was used for the slump tests and the rotary viscometer for the shear vane technique. The mechanical slump meter was designed to lift the cone or cylinder vertically at controlled lifting speeds.

3.2.1 THE VANE TECHNIQUE

The vane technique is the most straightforward technique for direct measurement of the yield stress. This technique assumes that the stress created by the vane is uniformly distributed everywhere on the cylindrical surfaces (including the bottom of the cylinder and the top of the cylinder for covered and uncovered conditions). As the vane rotates through the sample, the ideal response is a linear increase in stress (solid-like behaviour), followed by a clear break from linearity (at the transition from a solid-like state to a flowing fluid). The break is typically followed by either a maximum stress that falls off to a lower steady state stress or else by a break from linearity with a levelling off to a constant stress.

3.2.1.1 Calibration and testing

A general guideline for geometric proportions has been proposed (Nguyen & Boger, 1983 and 1985) for vane geometry when making yield stress measurements. The dimensions shown in Figure 3.1 are recommended for obtaining satisfactory measurements, taking into consideration the vane dimensions and system boundaries. The stress developed, when the vane is completely immersed in the sample and rotated slowly through the sample, is determined by Equation 2.18. A targeted rotational speed of 0.3 rpm was used for the margin of error vane test.

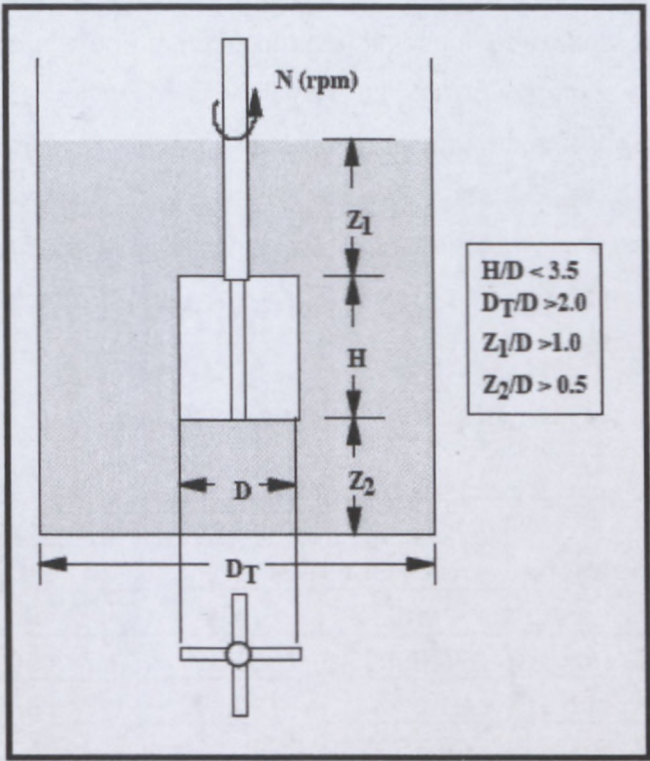


Figure 3. 1: Schematic diagram of a four-bladed vane in operation (Adapted from Boger et al., 1992)

In the case where the top of the vane is flush with the top of the sample, the torque developed is given by Equation 2.18. The difference between Equation 2.17 and Equation 2.18 is the 1/3 and 1/6 factors. The 1/3 factor involves the stresses at the top and bottom of the beaker, when the vane is totally immersed in the sample. The 1/6 factor is the stress at the bottom of the cylinder when the top of the vane is flush with the top of the sample. The vanes used in this study consisted of four identical blades welded symmetrically around a thin, rigid, small cylindrical shaft (as seen in Figure 3.1). The length of the blade for the big vane is 44 mm and the diameter is 22 mm, whereas the length of the blade as well as the diameter for the small vane is 22 mm.

The formula for yield stress is adapted for this aspect. For the aim of the experiment, two cylindrical containers were used for measurement, one for the large vane and the other for the small vane, and their height was divided into three equal parts, each part measuring the exact height of each vane for the container, as shown in Figure 3.4. Shear vane tests were conducted for four different concentrations of kaolin by inserting each vane to the 1/3 factor

and 1/6 factor, for the small and for the large. The technique used as the vane technique is for the top of the vane to be flush with the top of the sample in a wide container to regulate for slip effect. The summary of yield stress values is shown in Table 3.1 and the plots of yield stress as a function of solid concentration between the small vane and the large vane are shown in Figures 3.2a, 3.2b and 3.2c for the large vane 1/6 factor, large vane 1/3 factor & small vane 1/6 and small vane 1/3 factor combined; small vane 1/3 factor and small vane 1/6 factor and large vane 1/6 factor and small vane 1/3 factor respectively.

Table 3. 1: Summary of yield stress

Concentrations	Summary of Yield stresses			
	Small Vane		Large Vane	
	1/6	1/3	1/6	1/3
17 % 1st	90.0000	83.9800	76.4800	75.9900
17 % 2nd	91.8100	82.5700	74.5400	71.5300
17 % 3rd	94.7500	83.7000	76.7500	74.6000
18 % 1st	128.3400	116.0200	117.0600	106.6500
18 % 2nd	129.1500	114.6600	116.7800	115.1200
18 % 3rd	126.7400	115.5100	109.0500	111.7700
19 % 1st	169.0300	157.7500	141.3600	143.3100
19 % 2nd	172.1700	160.9700	146.8800	138.6900
19 % 3rd	177.4600	157.8600	145.2200	146.9000
20 % 1st	233.7400	218.2100	194.0900	191.5000
20 % 2nd	235.0700	204.1700	199.3300	189.2000
20 % 3rd	230.7900	212.9700	181.9400	191.7600

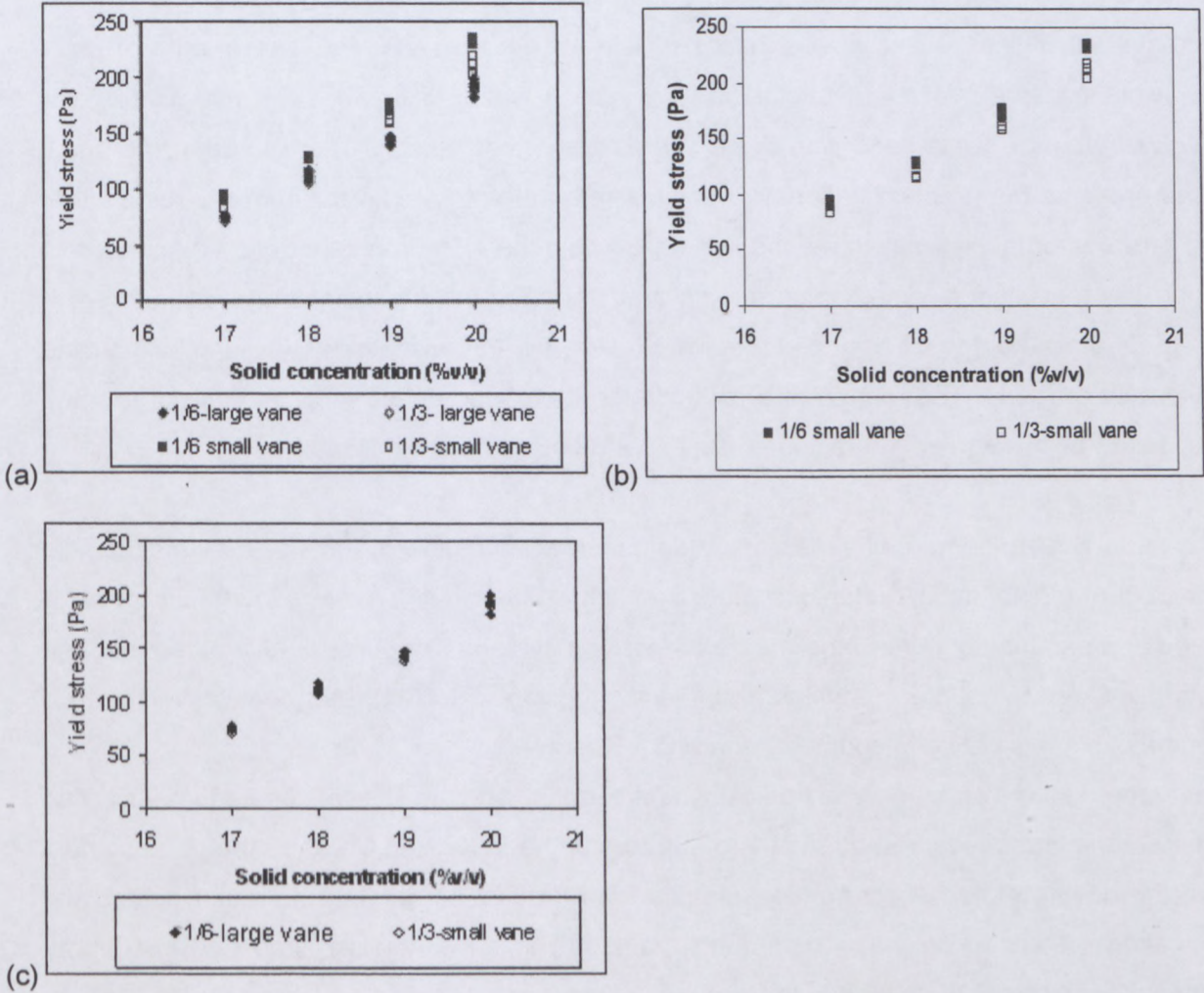


Figure 3. 2: Yield stress versus solid concentration. a) for the 1/6 and 1/3 factors for the small and large vane combined, b) 1/6 and 1/3 small vane combined and c) 1/6 large vane & 1/3 small vane.

3.2.1.2 Analysis of margin of error

Figure 3.2 shows the yield stress as a function of solid concentrations. The range of solid concentrations tested was between 17 % and 20 %. The result shows an increase in yield stresses as solid concentrations increase for the large vane (1/6 factor and 1/3 factor) and the small vane (1/6 factor and 1/3 factor). It was observed that the small vane, both in the 1/6 factor and in the 1/3 factor, produced a yield stress above 200 Pa, while the large vane did not exceed the yield stress of 200 Pa in either the 1/6 factor or the 1/3 factor, as shown in Table 3.1. The

large vane is in agreement with literature indicating that the yield vane technique is most suitable with fluids having yield stresses of less or equal to 200 Pa. The margin of error involving the small vane (1/6 factor and 1/3 factor) was $\pm 5\%$, while the margin of error involved with the large vane was $\pm 2\%$. This means that, arising from the data, the small vane presents the greatest uncertainty arising from the data. It is clear from the results that the errors of both the small vane and large are within the experimental errors experienced in using the four-bladed vane, which means that the effect of dimensions can be ignored. It assures that the torque detection system used by the viscometer is functioning and calibrated properly. The margin of error between them was determined and the large vane was taken as the agreed 1/6 factor for the experimental work for this study.

The general arrangement of vane apparatus as shown in Figure 3.3 has several mechanical components. The major setup includes a synchronous drive motor, a hydraulic gear, a spindle, a sample container, and a data acquisition system. The vane is fully automatic and controlled by a computer, in which a software program, US 2000, has been developed for control of signals between computer and MC 1 Rheometer.

The vane was driven by an electronically controlled DC motor. The torsional moment acting on the vane was measured by means of the torsion head located between the vane spindle and the driving motor. A control console provided facilities for setting the motor speed and indication meters for speed and torque readings. The drive, torsion head and instrument console are actually parts of the Rheolab MC 1 Rheometer.

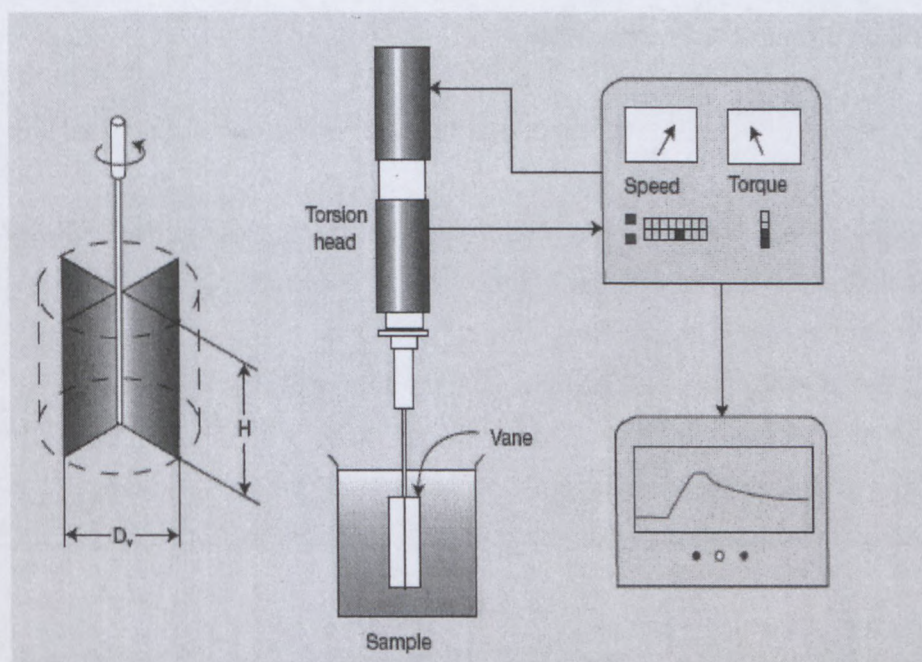


Figure 3. 3: Illustrating the vane technique for yield stress measurement (Adapted from Boger, 2006)

3.2.1.3 Mode of operation and theory

The yield stress measurements were obtained with a controlled strain rate rheometer.

In the strain rate controlled mode of operation, the vane was operated at a rotational speed of 0.3 rpm, to avoid the influence of viscous resistance and instrument inertia on the maximum torque, and also in the recommended range of 0.1 rpm to 0.9 rpm, as stated in the literature (section 2.10.2). The vane apparatus provides the most accurate technique to measure yield stress. The vane used is much bigger than the conventional shear vane and it is confined to be used on larger samples. The procedure for the vane technique for the experimental work is described as follows: a 176 ml plastic container containing 132 ml (see appendix E 5) of the suspension was raised slowly, as shown in Figure 3.4, by means of a jack, until just the top of the vane was even with the surface of the material. To limit interference caused by the wall of the beaker, care was taken to place the vane at the centre of the sample volume. The vane was then rotated at 0.3 rpm to obtain satisfactory yield stress measurements and the resulting torque was recorded with time until the maximum torque value was obtained. The yield stress was calculated using Equation 2.18, the vane dimensions and the measured maximum torque.

3.2.1.4 The equipment for measurement

The apparatus used for gathering the experimental data for the vane shear test were:

Rheometer – MC1 Paar Physica (most mid-range rheometers will suffice); the key criteria are good resolution of the torque and good range and control of rotational speed, in particular a capability for constant, very low rpm rotation. This is an instrument used to measure rheological properties of materials. The rotation speed is very important in this test as it determines the amount of torque that can be achieved, with the goal being to attain the maximum torque possible. Fresh material was loaded every time a vane test was conducted; the reason being that maximum torque is not realistic when a test is repeated on the same sample.

In the container (176 ml), the experimental measurement occurred in a “fixed” of material of tailings (i.e. the walls and bottom of the container were far enough from the vane so as to have no effect on the readings, as seen in Figure 3.4.



Figure 3. 4: MC 1 rheometer used for vane test

3.2.2 THE SLUMP METER

The slump meter was designed and constructed at the Flow Process Research Centre (FPRC) and the shear device for the test work was developed by the Mechanical Engineering department at the Cape Peninsula University of Technology (CPUT). It is a prototype developed from the traditional slump meter which was used to automate the hand-held cylinder. The slump meter is illustrated in Figure 3.5.

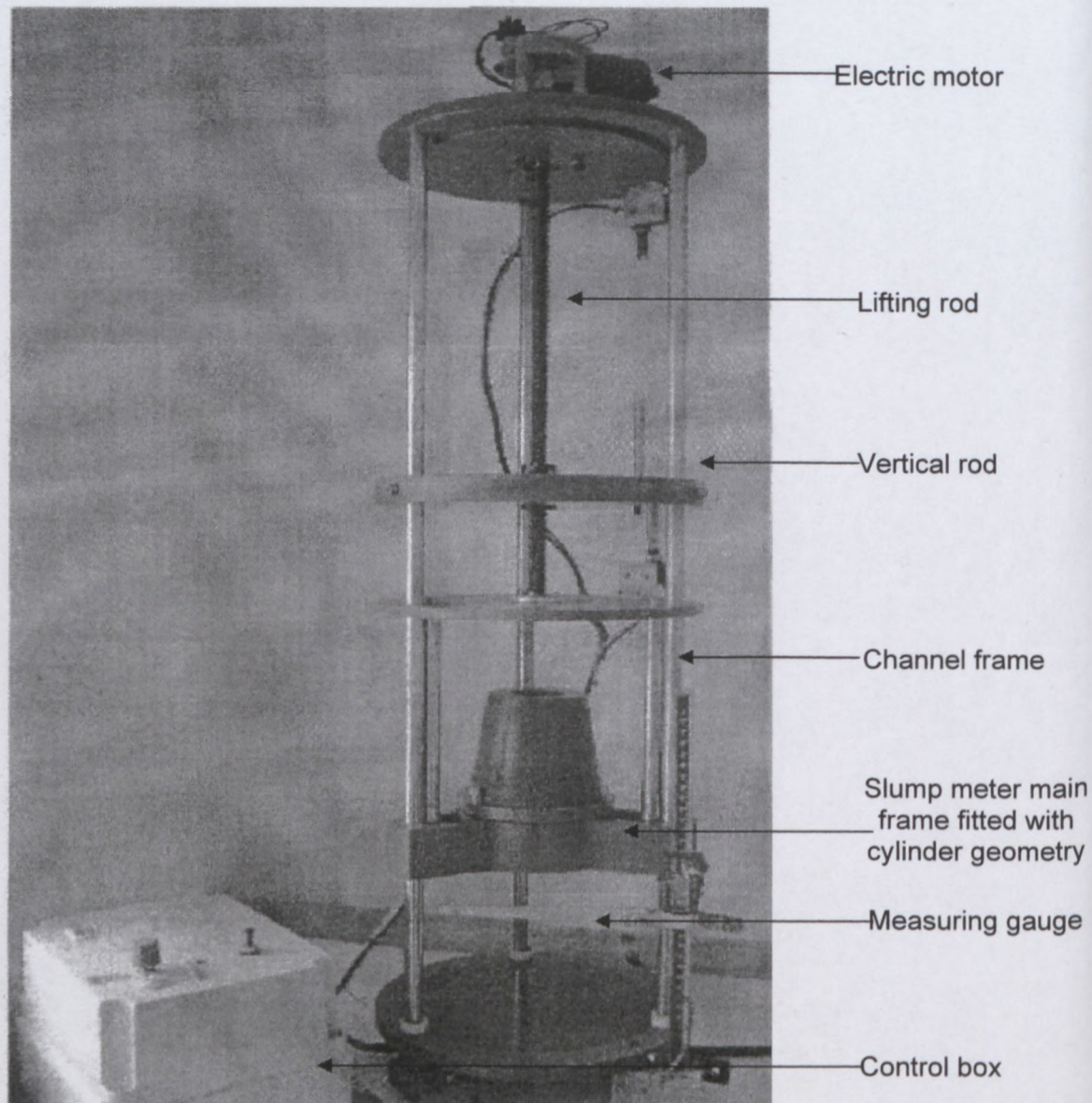


Figure 3. 5: The slump meter

3.2.2.1 Calibration and testing

The slump meter comprises of two main components, namely the slump meter frame and the control box. In addition two displacement transducers are used for measuring the geometry lifting displacement and slump displacement with time, the slump geometries are fitted in the frame and an electric motor is used to control the lifting rate of the slump geometry. The geometry (cone and cylinder) was inserted inside the slump meter main frame, and filled with the material to be tested (kaolin, kaolinite tailings, Laponite and kaolinite mine tailings (kaolinite tailings and sand)). The geometries were filled gradually, using a plastic spoon and a small plastic stirring ruler to remove any air bubbles trapped in

the material in the cone or cylinder. After smoothening of the top cone and cylinder, the control box, which was calibrated for 3 mm/s, 5 mm/s, 7 mm/s and 10 mm/s, was used to determine the actual lifting speeds. The highest and lowest points of the slumped material was taken as the slump height and height measured with the digital depth gauge; the lift speed was measured with a stopwatch to measure the time it took for the slump meter to start lifting the material and the time it took to leave the slump material. This was done immediately the geometry left the slumped material. For a few tests the slump height in the middle of the cone or cylinder were measured as well.

The slump meter shown in Figure 3.5 that was used to conduct the slump tests can be used at different lifting speeds. The speeds that can be utilised can start from as low as 3 mm/s to the highest speed of 21 mm/s. Different speeds ranging between 3 mm/s and 21 mm/s were used for each geometry. Before the slump test experiment was carried out, it was important to select the speeds for the slump test. The results recorded in Table 3.2, Tables E.6 and E.7 and E.8 in the Appendix E were obtained. The graphs showing the trend of the lifting speed for the six sets of the results were produced from the information in these tables.

The test was repeated four times. The results that were obtained indicated that the lifting speed for each set of a specific number tended to vary. In other words, the results showed inconsistencies. It was therefore decided to measure lift speed for each test individually. The set of results presented in the table and the graph led to the decision that the 3, 5, 7 and 10 as the control of the lifting device should be used for the experiments. Control of the lifting device 3, 5, 7 and 10 were then used to perform the slump test experiment.

Figure 3.6 below shows the trend in the lifting device control.

Table 3. 2: Calibration of the slump meter

Control	Lifting speed mm/s
2	3
3	6
4	9
5	11
6	15
7	17
8	21
9	23
10	27
11	27
12	27

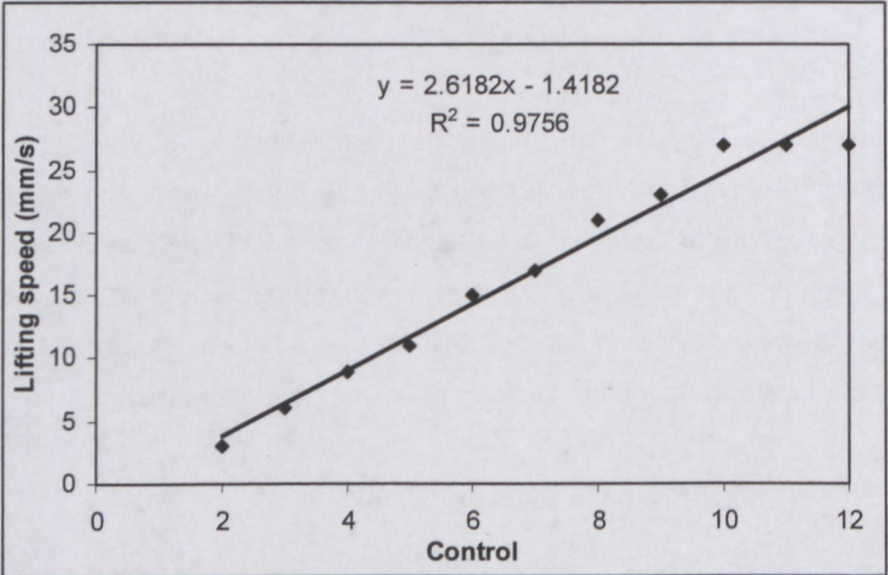


Figure 3. 6: The trend in the lifting device control

3.2.2.2 The geometries

All the experimental work completed with the slump meter was performed using the cone and cylinder geometry, both made of PVC and stainless steel, as depicted in Figure 3.7. The conical geometries for both PVC and stainless steel were 150 mm in height, with top and base diameter of 50 mm and 100 mm respectively and the cylindrical geometries were 100 mm in height, with a diameter of 100 mm.



Figure 3. 7: The stainless steel cone, PVC cone, stainless steel cylinder and PVC cylinder

3.2.3 THE HAND-HELD CYLINDER

The hand-held cylinder with a dimension of 75 mm in height to 75 mm in diameter is made of a stainless steel tube, as shown in Figure 3.8. The hand-held cylinder was also used for comparison with the tests performed while using the slump meter.

The loading of the sample into the hand-held cylinder was similar to the manner used in the cone/cylinder geometry with the slump meter. The hand-held cylinder was lifted slowly to avoid disturbing the slumping of the material. The highest point of the slumped material was taken as the slump height and the height was measured with the digital depth gauge.

Density and concentration were measured at the time of the test. To establish the effect of slip, application of silicon spray on the geometry was utilised and a test was performed.

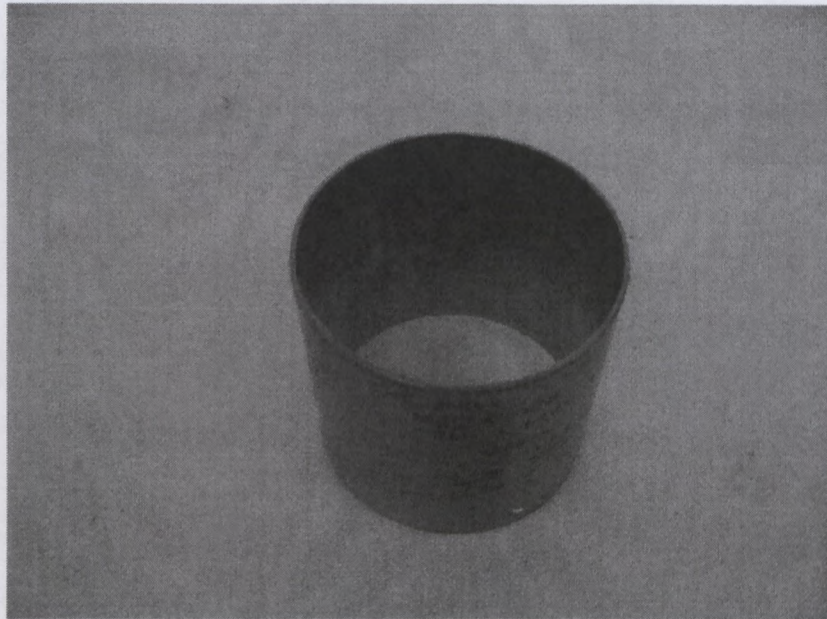


Figure 3. 8: Hand –held cylinder with dimensions of 75 mm in height and 75 mm in diameter

3.2.4 THE SHEAR MIXER

The procedure employed during the mixing of all the mix preparation (shear history) used in this research for the kaolinite mine tailings (kaolinite tailings and sand) is given below:

- The shear device is a mechanical device used for the shearing of the materials, as shown in Figure 3.9. The device was designed for shearing at 510 rpm. The consistency in the material is important as this determines the quality of the results obtained from experimental tests. Using a shear device is one means to achieve this, as it shears the material with water in such a way that a homogeneous mix is achieved.
- The shear mixer is equipped with a 1/2 HP motor and variable speed drive. Speeds range from 0-510 rpm, handling batches from 1-20 litres.

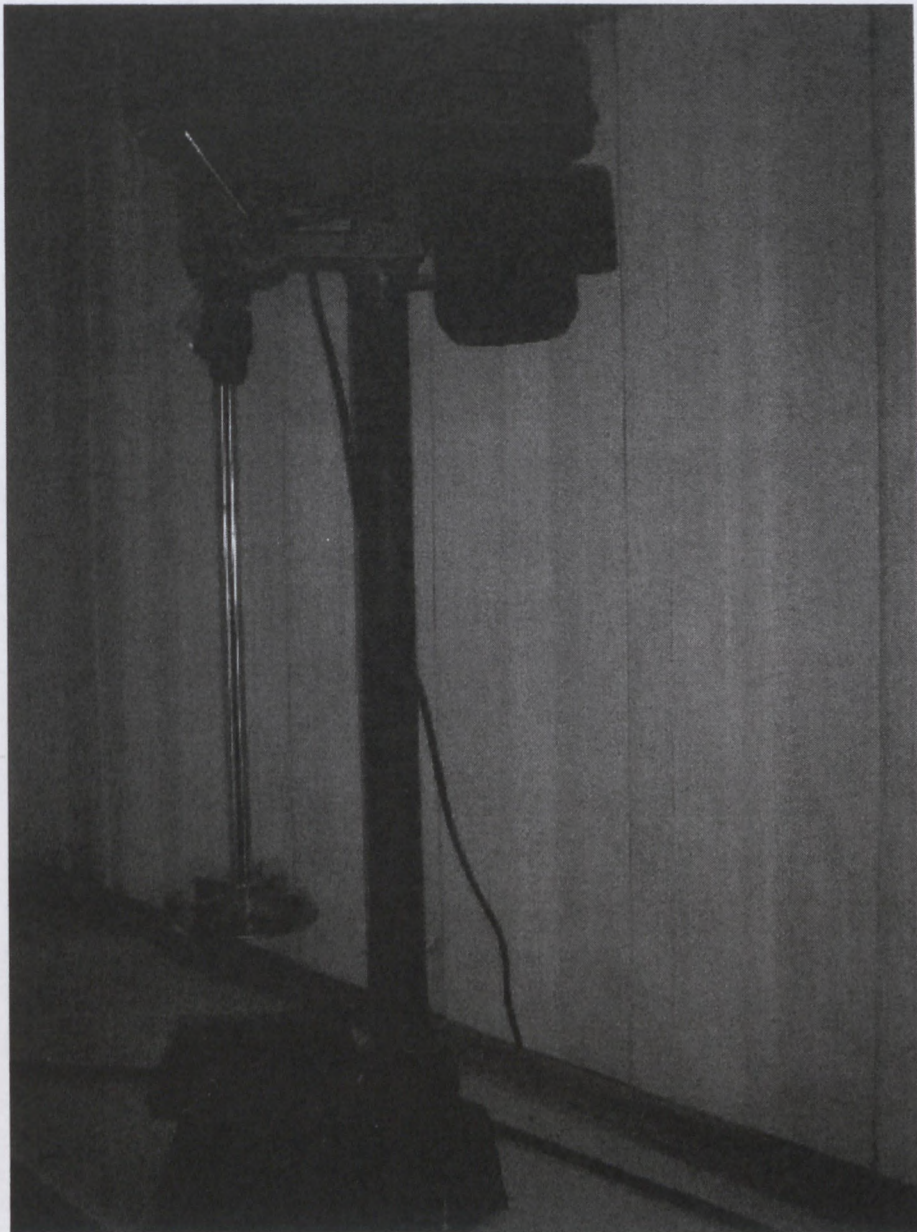


Figure 3. 9: The shearing device

3.2.5 THE HALOGEN MOISTURE ANALYSER

The determination of the sample's moisture content was performed using the Mettler Toledo HR83 Halogen moisture analyser. This moisture analyser uses a load cell that continuously measures the mass of the sample during the measurement, as well as a halogen heat lamp that is controlled by an infrared thermometer as shown in Table E 4.

3.3 EXPERIMENTAL PROCEDURES

The yield stress of the test materials was determined by using the slump technique and the direct technique (vane technique). The experimental procedures were strictly followed to avoid any experimental complications arising from an incomplete procedure. The materials were measured under the same conditions with respect to time and number of measuring points. The procedures used for the experimental work are as follows:

3.3.1 Yield stress measurement using the slump meter

The selected geometry (cone and cylinder) was placed inside the movable steel ring on the slump meter. The material (kaolin, kaolinite tailings, kaolinite mine tailings and Laponite) was then loaded inside the geometry with a spoon, in such a manner that voids in the material were eliminated. The material was loaded until it reached the top of the geometry.

At the top of the geometry, the material was levelled off with the use of a plastic rod, in such a way that a flat surface was maintained before the material was subjected to slump. After that, the selection of the lifting number inscribed in the control box follows, and the control box which moves the steel was switched on. The movable steel ring then starts to lift the geometry, causing the material to slump under its own weight. As the material is no longer supported by the geometry when this is lifted, the material starts to flow downwards due to the force of gravity. Figure 3.10 show an example of slump.

The slump was measured at the highest and lowest points as well as the middle of the slumped materials with a digital depth gauge and the lift speed was measured with a stopwatch. The slump height was measured at different positions on top of the slumped material to determine the effect of position of slump measuring position on the value of yield stress.

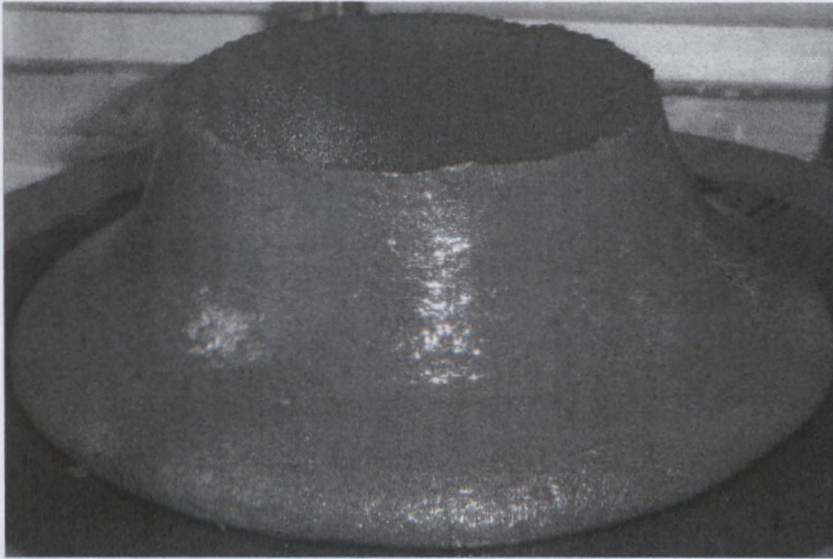


Figure 3. 10: Example of a slump for 18 % kaolinite mine tailings

3.3.2 Yield stress measurement using the vane techniques

The direct technique employed in this work for the measurement of the yield stress of the suspensions was the vane technique. The vane geometry consists of four thin rectangular blades welded to a thin, rigid, central, cylindrical shaft at right angles to each other, as shown in Figure 3.11.

A Paar Physica rheometer MC1 was used for measuring the rheological properties of the kaolin, kaolinite tailings, laponite and the kaolinite mine tailings. It is connected to the computer, which utilises a special program (US200). The vane technique basically involves inserting the vane probe into a sample of the material in a container rotated at a low speed of 0.3 rpm of 30 measuring points. The maximum-torque develops in the sample as the rheometer moves the spindle to meet the designated rotational speed. When the shear stress develops in the sample, the sample deforms elastically due to the stretching of the bonds in the network structure. At some point, the network begins to break under the shear stresses, as some of the bonds reach the elastic limit. The development of viscoelasticity is represented by the departure from linearity of the torque-time profile. At some point, the structure begins to break down completely and the relationship for calculating the yield stress can be shown, using an approximate derivation (Nguyen & Boger, 1983):

$$\tau_y = \frac{2M_o}{\pi d_v^3} \left(\frac{h_v}{d_v} + \frac{1}{6} \right)^{-1}$$

Equation 2.18

where D_v is the overall width of the vane (22 mm) and h_v is the vane height (44 mm), M_o is the maximum torque. This is often referred to as the static yield stress, since macroscopic flow has not occurred. Sample volumes were not deformed in anyway prior to measurement.

Measurements with these fixtures involved a wide gap between the vane and the outer cylinder of at least twice the diameter of the vane (Nguyen & Boger, 1983).

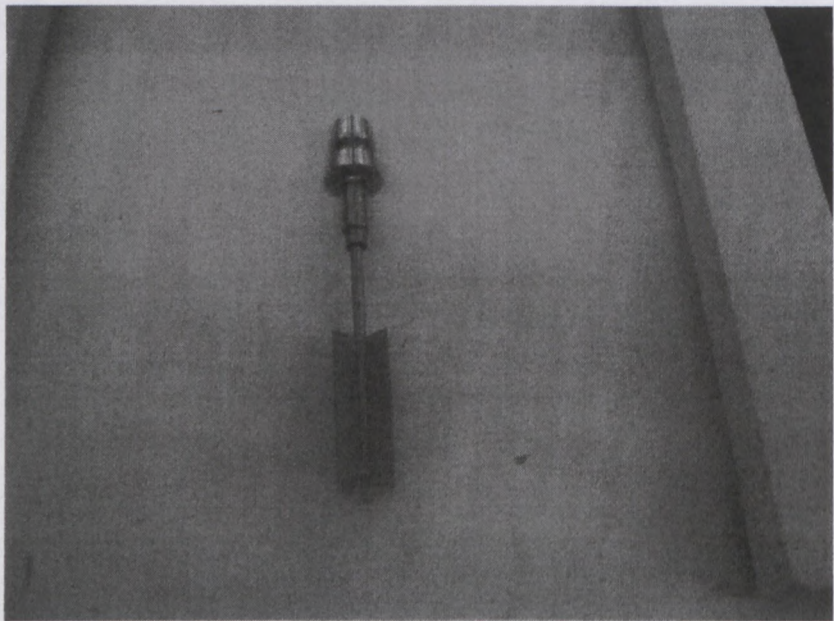


Figure 3. 11: Vane geometry with a 44 mm height and a 22 mm diameter

3.3.3 Yield stress measurement using the hand-held cylinder

After the slump measurement with the slump meter, the hand-held cylinder as seen in Figure 3.8, above, was used. This involves filling the geometry with a material (kaolin, laponite, kaolinite tailings and kaolinite mine tailings), lifting the hand-held cylinder off slowly and allowing the material to flow under its own weight. The highest point and lowest point of the slumped material was taken as the slump height and the height was measured with the digital depth gauge to an accuracy of 0.5 mm. Further tests were done using the middle point and highest point to determine the effect of position of slump measurement on the

value of the yield stress also using the hand-held cylinder. The profile of the final mound of material and as the difference between the initial and final heights can provide an estimation of the yield stress.

During the slump test, the hand-held cylinder, cone and cylinder geometry was sprayed with silicone spray applied to the sides of the cone, cylinder geometries and the hand-held cylinder, in an effort to reduce any complicating effects due to slip during lifting.

3.3.4 Shearing of the kaolinite tailings and sand

A rotating cylindrical shear mixer equipped with a stationary paddle assembly essentially forms the equipment used in these tests. The required amounts of kaolinite mine tailings (kaolinite tailings and sand) and water were poured together in the shear device to give a total volume of approximately three litres. The sample was first mixed by hand and afterwards the mixing blade was inserted to the required level afterwards. The shear mixer was rotated at a speed of 535 rpm for all the mixing measurements.

The consistency of the kaolinite mine tailings was indicated by the amount of deformation of a standardised coil spring connecting the stirring paddle and the stationary head, as shown in Figure 3.9. The kaolinite mine tailings (kaolinite tailings and sand) were kept in the shear device at this constant rotational speed and the consistency shear periods were recorded. After the mixing, a plastic spoon was used to remove the sample from the steel paddles for the shear vane test and slump measurements.

3.4 MATERIALS

The kaolin used for the experiment was provided by a mine in South Africa and transported in sealed 25 kg bags to the Flow Process Research Centre (FPRC) at the Cape Peninsula University of Technology (CPUT). Kaolin is one of the most abundant minerals in soils and sediments (Van, 1977) and one of the most widely used in industry. Kaolin is a 1:1 layer mineral with high chemical stability; it is the least reactive clay. The platelet- or lamella-like structural unit (Van, 1977) or sheet (thickness = 0.7 nm) is often piled up and forms a stack. Different arrangements can be defined, i.e. one-order with the initial unit, two-order when the particles are stacked sheets and, finally, three-order, with aggregates as packed particles.

Generally, regarding its well-packed structure, kaolin particles are not easily broken down and kaolin layers are easily separated. As the sample does not consist of 100 % kaolinite, it contains about 3 % mica; the sample is referred to as kaolin, not kaolinite, throughout this study. The kaolin used in this study is a commercial one. The tests were conducted using kaolin dispersed in water at different concentrations of 20 %, 18 %, 16 % and 14 % volume by total volume using tap water. All the materials (kaolin) were left to hydrate for 72 hours before determining their relative densities. Samples were mixed in 4-liter plastic buckets, which remained airtight until opened and mixed by hand for two minutes before testing.

3.4.1 Preparation of kaolin

The kaolin was delivered in 25 kg bags in a fine powder state to make up a fully homogenous non-Newtonian fluid and was mixed with clear water by hand until an uneven dispersion was obtained.

The dry density of kaolin is 2650 kg/m^3 and the volume-by-volume procedure was employed during the mixing for the experimental work. Kaolin can easily be mixed into a smooth, consistent mix to ascertain a homogenous mix throughout the bucket. No other additives were used. The measurements were determined after each mixing and as well as concentration.

3.4.2 Kaolinite tailings and preparation

Kaolinite tailings were obtained from a mine and supplied to the Cape Peninsula University of Technology in a 25 litre bucket. Kaolinite tailings are the most widespread mineral of the kaolin group, which also contains dickite, nacrite and halloysite (Chukwudi, 2008). The kaolinite tailings are what is left after minerals have been extracted from the industry.

3.4.2.1 Preparation of kaolinite tailings

The kaolinite tailings were mixed and allowed to stand. The supernatant water was decanted to achieve an initial high density and the decanted water was kept for dilution to attain a homogeneous mix. The kaolinite tailings were mixed slowly with a paddle and were adjusted using a vacuum pressure pump to ascertain the required concentration. Like kaolin, kaolinite

tailing tends to settle when left for some time. The concentrations were obtained by removing water using a vacuum pressure pump and calculating the new concentration. The concentrations of kaolinite tailings used in the experimental work were 14 %, 16 % 18 % and 20 % volume by total volume. The moisture content and relative density were determined. Relative densities were determined using the volumetric method. The displaced volumes and corresponding masses were determined and used to calculate the relative density. The moisture content was determined through water loss by heating at 60°C for this work. 60°C was used in this work because; it as the client, EXXARO's specification for the project.

3.4.3 Preparation of sand

The sand was prepared by mixing it with other, different, buckets of sand. The sand supplied commercially was sieved, using a 1 mm sieve plate at a minimised weight with water in another bucket, in order to remove oversized particles after the sieving. Solids were allowed to settle and the clear supernatant layer of water was decanted. Pin holes were created in the base of the bucket containing the new sand with fewer particles, to ensure that consistency was achieved. The sand was left in the bucket for 72 hours. After 72 hours the sand was placed in an oven at approximately 60 °C to ensure dry sand at zero moisture. At the end of the 72 hours, the sand was sieved to remove possible oversize that would negatively impact the results. After the sand preparation, the sand was stored in a bucket for experimental usage.

3.4.4 Mixture of kaolinite tailings and sand

Mixture of kaolinite tailings and sand in distilled water was done in order to achieve a higher representative particle size; the sand was introduced into the kaolinite tailings. Tests were conducted at different relative densities to determine the amount of kaolinite tailings needed to fully suspend within the mixture for shearing.

Table 3. 3: Example of mixture kaolinite tailings and sand

Set "kaolinite tailings plus sand" value		then goal seek (select "Sand Dry Ratio" - set to desired value "x" by changing "Sand Wt"					
Mixture	Mix components		Dry Ratio		Resultant Mixture		
	Sand (g)	301.9601143	90.0		Total Wt	479.426	
	Kaolinite tailings (g)	98.03988569	10.0		Total Volume	266.354	
	Water (g)	79.42616816			Rd	1.7999616	
	Kaolinite talling plus sand	400					
	Grams	Effective Wt %	Density	Volume	Effective Vol %	Rd	
Water	139.52	29.10	1.00	139.52	52.38		
Sand +45µm to - 1mm Fraction	305.91	63.81	2.68	114.15	42.86		
kaolinite tailings plus sand -45µm Fraction	33.99	7.09	2.68	12.68	4.76		
Total Sample	479.43	100.00		266.35	100.00	1.80	

The required masses for the different mixing ratios were calculated by using the volume ratios of sand in kaolinite tailings and kaolinite tailings in sand (above and below 45 micron fractions) together with the moisture content of the Kaolinite tailings and sand. The content of the dry sand and kaolinite tailings was determined to make up the required ratios of 90/10, 80/20 and 70/30. From the moisture content, the mass of wet kaolinite tailings required with the same dry mass were calculated to make up 100 g of the sand and kaolinite tailings mixture.

To make up a 90/10 mixture

The dry amount of solids in the kaolinite tailings can be calculated from the moisture content of the kaolinite tailings.

The Malvern results were used to calculate the fraction of kaolinite tailings in the sand and fraction of sand in the kaolinite tailings.

% Sand in kaolinite tailings = v % > 45 µm x Solids in kaolinite tailings

% Kaolinite tailings in kaolinite tailings = v % <45 µm x Solids in kaolinite tailings

% Sand in sand = v % > 45 µm

% Kaolinite tailings in sand = v % < 45µm

To calculate the effective amount of sand required = (sand in sand + sand in kaolinite tailings)

To calculate the effective amount of kaolinite tailings required = (kaolinite tailings in kaolinite tailings + kaolinite tailings in the sand)

The density of the sand, the kaolinite tailings and the solids were used to convert the volumes into masses.

The relative density of the final mixture was calculated from the equivalent mass and volume and water was added to adjust the density.

The required amounts of kaolinite tailings and water were poured together in the shear device to give a total volume of approximately three litres. The sample was first mixed by hand and, after inserting the mixing blade to the required level, the sample was mixed at 510 rpm for the four different shear periods. Samples were drawn after 10 seconds, 5 minutes, 10 minutes and 20 minutes to perform rheology tests of the kaolinite mine tailings.

For calculating the mass of dry sand and kaolinite tailings required to make up the desired mix ratio:

- Add sand then kaolinite tailings together in the shear mixer. The sample was mixed by hand to obtain a homogeneous mixture for every 2 minutes, and then sheared in the shearing mixer for the required shearing period (5 minutes, 10 minutes and 20 minutes).
- Sufficient sub-sample was taken out of the mix by spoon for the shearing vane test and the particle size analysis, and the remainder for the slump measurement using the hand-held fifty-cent rhoemeter and slump meter.

3.4.5 Laponite

Laponite is a white, granular powder that, when mixed with water, turns into a transparent, jelly-like substance. Laponite is a synthetic disc-shaped crystalline colloid that is widely used to modify rheological properties of liquids in applications such as cosmetics, paints, and inks

so that understanding its yield stress is of considerable practical as well as fundamental importance (Herman, 2007). Laponite is sensitive to sample preparation procedures.

Laponite (hydrous sodium lithium magnesium silicate) is a synthetic crystalline layered silicate colloid with crystal structure and composition closely resembling the natural smectite clay hectorite (Herman, 2007).

Although laponite can recover its physical structure quickly, it is a very fragile material and requires a lot of caution when handled. The laponite material contains crystals of small particles and it is also defined as synthetic layered silicate (Sofra & Boger, 2000).

Laponite is used in the industry as a thickener in toothpastes, paints and cosmetics and is also well known for its highly thixotropic behaviour and shear thinning.

Apart from industrial applications, Laponite-in-water is considered to be a model system for the study of phenomena such as glass transition and gelation (Cipelletti & Ramos, 2005).

The motivation for using laponite is because previous researchers have used laponite (Clayton et al, 2003) as a typical yield stress materials.

3.4.5.1 Preparation of laponite

Laponite was mixed to the required concentrations using; a mechanical stirrer. The mixing procedure was based on weight as the dry density of laponite was not clearly known. The structure of laponite makes it difficult to mix as lumps forms easily. In order to achieve a smooth, bubble-free, consistent mix, laponite has to be added to clean tap water gradually while simultaneously stirring it, with the stirrer adjusted to a suitable speed.

Once all the material has been added, the mix needs to be agitated for 2 minutes to ensure consistency of the material in the mixing container. This is imperative as the material mixed in the same container needs to be homogenous.

3.5 OTHER MEASURED VARIABLES

3.5.1 Determination of relative density

Non-Newtonian fluid density and relative density were determined using the technique described below. The apparatus used are Top pan balance, volumetric flasks (3x 250 ml), water bottle and plastic funnel and municipality water. The procedures that were used is as follows

- ✓ Obtain three clean empty (dry) volumetric flasks and mark with numbers 1, 2 and 3.
- ✓ Weigh each of the empty bottles and record their masses (Weight M_1).
- ✓ Half fill the volumetric flasks with test material mixture after through mixing of the test material
- ✓ Weigh and record the mass of each flask with the mixture (Weight M_2).
- ✓ Fill the bottles carefully with water until the meniscus coincides with the graduated mark, weigh and record the mass of each flask (Weight M_3).
- ✓ Empty the volumetric flasks and clean thoroughly.
- ✓ Fill the bottles carefully with water until meniscus coincides with the graduated mark level.
- ✓ Weigh and record the mass of each flask (Weight M_4).
- ✓ Measure the temperature of the water
- ✓ Weights recorded will be:

This procedure was repeated for three times consecutively tests using three different flasks. The average of the three was then taken as the relative density of the non-Newtonian fluid. The relative density (S_m) can be defined as ρ/ρ_w and can be expressed as

$$S_m = \frac{\text{mass of slurry sample}}{\text{mass of equal volume of water}} = \frac{M_2 - M_1}{(M_3 - M_2) - (M_4 - M_1)}$$

3.9

where:

- M_2 – Mass of flask + mixture
- M_3 – Mass of flask + mixture + water

M_4 – Mass of flask + water

$M_2 - M_1$ – Mass of mixture only

$M_4 - M_1 - M_3 - M_2$ – Mass displaced by mixture.

$$\text{Mixture Relative Density } Rd = \left(\frac{DM}{1.9982} \right) \quad 3.10$$

$F = 1.9982$ is relative to the density (g/ml) of water at 20 °C

The Volumetric Concentration (in %) of material may also be calculated, provided that the specific gravity of the dry solids is accurately known. The concentration for the sample was calculated using the following equation:

$$\% C_v = \frac{(\text{Mixture Relative density} - 1)}{(\text{Material specific gravity} - 1)} \times 100 \quad 3.11$$

Note: The above formula can only be used when the dry density of the material is known e.g. kaolin and Kaolinite tailings and sand = 2.65.

The errors in the individual measurements of density and relative density with using a chemical balance were extremely small. Several relative density measurements were performed on each sample of slurry and the largest difference in these measurements was taken as being more representative of the true error. The largest error in such measurements was found to be 0.2 %.

3.5.2 Determination of moisture content

The following procedure was used for the determination of Kaolinite tailings and sand moisture content, using the oven:

- Weigh the mass of the glass dish.
- Weigh mass of glass dish and Kaolinite tailings and sand sample.

- Dry in the oven at 60 °C.
- Put dry material (kaolinite tailings or Kaolinite tailings and sand) and glass dish in the desiccators for a fortnight to absorb all moisture.
- Weigh the mass of dry Kaolinite tailings and sand glass dish.

This procedure was repeated for three times consecutively tests using three different pans. The average of the three was then taken as the relative moisture content of the non-Newtonian fluid.

3.5.3 Determination of quantities of a mixture

The first step towards the process of mixing was to determine the amount of powder and amount of water to be mixed for a certain concentration. Due to a mixture being used for the slump technique and the vane technique, it was obligatory to mix a large amount of material.

A 12-litre volume was used for the experiments and this amount was mixed in a 15-litre bucket. Before the material was considered for its quantities, it was essential to know whether the amount of powder with the amount of water has a known dry density, in which case this information was going to determine the method by which the material would be mixed. There are two methods that can be used to mix the material, namely mixing volume by total volume and weight/weight. If the dry density of the material is known, it is important to use the volume/volume method. When the dry density of the powder is unknown, then the mixture will be mixed weight/weight. The calculation for a concentration was as follows:

A 20 % concentration was used as the example for calculating the quantities required to make a certain mixture.

$$\begin{aligned} &= 0.20 \times 12000 \text{ ml} \\ &= 2400 \text{ ml} \end{aligned}$$

2.4 litres was then converted into a mass in order to measure the quantity required for a mix on the measuring mass scale.

The conversion of volume to mass was done by equation 3.13, as shown below (for when the dry density is known).

$$\text{Dry density} = \frac{\text{Mass}}{\text{Volume}} \quad 3.12$$

$$\begin{aligned} \text{Therefore, } 2.65 &= \frac{\text{Mass}}{2400 \text{ ml}} \\ &= 6360 \text{ g} \end{aligned}$$

Mass of powder to be mixed = 6360 g

$$\begin{aligned} \text{Volume of water in the bucket to be mixed} &= 12000 \text{ ml} - 2400 \text{ ml} \\ &= 9600 \text{ ml} \end{aligned}$$

After the preparation, the kaolin had to be left undisturbed for a period of three days to allow it to gain network structure, as specified in the literature.

For kaolinite tailings, the calculations for the concentration were handled differently; because of the water content in the fluid, moisture content measurement had to be performed to observe the quantity of water present in the fluid. It was then possible to determine whether water had to be added or removed to produce the desired concentration. The calculations were done in terms of mass and then converted to volume.

For a sample of 20 kg of kaolinite tailings and moisture content of 60 % at 60°C:

$$20000 \times 0.60 = 12000 \text{ g of water in the sample}$$

$$20000 - 12000 = 8000 \text{ g of kaolinite tailings in the sample}$$

By converting to volume (specific gravity of kaolinite tailings = $2.65 \times 10^3 \text{ kg/m}^3$)

$$\frac{8000}{2.65} = 3019 \text{ ml of kaolinite tailings}$$

$$\text{Total volume} = 3019 + 12000 = 15019 \text{ ml}$$

% concentration of kaolinite tailings = $\frac{3019}{15019} = 20 \%$

Finally, to convert to, for example, 18 %, the molarity formula, as shown below, was used to determine the amount of water to be added.

$$C_1 \times V_1 = C_2 \times V_2$$

3.13

After adding water, the non-Newtonian fluid was remixed and was ready for use straight away, unlike kaolin.

3.6 NON-NEWTONIAN FLUID TEMPERATURE

The non-Newtonian fluid temperature was measured by dipping a glass thermometer with mercury into the non-Newtonian fluid in the morning and in the evening when the non-Newtonian fluid was changed in the bucket. Essentially the non-Newtonian fluid maintained a temperature of about 20°C for the duration of the experimental work. The maximum rise in temperature during a run was ± 1°C, but the rise was found to have a negligible effect on the actual test data. The kaolin and kaolinite tailings tests were done during the winter season while the test for the kaolinite mine tailings was done in the summer season. The Kaolinite tailings and sand temperature maintained an average constant temperature of 20°C during the testing.

3.7 SUMARRY OF THE RANGE OF MATERIALS TESTED

The values of yield stress obtained by the vane shear technique are shown in Table 3.3 for the kaolin, kaolinite tailing and the Laponite materials as well as Table 3.4 for the kaolinite mine tailings (kaolinite tailings and sand) material.

Table 3. 4: Yield stress results for all the materials and concentration using the vane technique

Materials	Concentrations (%v/v)	Yield stress (Nm ⁻²)
Kaolin	14	34
	16	49
	18	71
	20	136
Kaolinite tailing	14	51
	16	118
	18	216
	20	301
Laponite	4	100
	5	175
	6	243
	7	483

Concerning the concentration of solids used for the vane technique, as seen in Table 3.4, a distinction can be made between the materials when using the vane (FL 100 Z4) technique. The value of the yield stresses increases with an increase in the concentration of solids for all concentrations. In the sensitivity test (see Table 3.5), it was observed, when using the kaolinite tailings plus that the value of yield stress increased with an increase in the shearing period when the Kaolinite tailings and sand were sheared.

This discrepancy may be attributed to the breakdown of some of the assumptions discussed in Chapter 3 concerning vane theory, for less concentrated systems in which the contribution of the viscous stress might become significant in comparison with the network stress and where the shear stress distribution at yielding might not be uniform as assumed. Another reason could well be related to the progressive failure of the material, i.e., the yielding takes place mostly in front of each blade of the vane instead of at the edges. This observed difference was, however, not unexpected since the vane device at the present development stage was originally designed to measure the mechanical strength of materials that, in fact were highly concentrated suspensions.

Table 3. 5: Yield stress results for all the materials and concentration using the vane technique

Mixtures	Densities (Kg/m ³)	Shear periods (mins)	Yield stress (Pa)
90:10	1700	5	41
90:10	1700	10	62
90:10	1700	20	93
90:10	1750	5	74
90:10	1750	10	203
90:10	1750	20	356
90:10	1800	5	248
90:10	1800	10	309
90:10	1800	20	398
80:20	1600	5	67
80:20	1600	10	79
80:20	1600	20	82
80:20	1700	5	130
80:20	1700	10	161
80:20	1700	20	192
80:20	1800	5	264
80:20	1800	10	267
80:20	1800	20	269
70:30	1400	5	38
70:30	1400	10	40
70:30	1400	20	46
70:30	1500	5	59
70:30	1500	10	70
70:30	1500	20	87
70:30	1600	5	144
70:30	1600	10	168
70:30	1600	20	177

When loading a material during rheological measurement using the vane technique in measuring yield stress, it is important to load a fresh sample (not a broken down material structure) in each occurrence.

The maximum in the torque curve developed in the sample as the vane shear rheometer (FL 100 Z4) moves the spindle to meet the designated rotational speed, shear stress developed in the sample firstly, the sample deforms elastically due to the stretching of the bonds in the network structure. At some point, the network begins to break under the shear stresses when some of the bonds reach the elastic limit and the development of viscoelasticity is represented by the departure from linearity of the torque-time profile.

The reason for using a low torque in both the low and high concentration and the sensitivity test is that satisfactory yield stress measurements can be achieved only if the vane is rotated at sufficiently low speeds. At too high a rotational speed, significant viscous resistance, together with instrument inertia and insufficient damping, may introduce errors to the measured maximum torque and hence to the calculated yield stress.

The effect of rotational speed was studied in detail over a range of speeds from 0.1 to 256 rpm (Nguyen and Boger, 1983 and 1985). On the basis of these effects, it was concluded that the low operating range of vane rotational speeds (0.3 rpm) should be used in this work.

3.8 EXPERIMENTAL ERRORS

Any experimental measurement is subject to some degree of uncertainty or experimental error, excluding the tally of discrete objects. A primary aim is to identify the reliability of the measurements. A secondary goal is to identify limitations in the physical property measurements. Thus, steps must be taken to evaluate measurement errors. There are three steps in error analyses of most experiments. The first is the propagation of errors which can be performed before the experiment is performed; the second is the determination of the errors which occur during the experiment and, lastly, the comparison with accepted values performed after the experiment is completed (Poshusta, 2004 and Mbiya, 2003).

Every experimental result is subject to error. One can attempt to minimize errors but cannot eliminate them completely (Garland & Nibler, 1989).

3.8.1 Error theory

There are three types of errors, namely gross errors, systematic errors and random errors.

3.8.2 Gross error

Gross errors are due to blunders, equipment failure and power failure. A gross error is an immediate cause for rejection of measurements (Benzinger & Aksay, 1999; Garland & Nibler, 1989 and Nkomo, 2005).

3.8.3 Systematic error or cumulative error

Systematic errors or cumulative errors occur as a result of a constant bias in an experimental measurement. The clearest sources of systematic error in the case of both slump measurement and vane rheometry are due to known conditions. These conditions might be (Mbiya, 2003 and Nkomo, 2005)

- Natural (temperature variation due to viscous heating, faulty calibration, effect of slip)
- Instrumental (calibration graduation, incorrect alignment of the experimental setup, etc.)
- Personal (poor methods and inability of the experimenter to take correct readings)

3.8.4 Random error

Random errors are those errors that are due to chance variation. Most experimental processes meet with minor variations occurring by chance from event to event and following no systematic trend. They affect the precision of a measurement. Precision is sometimes called repeatability or reproducibility and is a measure of the variation between repeated measurements. In most cases, precision is improved by increasing the sample size (for example, number of repeated measurements). Thus, averaging repeated measurements

would often be the precision of the measurements provided $\left| \frac{X_1}{\bar{X}} \right| < 2$, for \bar{X} is the arithmetic mean and X_1 is the measurement (Mbiya, 2003 and Garland & Nibler, 1989).

Statistical analysis of experimental data

Statistics provide the essential tools for quantifying random errors, as well as assessing their effect on the conclusions drawn from the experimental data. The quality of the final research outputs from any statistical experiment depends on the quality of the raw experimental data. The most crucial abstract statistics about the precision and accuracy of experimental measurements are grouped into two categories: those that measure the precision of the measurements and those that measure the accuracy of the results (Mbiya, 2003 and Nkomo, 2005)

Precision of the measurements

The most crucial abstract statistics that have been developed to measure the precision of repeated measurements are

- The measure of central tendency, which is usually characterised by the arithmetic mean (denoted by \bar{X}) and is defined as follows:

$$\bar{X} = \frac{1}{N} \sum X_i$$

3.1

N is the number of measurements and X_i is the experimental measurement. For a large number of measurements ($N \geq 20$), the mean value \bar{X} is the most probable value.

- The measure of spreading, which is usually characterised by the standard deviation and by its variance (denoted s or s^2 respectively). The standard deviation (also referred to as the mean square deviation) is the measure of the width of the spread about the mean value. The less precise the measurement, the broader the frequency distribution and the larger the standard deviation and variance. For a finitely large sample ($N \geq 20$), the standard deviation and variance are accurately presented by Equations 3.2 and 3.3, respectively

$$S = \sqrt{\frac{\sum_{i=1}^N (X_i - \bar{X})^2}{N-1}} \tag{3.2}$$

The variance is the standard deviation squared,

$$S^2 = \frac{\sum_{i=1}^N (X_i - \bar{X})^2}{N-1} \tag{3.3}$$

The precision or the uncertainty of the mean value is presented by the standard deviation of the mean value (which is also referred to as the standard error, $S_{\bar{X}}$), and it is given by the following

$$S_{\bar{X}} = \frac{s}{\sqrt{N}} \tag{3.4}$$

The value of the overall standard deviation (s) is calculated from Equation 3.4. For non-normal distribution, the results are usually reported as $\bar{X} \pm \alpha$, where α is the confidence limit. This confidence limit α defines the range on both sides of the mean within which the true average value can be expected to be found with a given level of confidence (that is, the value within which the magnitude of the mean is certain to lie with a given level confidence). The confidence level and number of measurements (N) are often reported in brackets, for example 25.325 ± 10.427 (95%, $N = 30$). (Garland & Nibler, 1989). Calculation of α is given by

$$\alpha = \pm \frac{t_s}{\sqrt{N}} = \pm t_{s\bar{X}} \tag{3.5}$$

The value of t_s depends on both the type of frequency distribution and the level of confidence assumed for the calculation. For a large sample ($N \geq 20$) following the normal frequency distribution, $t = 1, 2$ and 3 for the confidence levels of 68.3 %, 95 % and 99 % respectively. It can be seen from Equation 3.5 that the standard error (s_x) is given by:

$$s_x = \pm \frac{\alpha}{t}$$

3.6

Finally, the measure of shapewhich is usually characterised by its skewness (that is, the frequency distribution's degree of distribution from symmetry) and by its kurtosis, α (i.e., the degree of concentration of data around the mode, the value with highest frequency and kurtosis is also referred to as peakedness). The position differences between the mean, median and mode (definition given in the glossary) are used to create arithmetic measures of skewness. In the case of zero skewness ($SK = 0$), there is a normal distribution where the mean is equal to both the mode and the median. For positive skewness ($SK > 0$), the frequency distribution tapers off more slowly toward the right of the mode. For negative skewness ($SK < 0$), the frequency distribution decreases more slowly towards the left of the mode. A formula exist to measure kurtosis, however, the extent of kurtosis can easily be determined by observing the frequency curve. The flatter the curve, the greater the spread of the data and, therefore, the larger the standard distribution.

Propagation of error

When many experiments measure the same physical quality and give a set of answers \overline{X}_1 with different errors α_1 , the best estimates of $\overline{X}_{overall}$ and its accuracy $\alpha_{overall}$ are found by statistically averaging the combined effect of the "N" number of the statistical parameter obtained from analysis of different sets of experimental measurements. This is done as follows:

- The most probable value or the mean ($\overline{X}_{overall}$) of the combined observation of N arithmetic averages (\overline{X} for 1. 2. 3....N) and is given by:

$$\overline{X}_{overall} = \frac{\sum_{i=1}^N \overline{X}}{\sum_{i=1}^N \frac{1}{\alpha_1^2}}$$

3.7

where the weighting function is the reciprocal of the square of the corresponding confidence limit, α_1 .

- The standard deviation (α_{overall}) of the mean for the combined observations of N confidence limits α_i (α_i for $i = 1, 2, 3, \dots, N$) is given by:

$$\frac{1}{\alpha_{\text{overall}}^2} = \sum_{i=1}^N \frac{1}{\alpha_i^2}$$

3.8

Thus each experiment is weighted by $\frac{1}{\alpha_i^2}$. In some sense, $\frac{1}{\alpha_i^2}$ gives the measure of the information quality of that experiment. The combined measure of dispersion α_{overall} or S_{overall} is also improved relative to any individual set and is closer to the most precise original measurement (Benzinger & Askay, 2004 and Garland & Nibler, 1989).

3.9 SUMMARY

Apparatus for the reliable collection of slump test and the vane test data for non- Newtonian fluids over yield stress measurement was constructed and commissioned. The mechanical equipment and apparatus used for the experimental work were the slump meter, the hand-held cylinder, Malvern moisture analyser, Malvern instrument (Mastersizer 2000) and MC1 Rheometer. The apparatus has been described fully and its use has enabled testing of the same non-Newtonian fluid over a wide range of rheological properties.

Calibration and test procedures were developed for the apparatus, so that valid and accurate yield stress data could be collected and the relevant non-Newtonian fluid properties could be measured.

The test technique for the shear vane test that was used was the constant rate procedure. The non-Newtonian fluid was sheared at a very low shear rate (0.3 rpm) and the shear rate measured. The effect of lifting speed and position of slump measurement on the value of yield stress were observed to determine both the even and the uneven nature on the top of the slump materials: this could be attributed to different materials used and the amount of moisture contained in the materials.

The solid materials used for non-Newtonian fluids preparation were kaolin, laponite, sand and kaolinite tailings. These non-Newtonian fluids were then tested in the apparatus and a database of the non-Newtonian fluid slump test and the shear vane test was compiled. The test results are presented in Chapter 4 and in the Appendix. Details of the test conditions and non-Newtonian fluid properties are presented for each test, together with a graphical presentation of yield stress as a function of lifting speed for the data, together with other relevant graphs.

Types of experimental errors were discussed and determined for the various types of experiments. Corrections to the experimental data obtained were needed, as precautionary measures were taken in advance to remove systematic experimental errors. The experimental errors pertaining to the apparatus and measurement methods have been analysed and quantified and were found to be within acceptable limits.

This database was used to evaluate the four models (approximate cylinder model, lump model, cone model and the cylinder model), the effect of lift speed, stability, position on slump measurement, etc. for the prediction of the flow behaviour of non-Newtonian fluids. This will be presented in Chapter 4 (Results and discussion).

CHAPTER 4

CHAPTER 4

RESULTS AND DISCUSSION

4.1 INTRODUCTION

This chapter provides a description of the procedures used in the analysis of results, and the discussions pertaining to the experimental results. The main aim of this chapter is to analyse, compare and discuss the test results obtained from the slump measurements and vane technique. The following aspects are discussed:

- Effect of position of slump measurement of yield stress.
- Validation of lump model.
- Effect of lift speed on measurement of yield stress.
- Effect of stability on measurement of yield stress.
- Effect of wall surface materials on measurement of yield stress.
- Effect of geometry on measurement of yield stress.
- Effect of slip on measurement of yield stress

Two sets of slump tests (with and without silicone spray) were conducted for every material to validate the effect of slip on the value of yield stress. The yield stress from the slump measurement was calculated using the approximate cylinder model, the lump model and the cylinder model.

The vane technique was used as the reference technique for calculating the yield stress. It is clear from the literature that the vane technique is the most widely used technique for measuring the yield stress. Standard statistical techniques were used in the analysis and comparison of the data sets of the experimental results, namely: the arithmetic mean and the standard deviation.

4.2 EFFECT OF POSITION OF SLUMP MEASUREMENT ON THE YIELD STRESS

One of the contradictions found in Chapter 2 (Section 2.13) is the point of measurement to determine the slump height. Conventionally, the slump height is measured at the highest point. (SABS, 1994). Pashias et al., (1996) smoothened the top of the cylinder geometry adapted for the conical slump test. They measured the midpoint of the slump height and lifted the cylinder slowly and evenly, but there was no evidence of the evaluation of the effect of position on slump measurement on the value of yield stress in their work. Gawu and Fourie (2004) measured the slump height at three lowest points in their work, but did not present enough evidence on effect of position of slump measurement on the yield stress value. The point where the slump height was measured was considered an important objective.

In this work, the slump measurements were taken in the highest and lowest points of the slumped material to establish what the effect of height variation would have on the value of the yield stress using the slump meter (cone and cylinder geometry) and the hand-held cylinder as shown in Figure 4.1. For a few of the slump tests the middle points of the slump heights were measured.

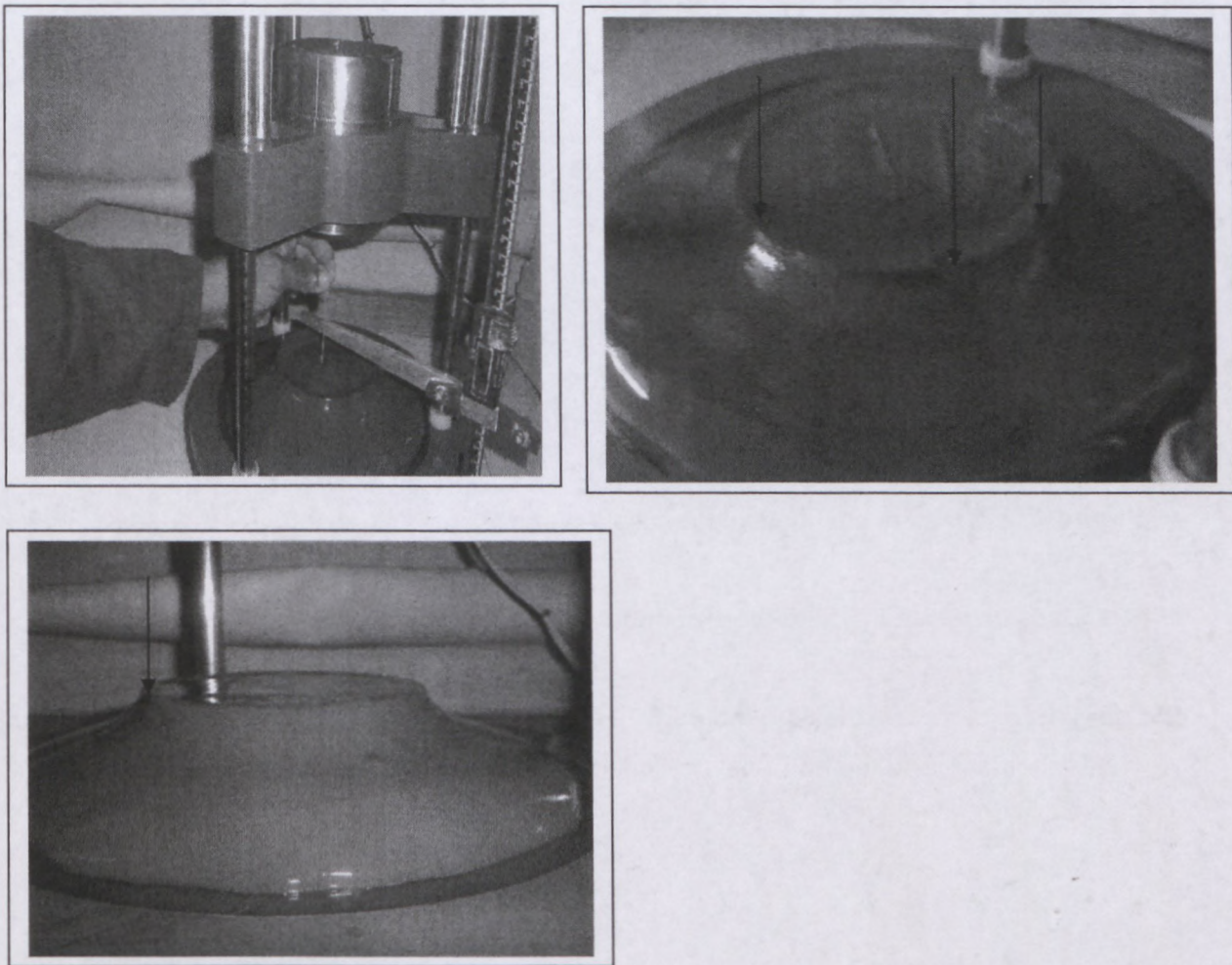


Figure 4. 1: Effect of slump height measuring position: (a) midpoint, (b) three lowest points and (c) highest point.

Figure 4.2, below, shows slump results for the cylinder geometry (stainless steel), cone geometry (stainless steel) and cylinder geometry (PVC) for various slump height points for 20 % v/v kaolinite tailings.

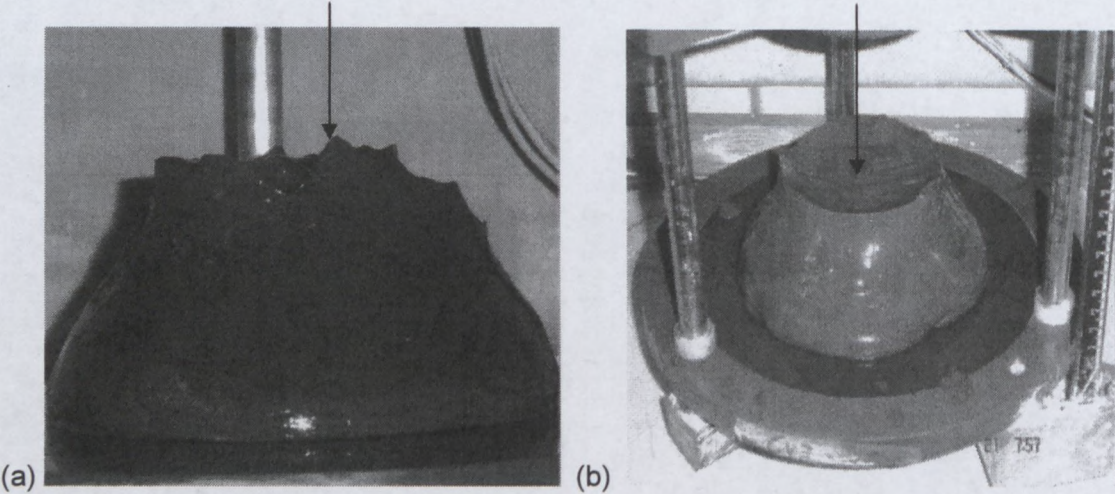


Figure 4. 2: Effect of slump height measuring position: (a) highest point, (b) middle point.

The surface on which the tests were conducted was made of PVC.

Table 4.1 contains the measurement of various positions of slump for the cone geometry, cylinder geometry and the hand-held cylinder using 20 % v/v kaolinite tailings.

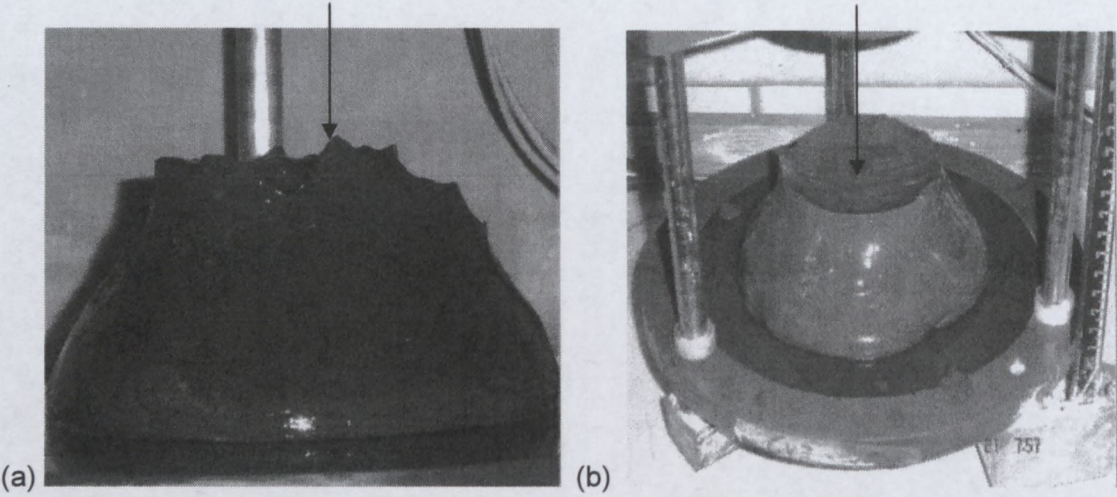


Figure 4. 2: Effect of slump height measuring position: (a) highest point, (b) middle point.

The surface on which the tests were conducted was made of PVC.

Table 4.1 contains the measurement of various positions of slump for the cone geometry, cylinder geometry and the hand-held cylinder using 20 % v/v kaolinite tailings.

Table 4. 1: Effect of position of slump measurement on yield stress

				Vane	Equations:		
Relative density		1.32		τ_y			
Density	(Kg/m ³)	1320		62.40			
$\dot{\gamma}$	(m.s ⁻¹)	9.81			$S' = \frac{h}{H}$	$\tau_y = 0.5(1 - S')e^{\sqrt{5}(s')}$	
Cone geometry : Stainless steel							Lump Model
Heights	Speed (mm.s ⁻¹)	Time	H (mm)	H _f (mm)	h (mm)	s'	τ_y
Highest	5.43	6.51	150	35.34	114.66	0.76	58.53
Middle	5.27	6.51	150	34.29	115.71	0.77	56.11
Lowest	5.22	6.51	150	33.95	116.05	0.77	55.33
Average						0.77	56.66
St. Deviation						0.00	1.36
% error						0.51%	2.40%
Cylinder geometry : Stainless steel							Lump Model
Heights	Speed (mm.s ⁻¹)	Time	H (mm)	H _f (mm)	h (mm)	s'	τ_y
Highest	5.83	6.42	100	37.45	62.55	0.63	78.89
Middle	5.66	6.42	100	36.36	64.44	0.64	75.16
Lowest	5.54	6.42	100	35.56	63.64	0.64	72.5
Average						0.64	75.52
St. Deviation						0.01	2.62
% error						1.22%	3.47%
Cone geometry : PVC							Lump Model
Heights	Speed (mm.s ⁻¹)	Time	H (mm)	H _f (mm)	h (mm)	s'	τ_y
Highest	6.34	5.43	150	34.44	115.56	0.77	56.45
Middle	6.14	5.43	150	33.36	116.64	0.78	54
Lowest	5.55	5.43	150	30.12	119.88	0.80	46.97
Average						0.78	52.47
St. Deviation						0.01	4.02
% error						1.56%	7.66%
Cylinder geometry : PVC							Lump Model
Heights	Speed (mm.s ⁻¹)	Time	H (mm)	H _f (mm)	h (mm)	s'	τ_y
Highest	7.24	4.8	100	34.77	65.23	0.65	69.92
Middle	7.13	4.8	100	34.2	65.8	0.66	68.1
Lowest	7.04	4.8	100	33.8	66.2	0.66	66.84
Average						0.66	68.29
St. Deviation						0.00	1.26
% error						0.61%	2.36%
Hand-held (fifty cent rheometer)							Lump Model
Heights	Speed (mm.s ⁻¹)	Time	H (mm)	H _f (mm)	h (mm)	s'	τ_y
Highest	11.81	2.63	75	31.07	43.93	0.59	70.12
Middle	11.62	2.63	75	30.56	44.44	0.59	66.84
Lowest	11.45	2.63	75	30.12	44.88	0.60	66.65
Average						0.59	67.87
St. Deviation						0.01	1.59
% error						0.87%	1.84%

Table 4.2 shows results from the repeatability test using the hand-held cylinder for kaolin, kaolinite tailings and laponite materials.

Table 4. 2: The repeatability of slump height and yield stress values using the hand-held cylinder for kaolin, kaolinite tailings and laponite materials.

	Kaolin				Kaolinite tailings				Mid-point				Laponite			
	14%	16%	18%	20%	14%	16%	18%	20%	4%	5%	6%	7%				
	h (mm)	h (mm)	h (mm)	h (mm)	h (mm)	h (mm)	h (mm)	h (mm)	h (mm)	h (mm)	h (mm)	h (mm)				
	36.91	26.25	17.77	11.06	32.04	22	25.02	26.7	36	26	8	1				
	35.7	28.7	16.52	9.71	31.6	24	25.54	27.83	35	26	10	2				
	36.95	27.1	16.2	12.28	32.84	23	27.61	28.08	40	26	13	2				
	36.52	27.43	16.83	11.08	32.16	23	26.06	27.54	37	26	10.33	1.67				
	0.71	0.93	0.68	1.13	0.51	0.82	1.12	0.6	2.16	0	2.05	0.47				
% error	2%	3%	4%	10%	2%	4%	4%	2%	6%	0%	20%	28%				
	14%	16%	18%	20%	14%	16%	18%	20%	4%	5%	6%	7%				
	τ_y	τ_y	τ_y	τ_y	τ_y	τ_y	τ_y	τ_y	τ_y	τ_y	τ_y	τ_y				
	136.16	193.07	245.64	330.63	161.03	181.43	222.3	245.1	116.17	157.48	260.61	350.15				
	141.44	181.56	253.98	348.3	164.89	212.42	221.37	239.4	108.99	157.48	245.69	331.36				
	135.98	189.88	256.17	312.86	167.04	218.21	224.55	235.6	102	157.48	225.88	331.36				
	137.86	188.17	251.93	330.6	164.32	204.02	222.74	240.03	109.05	157.48	244.06	337.62				
	3.1	5.94	5.56	17.72	2.48	16.15	1.33	3.9	5.79	0	14.22	8.86				
% error	2%	3%	2%	5%	2%	8%	1%	2%	5%	0%	6%	3%				

Figure 4.1 is an example of kaolinite tailings being tested using the cone and cylinder geometries. For the 150 mm cone, the minimum value of slump height was 33 mm and the maximum 42 mm. The maximum value of dimensionless slump was 0.62 and the minimum value was 0.60 with a corresponding maximum yield stress of 148 Pa and minimum yield stress of 56 Pa.

For the cylinder geometry, the minimum value of slump height was 34 mm and the maximum value was 36 mm. These measurements correspond to a maximum yield stress of 114 Pa and minimum yield stress of 64 Pa.

The minimum value of slump was 30 mm and the maximum value was 31 mm for the hand-held cylinder. These values correspond to a minimum yield stress of 58 Pa and maximum yield stress of 72 Pa.

The difference between the highest point and lowest point was measured to the accuracy of 0.5 mm for all the geometries and the hand-held cylinder, as stated in the previous chapter (Chapter 3), and taken as the representative slump height.

The variance for the yield stress values when using the cone geometry, cylinder geometry and the hand-held cylinder was $\pm 7\%$ when using the lump predictive model for all the measurements.

It can be seen in Table 4.1 that the slump heights and the values of yield stresses are very close to the maximum deviation of 8%.

Further tests were conducted in which the middle and the highest points were used, as shown in Figure 4.2, to determine the effect of position of the slump measurement when using kaolinite tailings. A cone geometry (stainless steel and PVC) and the hand-held cylinder were used (see Figure 4.2). A typical example is the 30 % v/v kaolinite tailings where, for the 100 mm cylinder, the maximum value was 48 mm and the minimum value of slump was 38 mm. These values correspond to a maximum yield stress of 278 Pa and a minimum yield stress of 238 Pa, which is a difference of 17 %. At 22 % v/v the difference in the value of yield stress was observed to be 24 %.

The effect of position on the slump where the slump height is measured was observed to vary according to the material. It seems as though different materials will have different slump-surfaces when tested. When they are uneven, this could have a significant effect on the value of the yield stress, depending on where the slump height is measured.

It was observed that, the cone geometry seems to have a more uneven surface than the cylinder geometry and the hand-held cylinder as shown in Figure 4.2.

Finally, it is recommended that the highest point be used for making accurate yield stress measurements using the slump technique. This work affirmed that the measurement of the highest point gives the values of yield stress comparable to that measured with the vane.

4.3 VALIDATION OF LUMP MODEL ON YIELD STRESS

The model used for measuring the yield stress from a conical slump was first employed by Murata in 1984 and was later corrected by Schowalter and Christensen (1998) to evaluate the workability and consistency of fresh concrete. The slump test was first adapted to a cylindrical geometry by Chandler (1986). It was adopted by Pashias et al., (1996) for a cylindrical geometry because of its simplicity. The cylinder model is generalised for any size cylinder.

Pashias et al., (1996) used the cone model to develop a simple relationship between the dimensionless slump and the dimensionless yield stress; their theoretical model is derived from a relationship between the pressure distribution and the stress distribution in a vertical cylinder composed of an incompressible material. The model assumes that all the horizontal planes remain horizontal, that is, the interface layer between yielded and unyielded material remains flat. In this development, the amount of the cylinder sample height reduced from the original height is referred to as the slump height.

When comparing the theoretical approach developed by Pashias et al., (1996), they predicted a dimensionless yield stress value up to 0.15 whereas Saak et al., (2004) when using the analytical technique predicted the dimensionless yield stress value up to 0.32. They observed that beyond the 0.15 dimensionless yield stress value the exact solution deviates from the experimental result.

Hallborn presented the lump model in 2005. The test materials used were zinc tailings and a fine alumina powder. This lump model was found to make better yield predictions than the cylinder model, particularly at low slumps (Hallborn, 2005). It is based on this that the validation of the lump model on the yield stress was prompted for investigation in this study.

The various materials (kaolin, kaolinite tailings, kaolinite mine tailings and laponite) were measured, using the shear vane rheometer immediately after mixing/shearing. The yield stress was measured using a controlled shear rate.

The slump data is represented in Tables A1 to A32 and Tables B1 to B32 for the slump meter and hand-held cylinder respectively in Appendices A and B.

Figure 4.3 illustrates the dimensionless slump height as a function of dimensionless yield stress for various suspensions (kaolin, kaolinite tailings, laponite and kaolinite mine tailings), along with the four theoretical predictive models, the lump, cylinder, cone and approximate cylinder models.

The slump test results using the hand-held cylinder as shown in Figure 4.3 was compared with data from previously published literature. In Figure 4.3, a dimensionless slump height of one means that there is no slumping while a dimensionless slump height of 0 corresponds to complete slumping. The dimensionless yield stress values were determined directly from the vane technique, while the dimensionless slump height values were determined directly from the slump height.

All the materials were tested using the mechanical slump meter as well as the stainless steel hand-held cylinder and results for the materials are presented in Figure 4.3. In Figure 4.4, the hand-held cylinder data using the lump model to calculate the yield stress is depicted. The values of yield stress obtained by the vane shear technique were used as a reference.

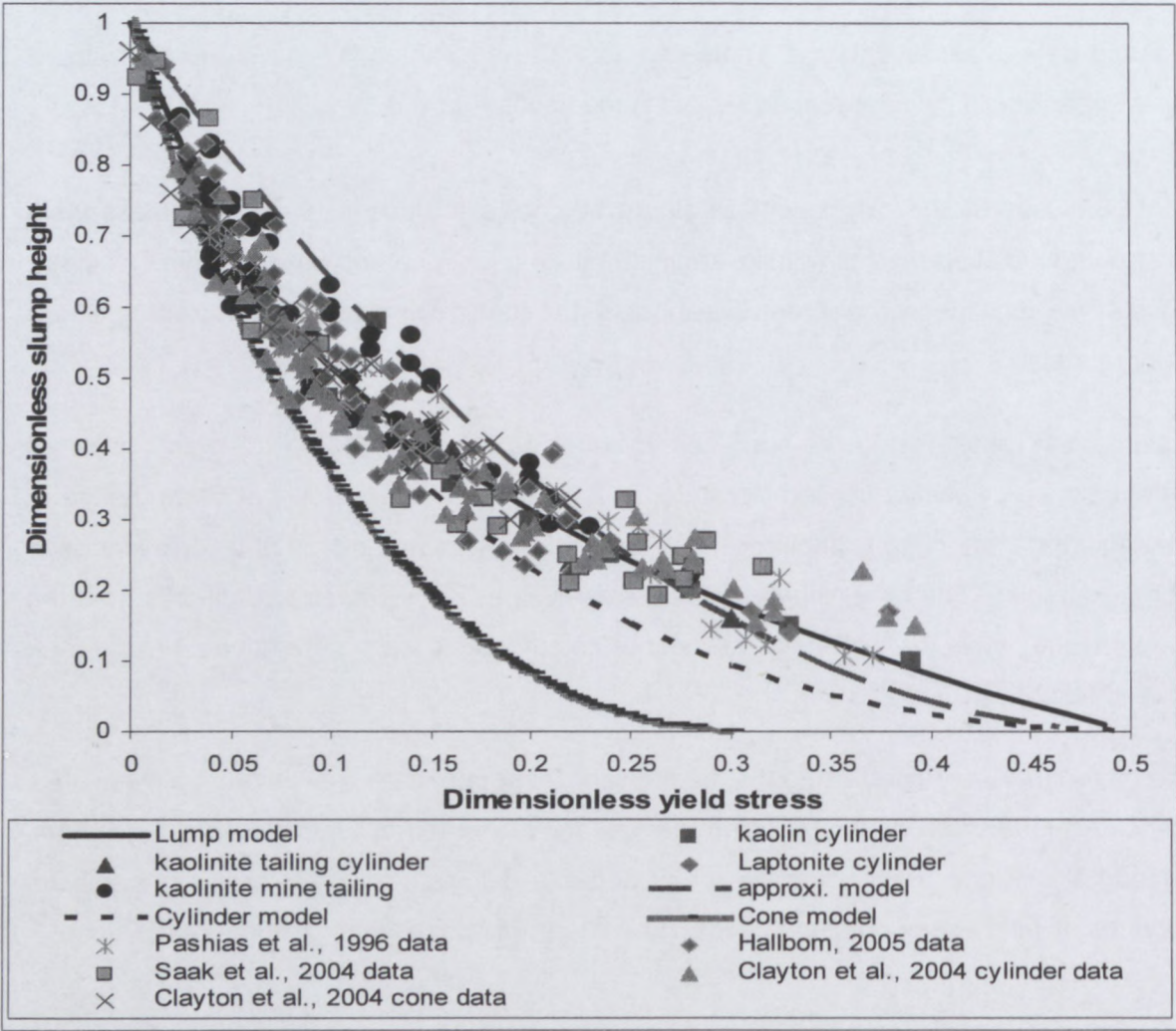


Figure 4. 3: Validation of Lump model for Hand-held cylinder

Figure 4.3 shows that, the approximate cylinder model over-predicts for dimensionless yield stress values ranging from 0 to 0.25. At higher dimensionless yield stress, the cylinder model under-predicted the data for dimensionless yield stresses ranging from 0.23 to 0.38.

The lump model fits the data very well over the range of slump heights (0 to 0.4) tested. The cylinder model fits the data at relatively medium slump heights, while the approximate cylinder model slightly under predicted the data at low to medium dimensionless yield stresses, but surprisingly, at higher dimensionless yield stresses (0.25 to 0.34), the approximate cylinder predicted the laponite data accurately. The cone model fits the data very well over the range tested at low dimensionless yield stresses (0.01 to 0.07) but at high dimensionless yield stresses

the cone model deviates from the data. The cone model performed poorly in relation to the relevant experimental data (which was measured with the cone geometry). It is difficult to fill the cone geometry properly with very viscous fluids and this could be one explanation for the discrepancy.

At low dimensionless yield stresses, the diameter of the top portion of the slump material was the same as the bottom diameter of the cone geometry, as shown in the previous chapter (Chapter 3, Figure 3.10) for the kaolinite mine tailings 18% v/v. The cone model assumes that the top portion of the slump material is unchanged, retaining the shape of the cone. Figure 3.10 shows that the top part of the sample did not yield when the cone was lifted.

In comparing the data from previous literature and the experimental data as shown in Figure 4.3, it is evident that the lump model predicted the yield stress well for all the data (0.01 to 0.4).

Figure 4.4, below, presents a plot of the dimensionless yield stress (vane test) as a function of the dimensionless yield stress (slump test) for all the materials tested (kaolin, kaolinite tailings and kaolinite mine tailings). In Figure 4.4, the hand-held cylinder data, using the lump model to calculate the yield stress, is depicted.

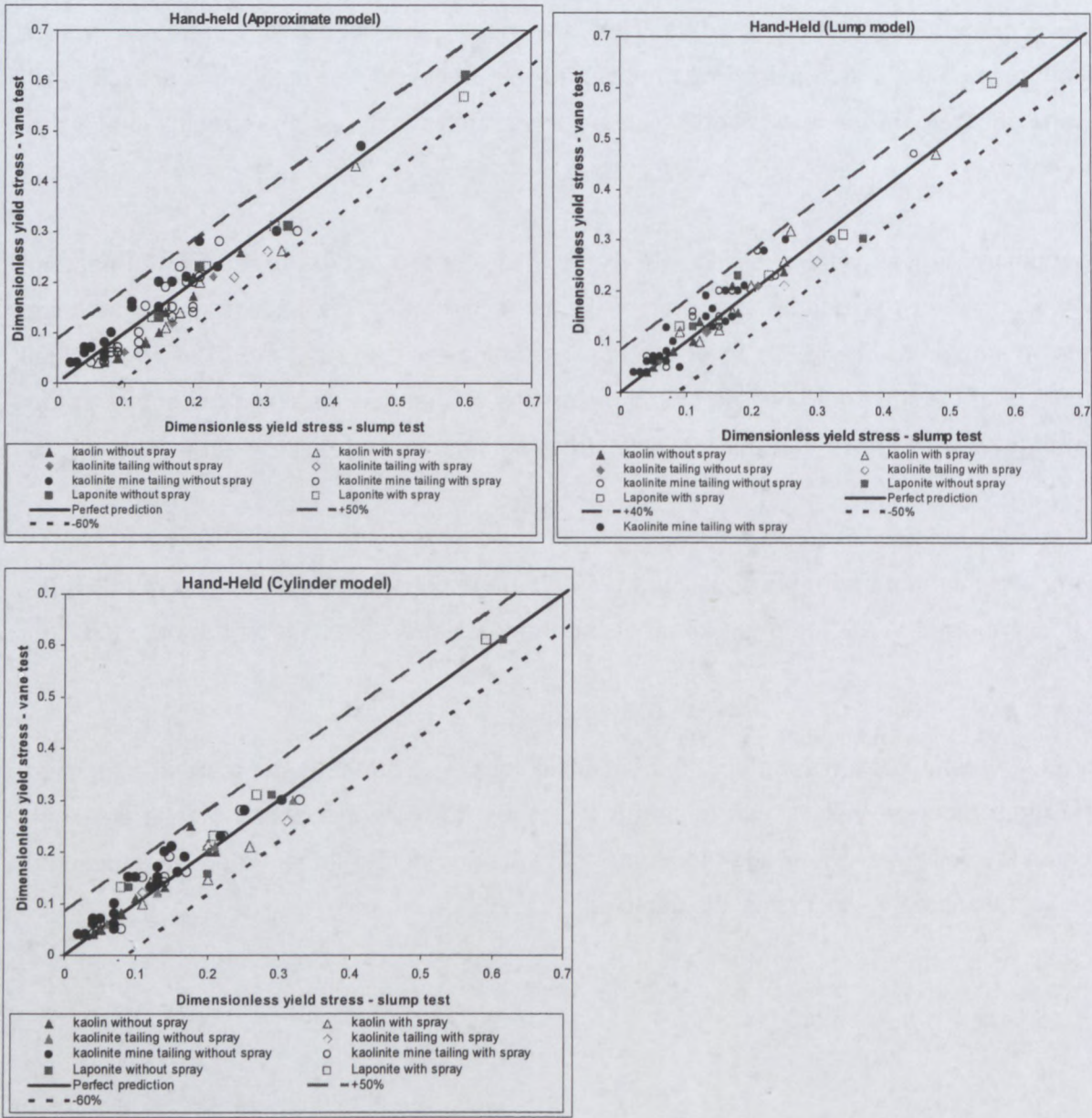


Figure 4. 4: Vane-measured yield stress compared with slump-calculated yield stress for the hand-held cylinder using the approximate cylinder, lump and cylinder model

The accuracy of the cone and cylinder slump models was assessed by comparing the yield stress determined using the vane technique with the yield stress determined via the slump test, as shown in Figure 4.4. The slump test gave good results compared to the vane data.

Table 4.3, below, presents a summary of the comparison of the models shown in Figure 4.4. The dimensionless yield stress values using the approximate cylinder, cylinder and lump

models were summarised together for each kaolin, laponite, kaolinite tailings and kaolinite mine tailings (kaolinite tailings and sand) to obtain Table 4.3.

Table 4. 3: Summary of validation of lump model using hand-held cylinder

Models	Ave. τ_y 'slump	Min τ_y 'slump	Max τ_y 'slump	St dev τ_y 'slump
Approximate Cylinder	0.16	0.04	0.48	60
Lump	0.11	0.01	0.33	50
Cylinder	0.12	0.01	0.44	60

Table D3 (summary for comparison of model) in Appendix D shows the summary for the comparison of models using the cone and cylinder geometry. The results of the investigation imply that the hand-held cylinder was best described in this work using the lump model from other theoretical predictive models (approximate cylinder model and the cylinder model) for this research and would be recommended for industrial applications and further research purposes.

Hallbom (2005) compared the lump and cylinder models in the measurement of tailings and found that, the lump model produces better results at low slump values than cylinder model. Haldenwang et al., (2007) compared the three models and found that, for most of the test however the lump model performed well over dimensionless yield stress values of 0.1 – 0.3. They also observed that the lump model seems to predict the value of yield stress better than the cylinder model and the approximate cylinder model. This work agrees with the work of Hallbom, (2005) and Haldenwang et al., (2007).

This work agrees with the work of Pashias et al., (1996), Clayton et al.,(2003) and Saak et al., (2004) when using the cylinder model, they said that the cylinder model accurately predicts the relationship between vane yield stress and cylinder slump height. They also said that the cylinder model is most accurate when the dimensionless yield stress is relatively low and the slump height is large.

In summary, this work confirmed that:

- The predictions were generally good across the whole range.
- The cylinder model gave better result than the approximate cylinder model.
- The lump model is an improvement over all previous models.

4.4 EFFECT OF LIFT SPEED ON YIELD STRESS

Viscosity and inertia effects do play a role in the slump at stoppage. This, in particular, means that the slump is affected by the lift velocity of the geometries of the slump meter and hand-held cylinder

Although it is difficult to propose a general demonstration for it, it seems reasonable to agree that viscous effects do play a role. Actually, for sufficiently slow flows, the yielding regions in the sample stop flowing when the yielding criterion is reached precisely. The unyielding regions keep their initial shape, so that the final sample shape should basically depend on the yield stress value and the initial shape of the material.

Figures 4.5 to 4.7, below, show plots of yield stress as a function of lifting speed (lump model) for three materials using a stainless steel cylinder, cone and the hand-held cylinder.

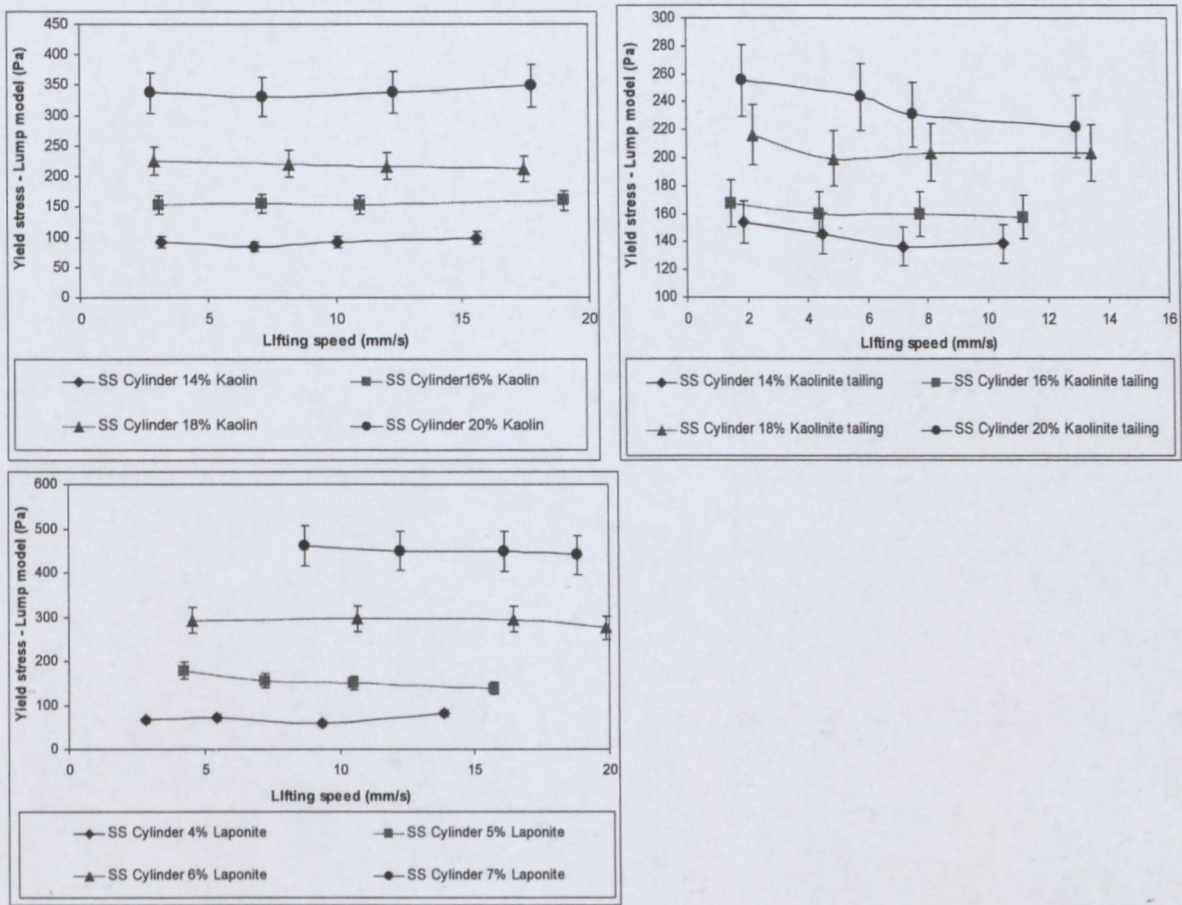


Figure 4. 5: The effect of lift speed on yield stress (lump model) for three materials using a stainless steel cylinder (Error bars +/- 15 %)

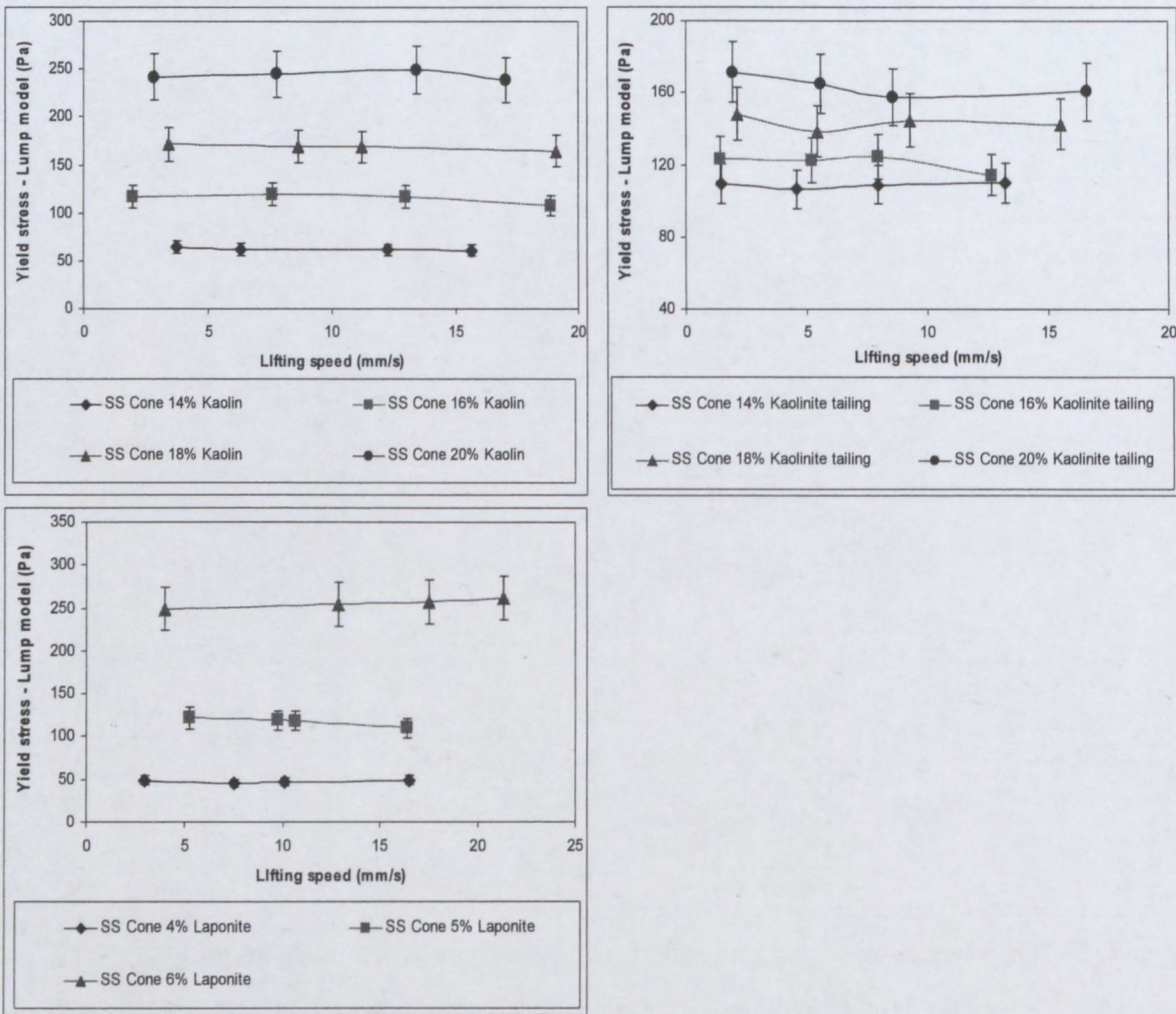


Figure 4. 6: The effect of lift speed on yield stress (lump model) for three materials using a stainless steel cone (Error bars +/- 15 %)

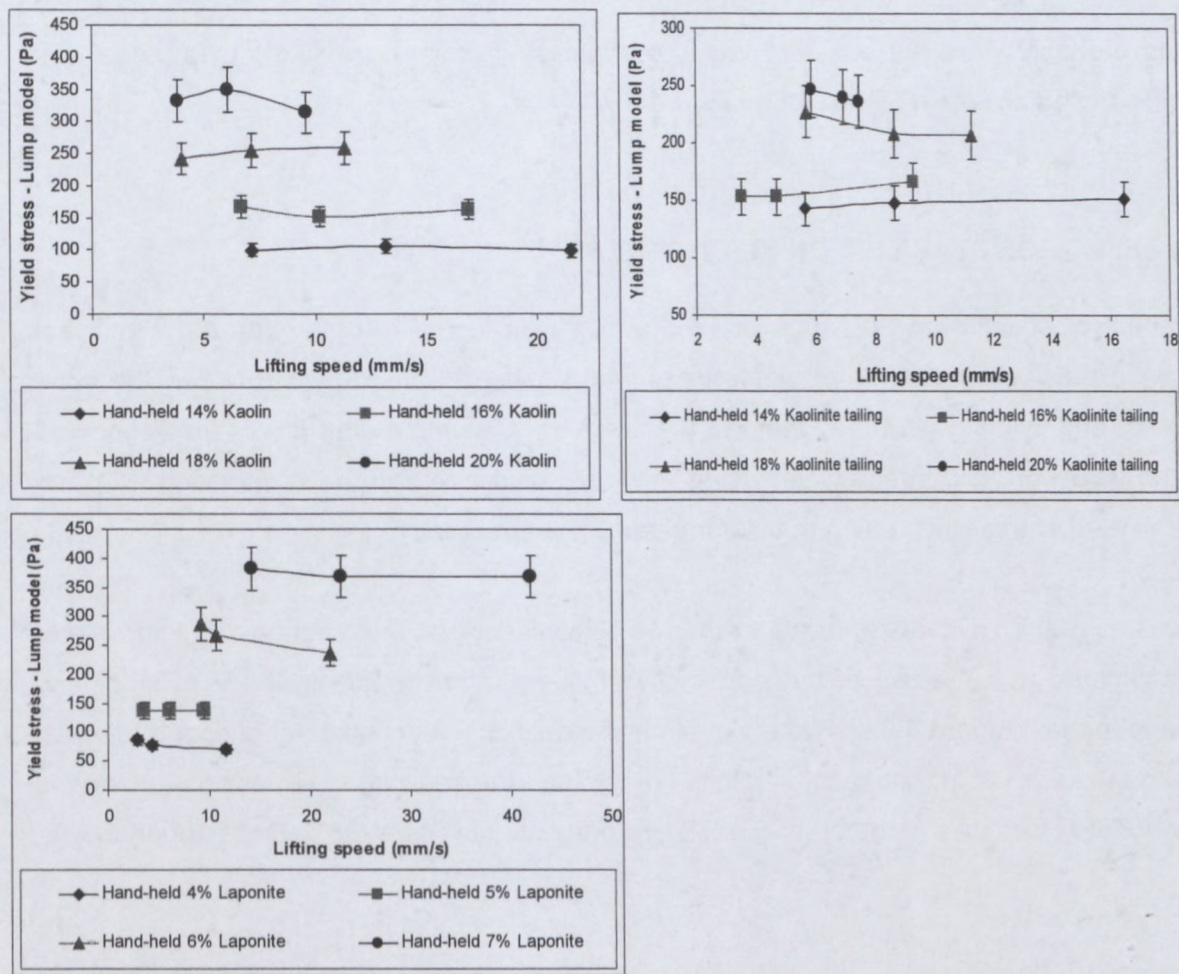


Figure 4. 7: The effect of lift speed on yield stress (lump model) for three materials using a hand-held cylinder (Error bars +/- 15 %)

The lifting speeds used varied from as low as 1.5 mm/s to as high as 20 mm/s for this work but at 7 % laponite lift speed was observed as 42 mm/s.

It is clear, from Figures 4.5 to 4.7 that, in terms of the rheological parameter of yield stress, the lift speed in the range tested did not have a significant effect on the yield stress value for all the materials when using the lump model.

The same trend was observed in almost all of the results with the geometries and the hand-held cylinder for the approximate cylinder and cylinder models when using the cylinder and cone PVC geometry shown in Tables D13, D14 and D15. In some instances, a slightly downward trend in the yield stresses with lift speed could be seen, but it was within the range of the experimental error of +/-15 %, as indicated by the error bar.

A lift speed of 42 mm/s was measured using the hand-held cylinder. These slow lifting speeds probably were not constant, but the effect of lift speed on yield stress value was insignificant, as shown in Figure 4.5 to Figure 4.7.

4.5 EFFECT OF STABILITY ON YIELD STRESS

The effect of stability on the value of yield stress was tested to determine the significant difference between the value of yield stress when using the hand-held cylinder, the cone geometry and cylinder geometry fitted to the mechanical slump meter. It was also observed that the value of yield stress when using the hand-held cylinder shows variation from the value of yield stress when using the slump meter measurement.

The values of the yield stress using the hand-held cylinder and the mechanical slump meter was estimated with the use of three predictive models (approximate cylinder, cylinder and the lump model). Figure 4.8 shows a plot of yield stress as a function of lift of speed for each of the materials (kaolin, Laponite, kaolinite tailings and the kaolinite mine tailings), using the lump model The results of the other models are presented in Table D6 to D19 (Appendix D).

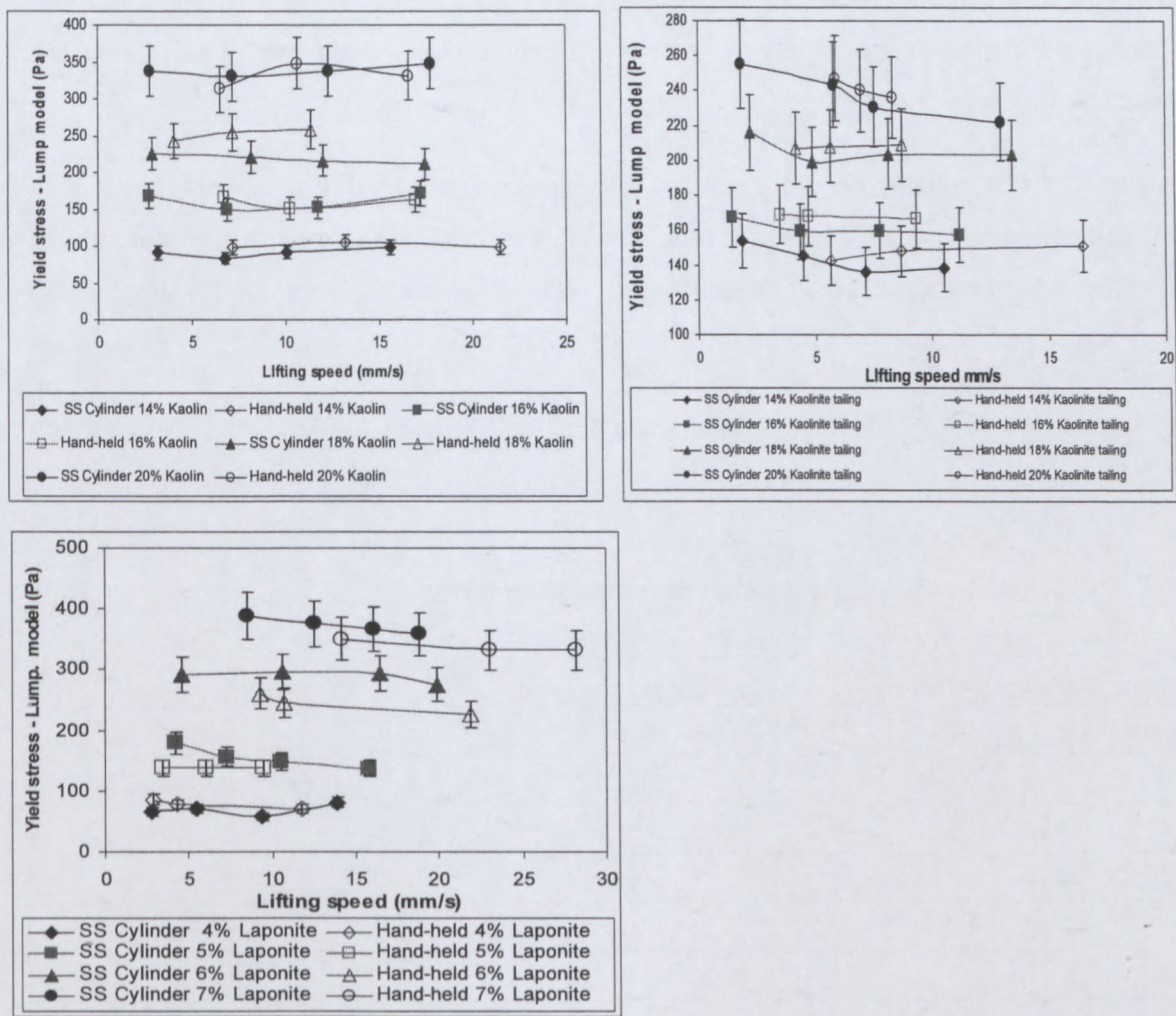


Figure 4. 8: Comparison of hand-held cylinder and slump meter yield stress (lump model), for three materials when using a stainless steel cylinder (Error bars are +/- 15 %)

The percentage error range for Figure 4.8 when using the lump model for the materials and concentrations tested is shown in Table 4.2.

It can be seen (in Figure 4.8) that the stability of the value of yield stress is approximately the same, more especially at the 14 % v/v, 16 % v/v and 20 % v/v concentrations. The value of yield stress at the 18 % v/v concentration when using the hand-held cylinder was observed to be slightly higher than the cylinder (stainless steel) for the kaolin material. For laponite material, the values of yield stress when using the hand-held cylinder was slightly lower that the value yield stress in using the cylinder stainless steel geometry, but at the 4 % v/v concentration the opposite was observed.

The results for the PVC cylinder with kaolin in four concentrations and the cone (stainless steel and PVC) cylinder, as well as the results for other materials are shown in Appendix D. The results were similar for all these.

4.6 EFFECT OF WALL SURFACE MATERIALS ON YIELD STRESS

One of the aims of this research was to assess the effect of wall surface material on the value of yield stress. The geometries with stainless steel and with PVC do have an effect on the value of slump height, which relates to the value of yield stress. In Chapter 2 it was explained that all the geometries were lifted manually by various previous researchers, irrespective of what geometry material was used (stainless steel or PVC). Cones and cylinders made of stainless steel and PVC used was controlled by a lifting rod attached to the lifting variable speed motor and pulley system in order to investigate and evaluate the effect of the wall surface material on the value of yield stress.

A series of slump experiments were conducted to enable a direct comparison of the wall surface effect. The following materials were tested; kaolin suspension at 14 % v/v, 16 % v/v, 18 % v/v and 20 % v/v; kaolinite tailings suspensions at 14 % v/v, 16 % v/v, 18 % v/v and 20 % v/v; laponite suspension at 4 % v/v, 5 % v/v, 6 % v/v and 7 % v/v and kaolinite mine tailings at 70:30, 80:20, 90:10 (with various relative densities).

Figure 4.9 presents a graph of the effect of wall surface materials on the value of yield stress measurements for three materials using a stainless steel and PVC cylinder.

The results for the PVC cylinder with kaolin in four concentrations and the cone (stainless steel and PVC) cylinder, as well as the results for other materials are shown in Appendix D. The results were similar for all these.

4.6 EFFECT OF WALL SURFACE MATERIALS ON YIELD STRESS

One of the aims of this research was to assess the effect of wall surface material on the value of yield stress. The geometries with stainless steel and with PVC do have an effect on the value of slump height, which relates to the value of yield stress. In Chapter 2 it was explained that all the geometries were lifted manually by various previous researchers, irrespective of what geometry material was used (stainless steel or PVC). Cones and cylinders made of stainless steel and PVC used was controlled by a lifting rod attached to the lifting variable speed motor and pulley system in order to investigate and evaluate the effect of the wall surface material on the value of yield stress.

A series of slump experiments were conducted to enable a direct comparison of the wall surface effect. The following materials were tested; kaolin suspension at 14 % v/v, 16 % v/v, 18 % v/v and 20 % v/v; kaolinite tailings suspensions at 14 % v/v, 16 % v/v, 18 % v/v and 20 % v/v; laponite suspension at 4 % v/v, 5 % v/v, 6 % v/v and 7 % v/v and kaolinite mine tailings at 70:30, 80:20, 90:10 (with various relative densities).

Figure 4.9 presents a graph of the effect of wall surface materials on the value of yield stress measurements for three materials using a stainless steel and PVC cylinder.

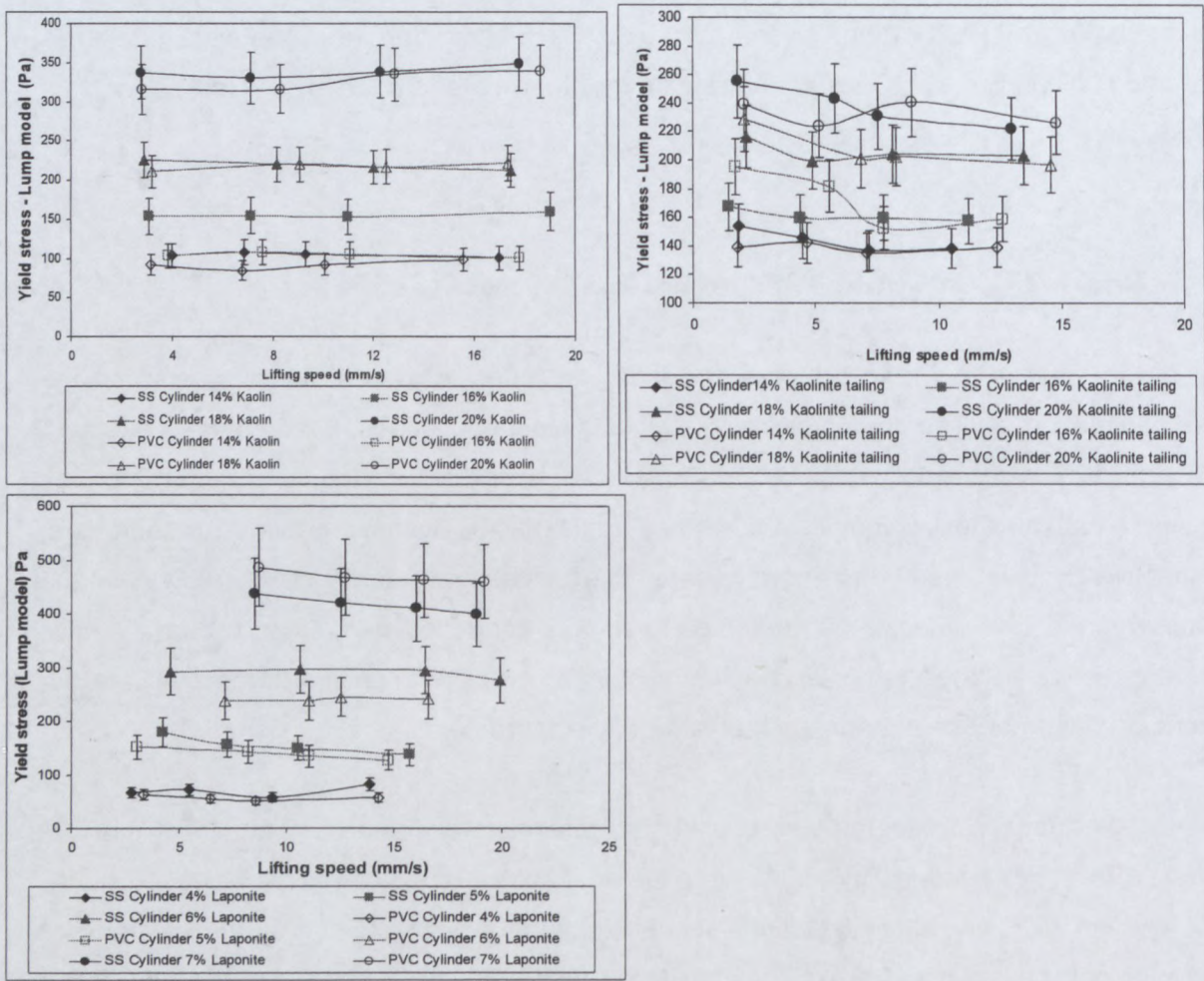


Figure 4. 9: Effect of wall surface materials on yield stress measurements for three materials using a stainless steel and PVC cylinder (SS and PVC) (Error bar is +/- 15 %)

It was seen from the results that the PVC cylinder geometry gave a lower value of yield stress than the cylinder stainless steel geometry at 4 % v/v, 5 % v/v and 6 % v/v for the laponite suspension especially at 7 % v/v. This result could have resulted from the difference of surface material. The error bar in Figure 4.9 is +/-15 % for the concentration and material used for this work and also for the graphs in Table D20 and Table D21 in Appendix D.

In some cases, however, the results could shift up or down slightly, mostly in the case of the kaolinite tailings. The kaolin results, as shown in Figure 4.1; Table D20 and Table D21 in Appendix D, show a result of the value of yield stress when using a stainless steel cylinder with slightly higher yield stress values than the cylinder PVC in all the three models. The laponite materials showed trends like the kaolin for three concentrations, as described above.

The results for the cone geometry when using stainless steel and PVC showed the same trend with kaolin materials when using the approximate model, the lump model and the cylinder. It was observed that the laponite material at 5 % v/v with the stainless steel and 5 % v/v with the PVC gave the same value of yield stress for the approximate cylinder model, but that it was different for the lump model and the cylinder model. There is a trend towards slightly different values of yield stress between the lump model and the cylinder model for the laponite material. For the kaolin material, the graphs (approximate cylinder model and the cylinder model) show the different trend in Figure 4.9. It was observed that the value of yield stress when using the stainless steel (lump model) showed higher value of yield stress than the PVC for the cone geometry test. This was also observed when using the laponite material for the cone geometry test when the approximate cylinder model, lump model and the cylinder model were used, as shown in Table D 21 in Appendix D.

With regard to the kaolinite material, it was observed that the results when using the approximate cylinder model and the cylinder model showed the same trend at all concentrations while the lump model produced a different trend. The approximate cylinder model gave higher values of yield stress, followed by the lump model and then the cylinder model.

Two materials with different surface properties were used (stainless steel and PVC) for the cone and the cylinder models with slight differences in roughness. It was observed during the slump measurement that materials stuck more to PVC material than to the stainless steel.

Finally, the effect of wall surface materials does not affect the value of yield stress much in the case of the materials tested, whether the material used is PVC or stainless steel.

4.7 EFFECT OF THE GEOMETRY ON YIELD STRESS

The effect of the geometry on the value of yield stress was also evaluated. The cone and cylinder geometries fitted to the mechanical slump meter and the hand-held cylinder were tested and results were compared.

Figure 4.10 plots the yield stress when using the lump model as a function of lifting speed for the stainless steel cylinder, stainless steel cone and the hand-held cylinder when using 14 % v/v, 16 % v/v, 18 % v/v and 20 % v/v for the kaolin, kaolinite tailings and laponite material. The results for the PVC cylinder, PVC cone and the hand-held cylinder when using the approximate cylinder and cylinder model for kaolin, kaolinite tailings and the laponite are shown in Table D22 and Table D23 in the Appendix. The error bars are +/-15 % for all the results when using the approximate cylinder model, lump model and the cylinder model, which confirm that the results are in the range of experimental error.

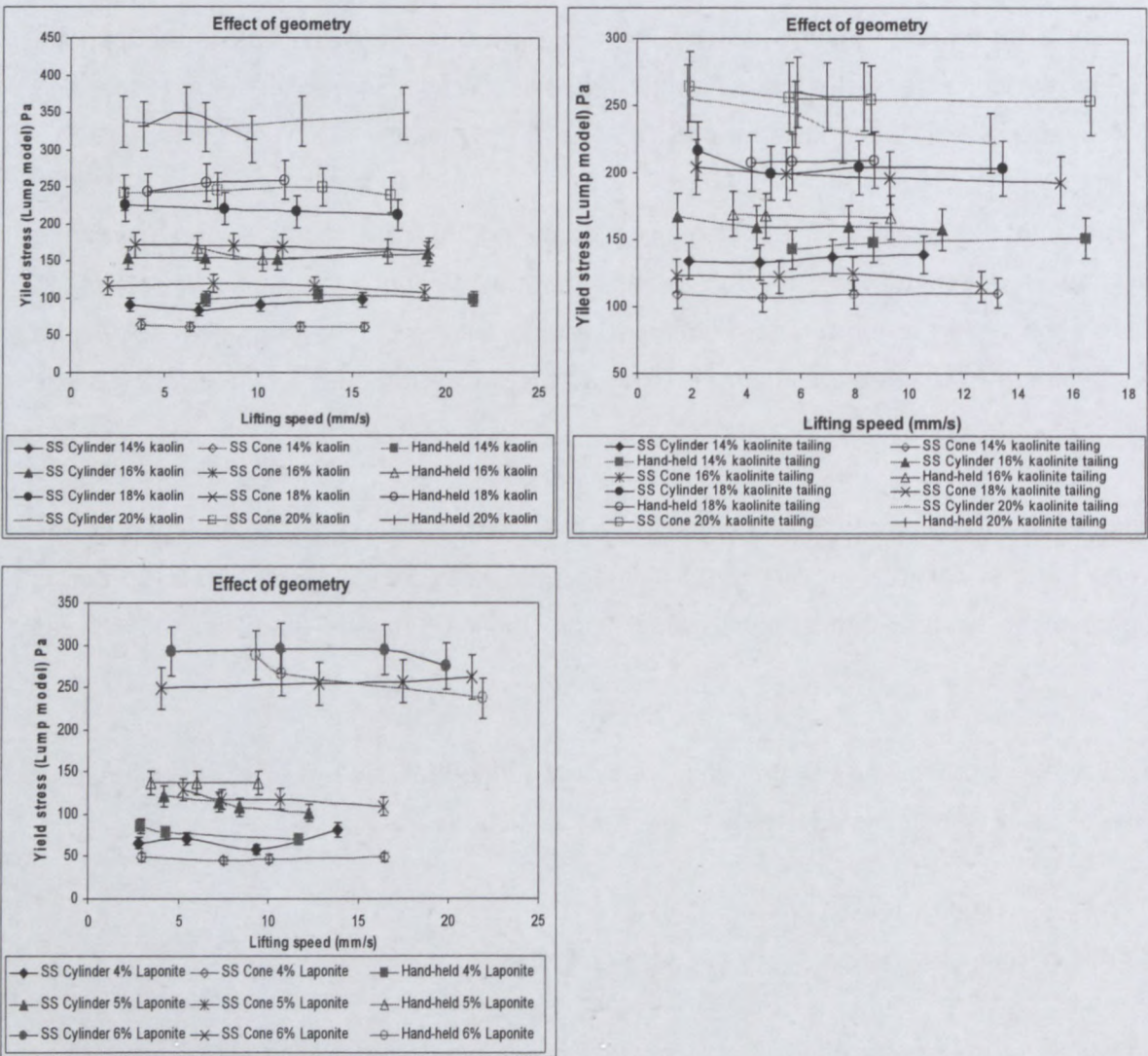


Figure 4. 10: The effect of the geometry on yield stress for kaolin, kaolinite tailings and laponite when using the lump model (Error bars +/-15 %)

It can be noticed in Figure 4.10 that the value of yield stress increases for the geometries and the hand-held cylinder as the concentrations increase. The hand-held cylinder gave the lowest yield stress value (327 Pa) at 14 % v/v, while it gave the highest value of yield stress (497 Pa) at 20 % v/v. It can also be seen in Figure 4.10 that the cylinder geometry gave a higher value of yield stress than the cone geometry for the stainless steel and the PVC for all the concentrations and materials.

The value of yield stress determined using the hand-held cylinder and the cone and cylinder geometry did not show much effect (± 2 % difference) when using the approximate cylinder model, lump model and the cylinder at low concentrations for all the materials tested. But for high concentrations, as seen in Figure 4.10, Table D22 and Table D23, the yield stresses showed a variation of ± 6 %. This is still within the range of experimental error.

The effect of the parameter was found to be insignificant on the value of the yield stress measurement.

4.8 EFFECT OF SLIP ON YIELD STRESS

The observation of slip effects in yield stress measurements with rotating vane rheometers led to this investigation.

During the slump test, the hand-held cylinder, as well as the cone and cylinder geometries, was sprayed with silicone spray to reduce the stickiness of the surface during lifting.

Slip can be determined by the roughness or smoothness of the wall inside the geometry used.

The results depicted in Figure 4.11, Figure 4.12 and Figure 4.13 show the yield stress measurements obtained when using the stainless steel cylinder geometry, stainless steel cone geometry and the stainless steel hand-held cylinder for all concentrations for kaolin with and without silicon spray.

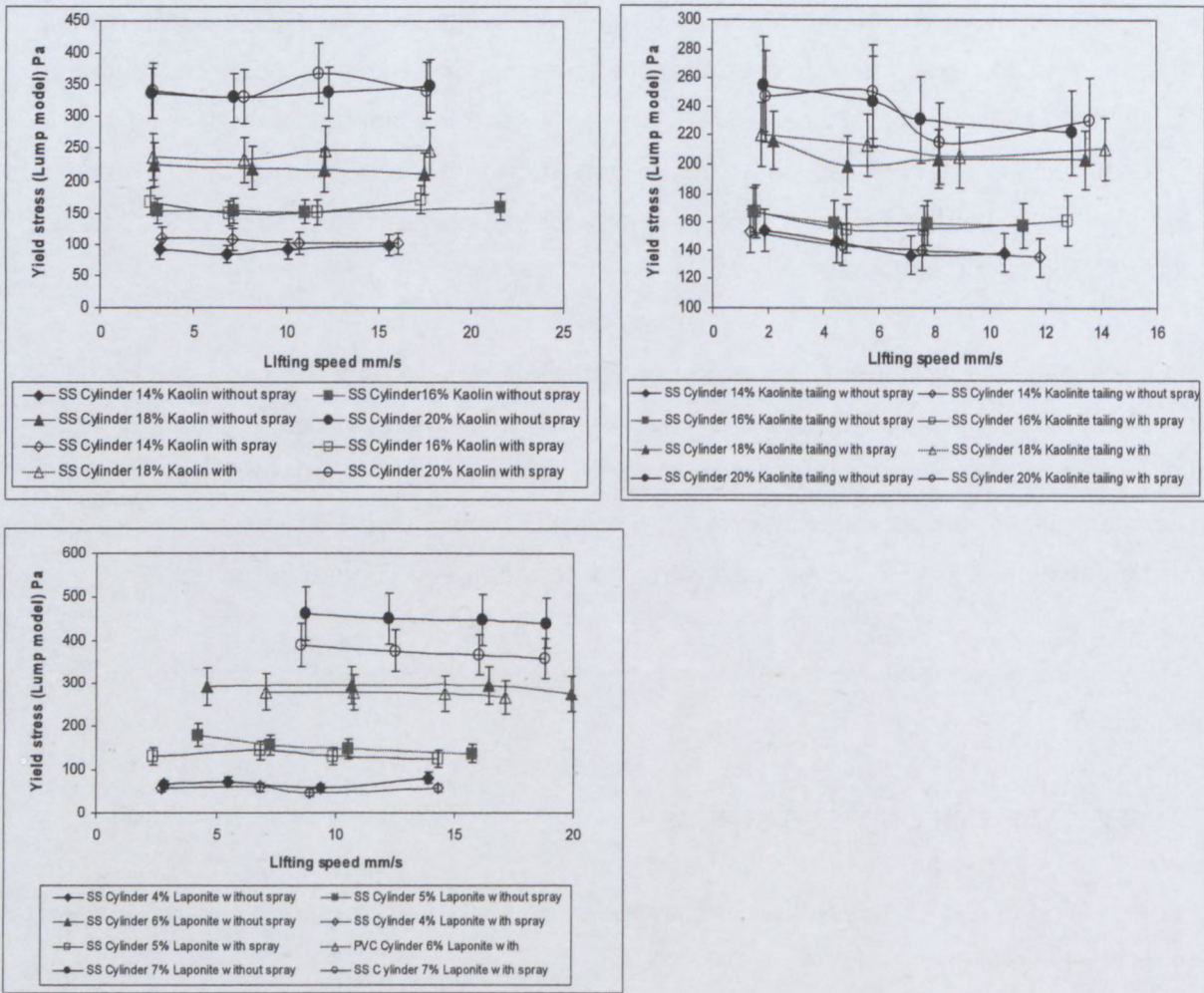


Figure 4. 11: Effect of slip on yield stress (lump model) for three materials, using a stainless steel cylinder (Error bars are +/- 15%)

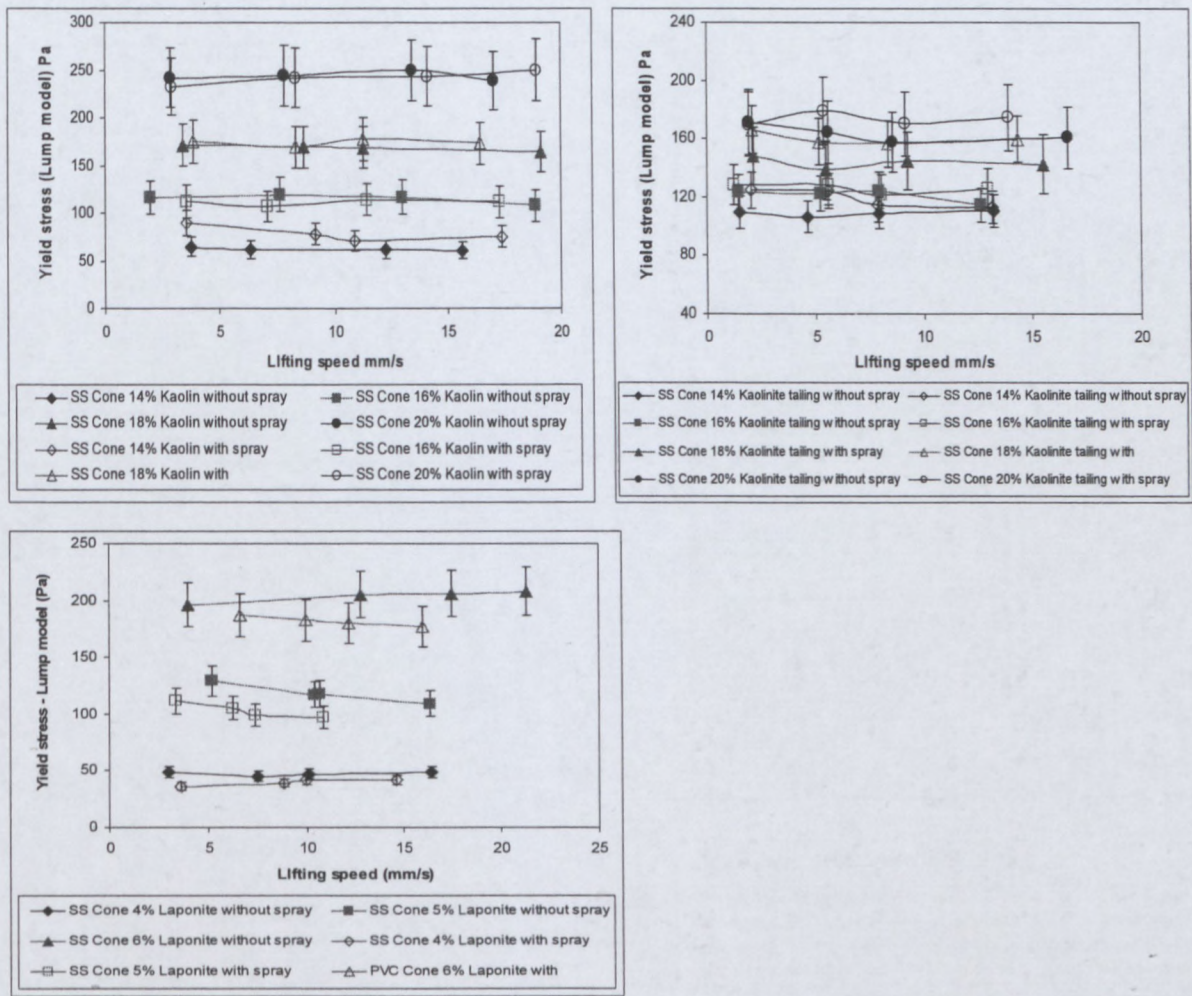


Figure 4. 12: Effect of slip on yield stress (lump model) for three materials, using a stainless steel cone (Error bars are +/- 15%)

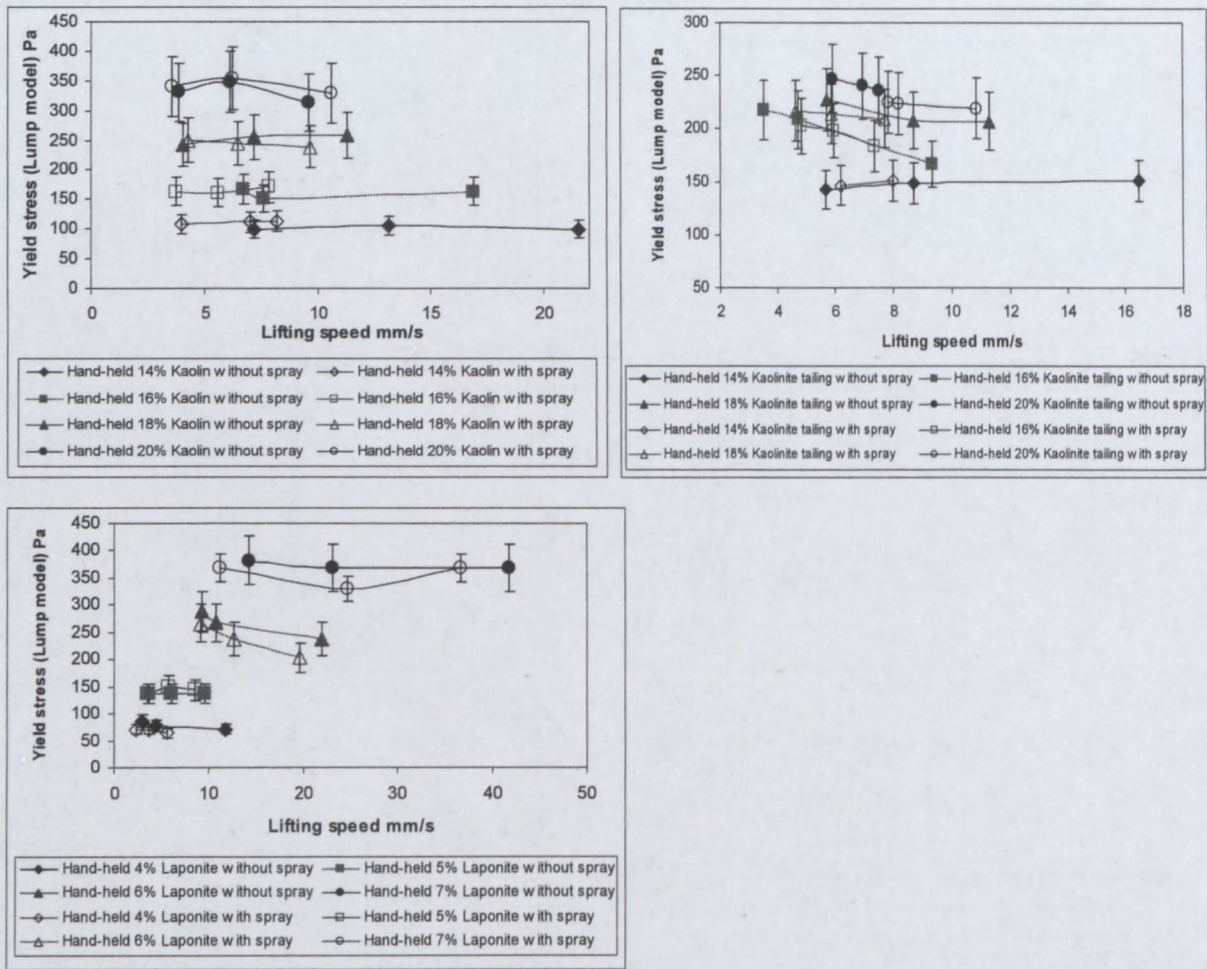


Figure 4. 13: Effect of slip on yield stress (lump model) for three materials, using a hand-held cylinder (Error bars are +/- 15%)

The difference between the values of yield stress recorded for the slump with and without the silicone spray was investigated and is shown in Figures 4.11, 4.12 and 4.13. The values of yield stress were evaluated using the lump model as a function of lifting speed. It is seen in Figures 4.11 to 4.13 that the effect of slip on the value of yield stress is insignificant; in some cases a slight downward trend in the value of yield stress with lift speed could be seen. The error bars are within the experimental error, which means that there are some indications that the values obtained in using with and without silicone spray did not have much effect on the value of the yield stress. The same trends were observed in all the results shown in Tables D4 to D9 which were obtained when using the PVC for kaolin, kaolinite tailings and laponite materials (Appendix D).

The effect of slip on the value of yield stress was measured in an endeavour to evaluate the effect of slip. The silicone spray was sprayed to the sides of the geometries and the hand-held cylinder to reduce wall friction during lifting, as this can affect the measurement of yield stress. It was observed that the effect of slip on the value of yield stress is negligible. It was conceptualised that, when the geometry is sprayed, it might improve the smoothness, thus enhancing the value of the yield stress. Several factors were found to contribute towards the value of yield stress measurement obtained, e.g. the loading of the material in the geometries and the hand-held cylinder.

Hallbom, (2005) studied the effect of slip on the geometry wall using a paste made from fine alumina powder with a 75 mm diameter cylinder, he found that 4.6 % to 21 % of the alumina paste remained in the cylinder.

From the work of Pashias et al. 1996, he propagated that the effect of slip, when using the hand hand-held cylinder was insignificant. These observations by the authors concur with the result shown in Figures 4.11 to 4.13 of the current work.

4.9 SUMMARY

Academic research is regularly driven by curiosity while industrial research is often driven by need (Boger et al., 2008).

Knowledge of rheological properties of suspensions is of paramount importance and correct measurement thereof provides useful information for the development of flow models for engineering applications, for the formulation of commercial production, design and process evaluation, quality control, and storage stability.

Slump testing is often used to indicate whether non-Newtonian fluid is likely to present difficulty in pumping, and at what concentration this can be expected.

The yield stress values of four materials at varying concentrations of solids and mix ratios were determined with the use of two techniques. The first set of values was measured using the hand-held cylinder and the mechanical slump meter technique. The second set was derived from measurements obtained by using the vane shear technique. The results

obtained from using the slump measurement and the vane shear techniques were graphically compared.

Results clearly showed that the slump height generated as a result of gravitational acceleration is a unique function of the yield stress. This result is consistent with findings for slump tests driven by gravitational acceleration alone obtained by Pashias et al., (1996), Haldenwang et al., (2007) and others.

The position where the slump height is taken on the slumped material can however, depending on the material, have a significant effect on the value of yield stress.

The materials tested induced an error as much as + 40 % and - 50 % for the hand-held cylinder using lump model for all the materials. The lump model for most of the experimental work predicted the value of yield stress better than the other theoretical predictive models over the range of materials and concentrations tested.

The approximate cylinder model gave a higher yield stress value than the lump model, while the cylinder model gave a lower value of yield stress. The hand-held cylinder slump test provided a reliable and simple test for evaluating the yield stress; without necessitating expensive and high cost equipment. The hand-held cylinder technique can therefore be employed as a reliable measurement of yield stress in the industry.

The four dimensionless models relating slump to yield stress were used for the analysis of the data. The results indicate that the cylinder model fits the experimental data for the cylindrical slump over a wide range of yield stress values for a variety of materials, including kaolin, kaolinite tailings and kaolinite mine tailings (kaolinite tailings and sand). The cone model did not fit the experimental data, but followed the cylinder model at low dimensionless yield stresses. The lump model gave better results than the other theoretical predictive models at low and high dimensionless yield stresses.

The lifting speed did not show much effect on the result of the yield stress. Within the accuracy of the experimental work, effect of lift speed is insignificant.

The effect of stability on the value of yield stress was observed not to have much effect on the yield stress measurement with respect to using the mechanical slump meter and the hand-held cylinder or the material used is stainless steel or PVC.

Yield stress values resulting from the use of stainless steel and PVC did not display much deviation from each other and it can be concluded that the material for the geometry does not have a major impact on the yield stress measurement.

The effect of slip on the value of yield stress was measured by spraying a silicone spray on the sides of the geometries and the hand-held cylinder in an endeavour to evaluate the effect of slip. It was observed that the effect of slip on the value of yield stress measurement is negligible.

To conclude, this work has shown that the slip, lifting speed, stability of the lifting device and material of the cylinder or cone, shape of device do not really effect the value of the yield stress for the materials tested. The material tested may have an effect on the position of where the slump height is measured as the top surface may be uneven and could result in errors of about 25%.

CHAPTER 5

CHAPTER 5

CONCLUSIONS AND RECOMMENDATIONS

5.1 INTRODUCTION

The yield stress of structured fluids is an important rheological parameter often used in engineering. Consequently there is a need for adequate measurement of yield stress as an engineering parameter. Industries produce large volumes of waste that should be disposed of according to environmentally acceptable standards, and in an economical manner. It is also essential that this waste to be thickened before being pumped to a disposal site, to save water.

Yield stress measurement using the slump technique and vane technique was reviewed. The hand-held cylinder was found to be, despite being manually-controlled, a very simple and quick way of determining the value of yield stress, requiring virtually no skill at all to perform. Use of this modified slump test might well become as common in the testing of thickened tailings as the conventional slump test is in concrete quality control (Gawu and Fourie, 2004).

The present experimental work was conducted in the Flow Process Research Centre (FPRC) at the Cape Peninsula University of Technology, Cape Town, South Africa. A mechanical slump meter developed at FPRC, as well as a hand-held cylinder and vane (FL 100 Z4) technique were used for the tests.

A technique that allows accurate determination of the yield stress of kaolin between 14 % v/v, 16 % v/v, 18 % v/v and 20 % v/v; kaolinite tailings between 14 % v/v, 16 % v/v, 18 % v/v and 20 % v/v; laponite between 4 % v/v, 5 % v/v, 6 % v/v and 7 % v/v, and kaolinite mine tailings (kaolinite tailings and sand) at mix ratios of 70/30, 80/20 and 90/10 with different densities was observed.

The main objective in this work was to evaluate the effect of position of slump measurement, validation of yield stress models and in addition, the effect of lift speed, stability, wall surface materials, geometry and slip on the measurement of yield stress. Work by Nguyen and

Boger (1983 & 1985), Pashias et al., (1996), Clayton et al., (2003), Saak et al., 2003, Hallbom, (2005), Gawu & Fourie, (2004) and Haldenwang et al., (2007) was found to be relevant.

In this chapter, a summary, and conclusions drawn from the present work are presented along with some recommendations for possible future work.

5.2 SUMMARY

Yield stress values of kaolin, laponite, kaolinite tailings and kaolinite mine tailings at various concentrations of solids were determined by comparing the slump technique with the vane technique.

The ASTM as well as SABS 143-86 describes the slump cone test for concrete. The dimensions of the slump cones and cylinders used in this work were within the range of sizes used by other researchers measuring yield stress of similar materials.

The experimental work was conducted with the mechanical slump meter, by which the speed of lift was controlled and lateral movement eliminated. The geometries (cone and cylinder) made of stainless steel and PVC was fitted to the mechanical slump meter. The hand-held cylinder was also used for the slump test, while the vane test was used as a reference technique.

The first set of yield stress values was measured using the vane shear technique while the second set of yield stress values was measured using the hand-held cylinder and the mechanical slump meter. The two sets of yield stress values were compared with four predictive theoretical models (approximate cylinder model, lump model, cylinder model and cone model).

It can be concluded that, although the materials tested may induce errors ranging to as much as +/- 40% for the complete database when using the hand-held cylinder for the lump model, the hand-held cylinder was observed to produce a reliable and simple test for evaluating the yield stress of kaolin, laponite, kaolinite tailings and kaolinite mine tailings (kaolinite tailings and sand).

This technique can therefore be recommended for industrial use to remedy the high cost of expensive equipment.

Care was taken with sample preparation and conditioning in conducting the tests. Details such as yield stress as a function of lifting speed were taken into account in the analysis, comparison and discussion of the results. Evaluation of this work revealed four significant points:

- The material tested may have an effect on the position where the slump height is measured as the top surface may be uneven and could result in errors of about 25%. The highest point gives results comparable to that of the vane.
- The validation of yield stress models used is significant. The Lump model seems to perform best for materials and concentrations tested.
- The simple slump test can be used to obtain yield stress values that are comparable to that obtained with the vane.
- The slip, lifting speed, stability of the lifting device and material of the cylinder or cone, shape of device do not really effect the value of the yield stress for the materials tested.

5.3 CONTRIBUTIONS

This thesis added mechanical slump-meter and hand-held cylinder data to the open literature for the yield stress measurement, which will be useful for thickening, pipeline transport, floc formation, pumping and product quality control.

5.4 CONCLUSIONS

There is a growing need to discover trustworthy and easy test techniques for measurement of yield stress. The results from testing kaolin, laponite, kaolinite tailings and kaolinite tailings (kaolinite tailings and sand) when using the hand-held cylinder show better yield stress

values compared to the results from the mechanical slump meter test. The vane technique was used as the reference technique for calculating the yield stress.

On completion of the work, the following conclusions are drawn:

- The position where the slump height is taken on the slump geometries and hand-held cylinder was observed. Some materials formed rough surfaces and in such cases the position where the slump is measured can have a significant effect on the value of the yield stress.
- The lump model predicted the value of yield stress better over the range of materials and concentrations tested. When compared with the vane test, the lump model predicted the value of yield stress within 40%.
- The lifting speed did not show much effect on the result of the yield stress. Within the accuracy of the experimental work, effect of lift speed on measurement of yield stress is insignificant.
- The effect of stability on the value of yield stress was observed not to have much effect on the yield stress measurement with respect to using the mechanical slump meter and the hand-held cylinder or the material used is stainless steel or PVC.
- The effect of slip on the value of yield stress was measured by spraying silicone spray on the sides of the cone geometries, cylinder geometries and the hand-held cylinder in an attempt to evaluate the effect of slip; the effect of slip on the value of yield stress was confirmed negligible in this research work.
- Yield stress values from stainless steel and PVC geometries did not display much deviation from each other; it can be concluded that the wall surface of the material does not have a major impact on yield stress values for the materials tested.
- The simple hand-held cylinder is indeed an instrument that can be used on site to measure the static yield stress of kaolin, kaolinite mine tailings, kaolinite tailings and laponite.

- From the results obtained it is recommended that the highest point can be used for making accurate yield stress measurements using the slump technique.

This work has shown that the slip, lifting speed, stability of the lifting device and material of the cylinder or cone, shape of device do not really effect the value of the yield stress for the materials tested. The material tested may have an effect on the position where the slump height is measured as the top surface may be uneven.

5.5 RECOMMENDATIONS

On reaching the end of this experimental programme, the following recommendations for future work are suggested:

- Further tests should be done to verify whether the yield stress measurements of other materials like Bentonite and other yield stress fluids will be similar to the existing found for open literature and this work using the same approach.
- With regard to the slump meter (from the base), the plate situated just above the geometry disturbs the loading process, especially when using cone geometry. The plate should be readjusted to facilitate testing.
- The length of the measuring gauge used in measuring the slump height should be increased. It was noticed that the device was unable to measure the points beyond the length of the gauge when the slump meter was being used for the slump tests.
- The materials that were tested induced error to as much as $\pm 40\%$ and $\pm 70\%$ for the hand-held cylinder lump model for all the materials. The hand-held cylinder test has found wide use in the industry for the measurement of yield stress. It is

recommended that care be taken in applying the procedure to new, prviously untested materials without at least carrying out some calibration tests using other, more accurate tests such as the vane shear rheometer test.

REFERENCES

REFERENCES

- Adams, M.J, Aydin I, Briscoe, B.J & Sinha S.K. (1997). A finite element analysis of the squeeze flow of an elasto-viscoplastic paste material. *Journal of Non-Newtonian Fluid Mechanics* 71:41–57.
- Alderman, N.J., Meeten, G.H. & Sherwood, J.D. (1991). Vane rheometry of Bentonite gels. *Journal of Non-Newtonian Fluid Mechanics*, 39:291.
- American Society for Testing and Materials standard test method for slump of Portland cement to concrete, ASTM, Philadelphia. 1922. ASTM: C – 143.
- Ancey, C. (2003). Role of particle network in concentrated mud suspensions, in Rickenmann Chen (eds.). *Debris-flow Hazards Mitigation: Mechanics, Prediction, and Assessment*, Volume 1. Rotterdam: Millpress, 257.
- AS 2701.5 Australia Standard, Standard Association of Australia, 1984.
- Astarita, G. (1990). Letter to the Editor: The Engineering reality of the yield stress. *Journal of Rheology*, 34(2):275.
- ASTM Designation C-143-90, (1996), Standard test method for slump of hydraulic cement concrete, Annual Book of ASTM Standards, 04.01, American Society for Testing Materials, Easton, MD, page. 85– 87
- Atkinson, C. & Sherwood, J.D. (1992). The torque on a rotating n-bladed vane in a Newtonian fluid or linear elastic medium. *Proceedings of the Royal Society London, Series A – Math. Phys. Eng. Sci.* (438):183-196.
- Baker, F.S, (1998), *Rheology – A practical approach to quality control*, Rheology conference, Shrewsbury, Paper 1, page 1 – 6.
- Banfill, P.F.G. (2003). The Rheology of fresh cement and concrete – A review. *Proceedings of the 11th International cement Chemistry congress*. Durban.
- Barnes, H.A. & Walters, K. (1985). The yield stress myth? *Rheological Acta*, 24:323-326.
-
- Maxwell Nyekwe Icheigbo: Investigation of factors effecting yield stress determinations using the slump test.

Barnes, H. A. & Carnali, J.O, (1989), The vane-in-cup as a novel rheometer geometry for shear thinning and thixotropic materials, *Journal of Rheology*, Vol. 34, No. 6, pp 841-864.

Barnes, H.A. (1995). A review of the slip (wall depletion) of polymer solutions, emulsions and particle suspensions in viscometers: its cause, character, and cure. *Journal of Non-Newtonian Fluid Mechanics*, 56:221.

Barnes, H.A. (1997). Thixotropy - a review. *Journal of Non-Newtonian Fluid Mechanics*, 70:1–33.

Barnes, H.A. & Carnali A (1989), The yield stress fluids, *Progress and Trends in Rheology Proceedings of the Fifth European Rheology conference*. Portoroz. Page 201.

Barnes, H.A., (1999). Yield stress – a review, or πάντα ρει – everything flows *Journal of Non-Newtonian Fluid Mechanics*. 81 (1999):133.

Barnes, H.A. (1999). A Brief history of the yield stress, Unilever Research Port Sunlight, Bebington, Wirral, L63 3JW Merseyside, United Kingdom.

Barnes, H.A. & Nguyen, Q.D. (2001). Rotating vane rheometry – a review. *Journal of Non-Newtonian Fluid Mechanics*, 98(1):1-14.

Barnes, H.A. & Bell, D. (2003). Controll-stress rotational rheometry: An historical review, *Korea-Australia rheology Journal*, 15 (14): 187.

Bartos, P.J.M., Sonebi, M. & Tamini, A.K. (2002). Workability and Rheology of fresh concrete, *Compendium of Test, Report of RILM Technical committee TC 145-WSM, workability of special concrete mixes*. Cachan Cedex, France: RILM publications. S.A R.L,

Bingham, E.C. (1922). *Fluidity and Plasticity*. New York: McGraw-Hill.

Bird, R.B., Grance, D. & Yorusso, B.J. (1983). The rheology and flow of viscoplastic materials. *Reverse. Chemical Engineering*, 1:1-70.

Maxwell Nyekwe Ichegbo: Investigation of factors effecting yield stress determinations using the slump test.

Blair, S.G.W. (1949). A survey of general and applied Rheology, 2nd edition. London: Pitman.

Blair, S.G.W. (1966). The success of Casson's equation. *Rheological Acta*, 5:184-187.

Boger, D.V. (2006). Paste and thickened Tailing. 2nd edition. Department of Chemical and Biomolecular Engineering, University of Melbourne, Australia.

Boger, D.V., Scales, P.J. & Sofra, F. (2008). Paste and thickened Tailing and the impact on the development of new Rheological Techniques. Department of Chemical and Biomolecular Engineering, University of Melbourne, Australia.

Carozza, S., Servias, C. & Roberts, A. (2000). Oscillatory Vane rheometry for complex materials. XIIIth International congress on Rheology. Cambridge, 3:321.

Chamberlain, J.A., Clayton, S., Landman, K.A. & Sader, J.E. (2003). Experimental validation of incipient failure of yield stress materials under gravitational loading. *Journal of Rheology*, 47(6):1317-1329.

Chandler, J.L., (1986). The stacking and solar drying process for disposal of bauxite tailings in Jamaica. Proceedings of the International Conference on Bauxite Tailings, Kingston, Jamaica. Jamaica Bauxite Institute, University of the West Indies, page: 101– 105.

Charm, S.E. (1963). Effect of yields stress on the power law constants of fluid food materials determined in low shear rate viscometers. *Industrial Engineering, Chemical Proceedings, Description and Development*, Volume 2:62-65.

Cheng C. H.R. and Parker B.R. (1976). The determination of wall-slip velocity in the coaxial cylinder viscometer. Proceedings of the seventh International congress on rheology, Gotenberg, Sweden, page 518-519.

Cheng, C.D.H. (1984). Further observations on the rheological behaviour of dense suspensions. *Powder Technology*, 37:255-273.

Cheng, C.D.H. (1986). Yield stress – A time-dependent property and how to measure it. *Rheological Acta*, 25(5):134.

Maxwell Nyekwe Ichegbo: Investigation of factors effecting yield stress determinations using the slump test.

- Chhabra, R.P. & Richardson, J.P. (1999). Non-Newtonian flow in the process industries. Oxford: Heinemann.
- Chong, J.S, Christiansen, E.B. & Baer, A.D. (1971). Rheology of Concentrated Suspensions. *Journal of Applied Polymer Science*, 15:2007-2021.
- Christopher, A. & Helene, J. (2006). Yield stress for particle suspensions within a clay dispersion, Cemagref, 2 Rue de la Papeterie, B.P. 76, 38402, Saint-Martin d'Heres Cedex, France.
- Christensen, G. (1991). Modelling the flow of fresh concrete: The slump test. Ph.D. Thesis, Princeton University, New Jersey, 08544-5263.
- Chukwudi, B C, (2008), Settling Behavior of Kaolinite Clay in the Absence of Flocculant, Department of Mechanical Engineering, Imo State University PMB 2000, Owerri, Nigeria.
- Clayton, S., Grice, T.G. & Boger, D.V. (2003). Analysis of the slump test for on-site yield stress measurement of mineral suspensions. Particulate Fluids Processing Centre, Department of Chemical Engineering, University of Melbourne, Australia. *Int. J. Miner. Process*, 70:3-21.
- Coussot P and Piau J.M, (1994), On the behaviour of fine mud suspensions, *Rheological Acta*, Volume 33, Page 175.
- Coussot, P., Proust, S. & Ancey, C. (1996). Rheological interpretation of deposits of yield stress fluids. *Journal of Non-Newtonian Fluid Mechanics*, 66:55.
- Coussot, P, Raynaud, J.S, Moucheron, P, Guilbaud, J.P, Huynh, T, Jarny, S & Lesueur, D, (2002b), "Coexistence of liquid and solid phases in flowing soft – glass materials", *Phys. Rev. Lett.* 88, 21830/ 1 - 4.
- Coussot, P., Nguyen, Q.D., Huynh, H.T. & Bonn, D. (2002). Viscosity bifurcation in thixotropic, yielding fluids. *Journal of Rheology*, 46:573-589.

Covey G.H and Stanmore B.R, (1981), Use of parallel plate plastometer for the characterization of viscous fluids with a yield stress, *Journal of Non-Newtonian fluid mechanics*, 8, 249-260.

Darby, R. & Cheremisoff, N.P. (1986). *Hydrodynamics of fluids and suspensions*. In *Encyclopedia of fluid mechanics*, 5th edition. Houston: Gulf.

De Kee, Daniel, Christopher, D.A., Max, H. & Kyle, F. (2004). Performance-Related test for Asphalt emulsions. Louisiana department of transportation and development, Louisiana transportation research centre, United States of America.

De Krester, R.G., Scales, P.J. & Boger, D.V. (1997). Clay-based tailings disposal: a case study on coal tailings. *Journal of American Institute of Chemical Engineers*, 43(7):1894-1904.

De Larrard, F, Sztikar, J.C, Hu, C & Joly, M (1994), Design of a rheometer for fluid concretes, in: P.J.M. Bartos (Ed.), *Proceedings of RILEM Workshop on Special Concretes: Workability and Mixing*, RILEM, Page . 201– 208.

Deepti, T. (2005). A new application for the Brookfield viscometer's Viscoelastic property determination. Department of Biological and Agricultural Engineering, Raleigh, North Carolina, USA.

Dobbie, T., Fleming, D.J. & Busby, J. (1998). Wall slip: Measuring and flow modelling for processing, *Rheology - A practical approach to quality control*. Rheology conference. Shrewsbury, Paper 11, Pages 1-5.

Domone, P. (1998). The slump flow test for high-workability concrete. *Cement concrete resources*, 28(2):177-182.0.

Evans, I.D. (1992). Letter to the Editor: On the nature of the yield stress. *Journal of Rheology*, 36(7):1313.

Ferraris, C.F. & Francois, D.L. (1998). Testing and modelling of fresh concrete rheology. Building and fire research laboratory, National Institute of standards and Technology, Gaithersburg, Maryland.

Maxwell Nyekwe Ichegebo: Investigation of factors effecting yield stress determinations using the slump test.

Fourie, A.B. & Dunn, F. (2007). Limitations to the use of the modified slump test for yield stress determination. Australian Centre for Geomechanics, Paste, Perth, Australia.

Gardiner, B.S., Dlugogorski, B.Z., Jamesson, G.T. & Chhabra, R.P.C. (1998). Yield stress measurement of aqueous foams in the dry limit. ARC Centre for Multiphase Processes. Department of Chemical Engineering, The University of Newcastle, Callaghan NSW 2308, Australia.

Garland, C.W & Nibler, J.W. (1989), "Experiments in Physical Chemistry", 5th Edition, McGraw Hill, New York, Chapter II, United States of America.

Garrido, V.R.H., Gonjalez, P.J. & Montalaban, R, (2003). Vane rheometry of an aqueous solution of worm-like micelles. *Revista Mexicana De Fisica*, 44(1):40. <http://www.ejournal.unam.mx/revmexfis/no481/RMF49107.pdf>

Garrido, P.A & Diaz, R.A, (2009). Analysis of the methodologies used for qualifying or setting the yield stress of copper tailings, Paste 2009, Vina del Mar, Chile.

Gawu, S.K.Y. & Fourie, A.B. (2004). Assessment of the modified slump test as a measure of the yield stress of high-density thickened tailing, *Journal of Geotechnical*, Canada, Volume 41: page 31-47.

Gebhard, S. (1994). A practical approach to Rheology and Rheometry, Karlsruhe: Gebrueder Haake Rheometers. 203.

Gladman, B.J., Usher, S.P. & Scales, P.J. (2006). Understanding the thickening process. Department of Chemical and Biomolecular Engineering, University of Melbourne, Australia.

Glenn III, T.A., Keener, K.M. & Daubert, C.R. (2000). A mixer viscometry approach to use vane tools as steady shear rheological attachments. *Journal of Applied Rheology*, 10(2):80.

Guo, J., Tiu, C., Uhlherr, P.H.T. & Fang, T.N. (2003). Yielding behaviour of organically treated anatase TiO_2 suspension. *Korea – Australia Rheology Journal*, 15(1):9.

- Hackley, V.A & Ferraris, C.F, (2001), In NIST special publication 946, guide to rheological nomenclature: Measurements in ceramic particulate systems, department of commerce, National Institute of standards and Technology (NIST) Technology administration, Gaithersburg, United States.
- Hadley D.W & Weber J.D, (1975), Rheological terminology, *Rheological Acta*, 14, 1098.
- Haldenwang, R., Slatter, P.T. & Masalova, I. (2007). The "Fifty Cent" Rheometer - Effect of Slip, Speed of Lift and Stability on Measurement of Yield Stress. *Paste* 2007. 10th International Seminar on Paste and Thickened Tailings. Adelaide, Australia. 211-218.
- Hallbom, D.J. (2005). The "Lump" Test. International seminar on paste and thickened tailings. Santiago, Chile. 73-97.
- Hartnett, J.P. & Hu, R.Y.Z. (1989). Technical Note: The yield stress – An Engineering Reality. *Journal of Rheology*, 33(4):671.
- Herman, C.Z (2007), Liquid, glass and gel: The phases of colloidal Laponite. *Journal of non-crystalline solids* 353, page 3891-3905.
- Heywood, N.I. & Cheng, D.C.H. (1984). Comparison of methods for predicting head loss in turbulent pipe flow of Non-Newtonian fluids. *Transaction Institute of measurement control*, 6:33-45.
- Heywood, N.I. & Brown, N.P. (1991). *Slurry handling: Design of solid-liquid systems*. Barking, U.K: Elsevier.
- Hobson, G.D. (1940), Industrial tailing, proceedings and development, *Journal of Institute of petroleum technology*, 26:533.
- James, A.E., Williams, D.J.A. & Williams, P.R. (1987). Direct measurement of static yield properties of cohesive suspensions. *Rheol. Acta*, 26:437-446.
- Kee, D.D. & Fong, C.F.C.M. (1993). Letter to the Editor: A true yield stress? *Journal of Rheology*, 37(4):775.

Keentok, M. (1982). The measurement of the yield stress of liquids, *Rheological Acta*, 21:325.

Keentok, M., Milthorpe, J.F. & Donovan, A.E. (1985). On the shearing zone around rotating vanes in plastic liquids: theory and experiment, *Journal of Non-Newtonian Fluid Mechanics*, 17(1):23.

Kochler, E.P. & Fowler, D.W. (2003) Shear dependence of the viscosity of aggregated suspensions, International centre for aggregates research, University of Texas, Austin, United States of America.

Kraynik, A.M. & Hansen, M.G. (1987). Foam Rheology: A model of viscous phenomena. *Journal of rheological act*, 31:175-205.

Krulis, M. & Rohm, M (2004). Adaptation of a vane tool for the viscosity determination of flavoured yoghurt. *Eur Food Res Technol*, Volume 218: 598.

Liddel, P.V. & Boger, D.V. (1996). Yield stress measurement with the vane. *Journal of Non-Newtonian Fluid Mechanics*, 63:235-261.

Lipscomb, G.G. & Denn, M.M. (1984). Flow of Bingham fluids in complex geometries, *Journal of Non-Newtonian Fluid Mechanics*, 14:337-346.

Liu, K. F. & Mei, C. C. (1989), Slow spreading of Bingham fluid on an inclined plane. *Journal Fluid Mech.* 207, 505-529.

Liu, Henry. 2003. Pipeline engineering. Lewis Publishers.

Macosko, C.W. (1994). *Rheology, principles, measurements*. New York: Wiley-VCH. 222-225.

Maia J. M and Covas J. A, (1998), Non- Conventional Rheological monitoring of polymer processing, *Rheology-A practical approach to Quality control*, Rheology conference, Shrewsbury, Paper 7, Page 1.

- Magnin, A. & Piau, J.M. (1990). Cone and plate rheometer of yield stress fluids, study of an aqueous gel. *Journal of Non-Newtonian Fluid Mechanics*, 36:85-108.
- Malkin, A. & Ya, E, (1994). *Rheology fundamentals*. Canada: Chem. Tec, 1:1 – 3, 4:62 – 66.
- Mbiya M. B, (2003), *Contraction and Expansion losses for non-Newtonian fluids*. Unpublished MTECH. Thesis, Cape Peninsula University of Technology, Cape Town, South Africa.
- McCabe, W. L; Smith J. C. & Harriott, P, (1993), *Unit Operations of Chemical Engineering*, International Editions, McGraw-Hill, Singapore, Chapter 3
- Meeker, S.P, Bonnetcaze, R.T & Cloitre, M, (2004), "Slip and flow of soft particle pastes", *Phys. Rev. Lett.* 92, 198302/1 – 4.
- Murata, J. (1984). Flow and deformation of fresh concrete. *Material of Construction*, Paris Volume 17: pages 117–129.
- Nguyen, Q.D. & Boger, D.V. (1983). Yield stress measurement for concentrated suspension. *J. Rheo.* 27:321-349.
- Nguyen, Q.D. & Boger, D.V. (1985). Direct yield stress measurement with the vane method, Department of chemical Engineering, University of Melbourne, Australia, *Journal of Rheology*, 27:335-347.
- Nguyen, Q.D. & Boger, D.V. (1992). Measuring the flow properties of yield stress fluids, *Annual review of fluid mechanics*, page 24-47.
- Nguyen, Q.D., Akroyd, T., Daniel, C., Kee. D. & Zhu, L. (2005). Yield stress measurements in suspensions: an inter-laboratory study. School of Chemical Engineering, University of Adelaide, Adelaide, SA 5005, Australia.
- Nielsen, S.S, (1998), *Food analysis*, in Aspen publishers, *Rheological principles for food analysis*, second edition, Gaithersburg, United States.

- Nkomo S. E, (2005), Using rheometry in prediction of pumping characteristics of highly concentrated water in oil explosive emulsions. Unpublished MTECH Thesis, Cape Peninsula University of Technology, Cape Town, South Africa.
- Oslen, R. S. (1999). The field vane shear web page [Online]. Available: <http://www.liquefaction.com/insitutests/vane/>
- Omura, A.P. & Steffe, J.E. (2001). Centrifugal slump test to measure yield stress. *Journal of food science*, 66(1), pages 34-53
- Pashias, N., Boger, D.V., Summers, J. & Glenister, D.J. (1996), A fifty-cent rheometer for yield stress measurement. *Journal of Rheology*, 40(6):1179-1189.
- Paterson, A. & Cooke, R. 1999. The design of slurry pipeline systems. Short course presented at the cape Technikon, Cape Town, 24-26 March, 1999.
- Patton, T.C. (1964). Paint flow and pigment dispersion. New York: Interscience Publishers.
- Peder C. F. Moller A, Mewis B. J and Bonn D, (2006), Yield stress and thixotropy: on the difficulty of measuring yield stresses in practice, *Journal of the Royal Society of Chemistry*, Volume 2, Page 274–283.
- Pernell, C.W., Foegeding, E.A. & Daubert, C.R. (2000). Measurement of the yield stress of protein foams by vane rheometry. *Journal of food science*, 65(1):110.
- Persello, J.A & Agassant J.F, (1994), *Rheology for polymer processing*, Elsevier, Amsterdam.
- Poshusta, R.D. Error analysis [Online]. Available: http://www.poshusta.chem.edu/sci_com/datanal/error.htm. [2004] August].
- Qui, C.G. & Rao, M.A. (1989). Effect of dispersed phase on the slip coefficient of applesauce in a concentric cylinder viscometer. *Journal of texture studies*, 20:57-70.
- Rao, M.A. & Cooley, H.J. (1984). Determination of Effective shear rates in rotational viscometers with complex Geometries. *Journal of Texture studies*, 15:327.
-
- Maxwell Nyekwe Ichegbo: Investigation of factors effecting yield stress determinations using the slump test.

Raynaud, J.S, Moucheron, P, Baudez J.C, Berrand, F, Guilbaud, J.P & Coussot, P, (2002), "Direct determination by nuclear magnetic resonance of the thixotropic and yielding behaviour of suspensions", *Journal Rheological*, 46, page 709 – 732.

Ritcey, G.W. (1989). *Tailings management*. Amsterdam: Elsevier.

Roberts, G.P & Barnes, H.A. (2001). New measurements of the flow-curves for Carbopol dispersions without slip artefacts. *Rheological Acta*, 40:499.

Rohm, A, & Haag J, (2002), *Aculyn 22 thickening*, 100 independence mall west, Philadelphia, Pa, United State.

Roussel, N., Stefani, C. & Lery, R. (2005). From mini-cone test to Abrams cone test: Measurement of cement-based materials yield stress using slump tests. *Cement and concrete Research*, 35:817-822.

Russell, J.L. (1939). *The scientific outlook Process Rheology society London service advertisers*: page 154-550.

Russel, N. (2006). Correlation between yield stress and slump: Comparison between numerical simulations and concrete rheometer results. *Material and structures* 39:501-509.

Saak, A.W, Jennings, H.M, & Shah, S.P. (2004). A generalized approach for the determination of yield stress by slump and slump flow. *Cement and Concrete Research* 34: 363–371.

SABS 862-: (1994). *Consistency of freshly mixed concrete – Slump test*. South African Bureau of Standards.

Savarmand, S. (2002). Rheological properties of concentrated aqueous silica suspensions: Effect of Ph and ions content. *Journal of Rheology*, 47:5.

Schowalter, W.R. & Christensen, G. (1987). Towards a rationalisation of the slump test for fresh concrete: comparisons of calculations and experiments. *J. Rheo.*, 42(4):865-870.

Maxwell Nyekwe Ichegbo: Investigation of factors effecting yield stress determinations using the slump test.

- Schurz, J. (1992). Letter to the Editor: A yield value in a true solution? *Journal of Rheology*, 36(7):1319.
- Sherwood, J.D. & Meeten, G.H. (1991). The use of the vane to measure the shear modulus of linear elastic solids. *Journal of Non-Newtonian Fluid Mechanics*, 41:101.
- Shook, C.W. & Roco, M.C. (1991). *Slurry flow: Principle and practical*. Butterworth Heinemann.
- Skelland A.H.P., 1967, *Non-Newtonian flow and heat transfer*, John Wiley & Sons, New York, NY.
- Slatter, P.T. (1994). *Transitional and turbulent flow of Non-Newtonian fluids in pipes*, Ph.D. thesis, University of Cape Town.
- Sofra, F. & Boger, D.V. (2000). Exploiting the Rheology of mine tailings for dry disposal in tailing and mine waste. *Proceedings of the 7th International conference*. Fort Collins, Colorado, 23-26 January, Rotterdam: A.A. Balkema. Pages 169-180.
- Sofra, F. & Boger, D.V. (2001a) Slope prediction for thickened tailings and pastes, in tailing and mine waste. *Proceedings of the 8th International conference*. Fort Collins, Colorado, 15th – 18th January. A.A Balkema: Rotterdam, Netherlands. Pages: 169-180.
- Sofra, F. & Boger, D.V. (2001b). Environmental rheology for waste minimization in the minerals industry. *Chemical Engineering Journal*, 86:319-330.
- Steffe, J.F. (1996). *Rheological methods in food process Engineering*. Second Edition. East Lansing: Freeman Press. Pages 2, 158, 200-201, 296, 316-317.
- Stokes, J.R. & Telford, J.H. (2004). Measuring the yield behaviour of structured fluids, *Journal of Non-Newtonian Fluid Mechanics*, 63:137-146.
- Stokes, J.R., Telford, J.H. & Williamson, R, (2005), The flowability of ice suspensions, *Journal of Rheology*, 49(1):139.
-
- Maxwell Nyekwe Ichegbo: Investigation of factors effecting yield stress determinations using the slump test.

- Talbert, S.H & Avitzur, B. (1996), *Elementary mechanics of plastic forming*, John Wiley and Sons, Hoboken City, Hudson County, New Jersey, United States of America.
- Tanigawa, Y. & Mori, H. (1989). Analytical study of deformation of fresh concrete. *Journal of engineering mechanics*, 115 (3), March.
- Tanigawa, Y., Mori, H. & Watanabe, K. (1991). Analytical and experimental studies on casting of fresh concrete into wall form. *Transcription of Japan concrete society*, 13.
- Tatsumi, D., Ishioka, S. & Matsumoto, T. (2002). Effect of Fiber concentration and axial ratio on the Rheological properties of cellulose fiber suspensions. *Journal of the Society of Rheology, Japan*, 30(1):27.
- Tattersall, G.H. & Bloomer, S.J. (1979). Further development of the two-point test for workability and extension of its range. *Magazine of Concrete Research*, 31:202-210.
- Tattersall, G.H. & Banfill, P.F.G. (1983). *The rheology of fresh concrete*. Boston: Pitman Publishing Incorporated.
- Tattersall, G.H. (1991). *Workability and quality control of concrete*. Spon: 262.
- Thomas, D.G. (1963). Non-Newtonian suspensions Part 1 - physical properties and laminar transport characteristics. *Industrial Engineering Chemical*, 55:18-29.
- Tran, Q.K. & Glumac, L. (2002). Study on filtered mud conveying at an alumina refinery. *Kraiser Engineers, Perth, Western Australia*, 6000.
- Traxler, R.N. (1961). *Asphalt*. New York: Reinhold Publishing Corporation.
- Troung, V.D. & Daubert, C.R. (2001). Textual characterization of Cheeses using vane Rheometry and Torsion analysis. *Journal of food science*, 66(5):716.
- Troung, V.D., Daubert, C.R., Drake, M.A. & Baxter, S.R. (2002). Vane Rheometry for Textual characterization of cheddar cheeses: Correlation with other Instrumental and sensory measurements. *LWT food science and Technology*, 35:305.

- Uhlherr, P.H.T., Guo, J., Fang, T.N. & Tiu, X.M. (2001). Static measurement of yield stress using a cylindrical penetrometer. *Korea-Australia Rheology Journal*, 14(1):17.
- Uhlherr, P.H.T., Guo, J., Tiu, X.M., Zhang, J.Z.Q., Zhou, J.Z.Q. & Fang, T.N. (2005). The shear-induced solid-liquid transition in yield stress materials with chemically different structures. *Journal of Non-Newtonian Fluid Mechanics*, 125:101.
- Umeya K, Isoda T, Ishii T, Sawamura K, (1969), Some observations on the flow properties of disperse Systems *Powder Technology*, 3, 259-266.
- Van Olphen, H. 1977. *An Introduction of Clay Colloid Chemistry*. Second Edition. John Wiley and Sons: New York, NY, United States of America.
- Walls, H.J., Caines, S.B., Sanchez, A.M. & Khan, S.A. (2003). Yield stress and wall slip phenomena. *Journal of Rheology*, 47(4):847.
- Williams, J A, Paddock, S W, Vorwerk K & Carroll, S B, (1994), *Nature (London)*; 368: 299 – 305
- Wilson, S.D.R. (1993). Squeezing flow of a Bingham material. *Journal of Non-Newtonian Fluid Mechanics*, 47:211-219.
- Wilson, K.C., Pugh, F.J., Addie, G.R., Visintainer, R.J. & Clift, R. (1993). Fluids with Non-Newtonian carrier fluids, up, down and sideways. 12th International Conference on slurry handling and pipeline transport. *Hydrotransport 12*, BHR Group: 657.
- Yan, J. & James, A.E. (1997). The yield surface of viscoelastic and plastic fluids in a vane viscometer, *Journal of Non-Newtonian Fluid Mechanics*, 70(1):237.
- Yetkin, Y, Mansour, R, & Thomas, W. K, (2000), Mixing and compaction temperatures for hot mix asphalt concrete, Bureau of Engineering Research, University of Texas at Austin, United State.
- Yoo, B., Rao, M A & Steffe. J F (1995), Yield stress of food dispersions with the vane method at controlled shear rate and shear stress. *Journal Texture Studies*, 26: 1-10.

Yoshimura, A.S, Prud'homme, R.K, Princen, H.M. & Kiss, A. (1987) A comparison of techniques for measuring yield stresses, *J. Rheol.* 31:699-710.

Zhang, M.X. & Nguyen, Q.D. (1996). Movement of the yield boundary of time-dependent yield stress fluids in coquette flow. *Proceedings of the 12th Congress on Rheology*. Quebec, 1996. 560.

Zhu, L, Sun N, Papadopoulos K, & De Kee, D. (2001). A slotted plate device for measuring static yield stress. *Journal of Rheology*, 45(5):1105.

APPENDICES

Appendix A- Slump Data

APPENDIX A – SLUMP DATA

Table A.1: Slump test for 14 % kaolin (without spray) using the slump meter

RESULTS ON SLUMP TEST : (KAOLIN 14%)										
Equations:										
Relative density Density ρ (Kg/m ³) (m.s ⁻¹)		$s' = \frac{h}{H}$		$\tau_y = \rho g H \tau'_y$		Approximate cylinder $\tau'_y = \frac{1}{2} - \frac{1}{2} \sqrt{s'}$		Vane τ_y 33.68		
$S = 1 - 2\tau_y (1 - \ln(2\tau_y))$										
Without silicone spray :										
Cone geometry : Stainless steel										
Number	Speed (mm.s ⁻¹)	Time	H (mm)	H _r (mm)	h (mm)	s'	τ'_y	τ_y	Calc. from vane	
10	3.75	10.23	150	38.4	111.6	0.74	0.07	121.35	0.02	
11	6.34	5.87	150	37.23	112.77	0.75	0.07	117.37	0.02	
12	12.25	3.02	150	37	113	0.75	0.07	116.59	0.02	
13	15.66	2.35	150	36.8	113.2	0.75	0.07	115.91	0.02	
Cylinder geometry : Stainless steel										
Number	Speed (mm.s ⁻¹)	Time	H (mm)	H _r (mm)	h (mm)	s'	τ'_y	τ_y		
10	3.18	13.01	100	41.4	58.6	0.59	0.12	138.02	0.03	
11	6.79	5.8	100	39.4	60.6	0.61	0.11	130.40	0.03	
12	10.07	4.12	100	41.5	58.5	0.59	0.12	138.41	0.03	
13	15.98	2.7	100	43.14	56.86	0.57	0.12	144.76	0.03	
Cone geometry : PVC										
Number	Speed (mm.s ⁻¹)	Time	H (mm)	H _r (mm)	h (mm)	s'	τ'_y	τ_y		
10	3.75	11.66	150	43.73	106.27	0.71	0.08	139.76	0.02	
11	7.45	5.39	150	40.16	109.84	0.73	0.07	127.38	0.02	
12	11.13	3.73	150	41.51	108.49	0.72	0.07	132.04	0.02	
13	19.15	2.2	150	42.12	107.88	0.72	0.08	134.15	0.02	
Cylinder geometry : PVC										
Number	Speed (mm.s ⁻¹)	Time	H (mm)	H _r (mm)	h (mm)	s'	τ'_y	τ_y		
10	4.03	11.02	100	44.36	55.64	0.56	0.13	149.55	0.03	
11	6.87	6.6	100	45.33	54.67	0.55	0.13	153.39	0.03	
12	8.63	4.8	100	41.42	58.58	0.59	0.12	138.10	0.03	
13	17.00	2.57	100	43.69	56.31	0.56	0.12	146.91	0.03	
Cylinder geometry : PVC										
Number	Speed (mm.s ⁻¹)	Time	H (mm)	H _r (mm)	h (mm)	s'	τ'_y	τ_y		
10	4.03	11.02	100	44.36	55.64	0.56	0.13	149.55	0.03	
11	6.87	6.6	100	45.33	54.67	0.55	0.13	153.39	0.03	
12	8.63	4.8	100	41.42	58.58	0.59	0.12	138.10	0.03	
13	17.00	2.57	100	43.69	56.31	0.56	0.12	146.91	0.03	
Cylinder geometry : PVC										
Number	Speed (mm.s ⁻¹)	Time	H (mm)	H _r (mm)	h (mm)	s'	τ'_y	τ_y		
10	4.03	11.02	100	44.36	55.64	0.56	0.13	149.55	0.03	
11	6.87	6.6	100	45.33	54.67	0.55	0.13	153.39	0.03	
12	8.63	4.8	100	41.42	58.58	0.59	0.12	138.10	0.03	
13	17.00	2.57	100	43.69	56.31	0.56	0.12	146.91	0.03	
Cylinder geometry : PVC										
Number	Speed (mm.s ⁻¹)	Time	H (mm)	H _r (mm)	h (mm)	s'	τ'_y	τ_y		
10	4.03	11.02	100	44.36	55.64	0.56	0.13	149.55	0.03	
11	6.87	6.6	100	45.33	54.67	0.55	0.13	153.39	0.03	
12	8.63	4.8	100	41.42	58.58	0.59	0.12	138.10	0.03	
13	17.00	2.57	100	43.69	56.31	0.56	0.12	146.91	0.03	
Cylinder geometry : PVC										
Number	Speed (mm.s ⁻¹)	Time	H (mm)	H _r (mm)	h (mm)	s'	τ'_y	τ_y		
10	4.03	11.02	100	44.36	55.64	0.56	0.13	149.55	0.03	
11	6.87	6.6	100	45.33	54.67	0.55	0.13	153.39	0.03	
12	8.63	4.8	100	41.42	58.58	0.59	0.12	138.10	0.03	
13	17.00	2.57	100	43.69	56.31	0.56	0.12	146.91	0.03	
Cylinder geometry : PVC										
Number	Speed (mm.s ⁻¹)	Time	H (mm)	H _r (mm)	h (mm)	s'	τ'_y	τ_y		
10	4.03	11.02	100	44.36	55.64	0.56	0.13	149.55	0.03	
11	6.87	6.6	100	45.33	54.67	0.55	0.13	153.39	0.03	
12	8.63	4.8	100	41.42	58.58	0.59	0.12	138.10	0.03	
13	17.00	2.57	100	43.69	56.31	0.56	0.12	146.91	0.03	
Cylinder geometry : PVC										
Number	Speed (mm.s ⁻¹)	Time	H (mm)	H _r (mm)	h (mm)	s'	τ'_y	τ_y		
10	4.03	11.02	100	44.36	55.64	0.56	0.13	149.55	0.03	
11	6.87	6.6	100	45.33	54.67	0.55	0.13	153.39	0.03	
12	8.63	4.8	100	41.42	58.58	0.59	0.12	138.10	0.03	
13	17.00	2.57	100	43.69	56.31	0.56	0.12	146.91	0.03	
Cylinder geometry : PVC										
Number	Speed (mm.s ⁻¹)	Time	H (mm)	H _r (mm)	h (mm)	s'	τ'_y	τ_y		
10	4.03	11.02	100	44.36	55.64	0.56	0.13	149.55	0.03	
11	6.87	6.6	100	45.33	54.67	0.55	0.13	153.39	0.03	
12	8.63	4.8	100	41.42	58.58	0.59	0.12	138.10	0.03	
13	17.00	2.57	100	43.69	56.31	0.56	0.12	146.91	0.03	
Cylinder geometry : PVC										
Number	Speed (mm.s ⁻¹)	Time	H (mm)	H _r (mm)	h (mm)	s'	τ'_y	τ_y		
10	4.03	11.02	100	44.36	55.64	0.56	0.13	149.55	0.03	
11	6.87	6.6	100	45.33	54.67	0.55	0.13	153.39	0.03	
12	8.63	4.8	100	41.42	58.58	0.59	0.12	138.10	0.03	
13	17.00	2.57	100	43.69	56.31	0.56	0.12	146.91	0.03	
Cylinder geometry : PVC										
Number	Speed (mm.s ⁻¹)	Time	H (mm)	H _r (mm)	h (mm)	s'	τ'_y	τ_y		
10	4.03	11.02	100	44.36	55.64	0.56	0.13	149.55	0.03	
11	6.87	6.6	100	45.33	54.67	0.55	0.13	153.39	0.03	
12	8.63	4.8	100	41.42	58.58	0.59	0.12	138.10	0.03	
13	17.00	2.57	100	43.69	56.31	0.56	0.12	146.91	0.03	
Cylinder geometry : PVC										
Number	Speed (mm.s ⁻¹)	Time	H (mm)	H _r (mm)	h (mm)	s'	τ'_y	τ_y		
10	4.03	11.02	100	44.36	55.64	0.56	0.13	149.55	0.03	
11	6.87	6.6	100	45.33	54.67	0.55	0.13	153.39	0.03	
12	8.63	4.8	100	41.42	58.58	0.59	0.12	138.10	0.03	
13	17.00	2.57	100	43.69	56.31	0.56	0.12	146.91	0.03	
Cylinder geometry : PVC										
Number	Speed (mm.s ⁻¹)	Time	H (mm)	H _r (mm)	h (mm)	s'	τ'_y	τ_y		
10	4.03	11.02	100	44.36	55.64	0.56	0.13	149.55	0.03	
11	6.87	6.6	100	45.33	54.67	0.55	0.13	153.39	0.03	
12	8.63	4.8	100	41.42	58.58	0.59	0.12	138.10	0.03	
13	17.00	2.57	100	43.69	56.31	0.56	0.12	146.91	0.03	
Cylinder geometry : PVC										
Number	Speed (mm.s ⁻¹)	Time	H (mm)	H _r (mm)	h (mm)	s'	τ'_y	τ_y		
10	4.03	11.02	100	44.36	55.64	0.56	0.13	149.55	0.03	
11	6.87	6.6	100	45.33	54.67	0.55	0.13	153.39	0.03	
12	8.63	4.8	100	41.42	58.58	0.59	0.12	138.10	0.03	
13	17.00	2.57	100	43.69	56.31	0.56	0.12	146.91	0.03	
Cylinder geometry : PVC										
Number	Speed (mm.s ⁻¹)	Time	H (mm)	H _r (mm)	h (mm)	s'	τ'_y	τ_y		
10	4.03	11.02	100	44.36	55.64	0.56	0.13	149.55	0.03	
11	6.87	6.6	100	45.33	54.67	0.55	0.13	153.39	0.03	
12	8.63	4.8	100	41.42	58.58	0.59	0.12	138.10	0.03	
13	17.00	2.57	100	43.69	56.31	0.56	0.12	146.91	0.03	
Cylinder geometry : PVC										
Number	Speed (mm.s ⁻¹)	Time	H (mm)	H _r (mm)	h (mm)	s'	τ'_y	τ_y		
10	4.03	11.02	100	44.36	55.64	0.56	0.13	149.55	0.03	
11	6.87	6.6	100	45.33	54.67	0.55	0.13	153.39	0.03	
12	8.63	4.8	100	41.42	58.58	0.59	0.12	138.10	0.03	
13	17.00	2.57	100	43.69	56.31	0.56	0.12	146.91	0.03	
Cylinder geometry : PVC										
Number	Speed (mm.s ⁻¹)	Time	H (mm)	H _r (mm)	h (mm)	s'	τ'_y	τ_y		
10	4.03	11.02	100	44.36	55.64	0.56	0.13	149.55	0.03	
11	6.87	6.6	100	45.33	54.67	0.55	0.13	153.39	0.03	
12	8.63	4.8	100	41.42	58.58	0.59	0.12	138.10	0.03	
13	17.00	2.57	100	43.69	56.31	0.56	0.12	146.91	0.03	
Cylinder geometry : PVC										
Number	Speed (mm.s ⁻¹)	Time	H (mm)	H _r (mm)	h (mm)	s'	τ'_y	τ_y		
10	4.03	11.02	100	44.36	55.64	0.56	0.13	149.55	0.03	
11	6.87	6.6	100	45.33	54.67	0.55	0.13	153.39	0.03	
12	8.63	4.8	100	41.42	58.58	0.59	0.12	138.10	0.03	
13	17.00	2.57	100	43.69	56.31	0.56	0.12	146.91	0.03	
Cylinder geometry : PVC										
Number	Speed (mm.s ⁻¹)	Time	H (mm)	H _r (mm)	h (mm)	s'	τ'_y	τ_y		
10	4.03	11.02	100	44.36	55.64	0.56	0.13	149.55	0.03	
11	6.87	6.6	100	45.33	54.67	0.55	0.13	153.39	0.03	
12	8.63	4.8	100	41.42	58.58	0.59	0.12	138.10	0.03	
13	17.00	2.57	100	43.69	56.31	0.56	0.12	146.91	0.03	
Cylinder geometry : PVC										
Number	Speed (mm.s ⁻¹)	Time	H (mm)	H _r (mm)	h (mm)	s'	τ'_y	τ_y		
10	4.03	11.02	100	44.36	55.64	0.56	0.13	149.55	0.03	
11	6.87	6.6	100	45.33	54.67	0.55	0.13	153.39	0.03	
12	8.63	4.8	100	41.42	58.58	0.59	0.12	138.10	0.03	
13	17.00	2.57	100	43.69	56.31	0.56	0.12	146.91	0.03	
Cylinder geometry : PVC										
Number	Speed (mm.s ⁻¹)	Time	H (mm)	H _r (mm)	h (mm)	s'	τ'_y	τ_y		
10	4.03	11.02	100	44.36	55.64	0.56	0.13	149.55	0.03	
11	6.87	6.6	100	45.33	54.67	0.55	0.			

Table A.2 Slump test for 14 % Kaolin (with spray) using the slump meter

Appendix A- Slump Data

RESULTS ON SLUMP TEST : (KAOLIN 14%)																									
Relative density Density g (Kg/m ³) (m.s ⁻¹)		1.201 1201 9.81		Equations: $s' = \frac{h}{H}$ $\tau_y = \rho g H \tau_y$		Approximate cylinder $\tau_y' = \frac{1}{2} - \frac{1}{2} \sqrt{s'}$		Vane τ_y 33.68		Lump model $\tau_y' = 0.5(1 - S') e^{\sqrt{3}(-s')}$		Cylinder model $S = 1 - 2\tau_y'(1 - \ln(2\tau_y'))$													
With silicone spray :																									
Cone geometry : Stainless steel																									
Number	Speed (mm.s ⁻¹)	Time	H (mm)	H _r (mm)	h (mm)	s'	τ_y'	Approx.cyl τ_y	Calc.from vane	τ_y'	Lump model	τ_y	Cylinder model τ_y												
10	3.56	13.39	150	47.63	102.37	0.68	0.09	153.52	0.02	0.05	0	85.97	0.05	4.03E-07	83.47										
11	9.11	4.79	150	43.65	106.35	0.71	0.08	139.48	0.02	0.04	0	75.25	0.04	5.88E-07	73.79										
12	10.85	3.78	150	41	109	0.73	0.07	130.27	0.02	0.04	0	68.55	0.04	3.76E-08	67.61										
13	17.38	2.45	150	42.57	107.43	0.72	0.08	135.71	0.02	0.04	0	72.47	0.04	3.37E-07	71.24										
Cylinder geometry : Stainless steel																									
Number	Speed (mm.s ⁻¹)	Time	H (mm)	H _r (mm)	h (mm)	s'	τ_y'	τ_y		τ_y'	Lump Model	τ_y	Cylinder model τ_y												
10	3.34	13.73	100	45.8	54.2	0.54	0.13	155.27	0.03	0.09	0	105.43	0.08	9.74E-07	95.72										
11	7.10	6.38	100	45.3	54.7	0.55	0.13	153.27	0.03	0.09	0	103.38	0.08	1.41E-07	94.11										
12	10.70	4.12	100	44.1	55.9	0.56	0.13	148.53	0.03	0.08	0	98.58	0.08	7.02E-07	90.30										
13	16.02	2.74	100	43.9	56.1	0.56	0.13	147.74	0.03	0.08	0	97.79	0.08	6.14E-07	89.67										
Cone geometry : PVC																									
Number	Speed (mm.s ⁻¹)	Time	H (mm)	H _r (mm)	h (mm)	s'	τ_y'	τ_y		τ_y'	Lump model	τ_y	Cylinder model τ_y												
10	4.28	10.54	150	45.1	104.9	0.70	0.08	144.56	0.02	0.04	0	79.06	0.04	9.55E-08	77.26										
11	8.22	5.29	150	43.5	106.5	0.71	0.08	138.96	0.02	0.04	0	74.86	0.04	5.00E-07	73.43										
12	12.01	3.59	150	43.1	106.9	0.71	0.08	137.56	0.02	0.04	0	73.83	0.04	2.63E-07	72.49										
13	16.64	2.47	150	41.1	108.9	0.73	0.07	130.62	0.02	0.04	0	68.79	0.04	4.63E-08	67.84										
Cylinder geometry : PVC																									
Number	Speed (mm.s ⁻¹)	Time	H (mm)	H _r (mm)	h (mm)	s'	τ_y'	τ_y		τ_y'	Lump model	τ_y	Cylinder model τ_y												
10	3.47	13.27	100	46	54	0.54	0.13	156.07	0.03	0.09	0	106.26	0.08	8.87E-07	96.37										
11	7.43	6.14	100	45.64	54.36	0.54	0.13	154.63	0.03	0.09	0	104.78	0.08	1.43E-07	95.20										
12	11.58	4	100	46.3	53.7	0.54	0.13	157.27	0.03	0.09	0	107.51	0.08	6.77E-07	97.35										
13	15.87	2.84	100	45.06	54.94	0.55	0.13	152.32	0.03	0.09	0	102.41	0.08	1.34E-07	93.34										

Table A.3 Slump test for 16 % Kaolin (without spray) using the slump meter

Appendix A- Slump Data

RESULTS ON SLUMP TEST : (KAOLIN 16%)													
Equations:													
<div>Relative density1.201</div> <div>Density (Kg/m³)1201</div> <div>g (m.s⁻¹)9.81</div> <div>g</div> <div>$s' = \frac{h}{H} \tau_y = \rho g H \tau_y$</div> <div>$\tau_y' = \frac{1}{2} - \frac{1}{2} \sqrt{s'}$</div> <div>$\tau_y' = 0.5(1 - S')e^{\sqrt{3}(1 - S')}$</div> <div>$S = 1 - 2\tau_y'(1 - \ln(2\tau_y'))$</div>													
Without silicone spray :													
Cone geometry : Stainless steel													
Number	Speed (mm.s ⁻¹)	Time	H (mm)	H _r (mm)	h (mm)	s'	τ_y'	Approx.cyl τ_y	Calc.from vane τ_y'	Lump model		Cylinder model	
10	1.98	23.2	150	45.9	104.1	0.69	0.08	147.51	0.03	0.05	0	81.27	79.27
11	7.59	7.34	150	55.7	94.3	0.63	0.10	183.01	0.03	0.06	0	110.44	104.75
12	12.97	4.24	150	55	95	0.63	0.10	180.42	0.03	0.06	0	108.18	102.82
13	18.88	2.77	150	52.3	97.7	0.65	0.10	170.50	0.03	0.06	0	99.71	95.55
Cylinder geometry : Stainless steel													
Number	Speed (mm.s ⁻¹)	Time	H (mm)	H _r (mm)	h (mm)	s'	τ_y'	τ_y	τ_y'	Lump model		Cylinder model	
10	3.07	17.5	100	53.8	46.2	0.46	0.16	188.68	0.04	0.12	0	142.38	123.81
11	7.13	7.56	100	53.9	46.1	0.46	0.16	189.12	0.04	0.12	0	142.89	124.19
12	10.98	4.88	100	53.6	46.4	0.46	0.16	187.82	0.04	0.12	0	141.36	123.06
13	21.61	2.54	100	54.9	45.1	0.45	0.16	193.48	0.04	0.13	0	148.08	128.01
Cone geometry : PVC													
Number	Speed (mm.s ⁻¹)	Time	H (mm)	H _r (mm)	h (mm)	s'	τ_y'	τ_y	τ_y'	Lump model		Cylinder model	
10	4.31	13.01	150	56.1	93.9	0.63	0.10	184.50	0.03	0.06	0	111.75	105.86
11	7.79	7.05	150	54.9	95.1	0.63	0.10	180.05	0.03	0.06	0	107.86	102.55
12	11.47	4.62	150	53	97	0.65	0.10	173.05	0.03	0.06	0	101.86	97.41
13	16.38	3.2	150	52.4	97.6	0.65	0.10	170.86	0.03	0.06	0	100.02	95.82
Cylinder geometry : PVC													
Number	Speed (mm.s ⁻¹)	Time	H (mm)	H _r (mm)	h (mm)	s'	τ_y'	τ_y	τ_y'	Lump model		Cylinder model	
10	3.84	14.28	100	54.8	45.2	0.45	0.16	193.04	0.04	0.13	0	147.56	127.62
11	7.61	7.2	100	54.8	45.2	0.45	0.16	193.04	0.04	0.13	0	147.56	127.62
12	11.08	4.91	100	54.4	45.6	0.46	0.16	191.29	0.04	0.12	0	145.47	126.09
13	17.80	3.04	100	54.1	45.9	0.46	0.16	189.98	0.04	0.12	0	143.92	124.95

Table A.4 Slump test for 16 % Kaolin (with spray) using the slump meter

Appendix A- Slump Data

RESULTS ON SLUMP TEST : (KAOLIN 16%)									
Equations:									
Relative density Density g		$s' = \frac{h}{H}$		$\tau_y = \rho g H \tau_y'$		Approximate cylinder			
1.201 1201 (Kg/m ³)		1.201 1201 (m.s ⁻¹)		$\tau_y' = \frac{1}{2} - \frac{1}{2} \sqrt{s'}$		$\tau_y' = \frac{1}{2} - \frac{1}{2} \sqrt{s'}$			
9.81		9.81		48.32		48.32			
Cylinder model									
$S = 1 - 2\tau_y'(1 - \ln(2\tau_y'))$									
Lump model									
$\tau_y' = 0.5(1 - S')e^{\sqrt{3}(-S')}$									
Cylinder model									
$S = 1 - 2\tau_y'(1 - \ln(2\tau_y'))$									
With silicone spray :									
Cone geometry : Stainless steel									
Number	Speed (mm.s ⁻¹)	Time	H (mm)	H _r (mm)	h (mm)	s'	τ_y'	Approx.cyl τ_y	Calc. from vane
10	3.55	15.12	150	53.7	96.3	0.64	0.10	175.62	0.03
11	7.04	7.4	150	52.1	97.9	0.65	0.10	169.77	0.03
12	11.41	4.75	150	54.2	95.8	0.64	0.10	177.46	0.03
13	17.29	3.1	150	53.6	96.4	0.64	0.10	175.26	0.03
Cylinder geometry : Stainless steel									
Number	Speed (mm.s ⁻¹)	Time	H (mm)	H _r (mm)	h (mm)	s'	τ_y'	Lump Model τ_y	Cylinder model τ_y
10	2.69	20.99	100	56.453	43.547	0.44	0.17	200.35	0.13
11	6.95	7.7	100	53.5	46.5	0.47	0.16	187.38	0.12
12	12.40	4.58	100	56.8	43.2	0.43	0.17	201.90	0.13
13	15.88	3.29	100	52.26	47.74	0.48	0.15	182.06	0.11
Cone geometry : PVC									
Number	Speed (mm.s ⁻¹)	Time	H (mm)	H _r (mm)	h (mm)	s'	τ_y'	Lump model τ_y	Cylinder model τ_y
10	3.37	15.95	150	53.8	96.2	0.64	0.10	175.99	0.06
11	7.32	6.85	150	50.15	99.85	0.67	0.09	162.69	0.05
12	10.31	5.16	150	53.2	96.8	0.65	0.10	173.79	0.06
13	16.45	3.18	150	52.3	97.7	0.65	0.10	170.50	0.06
Cylinder geometry : PVC									
Number	Speed (mm.s ⁻¹)	Time	H (mm)	H _r (mm)	h (mm)	s'	τ_y'	Lump model τ_y	Cylinder model τ_y
10	3.36	16.15	100	54.2	45.8	0.46	0.16	190.42	0.12
11	7.47	7.35	100	54.9	45.1	0.45	0.16	193.48	0.13
12	10.36	5.02	100	52	48	0.48	0.15	180.96	0.11
13	15.80	3.36	100	53.1	46.9	0.47	0.16	185.66	0.12

Table A.5 Slump test for 18 % Kaolin (without spray) using the slump meter

RESULTS ON SLUMP TEST : (KAOLIN 18%)

Equations:

$$\tau_y = \frac{H}{\eta} = \rho g H \tau_y$$

Relative density	1.269
Density	1269
ρ	9.81

Without silicone spray :												
Cone geometry : Stainless steel												
Number	Speed (mm.s ⁻¹)	Time	H (mm)	H _r (mm)	h (mm)	s'	τ _y '	τ _y	Approx.cyl	Calc.from vane	τ _y	τ _y '
10	3.42	20.06	150	68.6	81.4	0.54	0.13	245.87	0	0.09	166.81	0.08
11	8.65	7.88	150	68.2	81.8	0.55	0.13	244.18	0	0.04	165.07	0.08
12	11.24	6.05	150	68	82	0.55	0.13	243.34	0	0.04	164.21	0.08
13	19.09	3.51	150	67	83	0.55	0.13	239.15	0	0.04	159.94	0.08
Cylinder geometry : Stainless steel												
Number	Speed (mm.s ⁻¹)	Time	H (mm)	H _r (mm)	h (mm)	s'	τ _y '	τ _y	Lump model	τ _y	τ _y '	
10	2.91	22.34	100	64.9	35.1	0.35	0.20	253.68	0	0.06	219.95	0.15
11	8.18	7.84	100	64.1	35.9	0.36	0.20	249.50	0	0.06	214.25	0.14
12	12.02	5.29	100	63.6	36.4	0.36	0.20	246.91	0	0.06	210.74	0.14
13	17.45	3.61	100	63	37	0.37	0.20	243.83	0	0.06	206.59	0.14
Cone geometry : PVC												
Number	Speed (mm.s ⁻¹)	Time	H (mm)	H _r (mm)	h (mm)	s'	τ _y '	τ _y	Lump model	τ _y	τ _y '	
10	3.40	19.5	150	66.3	83.7	0.56	0.13	236.22	0	0.08	156.99	0.08
11	9.20	6.88	150	63.3	86.7	0.58	0.12	223.83	0	0.08	144.78	0.07
12	12.20	5.43	150	66.26	83.74	0.56	0.13	236.06	0	0.04	156.82	0.08
13	18.62	3.56	150	66.29	83.71	0.56	0.13	236.18	0	0.04	156.95	0.08
Cylinder geometry : PVC												
Number	Speed (mm.s ⁻¹)	Time	H (mm)	H _r (mm)	h (mm)	s'	τ _y '	τ _y	Lump model	τ _y	τ _y '	
10	3.22	19.46	100	62.72	37.28	0.37	0.19	242.40	0	0.06	204.68	0.14
11	9.09	7.05	100	64.11	35.89	0.36	0.20	249.55	0	0.06	214.32	0.14
12	12.52	5.08	100	63.62	36.38	0.36	0.20	247.01	0	0.06	210.88	0.14
13	17.33	3.71	100	64.3	35.7	0.36	0.20	250.54	0	0.06	215.66	0.14
Cylinder geometry : Stainless steel												
Number	Speed (mm.s ⁻¹)	Time	H (mm)	H _r (mm)	h (mm)	s'	τ _y '	τ _y	Lump model	τ _y	τ _y '	
10	2.91	22.34	100	64.9	35.1	0.35	0.20	253.68	0	0.06	219.95	0.15
11	8.18	7.84	100	64.1	35.9	0.36	0.20	249.50	0	0.06	214.25	0.14
12	12.02	5.29	100	63.6	36.4	0.36	0.20	246.91	0	0.06	210.74	0.14
13	17.45	3.61	100	63	37	0.37	0.20	243.83	0	0.06	206.59	0.14
Cylinder geometry : PVC												
Number	Speed (mm.s ⁻¹)	Time	H (mm)	H _r (mm)	h (mm)	s'	τ _y '	τ _y	Lump model	τ _y	τ _y '	
10	3.40	19.5	150	66.3	83.7	0.56	0.13	236.22	0	0.08	156.99	0.08
11	9.20	6.88	150	63.3	86.7	0.58	0.12	223.83	0	0.08	144.78	0.07
12	12.20	5.43	150	66.26	83.74	0.56	0.13	236.06	0	0.08	156.82	0.08
13	18.62	3.56	150	66.29	83.71	0.56	0.13	236.18	0	0.08	156.95	0.08
Cylinder geometry : Stainless steel												
Number	Speed (mm.s ⁻¹)	Time	H (mm)	H _r (mm)	h (mm)	s'	τ _y '	τ _y	Lump model	τ _y	τ _y '	
10	2.91	22.34	100	64.9	35.1	0.35	0.20	253.68	0	0.06	219.95	0.15
11	8.18	7.84	100	64.1	35.9	0.36	0.20	249.50	0	0.06	214.25	0.14
12	12.02	5.29	100	63.6	36.4	0.36	0.20	246.91	0	0.06	210.74	0.14
13	17.45	3.61	100	63	37	0.37	0.20	243.83	0	0.06	206.59	0.14
Cylinder geometry : PVC												
Number	Speed (mm.s ⁻¹)	Time	H (mm)	H _r (mm)	h (mm)	s'	τ _y '	τ _y	Lump model	τ _y	τ _y '	
10	3.40	19.5	150	66.3	83.7	0.56	0.13	236.22	0	0.08	156.99	0.08
11	9.20	6.88	150	63.3	86.7	0.58	0.12	223.83	0	0.08	144.78	0.07
12	12.20	5.43	150	66.26	83.74	0.56	0.13	236.06	0	0.08	156.82	0.08
13	18.62	3.56	150	66.29	83.71	0.56	0.13	236.18	0	0.08	156.95	0.08
Cylinder geometry : Stainless steel												
Number	Speed (mm.s ⁻¹)	Time	H (mm)	H _r (mm)	h (mm)	s'	τ _y '	τ _y	Lump model	τ _y	τ _y '	
10	2.91	22.34	100	64.9	35.1	0.35	0.20	253.68	0	0.06	219.95	0.15
11	8.18	7.84	100	64.1	35.9	0.36	0.20	249.50	0	0.06	214.25	0.14
12	12.02	5.29	100	63.6	36.4	0.36	0.20	246.91	0	0.06	210.74	0.14
13	17.45	3.61	100	63	37	0.37	0.20	243.83	0	0.06	206.59	0.14
Cylinder geometry : PVC												
Number	Speed (mm.s ⁻¹)	Time	H (mm)	H _r (mm)	h (mm)	s'	τ _y '	τ _y	Lump model	τ _y	τ _y '	
10	3.40	19.5	150	66.3	83.7	0.56	0.13	236.22	0	0.08	156.99	0.08
11	9.20	6.88	150	63.3	86.7	0.58	0.12	223.83	0	0.08	144.78	0.07
12	12.20	5.43	150	66.26	83.74	0.56	0.13	236.06	0	0.08	156.82	0.08
13	18.62	3.56	150	66.29	83.71	0.56	0.13	236.18	0	0.08	156.95	0.08
Cylinder geometry : Stainless steel												
Number	Speed (mm.s ⁻¹)	Time	H (mm)	H _r (mm)	h (mm)	s'	τ _y '	τ _y	Lump model	τ _y	τ _y '	
10	2.91	22.34	100	64.9	35.1	0.35	0.20	253.68	0	0.06	219.95	0.15
11	8.18	7.84	100	64.1	35.9	0.36	0.20	249.50	0	0.06	214.25	0.14
12	12.02	5.29	100	63.6	36.4	0.36	0.20	246.91	0	0.06	210.74	0.14
13	17.45	3.61	100	63	37	0.37	0.20	243.83	0	0.06	206.59	0.14
Cylinder geometry : PVC												
Number	Speed (mm.s ⁻¹)	Time	H (mm)	H _r (mm)	h (mm)	s'	τ _y '	τ _y	Lump model	τ _y	τ _y '	
10	3.40	19.5	150	66.3	83.7	0.56	0.13	236.22	0	0.08	156.99	0.08
11	9.20	6.88	150	63.3	86.7	0.58	0.12	223.83	0	0.08	144.78	0.07
12	12.20	5.43	150	66.26	83.74	0.56	0.13	236.06	0	0.08	156.82	0.08
13	18.62	3.56	150	66.29	83.71	0.56	0.13	236.18	0	0.08	156.95	0.08
Cylinder geometry : Stainless steel												
Number	Speed (mm.s ⁻¹)	Time	H (mm)	H _r (mm)	h (mm)	s'	τ _y '	τ _y	Lump model	τ _y	τ _y '	
10	2.91	22.34	100	64.9	35.1	0.35	0.20	253.68	0	0.06	219.95	0.15
11	8.18	7.84	100	64.1	35.9	0.36	0.20	249.50	0	0.06	214.25	0.14
12	12.02	5.29	100	63.6	36.4	0.36	0.20	246.91	0	0.06	210.74	0.14
13	17.45	3.61	100	63	37	0.37	0.20	243.83	0	0.06	206.59	0.14
Cylinder geometry : PVC												
Number	Speed (mm.s ⁻¹)	Time	H (mm)	H _r (mm)	h (mm)	s'	τ _y '	τ _y	Lump model	τ _y	τ _y '	
10	3.40	19.5	150	66.3	83.7	0.56	0.13	236.22	0	0.08	156.99	0.08
11	9.20	6.88	150	63.3	86.7	0.58	0.12	223.83	0	0.08	144.78	0.07
12	12.20	5.43	150	66.26	83.74	0.56	0.13	236.06	0	0.08	156.82	0.08
13	18.62	3.56	150	66.29	83.71	0.56	0.13	236.18	0	0.08	156.95	0.08
Cylinder geometry : Stainless steel												
Number	Speed (mm.s ⁻¹)	Time	H (mm)	H _r (mm)	h (mm)	s'	τ _y '	τ _y	Lump model	τ _y	τ _y '	
10	2.91	22.34	100	64.9	35.1	0.35	0.20	253.68	0	0.06	219.95	0.15
11	8.18	7.84	100	64.1	35.9	0.36	0.20	249.50	0	0.06	214.25	0.14
12	12.02	5.29	100	63.6	36.4	0.36	0.20	246.91	0	0.06	210.74	0.14
13	17.45	3.61	100	63	37	0.37	0.20	243.83	0	0.06	206.59	0.14
Cylinder geometry : PVC												
Number	Speed (mm.s ⁻¹)	Time	H (mm)	H _r (mm)	h (mm)	s'	τ _y '	τ _y	Lump model	τ _y	τ _y '	
10	3.40	19.5	150	66.3	83.7	0.56	0.13	236.22	0	0.08	156.99	0.08
11	9.20	6.88	150	63.3	86.7	0.58	0.12	223.83	0	0.08	144.78	0.07
12	12.20	5.43	150	66.26	83.74	0.56	0.13	236.06	0	0.08	156.82	0.08
13	18.62	3.56	150	66.29	83.71	0.56	0.13	236.18	0	0.08	156.95	0.08
Cylinder geometry : Stainless steel												
Number	Speed (mm.s ⁻¹)	Time	H (mm)	H _r (mm)	h (mm)	s'	τ _y '	τ _y	Lump model	τ _y	τ _y '	
10	2.91	22.34	100	64.9	35.1	0.35	0.20	253.68	0	0.06	219.95	0.15
11	8.18	7.84	100	64.1	35.9	0.36	0.20	249.50	0	0.06	214.25	0.14
12	12.02	5.29	100	63.6	36.4	0.36	0.20	246.91	0	0.06	210.74	0.14
13	17.45	3.61	100	63	37	0.37	0.20	243.83	0	0.06	206.59	0.14
Cylinder geometry : PVC												
Number	Speed (mm.s ⁻¹)	Time	H (mm)	H _r (mm)	h (mm)	s'	τ _y '	τ _y	Lump model	τ _y	τ _y '	
10	3.40	19.5	150	66.3	83.7	0.56	0.13	236.22	0	0.08	156.99	0.08
11	9.20	6.88	150	63.3	86.7	0.58	0.12	223.83	0	0.08	144.78	0.07
12	12.20	5.43	150	66.26	83.74	0.56	0.13	236.06	0	0.08	156.82	0.08
13	18.62	3.56	150	66.29	83.71	0.56	0.13	236.18	0	0.08	156.95	0.08
Cylinder geometry : Stainless steel												
Number	Speed (mm.s ⁻¹)	Time	H (mm)	H _r (mm)	h (mm)	s'	τ _y '	τ _y	Lump model	τ _y	τ _y '	
10	2.91	22.34	100	64.9	35.1	0.35	0.20	253.68	0	0.06	219.95	0.15
11	8.18	7.84	100	64.1	35.9	0.36	0.20	249.50	0	0.06	214.25	0.14
12	12.02	5.29	100	63.6	36.4	0.36	0.20	246.91	0	0.06	210.74	0.14
13	17.45	3.61	100	63	37	0.37	0.20	243.83	0	0.06	206.59	0.14
Cylinder geometry : PVC												
Number	Speed (mm.s ⁻¹)	Time	H (mm)	H _r (mm)	h (mm)	s'	τ _y '	τ _y	Lump model	τ _y	τ _y '	
10	3.40	19.5	150	66.3	83.7	0.56	0.13	236.22	0	0.08	156.99	0.08
11	9.20	6.88	150	63.3	86.7	0.58	0.12	223.83	0	0.08	144.78	0.07
12	12.20	5.43	150	66.26	83.74	0.56	0.13	236.06	0	0.08	156.82	0.08
13	18.62	3.56	150	66.29	83.71	0.56	0.13	236.18	0	0.08	156.95	0.08
Cylinder geometry : Stainless steel												
Number	Speed (mm.s ⁻¹)	Time										

Table A.6 Slump test for 18 % Kaolin (with spray) using the slump meter

Appendix A- Slump Data

RESULTS ON SLUMP TEST : (KAOLIN 18%)															
Equations:															
Relative density Density g		$s' = \frac{h}{H}$		$\tau_y = \rho g H \tau_y'$			$\tau_y' = \frac{1}{2} - \frac{1}{2} \sqrt{s'}$			Lump model $\tau_y' = 0.5(1 - S')e^{\sqrt{3}(-S')}$		Cylinder model $S = 1 - 2\tau_y'(1 - \ln(2\tau_y'))$			
1.269 1269 (Kg/m ³)										Vane τ_y 135.83					
9.81 (m.s ⁻¹)															
With silicone spray :															
Cone geometry : Stainless steel															
Number	Speed (mm.s ⁻¹)	Time	H (mm)	H _r (mm)	h (mm)	s'	τ_y'	τ_y	Approx.cyl	Calc.from vane	τ_y'	τ_y	τ_y'	Cylinder model	τ_y
10	3.86	18	150	69.5	80.5	0.54	0.13	249.69	τ_y	0.04	0.09	170.76	0.08	6.47E-07	154.59
11	8.30	8.2	150	68.1	81.9	0.55	0.13	243.76	τ_y	0.04	0.09	164.64	0.08	1.43E-07	149.79
12	11.24	6.23	150	70	80	0.53	0.13	251.81	τ_y	0.04	0.09	172.99	0.08	2.65E-07	156.33
13	16.43	4.2	150	69	81	0.54	0.13	247.56	τ_y	0.04	0.09	168.56	0.08	8.87E-07	152.87
Cylinder geometry : Stainless steel															
Number	Speed (mm.s ⁻¹)	Time	H (mm)	H _r (mm)	h (mm)	s'	τ_y'	τ_y			τ_y'	τ_y	τ_y'	Cylinder model	τ_y
10	2.86	23.22	100	66.4	33.6	0.34	0.21	261.64	τ_y	0.06	0.19	230.95	0.15	4.36E-07	188.19
11	7.74	8.5	100	65.8	34.2	0.34	0.21	258.43	τ_y	0.06	0.18	226.50	0.15	3.53E-07	185.09
12	12.09	5.61	100	67.8	32.2	0.32	0.22	269.24	τ_y	0.06	0.19	241.61	0.16	4.42E-07	195.60
13	17.80	3.8	100	67.63	32.37	0.32	0.22	268.31	τ_y	0.06	0.19	240.30	0.16	4.67E-07	194.68
Cone geometry : PVC															
Number	Speed (mm.s ⁻¹)	Time	H (mm)	H _r (mm)	h (mm)	s'	τ_y'	τ_y			τ_y'	τ_y	τ_y'	Cylinder model	τ_y
10	2.95	22.65	150	66.8	83.2	0.55	0.13	238.31	τ_y	0.04	0.09	159.09	0.08	8.76E-07	145.40
11	8.11	8.1	150	65.7	84.3	0.56	0.13	233.73	τ_y	0.04	0.08	154.50	0.08	5.69E-07	141.74
12	11.35	5.87	150	66.6	83.4	0.56	0.13	237.47	τ_y	0.04	0.08	158.25	0.08	8.26E-07	144.73
13	17.04	3.89	150	66.3	83.7	0.56	0.13	236.22	τ_y	0.04	0.08	156.99	0.08	7.45E-07	143.73
Cylinder geometry : PVC															
Number	Speed (mm.s ⁻¹)	Time	H (mm)	H _r (mm)	h (mm)	s'	τ_y'	τ_y			τ_y'	τ_y	τ_y'	Cylinder model	τ_y
10	3.01	22.5	100	67.8	32.2	0.32	0.22	269.24	τ_y	0.06	0.19	241.61	0.16	4.42E-07	195.60
11	7.50	8.87	100	66.5	33.5	0.34	0.21	262.18	τ_y	0.06	0.19	231.70	0.15	4.48E-07	188.71
12	11.66	5.71	100	66.6	33.4	0.33	0.21	262.72	τ_y	0.06	0.19	232.45	0.15	4.58E-07	189.23
13	17.28	3.78	100	65.3	34.7	0.35	0.21	255.78	τ_y	0.06	0.18	222.84	0.15	2.76E-07	182.54

Table A.7 Slump test for 20 % Kaolin (without spray) using the slump meter

Appendix A- Slump Data

RESULTS ON SLUMP TEST : (KAOLIN 20%)														
Relative density Density g			1.31 1310 9.81			Equations: $s' = \frac{h}{H}$			$\tau_y = \rho g H \tau'_y$			Approximate cylinder $\tau'_y = \frac{1}{2} - \frac{1}{2} \sqrt{s'}$		
Without silicone spray :														
Cone geometry : Stainless steel														
Number	Speed (mm.s ⁻¹)	Time	H (mm)	H _t (mm)	h (mm)	s'	τ'_y	Approx.cyl τ_y	Calc. from vane τ_y	τ'_y	Lump Model τ_y	τ'_y	Lump model τ_y	Cylinder model τ_y
10	2.84	28.34	150	80.6	69.4	0.46	0.16	308.24	0.07	0.12	0	0.10	8.88E-07	202.16
11	7.79	10.41	150	81.1	68.9	0.46	0.16	310.60	0.07	0.12	0	0.11	7.05E-07	204.22
12	13.43	6.1	150	81.9	68.1	0.45	0.16	314.41	0.07	0.12	0	0.11	9.29E-07	207.55
13	17.04	4.7	150	80.1	69.9	0.47	0.16	305.88	0.07	0.12	0	0.10	2.61E-07	200.11
Cylinder geometry : Stainless steel														
Number	Speed (mm.s ⁻¹)	Time	H (mm)	H _t (mm)	h (mm)	s'	τ'_y	τ_y		τ'_y	Lump model τ_y	τ'_y	Cylinder model τ_y	τ_y
10	2.77	27.5	100	76.2	23.8	0.24	0.26	329.08	0.11	0.25	0	0.20	5.48E-07	253.88
11	6.96	10.85	100	75.5	24.5	0.25	0.25	324.51	0.11	0.25	0	0.19	4.64E-07	249.08
12	12.31	6.2	100	76.3	23.7	0.24	0.26	328.74	0.11	0.25	0	0.20	5.58E-07	254.57
13	17.77	4.35	100	77.3	22.7	0.23	0.26	336.41	0.11	0.26	0	0.20	5.92E-07	261.61
Cone geometry : PVC														
Number	Speed (mm.s ⁻¹)	Time	H (mm)	H _t (mm)	h (mm)	s'	τ'_y	τ_y		τ'_y	Lump model τ_y	τ'_y	Cylinder model τ_y	τ_y
10	3.63	21.24	150	77	73	0.49	0.15	291.45	0.07	0.11	0	0.10	9.34E-07	187.69
11	6.88	11.34	150	78	72	0.48	0.15	296.07	0.07	0.11	0	0.10	2.53E-07	191.64
12	11.69	6.5	150	76	74	0.49	0.15	286.86	0.07	0.11	0	0.10	7.64E-07	183.78
13	15.71	4.9	150	77	73	0.49	0.15	291.45	0.07	0.11	0	0.10	9.34E-07	187.69
Cylinder geometry : PVC														
Number	Speed (mm.s ⁻¹)	Time	H (mm)	H _t (mm)	h (mm)	s'	τ'_y	τ_y		τ'_y	Lump model τ_y	τ'_y	Cylinder model τ_y	τ_y
10	2.69	27.53	100	74	26	0.26	0.25	314.91	0.11	0.24	0	0.19	7.67E-07	239.12
11	6.96	10.64	100	74.1	25.9	0.26	0.25	315.55	0.11	0.24	0	0.19	7.98E-07	239.78
12	10.44	7.28	100	76	24	0.24	0.26	327.77	0.11	0.25	0	0.20	5.27E-07	252.50
13	18.68	4.09	100	76.4	23.6	0.24	0.26	330.40	0.11	0.25	0	0.20	5.67E-07	255.26

Table A.8 Slump test for 20 % Kaolin (with spray) using the slump meter

RESULTS ON SLUMP TEST : (KAOLIN 20%)										Approximate cylinder		Lump model		Cylinder model	
Equations:										$\tau_y' = \frac{1}{2} - \frac{1}{2} \sqrt{s'}$		$\tau_y' = 0.5(1 - S') e^{\sqrt{3}(-s')}$		$S = 1 - 2\tau_y'(1 - \ln(2\tau_y'))$	
Relative density Density ρ (Kg/m ³) (m.s ⁻¹)		$s' = \frac{h}{H}$		$\tau_y = \rho g H \tau_y'$		Vane τ_y									
1.31 1310	9.81						135.83								
With silicone spray :															
Cone geometry : Stainless steel										Approx.cyl	Calc. from vane				
Number	Speed (mm.s ⁻¹)	Time	H (mm)	H _r (mm)	h (mm)	s'	τ_y'	τ_y	τ_y'	Lump model	τ_y	τ_y'	Cylinder model	τ_y	
10	19.27	4.1	150	79	71	0.47	0.16	300.72	0.07	0	223.61	0.10	2.76E-07	195.64	
11	19.66	4.1	150	80.6	69.4	0.46	0.16	308.24	0.07	0	232.39	0.10	8.88E-07	202.16	
12	19.73	4.1	150	80.9	69.1	0.46	0.16	309.66	0.07	0	234.06	0.11	7.86E-07	203.39	
13	20.00	4.1	150	82	68	0.45	0.16	314.88	0.07	0	240.28	0.11	6.68E-07	207.97	
Cylinder geometry : Stainless steel															
Number	Speed (mm.s ⁻¹)	Time	H (mm)	H _r (mm)	h (mm)	s'	τ_y'	τ_y	τ_y'	Lump Model	τ_y	τ_y'	Cylinder model	τ_y	
10	19.13	4	100	76.5	23.5	0.24	0.26	331.06	0.11	0	327.19	0.20	5.75E-07	255.96	
11	18.90	4	100	75.6	24.4	0.24	0.25	325.16	0.11	0	318.34	0.19	4.77E-07	249.76	
12	19.78	4	100	79.1	20.9	0.21	0.27	348.80	0.11	0	353.89	0.21	2.06E-07	274.85	
13	19.15	4	100	76.6	23.4	0.23	0.26	331.73	0.11	0	328.19	0.20	5.82E-07	256.66	
Cone geometry : PVC															
Number	Speed (mm.s ⁻¹)	Time	H (mm)	H _r (mm)	h (mm)	s'	τ_y'	τ_y	τ_y'	Lump model	τ_y	τ_y'	Cylinder model	τ_y	
10	20.74	3.8	150	78.8	71.2	0.47	0.16	299.79	0.07	0	222.53	0.10	2.73E-07	194.84	
11	20.68	3.8	150	78.6	71.4	0.48	0.16	298.86	0.07	0	221.45	0.10	2.70E-07	194.03	
12	20.87	3.8	150	79.3	70.7	0.47	0.16	302.13	0.07	0	225.24	0.10	2.77E-07	196.85	
13	21.55	3.8	150	81.9	68.1	0.45	0.16	314.41	0.07	0	239.71	0.11	9.29E-07	207.55	
Cylinder geometry : PVC															
Number	Speed (mm.s ⁻¹)	Time	H (mm)	H _r (mm)	h (mm)	s'	τ_y'	τ_y	τ_y'	Lump model	τ_y	τ_y'	Cylinder model	τ_y	
10	17.20	4.5	100	77.4	22.6	0.23	0.26	337.09	0.11	0	336.24	0.20	5.86E-07	262.33	
11	17.51	4.5	100	78.8	21.2	0.21	0.27	346.70	0.11	0	350.72	0.21	4.02E-08	272.59	
12	17.29	4.5	100	77.8	22.2	0.22	0.26	339.80	0.11	0	340.33	0.21	5.36E-07	265.22	
13	17.07	4.5	100	76.8	23.2	0.23	0.26	333.06	0.11	0	330.18	0.20	5.93E-07	258.07	

Table A.9 Slump test for 14 % Kaolinite tailing (without spray) using the slump meter

Appendix A- Slump Data

RESULTS ON SLUMP TEST : (KAOLINITE TAILING 14%)																										
Relative density Density ρ		(Kg/m ³) (m.s ⁻¹)		Equations: $s' = \frac{h}{H}$		$\tau_y = \rho g H \tau_y'$		$\tau_y' = \frac{1}{2} - \frac{1}{2} \sqrt{s'}$		Vane τ_y 50.52		Lump model $\tau_y' = 0.5(1-s')e^{\sqrt[3]{s'}}$		Cylinder model $S = 1 - 2\tau_y'(1 - \ln(2\tau_y'))$												
Without silicone spray :																										
Cone geometry : Stainless steel																										
Number	Speed (mm.s ⁻¹)	Time	H (mm)	H _r (mm)	h (mm)	s'	τ_y'	τ_y	Approx.cyl	Calc.from vane	τ_y'	Lump Model	τ_y	τ_y'	Cylinder model											
10	1.47	34.7	150	51	99	0.66	0.09	166.46			0.03	0	96.18	0.05	2.80E-07											
11	4.62	10.84	150	50.09	99.91	0.67	0.09	166.46			0.03	0	93.48	0.05	2.23E-07											
12	8.02	6.39	150	51.25	98.75	0.66	0.09	166.46			0.03	0	96.93	0.05	2.91E-07											
13	13.24	3.87	150	51.25	98.75	0.66	0.09	166.46			0.03	0	96.93	0.05	2.91E-07											
Cylinder geometry : Stainless steel																										
Number	Speed (mm.s ⁻¹)	Time	H (mm)	H _r (mm)	h (mm)	s'	τ_y'	τ_y			τ_y'	Lump model	τ_y	τ_y'	Cylinder model											
10	1.89	27.7	100	52.29	47.71	0.48	0.15	182.95			0.04	0	135.37	0.10	2.66E-07											
11	4.49	11.3	100	50.78	49.22	0.49	0.15	182.95			0.04	0	128.07	0.10	7.95E-07											
12	7.17	6.84	100	49.05	50.95	0.51	0.15	182.95			0.04	0	120.05	0.09	3.45E-07											
13	10.51	4.7	100	49.42	50.58	0.51	0.15	182.95			0.04	0	121.74	0.09	4.33E-07											
Cone geometry : PVC																										
Number	Speed (mm.s ⁻¹)	Time	H (mm)	H _r (mm)	h (mm)	s'	τ_y'	τ_y			τ_y'	Lump model	τ_y	τ_y'	Cylinder model											
10	1.77	30.32	150	53.68	96.32	0.64	0.10	176.28			0.03	0	104.42	0.06	5.86E-07											
11	5.22	10.81	150	56.45	93.55	0.62	0.10	176.28			0.03	0	113.37	0.06	7.04E-07											
12	7.56	6.6	150	49.87	100.13	0.67	0.10	176.28			0.03	0	92.83	0.05	2.06E-07											
13	13.01	3.89	150	50.61	99.39	0.66	0.10	176.28			0.03	0	95.02	0.05	2.59E-07											
Cylinder geometry : PVC																										
Number	Speed (mm.s ⁻¹)	Time	H (mm)	H _r (mm)	h (mm)	s'	τ_y'	τ_y			τ_y'	Lump model	τ_y	τ_y'	Cylinder model											
10	1.82	27.15	100	49.53	50.47	0.50	0.14	171.30			0.04	0	122.24	0.09	4.61E-07											
11	4.66	10.76	100	50.12	49.88	0.50	0.14	171.30			0.04	0	124.97	0.09	6.16E-07											
12	7.10	6.88	100	48.83	51.17	0.51	0.14	171.30			0.04	0	119.06	0.09	2.96E-07											
13	12.38	4	100	49.5	50.5	0.51	0.14	171.30			0.04	0	122.10	0.09	4.53E-07											

Table A.10 Slump test for 14 % Kaolinite tailing (with spray) using the slump meter

Appendix A- Slump Data

RESULTS ON SLUMP TEST : (KAOLINITE TAILING 14%)												
Equations:												
Relative density Density g	(Kg/m ³) (m.s ⁻¹)	1.206 1206 9.81	$s' = \frac{h}{H}$		$\tau_y = \frac{\rho g H \tau_y}{H}$							
Cylinder geometry : Stainless steel												
Number	Speed (mm.s ⁻¹)	Time	H (mm)	H ₁ (mm)	h (mm)	s'						
10	2.03	27.23	150	55.29	94.71	0.63	τ_y'	τ_y	Approx.cyl	Calc. from vane		
11	5.58	9.88	150	55.17	94.83	0.63	0.10	182.25	τ_y			
12	7.89	6.65	150	52.44	97.56	0.65	0.10	182.25	0.06	0.03	0.06	Lump model
13	14.11	3.69	150	52.08	97.92	0.65	0.10	182.25	0.06	0.03	0.06	Lump model
Cylinder geometry : Stainless steel												
Number	Speed (mm.s ⁻¹)	Time	H (mm)	H ₁ (mm)	h (mm)	s'	τ_y'	τ_y				
10	1.35	38.78	100	52.19	47.81	0.48	0.15	182.52	0.11	0.04	0.10	Cylinder model
11	4.67	10.79	100	50.43	49.57	0.50	0.15	182.52	0.11	0.04	0.09	Cylinder model
12	7.58	6.56	100	49.71	50.29	0.50	0.15	182.52	0.04	0.04	0.09	Cylinder model
13	11.81	4.13	100	48.79	51.21	0.51	0.15	182.52	0.10	0.04	0.09	Cylinder model
Cone geometry : PVC												
Number	Speed (mm.s ⁻¹)	Time	H (mm)	H ₁ (mm)	h (mm)	s'	τ_y'	τ_y				
10	2.09	25.38	150	53.02	96.98	0.65	0.10	173.85	0.06	0.03	0.06	Cylinder model
11	4.46	10.12	150	45.18	104.82	0.70	0.10	173.85	0.04	0.03	0.04	Cylinder model
12	8.31	6.1	150	50.7	99.3	0.66	0.10	173.85	0.05	0.03	0.05	Cylinder model
13	12.51	4.2	150	52.56	97.44	0.65	0.10	173.85	0.06	0.03	0.05	Cylinder model
Cylinder geometry : PVC												
Number	Speed (mm.s ⁻¹)	Time	H (mm)	H ₁ (mm)	h (mm)	s'	τ_y'	τ_y				
10	1.65	32.61	100	53.69	46.31	0.46	0.16	188.99	0.12	0.04	0.10	Cylinder model
11	4.56	10.73	100	48.9	51.1	0.51	0.16	188.99	0.10	0.04	0.09	Cylinder model
12	6.89	7.13	100	49.12	50.88	0.51	0.16	188.99	0.10	0.04	0.09	Cylinder model
13	9.99	4.8	100	47.94	52.06	0.52	0.16	188.99	0.10	0.04	0.09	Cylinder model

Appendix A- Slump Data

RESULTS ON SLUMP TEST : (KAOLINITE TAILING 16%)												
Equations:												
Relative density Density g	(Kg/m ³) (m.s ⁻¹)	1.338 1338 9.81	$h \tau_y = \rho g H \tau_y$ $s' = \frac{h}{H} \tau_y$					$\tau_y' = \frac{1}{2} - \frac{1}{2} \sqrt{s'}$			Vane	
											τ_y	
											117.62	
Without silicone spray :												
Cone geometry : Stainless steel												
Number	Speed (mm.s ⁻¹)	Time	H (mm)	H _r (mm)	h (mm)	s'	τ_y'	Approx.cyl	Calc. from vane	τ_y'	Lump Model	τ_y
10	1.44	37.77	150	54.37	95.63	0.64	0.10	198.41	0.06	0.06	0	118.27
11	5.20	10.43	150	54.24	95.76	0.64	0.10	197.87	0.06	0.06	0	117.81
12	7.94	6.9	150	54.78	95.22	0.63	0.10	200.09	0.06	0.06	0	119.73
13	12.65	4.11	150	52.01	97.99	0.65	0.10	188.77	0.06	0.06	0	110.10
Cylinder geometry : Stainless steel												
Number	Speed (mm.s ⁻¹)	Time	H (mm)	H _r (mm)	h (mm)	s'	τ_y'	τ_y	τ_y'	τ_y	Lump model	τ_y
10	1.46	34.74	100	50.76	49.24	0.49	0.15	195.76	0.09	0.11	0	141.98
11	4.39	10.9	100	47.83	52.17	0.52	0.14	182.26	0.09	0.10	0	127.16
12	7.76	6.63	100	51.47	48.53	0.49	0.15	199.10	0.09	0.11	0	145.75
13	13.02	3.81	100	49.6	50.4	0.50	0.15	190.37	0.09	0.10	0	135.97
Cone geometry : PVC												
Number	Speed (mm.s ⁻¹)	Time	H (mm)	H _r (mm)	h (mm)	s'	τ_y'	τ_y	τ_y'	τ_y	Lump model	τ_y
10	1.31	43.13	150	56.41	93.59	0.62	0.11	206.83	0.06	0.06	0	125.64
11	5.05	10.66	150	53.81	96.19	0.64	0.10	196.11	0.06	0.06	0	116.30
12	8.69	6.32	150	54.9	95.1	0.63	0.10	200.59	0.06	0.06	0	120.16
13	14.63	3.81	150	55.73	94.27	0.63	0.10	204.02	0.06	0.06	0	123.15
Cylinder geometry : PVC												
Number	Speed (mm.s ⁻¹)	Time	H (mm)	H _r (mm)	h (mm)	s'	τ_y'	τ_y	τ_y'	τ_y	Lump model	τ_y
10	1.65	33.68	100	55.55	44.45	0.44	0.17	218.74	0.09	0.13	0	168.82
11	5.59	10.12	100	56.53	43.47	0.43	0.17	223.59	0.09	0.13	0	174.74
12	7.78	6.63	100	51.61	48.39	0.48	0.15	199.76	0.09	0.11	0	146.50
13	12.60	4.19	100	52.78	47.22	0.47	0.16	205.31	0.09	0.12	0	152.89
Cylinder model												
$S=1-2\tau_y'(1-\ln(2\tau_y'))$												

Table A.12 Slump test for 16 % Kaolinite tailing (with spray) using the slump meter

Appendix A- Slump Data

RESULTS ON SLUMP TEST : (KAOLINITE TAILING 16%)												
Equations:												
Relative density Density g (Kg/m ³) (m.s ⁻¹)	1.338 1338 9.81	$s' = \frac{h}{H}$		$\tau_y = \rho g H \tau_y'$		$\tau_y' = \frac{1}{2} - \frac{1}{2} \sqrt{s'}$		Approximate cylinder		Lump model		Cylinder model
With silicone spray :												
Cone geometry : Stainless steel												
Number	Speed (mm.s ⁻¹)	Time	H (mm)	H _r (mm)	h (mm)	s'	τ_y'	Approx.cyl τ_y	Calc.from vane	τ_y'	Lump model τ_y	Cylinder model τ_y
10	1.25	44.61	150	55.84	94.16	0.63	0.10	204.47	0.06	0.06	0	9.36E-07
11	5.62	9.94	150	55.89	94.11	0.63	0.10	204.68	0.06	0.06	0	7.97E-07
12	8.05	6.72	150	54.08	95.92	0.64	0.10	197.21	0.06	0.06	0	7.66E-07
13	12.93	4.26	150	55.1	94.9	0.63	0.10	201.41	0.06	0.06	0	7.49E-07
Cylinder geometry : Stainless steel												
Number	Speed (mm.s ⁻¹)	Time	H (mm)	H _r (mm)	h (mm)	s'	τ_y'	τ_y		τ_y'	Lump Model τ_y	Cylinder model τ_y
10	1.56	34.74	100	54.24	45.76	0.46	0.16	212.33	0.09	0.12	0	5.82E-07
11	4.84	10.78	100	52.13	47.87	0.48	0.15	202.21	0.09	0.11	0	2.59E-07
12	7.64	6.81	100	52	48	0.48	0.15	201.60	0.09	0.11	0	2.53E-07
13	12.78	4.16	100	53.17	46.83	0.47	0.16	207.17	0.09	0.12	0	2.72E-07
Cone geometry : PVC												
Number	Speed (mm.s ⁻¹)	Time	H (mm)	H _r (mm)	h (mm)	s'	τ_y'	τ_y		τ_y'	Lump model τ_y	Cylinder model τ_y
10	1.26	43.97	150	55.34	94.66	0.63	0.10	202.40	0.06	0.06	0	9.44E-07
11	4.79	11.3	150	54.15	95.85	0.64	0.10	197.50	0.06	0.06	0	3.80E-07
12	8.37	6.3	150	52.72	97.28	0.65	0.10	191.65	0.06	0.06	0	2.63E-07
13	11.15	4.94	150	55.09	94.91	0.63	0.10	201.37	0.06	0.06	0	7.41E-07
Cylinder geometry : PVC												
Number	Speed (mm.s ⁻¹)	Time	H (mm)	H _r (mm)	h (mm)	s'	τ_y'	τ_y		τ_y'	Lump model τ_y	Cylinder model τ_y
10	1.52	34.74	100	52.96	47.04	0.47	0.16	206.17	0.09	0.12	0	2.76E-07
11	4.77	10.78	100	51.39	48.61	0.49	0.15	198.72	0.09	0.11	0	9.47E-07
12	7.42	6.81	100	50.52	49.48	0.49	0.15	194.64	0.09	0.11	0	7.25E-07
13	12.74	4.16	100	52.99	47.01	0.47	0.16	206.31	0.09	0.12	0	2.76E-07

Table A.13 Slump test for 18 % Kaolinite tailing (without spray) using the slump meter

Appendix A- Slump Data

RESULTS ON SLUMP TEST : (KAOLINITE TAILING 18%)											
Equations:											
Relative density Density g		1.365 1365 9.81		$s' = \frac{h}{H}$		$\tau_y = \rho g H \tau_y$		$\tau_y' = \frac{1}{2} - \frac{1}{2} \sqrt{s'}$		$\tau_y' = 0.5(1-S')e^{\sqrt[3]{3(-S')}}$ $S=1-2\tau_y'(1-\ln(2\tau_y'))$	
Without silicone spray :											
Cone geometry : Stainless steel											
Number	Speed (mm.s ⁻¹)	Time	H (mm)	H _r (mm)	h (mm)	s'	τ_y'	Approx.cyl τ_y	Calc.from vane τ_y'	Lump Model τ_y	Cylinder model τ_y
10	9.29	6.4	150	59.45	90.55	0.60	0.11	224.00	0.11	0	4.39E-08
11	8.93	6.4	150	57.12	92.88	0.62	0.11	214.02	0.11	0	1.19E-08
12	9.16	6.4	150	58.63	91.37	0.61	0.11	220.47	0.11	0	9.32E-07
13	9.08	6.4	150	58.1	91.9	0.61	0.11	218.20	0.11	0	8.39E-08
Cylinder geometry : Stainless steel											
Number	Speed (mm.s ⁻¹)	Time	H (mm)	H _r (mm)	h (mm)	s'	τ_y'	τ_y	τ_y'	Lump model τ_y	Cylinder model τ_y
10	14.07	4.3	100	60.48	39.52	0.40	0.19	248.63	0.16	0	3.14E-07
11	13.51	4.3	100	58.11	41.89	0.42	0.18	236.19	0.16	0	2.64E-07
12	13.66	4.3	100	58.74	41.26	0.41	0.18	239.47	0.16	0	2.35E-07
13	13.64	4.3	100	58.65	41.35	0.41	0.18	239.00	0.16	0	2.65E-07
Cone geometry : PVC											
Number	Speed (mm.s ⁻¹)	Time	H (mm)	H _r (mm)	h (mm)	s'	τ_y'	τ_y	τ_y'	Lump model τ_y	Cylinder model τ_y
10	12.15	4.8	150	58.3	91.7	0.61	0.11	219.06	0.11	0	4.34E-07
11	12.10	4.8	150	58.1	91.9	0.61	0.11	218.20	0.11	0	8.39E-08
12	11.68	4.8	150	56.07	93.93	0.63	0.10	209.57	0.11	0	6.17E-07
13	11.62	4.8	150	55.79	94.21	0.63	0.10	208.39	0.11	0	4.88E-07
Cylinder geometry : PVC											
Number	Speed (mm.s ⁻¹)	Time	H (mm)	H _r (mm)	h (mm)	s'	τ_y'	τ_y	τ_y'	Lump model τ_y	Cylinder model τ_y
10	13.21	4.7	100	62.1	37.9	0.38	0.19	257.35	0.16	0	3.31E-07
11	12.40	4.7	100	58.3	41.7	0.42	0.18	237.18	0.16	0	2.93E-07
12	12.46	4.7	100	58.56	41.44	0.41	0.18	238.53	0.16	0	2.85E-07
13	12.28	4.7	100	57.71	42.29	0.42	0.17	234.13	0.16	0	1.51E-07

Table A. 14 Slump test for 18 % Kaolinite tailing (with spray) using the slump meter

Appendix A- Slump Data

RESULTS ON SLUMP TEST : (KAOLINITE TAILING 18%)											
Equations:											
Relative density Density ρ (Kg/m ³) (m.s ⁻¹)		1.365 1365 9.81	$s' = \frac{h}{H}$			$\tau_y = \rho g H \tau_y'$			$\tau_y' = \frac{1}{2} - \frac{1}{2} \sqrt{s'}$		
With silicone spray :											
Cone geometry : Stainless steel											
Number	Speed (mm.s ⁻¹)	Time	H (mm)	H _r (mm)	h (mm)	s'	τ_y'	Approx.cyl τ_y	Calc. from vane τ_y'	Lump model τ_y	Cylinder model τ_y'
10	15.51	4.1	150	63.6	86.4	0.58	0.12	242.09	0.11	0	1.87E-07
11	15.06	4.1	150	61.74	88.26	0.59	0.12	233.93	0.11	0	5.90E-07
12	15.57	4.1	150	63.82	86.18	0.57	0.12	233.93	0.11	0	6.77E-07
13	15.16	4.1	150	62.15	87.85	0.59	0.12	235.72	0.11	0	6.36E-07
Cylinder geometry : Stainless steel											
Number	Speed (mm.s ⁻¹)	Time	H (mm)	H _r (mm)	h (mm)	s'	τ_y'	τ_y	τ_y'	Lump Model τ_y	Cylinder model τ_y'
10	15.26	4	100	61.03	38.97	0.39	0.19	251.57	0.16	0	4.30E-07
11	15.01	4	100	60.05	39.95	0.40	0.18	246.35	0.16	0	2.04E-07
12	14.73	4	100	58.91	41.09	0.41	0.18	240.35	0.16	0	1.43E-07
13	14.92	4	100	59.68	40.32	0.40	0.18	244.39	0.16	0	1.15E-07
Cone geometry : PVC											
Number	Speed (mm.s ⁻¹)	Time	H (mm)	H _r (mm)	h (mm)	s'	τ_y'	τ_y	τ_y'	Lump model τ_y	Cylinder model τ_y'
10	15.79	3.8	150	60.01	89.99	0.60	0.11	226.42	0.11	0	6.27E-07
11	15.80	3.8	150	60.05	89.95	0.60	0.11	226.59	0.11	0	8.97E-07
12	15.50	3.8	150	58.91	91.09	0.61	0.11	221.68	0.11	0	4.02E-08
13	15.71	3.8	150	59.68	90.32	0.60	0.11	224.99	0.11	0	7.25E-07
Cylinder geometry : PVC											
Number	Speed (mm.s ⁻¹)	Time	H (mm)	H _r (mm)	h (mm)	s'	τ_y'	τ_y	τ_y'	Lump model τ_y	Cylinder model τ_y'
10	13.34	4.5	100	60.01	39.99	0.40	0.18	246.14	0.16	0	1.94E-07
11	13.50	4.5	100	60.76	39.24	0.39	0.19	250.13	0.16	0	3.79E-07
12	12.60	4.5	100	56.72	43.28	0.43	0.17	229.06	0.16	0	6.55E-07
13	13.11	4.5	100	59	41	0.41	0.18	240.82	0.16	0	7.48E-08

Appendix A- Slump Data

RESULTS ON SLUMP TEST : (KAOLINITE TAILING 20%)													
Equations:													
Relative density Density ρ (Kg/m ³) (m.s ⁻¹)		1.37 1370 9.81		$s' = \frac{h}{H} \tau_y = \rho g H \tau_y$									
$\tau_y' = \frac{1}{2} - \frac{1}{2} \sqrt{s'}$													
Approximate cylinder		Vane τ_y 300.93		$\tau_y' = 0.5(1 - s')e^{\sqrt{3}(s')}$									
Lump model		$S = 1 - 2\tau_y'(1 - \ln(2\tau_y'))$											
Cylinder model													

Without silicone spray :													
Cone geometry : Stainless steel													
Number	Speed (mm.s ⁻¹)	Time	H (mm)	H _r (mm)	h (mm)	s'				Approx.cyl			
10	1.92	32.98	150	63.35	86.65	0.58	0.12	0.12	0.15	0.08	Lump Model	τ_y	τ_y
11	5.59	11.08	150	61.89	88.11	0.59	0.12	0.12	0.15	0.07	0	156.52	144.77
12	8.59	7.02	150	60.32	89.68	0.60	0.11	0.11	0.15	0.07	0	150.36	139.76
13	16.63	3.67	150	61.02	88.98	0.59	0.11	0.11	0.15	0.07	0	143.91	134.47
Cylinder geometry : Stainless steel													
Number	Speed (mm.s ⁻¹)	Time	H (mm)	H _r (mm)	h (mm)	s'	τ_y'	τ_y					
10	1.85	34.74	100	64.3	35.7	0.36	0.20	0.20	0.22	0.17	Lump model	τ_y	τ_y
11	5.82	10.81	100	62.87	37.13	0.37	0.20	0.20	0.22	0.17	0	232.82	191.65
12	7.54	8.13	100	61.28	38.72	0.39	0.19	0.19	0.22	0.16	0	222.08	184.11
13	12.96	4.64	100	60.15	39.85	0.40	0.18	0.18	0.22	0.15	0	210.58	176.00
Cone geometry : PVC													
Number	Speed (mm.s ⁻¹)	Time	H (mm)	H _r (mm)	h (mm)	s'	τ_y'	τ_y					
10	3.25	19.54	150	63.44	86.56	0.58	0.12	0.12	0.15	0.08	Lump model	τ_y	τ_y
11	4.88	12.3	150	60	90	0.60	0.11	0.11	0.15	0.07	0	156.91	145.08
12	8.72	6.9	150	60.19	89.81	0.60	0.11	0.11	0.15	0.07	0	142.62	133.41
13	17.38	3.52	150	61.16	88.84	0.59	0.12	0.12	0.15	0.07	0	143.39	134.04
Cylinder geometry : PVC													
Number	Speed (mm.s ⁻¹)	Time	H (mm)	H _r (mm)	h (mm)	s'	τ_y'	τ_y					
10	2.12	29.43	100	62.36	37.64	0.38	0.19	0.19	0.22	0.16	Lump model	τ_y	τ_y
11	5.15	11.71	100	60.36	39.64	0.40	0.19	0.19	0.22	0.15	0	218.34	181.48
12	8.94	6.99	100	62.5	37.5	0.38	0.19	0.19	0.22	0.16	0	204.14	171.43
13	14.77	4.11	100	60.72	39.28	0.39	0.19	0.19	0.22	0.15	0	219.36	182.20
											0	206.64	173.21

Table A.16 Slump test for 20 % Kaolinite tailing (with spray) using the slump meter

Appendix A- Slump Data

RESULTS ON SLUMP TEST : (4% LAPTONITE)													Approximate cylinder		Lump model		Cylinder model	
Equations:													Vane					
													τ_y					
													100.08					

Table A.18 Slump test for 4 % Laponite (with spray) using the slump meter

Appendix A- Slump Data

RESULTS ON SLUMP TEST : (4% LAPTONITE)															
Relative density Density g		1.028 Equations: 1028 9.81		$\tau_y = \frac{h}{H} \tau_y = \rho g H \tau_y'$		$\tau_y' = \frac{1}{2} - \frac{1}{2} \sqrt{s'}$		Approximate cylinder		Vane		Lump model $\tau_y' = 0.5(1 - S') e^{\sqrt{3}(-s')}$		Cylinder model $S = 1 - 2\tau_y'(1 - \ln(2\tau_y'))$	
										τ_y					
										100.08					
With silicone spray :															
Cone geometry : Stainless steel															
Number	Speed (mm.s ⁻¹)	Time	H (mm)	H _t (mm)	h (mm)	s'	τ_y'	τ_y	τ_y'	Calc from vane	τ_y'	Lump model	τ_y	Cylinder model	τ_y
3	3.66	11.75	150	43	107	0.71	0.08	117.54	0.07		63.03	0	56.63	2.05E-07	61.89
5	8.85	4.52	150	40	110	0.73	0.07	108.65	0.07		56.63	0	56.63	2.80E-07	55.97
7	9.94	3.22	150	32	118	0.79	0.06	85.51	0.07		41.31	-1E-06	41.31	4.22E-07	41.29
10	14.61	2.19	150	32	118	0.79	0.06	85.51	0.07		41.31	-1E-06	41.31	4.22E-07	41.29
Cylinder geometry : Stainless steel															
Number	Speed (mm.s ⁻¹)	Time	H (mm)	H _t (mm)	h (mm)	s'	τ_y'	τ_y	τ_y'		τ_y	Lump model	τ_y	Cylinder model	τ_y
3	2.741	12.77	100	35	65	0.65	0.10	97.71	0.10		57.25	0	57.25	-2.88754E-07	54.83
5	6.792	5.3	100	36	64	0.64	0.10	100.85	0.10		59.91	0	59.91	4.69047E-07	57.12
7	8.908	3.48	100	31	69	0.69	0.08	85.39	0.10		47.31	0	47.31	4.17781E-07	46.07
10	14.286	2.45	100	35	65	0.65	0.10	97.71	0.10		57.25	0	57.25	3.65074E-07	54.83
Cone geometry : PVC															
Number	Speed (mm.s ⁻¹)	Time	H (mm)	H _t (mm)	h (mm)	s'	τ_y'	τ_y	τ_y'		τ_y	Lump model	τ_y	Cylinder model	τ_y
3	1.719	19.78	150	34	116	0.77	0.06	91.22	0.07		44.91	-1E-06	44.91	7.79507E-07	44.81
5	4.472	7.38	150	33	117	0.78	0.06	88.36	0.07		43.09	-1E-06	43.09	5.80615E-07	43.04
7	11.180	3.22	150	36	114	0.76	0.06	96.98	0.07		48.67	0	48.67	3.91128E-07	48.43
10	15.652	2.3	150	36	114	0.76	0.06	96.98	0.07		48.67	0	48.67	3.91128E-07	48.43
Cylinder geometry : PVC															
Number	Speed (mm.s ⁻¹)	Time	H (mm)	H _t (mm)	h (mm)	s'	τ_y'	τ_y	τ_y'		τ_y	Lump model	τ_y	Cylinder model	τ_y
3	3.177	11.33	100	36	64	0.64	0.10	100.85	0.10		59.91	0	59.91	7.57309E-07	57.12
5	5.596	6.79	100	38	62	0.62	0.11	107.20	0.10		65.47	0	65.47	-7.42133E-07	61.84
7	9.067	3.86	100	35	65	0.65	0.10	97.71	0.10		57.25	0	57.25	-4.04901E-07	54.83
10	16.990	2.06	100	35	65	0.65	0.10	97.71	0.10		57.25	0	57.25	8.43986E-07	54.83

Table A.19 Slump test for 5 % Laponite (without spray) using the slump meter

Appendix A- Slump Data

RESULTS ON SLUMP TEST : (LAPTONITE 5%) Equations: $s' = \frac{h}{H} \tau_y = \rho g H \tau_y$ $\tau_y' = \frac{1}{2} \frac{1}{2} \frac{1}{2} \sqrt{s'}$ $\tau_y' = 0.5(1 - s') e^{\sqrt{3}(-s')}$ $S = 1 - 2\tau_y'(1 - \ln(2\tau_y'))$											
Without silicone spray :			Stainless steel			PVC			Cylinder model		
Number	Speed (mm.s ⁻¹)	Time	H (mm)	H _r (mm)	h (mm)	s'	τ_y'	τ_y	τ_y'	τ_y	τ_y
3	5.23	15.20	150	79.45	70.55	0.47	0.157	240.62	0.12	179.62	156.90
5	10.39	7.47	150	77.65	72.35	0.48	0.153	233.96	0.11	171.94	151.17
7	10.64	5.92	150	63.00	87.00	0.58	0.119	182.59	0.08	117.79	109.07
10	16.38	3.68	150	60.27	89.73	0.60	0.113	173.51	0.07	109.19	102.04
Cylinder geometry : Stainless			Stainless steel			PVC			Cylinder model		
Number	Speed (mm.s ⁻¹)	Time	H (mm)	H _r (mm)	h (mm)	s'	τ_y'	τ_y	τ_y'	τ_y	τ_y
3	4.22	15.3	100	64.57	35.43	0.35	0.20	206.66	0.17	178.47	146.71
5	7.22	8.37	100	60.47	39.53	0.40	0.19	189.56	0.15	155.68	130.66
7	10.49	5.63	100	59.08	40.92	0.41	0.18	183.96	0.15	148.48	125.53
10	15.72	3.61	100	56.75	43.25	0.43	0.17	174.79	0.13	136.99	117.25
Cone geometry : PVC			PVC			Cylinder model			Cylinder model		
Number	Speed (mm.s ⁻¹)	Time	H (mm)	H _r (mm)	h (mm)	s'	τ_y'	τ_y	τ_y'	τ_y	τ_y
3	3.29	19.5	150	64.06	85.94	0.57	0.12	186.16	0.08	121.24	111.87
5	8.99	6.88	150	61.87	88.13	0.59	0.12	178.82	0.07	114.18	106.13
7	11.02	5.43	150	59.84	90.16	0.60	0.11	172.10	0.07	107.87	100.96
10	16.15	3.56	150	57.5	92.5	0.62	0.11	164.44	0.07	100.89	95.14
Cylinder geometry : PVC			PVC			Cylinder model			Cylinder model		
Number	Speed (mm.s ⁻¹)	Time	H (mm)	H _r (mm)	h (mm)	s'	τ_y'	τ_y	τ_y'	τ_y	τ_y
3	32.67	3.06	19.46	100	59.57	40.43	0.40	0.18	0.15	150.99	127.32
5	12.18	8.21	7.05	100	57.9	42.1	0.42	0.18	0.14	142.57	121.28
7	9.06	11.03	5.08	100	56.04	43.96	0.44	0.17	0.13	133.62	114.80
10	6.79	14.73	3.71	100	54.63	45.37	0.45	0.16	0.12	127.12	110.04

Table A.20 Slump test for 5 % Laponite (with spray) using the slump meter

Appendix A- Slump Data

[illegible]

Table A.21 Slump test for 6 % Laponite (without spray) using the slump meter

Appendix A- Slump Data

RESULTS ON SLUMP TEST : (LAPTONITE 6%)																
Relative density Density (Kg/m ³) g (m.s ⁻¹)		1.052 Equations: 1052 9.81 s' =		h H		τ _y = ρgHτ' _y		τ' _y = $\frac{1}{2} \frac{1}{2} \sqrt{s'}$		Vane τ _y 243.03		Lump model τ' _y = 0.5(1 - S')e ^{√3(-S')}		Cylinder model S = 1 - 2τ' _y (1 - ln(2τ' _y))		
Without silicone spray :																
Cone geometry : Stainless steel									App cyl		Calc from vane					
Number	Speed (mm.s ⁻¹)	Time	H (mm)	H _r (mm)	h (mm)	s'	τ' _y	τ _y	τ' _y	Lump model	τ _y	τ' _y	Cylinder model	τ _y	τ' _y	
3	4.01	23.2	150	92.98	57.02	0.38	0.19	296.79	0.16	0	248.37	0.13	6.26E-07	206.83		
5	12.81	7.34	150	93.99	56.01	0.37	0.19	301.04	0.16	0	254.01	0.14	9.18E-07	210.81		
7	22.26	4.24	150	94.40	55.60	0.37	0.20	302.77	0.16	0	256.33	0.14	3.39E-07	212.44		
10	34.40	2.77	150	95.30	54.70	0.36	0.20	306.60	0.16	0	261.48	0.14	7.29E-07	216.06		
Cylinder geometry : Stainless steel																
Number	Speed (mm.s ⁻¹)	Time	H (mm)	H _r (mm)	h (mm)	s'	τ' _y	τ _y	τ' _y	Lump model	τ _y	τ' _y	Cylinder model	τ _y	τ' _y	
3	4.57	17.50	100.00	80.00	20.00	0.20	0.28	391.80	0.24	0	291.94	0.22	1.20E-07	226.27		
5	10.63	7.56	100.00	80.39	19.61	0.20	0.28	394.91	0.24	0	295.36	0.22	3.38E-07	228.73		
7	16.44	4.88	100.00	80.25	19.75	0.20	0.28	393.79	0.24	0	294.13	0.22	3.26E-07	227.84		
10	30.71	2.54	100.00	78.00	22.00	0.22	0.27	376.33	0.24	0	274.96	0.21	3.75E-07	214.15		
Cone geometry : PVC																
Number	Speed (mm.s ⁻¹)	Time	H (mm)	H _r (mm)	h (mm)	s'	τ' _y	τ _y	τ' _y	Lump model	τ _y	τ' _y	Cylinder model	τ _y	τ' _y	
3	5.89	13.61	150.00	80.10	69.90	0.47	0.16	244.94	0.16	0	184.40	0.10	5.26E-07	160.70		
5	9.66	7.80	150.00	75.35	74.65	0.50	0.15	227.33	0.16	0	164.20	0.09	8.18E-07	145.57		
7	13.92	5.45	150.00	75.84	74.16	0.49	0.15	229.12	0.16	0	166.21	0.10	6.28E-07	147.09		
10	16.89	4.50	150.00	76.00	74.00	0.49	0.15	229.71	0.16	0	166.87	0.10	5.35E-07	147.59		
Cylinder geometry : PVC																
Number	Speed (mm.s ⁻¹)	Time	H (mm)	H _r (mm)	h (mm)	s'	τ' _y	τ _y	τ' _y	Lump model	τ _y	τ' _y	Cylinder model	τ _y	τ' _y	
3	7.12	10.27	100.00	73.08	26.92	0.27	0.24	247.57	0.24	0	236.57	0.18	2.21E-07	187.29		
5	11.01	6.63	100.00	73.01	26.99	0.27	0.24	247.22	0.24	0	236.05	0.18	1.99E-07	186.93		
7	12.54	5.90	100.00	74.01	25.99	0.26	0.25	252.22	0.24	0	243.47	0.19	1.21E-07	192.08		
10	16.60	4.43	100.00	73.55	26.45	0.26	0.24	249.91	0.24	0	240.04	0.18	6.24E-07	189.69		

Table A.22 Slump test for 6 % Laponite (with spray) using the slump meter

Appendix A- Slump Data

RESULTS ON SLUMP TEST : (LAPTONITE 6%)									
Relative density Density g (Kg/m ³) (m.s ⁻³)		1.052 Equations: 1052 9.81		$s' = \frac{h}{H} \tau_y = \rho g H \tau_y'$		Approximate cylinder $\tau_y' = \frac{1}{2} \frac{1}{\sqrt{s'}}$		Vane τ_y 243.03	
								Lump model $\tau_y' = 0.5(1 - S') e^{\sqrt{3}(-S')}$	
								Cylinder model $S = 1 - 2\tau_y'(1 - \ln(2\tau_y'))$	
With silicone spray :									
Cone geometry : Stainless steel									
Number	Speed (mm.s ⁻¹)	Time	H (mm)	H _r (mm)	h (mm)	s'	τ_y'	τ_y	τ_y'
3	6.66	12.10	150	80.60	69.40	0.46	0.16	246.83	162.34
5	9.96	8.00	150	79.65	70.35	0.47	0.16	243.24	159.22
7	12.16	6.50	150	79.05	70.95	0.47	0.16	241.00	157.27
10	16.00	4.90	150	78.41	71.59	0.48	0.15	238.61	155.21
Cylinder geometry : Stainless steel									
Number	Speed (mm.s ⁻¹)	Time	H (mm)	H _r (mm)	h (mm)	s'	τ_y'	τ_y	τ_y'
3	7.05	11.14	100	78.50	21.50	0.22	0.27	275.95	217.11
5	10.72	7.31	100	78.37	21.63	0.22	0.27	275.23	216.34
7	14.58	5.35	100	78.02	21.98	0.22	0.27	273.31	214.27
10	17.11	4.50	100	77.00	23.00	0.23	0.26	267.77	208.38
Cone geometry : PVC									
Number	Speed (mm.s ⁻¹)	Time	H (mm)	H _r (mm)	h (mm)	s'	τ_y'	τ_y	τ_y'
3	6.08	12.50	150	76.00	74.00	0.49	0.15	229.71	147.59
5	10.14	7.31	150	74.10	75.90	0.51	0.14	222.79	141.74
7	13.94	5.30	150	73.89	76.11	0.51	0.14	222.03	141.10
10	15.84	4.61	150	73.00	77.00	0.51	0.14	218.83	138.42
Cylinder geometry : PVC									
Number	Speed (mm.s ⁻¹)	Time	H (mm)	H _r (mm)	h (mm)	s'	τ_y'	τ_y	τ_y'
3	7.29	10.01	100	73.01	73.01	0.73	0.15	153.14	136.48
5	10.88	6.78	100	73.80	73.80	0.74	0.15	153.14	140.95
7	14.38	5.14	100	73.90	73.90	0.74	0.15	153.14	141.52
10	17.38	4.20	100	73.00	73.00	0.73	0.15	153.14	136.42

Table A.23 Slump test for 7 % Laponite (without spray) using the slump meter

Appendix A- Slump Data

RESULTS ON SLUMP TEST : (LAPTONITE 7%)																
Relative density Density (Kg/m ³) g			1.052 Equations: 1052 9.81			$s' = \frac{h}{H} \tau_y = \rho g H s'$			Approximate cylinder $\tau_y' = \frac{1}{2} \frac{1}{2} \sqrt{s'}$		Vane τ_y 482.48		Lump model $\tau_y' = 0.5(1-S')e^{\sqrt{3}(-S')}$		Cylinder model $S=1-2\tau_y'(1-\ln(2\tau_y'))$	
Without silicone spray :																
Cone geometry : Stainless steel																
Number	Speed (mm.s ⁻¹)	Time	H (mm)	H _r (mm)	h (mm)	s'	τ_y'	τ_y	τ_y'	τ_y	τ_y'	τ_y	τ_y'	τ_y	τ_y'	τ_y
			150													
			150													
			150													
			150													
Cylinder geometry : Stainless steel																
Number	Speed (mm.s ⁻¹)	Time	H (mm)	H _r (mm)	h (mm)	s'	τ_y'	τ_y	τ_y'	τ_y	τ_y'	τ_y	τ_y'	τ_y	τ_y'	τ_y
3	8.71	10.97	100	95.60	4.40	0.04	0.40	411.26	0.46	0	461.02	0.36	3.10E-07	373.88		
5	12.24	7.73	100	94.65	5.35	0.05	0.38	400.05	0.46	0	448.99	0.35	2.76E-07	359.75		
7	16.14	5.86	100	94.60	5.40	0.05	0.38	399.49	0.46	0	448.36	0.34	5.22E-07	359.04		
10	18.83	4.99	100	93.94	6.06	0.06	0.38	392.31	0.46	0	440.17	0.34	6.14E-07	350.09		
Cone geometry : PVC																
Number	Speed (mm.s ⁻¹)	Time	H (mm)	H _r (mm)	h (mm)	s'	τ_y'	τ_y	τ_y'	τ_y	τ_y'	τ_y	τ_y'	τ_y	τ_y'	τ_y
			150													
			150													
			150													
			150													
Cylinder geometry : PVC																
Number	Speed (mm.s ⁻¹)	Time	H (mm)	H _r (mm)	h (mm)	s'	τ_y'	τ_y	τ_y'	τ_y	τ_y'	τ_y	τ_y'	τ_y	τ_y'	τ_y
3	9.43	10.58	100	99.78	0.22	0.00	0.48	496.01	0.46	0	520.42	0.50	0.0022	520.43		
5	12.79	7.70	100	98.50	1.50	0.02	0.44	456.68	0.46	0	499.47	0.42	4.16E-07	432.92		
7	16.10	5.99	100	96.42	3.58	0.04	0.41	421.95	0.46	0	471.62	0.37	2.83E-07	387.53		
10	20.10	4.70	100	94.47	5.53	0.06	0.48	496.01	0.46	0	446.74	0.34	5.21E-07	357.23		

Table A.24 Slump test for 7 % Laponite (with spray) using the slump meter

Appendix A- Slump Data

RESULTS ON SLUMP TEST : (LAPTONITE 7%)									
Relative density Density (Kg/m ³) g		1.052 Equations: 1052 9.81 s' =		h H		$\tau_y = \rho g H s'$			
With silicone spray :								Approximate cylinder	
Cone geometry : Stainless steel								$\tau_y = \frac{1}{2} \frac{1}{2} \sqrt{s'}$	
Number	Speed (mm.s ⁻¹)	Time	H (mm)	H _r (mm)	h (mm)	s'	τ_y'	τ_y	τ_y
			150						
			150						
			150						
Cylinder geometry : Stainless steel									
Number	Speed (mm.s ⁻¹)	Time	H (mm)	H _r (mm)	h (mm)	s'	τ_y'	τ_y	τ_y
3	8.51	11.01	100	93.66	6.34	0.06	0.37	389.38	4.63E-07
5	12.50	7.38	100	92.26	7.74	0.08	0.36	375.64	8.81E-08
7	16.03	5.70	100	91.35	8.65	0.09	0.35	367.36	6.93E-07
10	18.82	4.80	100	90.32	9.68	0.10	0.34	358.50	7.62E-07
Cone geometry : PVC									
Number	Speed (mm.s ⁻¹)	Time	H (mm)	H _r (mm)	h (mm)	s'	τ_y'	τ_y	τ_y
3			150						
5			150						
7			150						
10			150						
Cylinder geometry : PVC									
Number	Speed (mm.s ⁻¹)	Time	H (mm)	H _r (mm)	h (mm)	s'	τ_y'	τ_y	τ_y
3	8.73	11.17	100	97.53	2.47	0.02	0.42	438.63	3.90E-07
5	12.76	7.53	100	96.06	3.94	0.04	0.40	417.12	6.56E-07
7	16.38	5.84	100	95.65	4.35	0.04	0.40	411.88	6.93E-07
10	19.20	4.97	100	95.40	4.60	0.05	0.39	408.80	6.51E-07

Table A.25 Slump test for 5 mins 90:10 at relative density of 1.75 Kaolinite tailings and sand using the slump meter

Appendix A- Slump Data

RESULTS ON THE SLUMP TEST: (10mins 90:10 at 1.75)									
Equations: $1.75 \quad s' = \frac{h}{H} \quad \tau_y = \rho g H \tau_y$ $1750 \quad s' = \frac{h}{H} \quad \tau_y = \rho g H \tau_y$ $9.81 \quad s' = \frac{h}{H} \quad \tau_y = \rho g H \tau_y$									
Without silicone spray :									
Cone geometry : Stainless steel									
Number	Speed (mm.s ⁻¹)	Time	H (mm)	H _r (mm)	h (mm)	s'	Approx. cyl		
10	7.51	4.33	150	32.52	117.48	0.78	τ_y	τ_y	τ_y
Cylinder geometry : Stainless steel							0.06	148.09	
Number	Speed (mm.s ⁻¹)	Time	H (mm)	H _r (mm)	h (mm)	s'	τ_y	τ_y	τ_y
10	6.99	4.46	100	31.18	68.82	0.69	0.09	146.29	
Cone geometry : PVC									
Number	Speed (mm.s ⁻¹)	Time	H (mm)	H _r (mm)	h (mm)	s'	τ_y	τ_y	τ_y
10	7.69	4.45	150	34.21	115.79	0.77	0.06	156.31	
Cylinder geometry : PVC									
Number	Speed (mm.s ⁻¹)	Time	H (mm)	H _r (mm)	h (mm)	s'	τ_y	τ_y	τ_y
10	6.98	4.32	100	30.14	69.86	0.70	0.08	140.93	
With silicone spray :									
Cone geometry : Stainless steel									
Number	Speed (mm.s ⁻¹)	Time	H (mm)	H _r (mm)	h (mm)	s'	Approx. cyl		
10	7.70	4.46	150	34.32	115.68	0.77	τ_y	τ_y	τ_y
Cylinder geometry : Stainless steel							0.06	156.85	
Number	Speed (mm.s ⁻¹)	Time	H (mm)	H _r (mm)	h (mm)	s'	τ_y	τ_y	τ_y
10	8.22	4.27	100	35.12	64.88	0.65	0.10	166.97	
Cone geometry : PVC									
Number	Speed (mm.s ⁻¹)	Time	H (mm)	H _r (mm)	h (mm)	s'	τ_y	τ_y	τ_y
10	7.62	4.61	150	35.12	114.88	0.77	0.06	160.77	
Cylinder geometry : PVC									
Number	Speed (mm.s ⁻¹)	Time	H (mm)	H _r (mm)	h (mm)	s'	τ_y	τ_y	τ_y
10	8.57	3.81	100	32.64	67.36	0.67	0.09	153.88	
Vane							Calc. from vane		
							τ_y		
							203.20		
Lump model							τ_y	τ_y	τ_y
							0	71.89	71.83
Cylinder model							τ_y	τ_y	τ_y
							0	81.26	79.08
Lump model							τ_y	τ_y	τ_y
							0	77.12	76.92
Cylinder model							τ_y	τ_y	τ_y
							0	77.15	75.37
Lump Model							τ_y	τ_y	τ_y
							0	77.47	77.25
Cylinder model							τ_y	τ_y	τ_y
							0	97.99	93.80
Lump Model							τ_y	τ_y	τ_y
							0	80.01	79.71
Cylinder model							τ_y	τ_y	τ_y
							0	87.24	84.40

Table A.27 Slump test for 20 mins 90:10 at relative density of 1.75 Kaolinite tailings and sand using the slump meter

Appendix A- Slump Data

RESULTS ON THE SLUMP TEST: (5mins 90:10 at 1.8)												
Relative density Density (Kg/m ³) g (m.s ⁻¹)	Equations: $s' = \frac{1.8}{1800} h \tau_y = \frac{\rho g H \tau_y}{H}$											
	$\tau_y' = \frac{1}{2} - \frac{1}{2} \sqrt{s'}$											
	Approximate cylinder											
Lump model												
Cylinder model												
$S' = 1 - 2\tau_y' (1 - \ln(2\tau_y'))$												
Without silicone spray :												
Cone geometry : Stainless steel												
Number	Speed (mm.s ⁻¹)	Time	H (mm)	H _r (mm)	h (mm)	s'	τ_y'	Approx.cyl τ_y	Calc. from vane τ_y'	τ_y'	Lump Model τ_y	Cylinder model τ_y
10	10.43	4.36	150	45.46	104.54	0.70	0.08	218.75	0.09	0.05	0	120.03
Cylinder geometry : Stainless steel												
Number	Speed (mm.s ⁻¹)	Time	H (mm)	H _r (mm)	h (mm)	s'	τ_y'	τ_y	0.14	0.08	0	149.53
10	10.59	4.19	100	44.38	55.62	0.56	0.13	224.44				136.77
Cone geometry : PVC												
Number	Speed (mm.s ⁻¹)	Time	H (mm)	H _r (mm)	h (mm)	s'	τ_y'	τ_y	0.09	0.04	0	111.20
10	10.52	4.11	150	43.22	106.78	0.71	0.08	206.97				109.15
Cylinder geometry : PVC												
Number	Speed (mm.s ⁻¹)	Time	H (mm)	H _r (mm)	h (mm)	s'	τ_y'	τ_y	0.14	0.10	0	172.05
10	10.95	4.38	100	47.98	52.02	0.52	0.14	246.11				154.40
With silicone spray :												
Cone geometry : Stainless steel												
Number	Speed (mm.s ⁻¹)	Time	H (mm)	H _r (mm)	h (mm)	s'	τ_y'	Approx.cyl τ_y	Calc. from vane	τ_y'	Lump Model τ_y	Cylinder model τ_y
10	11.07	4.3	150	47.58	102.42	0.68	0.09	230.02	0.09	0.05	0	128.74
Cylinder geometry : Stainless steel												
Number	Speed (mm.s ⁻¹)	Time	H (mm)	H _r (mm)	h (mm)	s'	τ_y'	τ_y	0.14	0.09	0	162.97
10	10.12	4.6	100	46.57	53.43	0.53	0.13	237.54				147.35
Cone geometry : PVC												
Number	Speed (mm.s ⁻¹)	Time	H (mm)	H _r (mm)	h (mm)	s'	τ_y'	τ_y	0.09	0.04	0	117.67
10	10.68	4.2	150	44.87	105.13	0.70	0.08	215.63				115.05
Cylinder geometry : PVC												
Number	Speed (mm.s ⁻¹)	Time	H (mm)	H _r (mm)	h (mm)	s'	τ_y'	τ_y	0.14	0.10	0	176.69
10	11.56	4.21	100	48.68	51.32	0.51	0.14	250.41				157.96

Table A.29 Slump test for 10 mins 90:10 at relative density of 1.8 Kaolinite tailings and sand using the slump meter

Appendix A- Slump Data

RESULTS ON THE SLUMP TEST: (10mins 90:10 at 1.8)													
Equations: $\tau_y = \frac{h}{H} \tau_y = \rho g H \tau_y$ $s' = \frac{1}{2} - \frac{1}{2} \sqrt{s'}$													
Relative density Density (Kg/m ³) ρ (m.s ⁻¹)													
Without silicone spray : Cone geometry : Stainless steel													
Number	Speed (mm.s ⁻¹)	Time	H (mm)	H _r (mm)	h (mm)	s'	τ_y	Approx.cyl	Vane τ_y	Lump model	Cylinder model		
10	10.44	5.13	150	53.54	96.46	0.64	0.10	282.33	308.21	0	0.06	τ_y	$S' = 1 - 2\tau_y (1 - \ln(2\tau_y))$
Cylinder geometry : Stainless steel													
Number	Speed (mm.s ⁻¹)	Time	H (mm)	H _r (mm)	h (mm)	s'	τ_y						
10	10.44	5.06	100	52.84	47.16	0.47	0.16	276.58	0.18	0	0.12	τ_y	τ_y
Cone geometry : PVC													
Number	Speed (mm.s ⁻¹)	Time	H (mm)	H _r (mm)	h (mm)	s'	τ_y						
10	10.89	5.08	150	55.32	94.68	0.63	0.10	272.18	0.12	0	0.06	τ_y	τ_y
Cylinder geometry : PVC													
Number	Speed (mm.s ⁻¹)	Time	H (mm)	H _r (mm)	h (mm)	s'	τ_y						
10	11.46	4.8	100	55.01	44.99	0.45	0.16	290.70	0.18	0	0.13	τ_y	τ_y
With silicone spray :													
Cone geometry : Stainless steel													
Number	Speed (mm.s ⁻¹)	Time	H (mm)	H _r (mm)	h (mm)	s'	τ_y	Approx.cyl	Calc.from vane				
10	9.21	6.14	150	56.54	93.46	0.62	0.11	278.98	0.12	0	0.06	τ_y	τ_y
Cylinder geometry : Stainless steel													
Number	Speed (mm.s ⁻¹)	Time	H (mm)	H _r (mm)	h (mm)	s'	τ_y						
10	9.03	6.12	100	55.26	44.74	0.45	0.17	292.35	0.18	0	0.13	τ_y	τ_y
Cone geometry : PVC													
Number	Speed (mm.s ⁻¹)	Time	H (mm)	H _r (mm)	h (mm)	s'	τ_y						
10	9.77	5.82	150	56.85	93.15	0.62	0.11	280.72	0.12	0	0.06	τ_y	τ_y
Cylinder geometry : PVC													
Number	Speed (mm.s ⁻¹)	Time	H (mm)	H _r (mm)	h (mm)	s'	τ_y						
10	8.69	6.41	100	55.68	44.32	0.44	0.17	295.12	0.18	0	0.13	τ_y	τ_y

Table A.30 Slump test for 20 mins 90:10 at relative density of 1.8 Kaolinite tailings and sand using the slump meter

Appendix A- Slump Data

RESULTS ON THE SLUMP TEST: (20mins 90:10 at 1.8)											
Relative density Density (Kg/m ³) g (m.s ⁻¹)		1.8 1800 9.81		Equations: $s' = \frac{h}{H}$ $\tau_y = \rho g H \tau'_y$		$\tau'_y = \frac{1}{2} - \frac{1}{2} \sqrt{s'}$		Vane τ_y 397.83		$\tau'_y = 0.5(1 - S') e^{\sqrt{3}(-s')}$ $S' = 1 - 2\tau'_y (1 - \ln(2\tau'_y))$	
Without silicone spray :											
Cone geometry : Stainless steel								Approx.cyl	Calc. from vane		
Number	Speed (mm.s ⁻¹)	Time	H (mm)	H _r (mm)	h (mm)	s'	τ'_y	τ_y	τ'_y	Lump Model	Cylinder model
10	9.31	6.89	150	64.12	85.88	0.57	0.12	322.27	0.15	0	210.01
Cylinder geometry : Stainless steel											
Number	Speed (mm.s ⁻¹)	Time	H (mm)	H _r (mm)	h (mm)	s'	τ'_y	τ_y		Lump model	Cylinder model
10	9.96	6.35	100	63.25	36.75	0.37	0.20	347.67	0.23	0	295.48
Cone geometry : PVC											
Number	Speed (mm.s ⁻¹)	Time	H (mm)	H _r (mm)	h (mm)	s'	τ'_y	τ_y	0.15	0	206.72
10	9.66	6.58	150	63.54	86.46	0.58	0.12	318.89			
Cylinder geometry : PVC											
Number	Speed (mm.s ⁻¹)	Time	H (mm)	H _r (mm)	h (mm)	s'	τ'_y	τ_y		Lump model	Cylinder model
10	9.75	6.58	100	64.15	35.85	0.36	0.20	354.26	0.23	0	304.39
With silicone spray :											
Cone geometry : Stainless steel								Approx.cyl	Calc. from vane		
Number	Speed (mm.s ⁻¹)	Time	H (mm)	H _r (mm)	h (mm)	s'	τ'_y	τ_y		Lump Model	Cylinder model
10	9.71	6.56	150	63.68	86.32	0.58	0.12	319.70	0.15	0	207.51
Cylinder geometry : Stainless steel											
Number	Speed (mm.s ⁻¹)	Time	H (mm)	H _r (mm)	h (mm)	s'	τ'_y	τ_y		Lump Model	Cylinder model
10	9.84	6.48	100	63.78	36.22	0.36	0.20	351.54	0.23	0	300.71
Cone geometry : PVC											
Number	Speed (mm.s ⁻¹)	Time	H (mm)	H _r (mm)	h (mm)	s'	τ'_y	τ_y		Lump Model	Cylinder model
10	9.97	6.49	150	64.68	85.32	0.57	0.12	325.54	0.15	0	213.22
Cylinder geometry : PVC											
Number	Speed (mm.s ⁻¹)	Time	H (mm)	H _r (mm)	h (mm)	s'	τ'_y	τ_y		Lump Model	Cylinder model
10	9.89	6.53	100	64.58	35.42	0.35	0.20	357.44	0.23	0	308.73

Table A.31 Slump test for 5 mins 80:20 at relative density of 1.6 Kaolinite tailings and sand using the slump meter

Appendix A- Slump Data

RESULTS ON THE SLUMP TEST: (5mins 80:20 at 1.6)										Approximate cylinder		Lump model			Cylinder model		
Equations: $s' = \frac{h}{H} \tau_y = \rho g H \tau_y'$										$\tau_y' = -\frac{1}{2} \frac{1}{2} \sqrt{s'}$		$\tau_y' = 0.5(1 - S') e^{\sqrt{3}(-S')}$			$S' = 1 - 2\tau_y'(1 - \ln(2\tau_y'))$		
Relative density Density (Kg/m ³) g (m.s ⁻¹)										Vane τ_y 66.84							
Without silicone spray :										Calc from vane							
Cone geometry : Stainless steel										Approx.cyl							
Number	Speed (mm.s ⁻¹)	Time	H (mm)	H _r (mm)	h (mm)	s'	τ_y'	τ_y	τ_y'	τ_y'	τ_y	Lump Model	τ_y'	τ_y	Cylinder model	τ_y'	
10	6.47	3.76	150	24.32	125.68	0.84	0.04	99.65	0.03	0.02	44.72	0	0.02	44.72	4.05E-07	44.69	
Cylinder geometry : Stainless steel																	
Number	Speed (mm.s ⁻¹)	Time	H (mm)	H _r (mm)	h (mm)	s'	τ_y'	τ_y	τ_y'	τ_y'	τ_y	Lump model	τ_y'	τ_y	Cylinder model	τ_y'	
10	6.56	3.83	100	25.12	74.88	0.75	0.07	105.69	0.04	0.03	53.89	0	0.03	53.89	1.11E-07	53.48	
Cone geometry : PVC																	
Number	Speed (mm.s ⁻¹)	Time	H (mm)	H _r (mm)	h (mm)	s'	τ_y'	τ_y	τ_y'	τ_y'	τ_y	Lump Model	τ_y'	τ_y	Cylinder model	τ_y'	
10	6.56	3.61	150	23.67	126.33	0.84	0.04	96.87	0.03	0.02	43.20	0	0.02	43.20	3.17E-07	43.13	
Cylinder geometry : PVC																	
Number	Speed (mm.s ⁻¹)	Time	H (mm)	H _r (mm)	h (mm)	s'	τ_y'	τ_y	τ_y'	τ_y'	τ_y	Lump Model	τ_y'	τ_y	Cylinder model	τ_y'	
10	5.83	4.17	100	24.31	75.69	0.76	0.07	102.02	0.04	0.03	51.43	0	0.03	51.43	6.67E-07	51.14	
With silicone spray :										Calc from vane							
Cone geometry : Stainless steel										Approx.cyl							
Number	Speed (mm.s ⁻¹)	Time	H (mm)	H _r (mm)	h (mm)	s'	τ_y'	τ_y	τ_y'	τ_y'	τ_y	Lump Model	τ_y'	τ_y	Cylinder model	τ_y'	
10	6.36	4.15	150	26.41	123.59	0.82	0.05	108.65	0.03	0.02	49.74	0	0.02	49.74	3.41E-07	49.79	
Cylinder geometry : Stainless steel																	
Number	Speed (mm.s ⁻¹)	Time	H (mm)	H _r (mm)	h (mm)	s'	τ_y'	τ_y	τ_y'	τ_y'	τ_y	Lump Model	τ_y'	τ_y	Cylinder model	τ_y'	
10	6.55	4.31	100	28.21	71.79	0.72	0.08	119.85	0.04	0.04	63.85	0	0.04	63.85	3.12E-07	62.80	
Cone geometry : PVC																	
Number	Speed (mm.s ⁻¹)	Time	H (mm)	H _r (mm)	h (mm)	s'	τ_y'	τ_y	τ_y'	τ_y'	τ_y	Lump Model	τ_y'	τ_y	Cylinder model	τ_y'	
10	6.97	3.73	150	25.98	124.02	0.83	0.05	106.79	0.03	0.02	48.69	0	0.02	48.69	4.00E-07	48.72	
Cylinder geometry : PVC																	
Number	Speed (mm.s ⁻¹)	Time	H (mm)	H _r (mm)	h (mm)	s'	τ_y'	τ_y	τ_y'	τ_y'	τ_y	Lump Model	τ_y'	τ_y	Cylinder model	τ_y'	
10	5.97	4.5	100	26.87	73.13	0.73	0.07	113.67	0.04	0.04	59.42	0	0.04	59.42	5.80E-07	58.69	

Table A.32 Slump test for 10 mins 80:20 at relative density of 1.6 Kaolinite tailings and sand using the slump meter

Appendix A- Slump Data

RESULTS ON THE SLUMP TEST: (10mins 80:20 at 1.6)										Approximate cylinder		Lump model		Cylinder model											
Equations: $\tau_y = \frac{h}{H} \rho g H \tau_y'$ $\tau_y' = \frac{1}{2} - \frac{1}{2} \sqrt{s'}$										$\tau_y' = 0.5(1 - S') e^{\sqrt{3}(-S')}$ $S' = 1 - 2\tau_y'(1 - \ln(2\tau_y'))$		Vane τ_y 78.68		Lump Model 0		τ_y' 0.02		τ_y 50.24		τ_y' 0.02		Cylinder model 8.63E-07		τ_y 50.28	
Without silicone spray :										Approx.cyl		Lump Model		τ_y'		τ_y		Cylinder model		τ_y					
Cone geometry : Stainless steel		H (mm)		H _r (mm)		h (mm)		s'		τ_y'		τ_y		τ_y'		τ_y		Cylinder model		τ_y					
10	6.79	3.92	26.61	150	123.39	0.82	0.05	0.05	109.51	0.03		0		0.02		50.24		0.02		8.63E-07					
Cylinder geometry : Stainless steel										τ_y		Lump model		τ_y'		τ_y		Cylinder model		τ_y		Cylinder model			
10	5.92	4.46	26.42	100	73.58	0.74	0.07	0.07	111.61	0.05		0		0.04		57.97		0.04		1.29E-07					
Cone geometry : PVC										τ_y		Lump Model		τ_y'		τ_y		Cylinder model		τ_y		Cylinder model			
10	6.06	4.32	26.16	150	123.84	0.83	0.05	0.05	107.57	0.03		0		0.02		49.13		0.02		9.16E-07					
Cylinder geometry : PVC										τ_y		Lump Model		τ_y'		τ_y		Cylinder model		τ_y		Cylinder model			
10	6.21	4	24.82	100	75.18	0.75	0.07	0.07	104.33	0.05		0		0.03		52.97		0.03		7.36E-07					
With silicone spray :										Approx.cyl		Lump Model		τ_y'		τ_y		Cylinder model		τ_y		Cylinder model			
Cone geometry : Stainless steel		H (mm)		H _r (mm)		h (mm)		s'		τ_y'		Lump Model		τ_y'		54.05		0.02		4.27E-07					
10	6.83	4.12	28.13	150	121.87	0.81	0.05	0.05	116.11	0.03		0		0.02		54.05		0.02		4.27E-07					
Cylinder geometry : Stainless steel										τ_y		Lump Model		τ_y'		τ_y		Cylinder model		τ_y		Cylinder model			
10	7.15	4.09	29.24	100	70.76	0.71	0.08	0.08	124.63	0.05		0		0.04		67.37		0.04		2.68E-07					
Cone geometry : PVC										τ_y		Lump Model		τ_y'		τ_y		Cylinder model		τ_y		Cylinder model			
10	6.14	4.57	28.05	150	121.95	0.81	0.05	0.05	115.76	0.03		0		0.02		53.84		0.02		4.13E-07					
Cylinder geometry : PVC										τ_y		Lump Model		τ_y'		τ_y		Cylinder model		τ_y		Cylinder model			
10	6.41	4.17	26.73	100	73.27	0.73	0.07	0.07	113.03	0.05		0		0.04		58.97		0.04		-3.37E-07					

Table A.33 Slump test for 20 mins 80:20 at relative density of 1.6 Kaolinite tailings and sand using the slump meter

Appendix A- Slump Data

RESULTS ON THE SLUMP TEST: (20mins 80:20 at 1.6)													
Equations: h 1.7 $s' = \frac{h}{H}$ 1700 $\tau_y = \rho g H \tau_y$ 9.81						$\tau_y' = \frac{1}{2} - \frac{1}{2} \sqrt{s'}$			Approximate cylinder		Cylinder model		
Relative density Density (Kg/m ³) g (m.s ⁻¹)						$\tau_y' = 0.5(1 - S')e^{\sqrt{3}(-S')}$						$S' = 1 - 2\tau_y'(1 - \ln(2\tau_y'))$	
						Vane							
						τ_y							
						82.27284							
Without silicone spray :						Calc from vane							
Cone geometry : Stainless steel						τ_y'		Lump Model		τ_y		Cylinder model	
Number Speed (mm.s ⁻¹) Time						0.04		0		56.13		6.23E-07	
10 7.5 3.88													
Cylinder geometry : Stainless steel						τ_y'		Lump model		τ_y		Cylinder model	
Number Speed (mm.s ⁻¹) Time						0.05		0		66.68		3.33E-07	
10 7.0 4.12													
Cone geometry : PVC						τ_y'		Lump Model		τ_y		Cylinder model	
Number Speed (mm.s ⁻¹) Time						0.040		0		54.92		4.91E-07	
10 7.1 4													
Cylinder geometry : PVC						τ_y'		Lump Model		τ_y		Cylinder model	
Number Speed (mm.s ⁻¹) Time						0.05		0		57.30		2.34E-07	
10 7.4 3.56													
With silicone spray :													
Cone geometry : Stainless steel						Calc from vane		Lump Model		τ_y		Cylinder model	
Number Speed (mm.s ⁻¹) Time						0.04		0		57.66		3.69E-07	
10 7.6 3.91													
Cylinder geometry : Stainless steel						τ_y'		Lump Model		τ_y		Cylinder model	
Number Speed (mm.s ⁻¹) Time						0.05		0		70.50		1.80E-07	
10 7.1 4.26													
Cone geometry : PVC						τ_y'		Lump Model		τ_y		Cylinder model	
Number Speed (mm.s ⁻¹) Time						0.04		0		56.72		3.58E-07	
10 7.0 4.17													
Cylinder geometry : PVC						τ_y'		Lump Model		τ_y		Cylinder model	
Number Speed (mm.s ⁻¹) Time						0.05		0		64.35		4.24E-07	
10 7.2 3.96													

Table A.34 Slump test for 5 mins 90:10 at relative density of 1.75 Kaolinite tailings and sand using the slump meter

Appendix A- Slump Data

RESULTS ON THE SLUMP TEST: (5mins 80:20 at 1.7)										Approximate cylinder		Lump model		Cylinder model	
<div>Equations:</div> $\tau_y = \frac{h}{H} \rho g H \tau_y'$ $\tau_y' = \frac{1}{2} - \frac{1}{2} \sqrt{s'}$										<div>Vane</div> τ_y'		$\tau_y' = 0.5(1 - S') e^{\sqrt[3]{3(-s')}}$		$S' = 1 - 2\tau_y'(1 - \ln(2\tau_y'))$	
										130.04					
Without silicone spray :										Approx.cyl		Lump Model		Cylinder model	
Cone geometry : Stainless steel															
Number	Speed (mm.s ⁻¹)	H (mm)	H _c (mm)	h (mm)	s'	τ_y'	τ_y	Time		τ_y'	τ_y	τ_y'	τ_y	τ_y'	τ_y
10	7.63	150	40.23	109.77	0.73	0.07	180.80	5.27		0.04	94.44	0.04	0	0.04	93.29
Cylinder geometry : Stainless steel															
Number	Speed (mm.s ⁻¹)	H (mm)	H _c (mm)	h (mm)	s'	τ_y'	τ_y	Time		τ_y'	τ_y	τ_y'	τ_y	τ_y'	τ_y
10	7.71	100	41.53	58.47	0.58	0.12	196.24	5.39		0.08	125.78	0.07	0	0.07	116.76
Cone geometry : PVC															
Number	Speed (mm.s ⁻¹)	H (mm)	H _c (mm)	h (mm)	s'	τ_y'	τ_y	Time		τ_y'	τ_y	τ_y'	τ_y	τ_y'	τ_y
10	7.66	150	35.3	114.7	0.76	0.06	157.03	4.61		0.03	78.28	0.03	0	0.03	77.97
Cylinder geometry : PVC												Lump Model		Cylinder model	
Number	Speed (mm.s ⁻¹)	H (mm)	H _c (mm)	h (mm)	s'	τ_y'	τ_y	Time		τ_y'	τ_y	τ_y'	τ_y	τ_y'	τ_y
10	8.32	100	37.79	62.21	0.62	0.11	176.16	4.54		0.06	107.28	0.06	0	0.06	101.43
With silicone spray :															
Cone geometry : Stainless steel										Approx.cyl		Lump Model		Cylinder model	
Number	Speed (mm.s ⁻¹)	H (mm)	H _c (mm)	h (mm)	s'	τ_y'	τ_y	Time		τ_y'	τ_y	τ_y'	τ_y	τ_y'	τ_y
10	7.01	150	40.17	109.83	0.73	0.07	180.50	7.01		0.04	94.24	0.04	0	0.04	93.10
Cylinder geometry : Stainless steel												Lump Model		Cylinder model	
Number	Speed (mm.s ⁻¹)	H (mm)	H _c (mm)	h (mm)	s'	τ_y'	τ_y	Time		τ_y'	τ_y	τ_y'	τ_y	τ_y'	τ_y
10	7.59	100	37.28	62.72	0.63	0.10	173.47	4.91		0.08	104.90	0.06	0	0.06	99.42
Cone geometry : PVC												Lump Model		Cylinder model	
Number	Speed (mm.s ⁻¹)	H (mm)	H _c (mm)	h (mm)	s'	τ_y'	τ_y	Time		τ_y'	τ_y	τ_y'	τ_y	τ_y'	τ_y
10	6.98	150	39.98	110.02	0.73	0.07	179.58	5.73		0.04	93.58	0.04	0	0.04	92.49
Cylinder geometry : PVC												Lump Model		Cylinder model	
Number	Speed (mm.s ⁻¹)	H (mm)	H _c (mm)	h (mm)	s'	τ_y'	τ_y	Time		τ_y'	τ_y	τ_y'	τ_y	τ_y'	τ_y
10	8.19	100	36.87	63.13	0.63	0.10	171.32	4.5		0.06	103.01	0.06	0	0.06	97.82

Table A.35 Slump test for 10 mins 80:20 at relative density of 1.7 Kaolinite tailings and sand using the slump meter

Appendix A- Slump Data

RESULTS ON THE SLUMP TEST: (10mins 80:20 at 1.7)										Approximate cylinder		Lump model		Cylinder model		
Relative density Density (Kg/m ³) g (m.s ⁻¹)		Equations: $1.7 \tau_y = \rho g H \tau_y$ $1700 s' = \frac{h}{H}$ 9.81								Vane τ_y 161.23		$\tau_y' = 0.5(1-S')e^{\sqrt{3}(-s')}$		$S' = 1-2\tau_y'(1-\ln(2\tau_y'))$		
Without silicone spray :										Approx.cyl	Calc.from vane					
Cone geometry : Stainless steel																
Number	Speed (mm.s ⁻¹)	Time	H (mm)	H _r (mm)	h (mm)	s'				τ_y'	τ_y		τ_y'	Cylinder model	τ_y	
10	8.11	5.03	150	40.78	109.22	0.73				0.07	183.48	0.06	0.04	5.219E-07	95.07	
Cylinder geometry : Stainless steel																
Number	Speed (mm.s ⁻¹)	Time	H (mm)	H _r (mm)	h (mm)	s'				τ_y'	τ_y		τ_y'	Cylinder model	τ_y	
10	8.74	4.56	100	39.86	60.14	0.60				0.11	187.20	0.10	0.07	1.205E-07	109.78	
Cone geometry : PVC																
Number	Speed (mm.s ⁻¹)	Time	H (mm)	H _r (mm)	h (mm)	s'				τ_y'	τ_y		τ_y'	Cylinder model	τ_y	
10	8.12	5.02	150	40.74	109.26	0.73				0.07	183.28	0.06	0.04	4.154E-07	94.94	
Cylinder geometry : PVC																
Number	Speed (mm.s ⁻¹)	Time	H (mm)	H _r (mm)	h (mm)	s'				τ_y'	τ_y		τ_y'	Cylinder model	τ_y	
10	7.94	4.7	100	37.32	62.68	0.63				0.10	173.69	0.10	0.06	4.657E-07	99.58	
With silicone spray :																
Cone geometry : Stainless steel										Approx.cyl	Calc.from vane					
Number	Speed (mm.s ⁻¹)	Time	H (mm)	H _r (mm)	h (mm)	s'				τ_y'	τ_y		τ_y'	Cylinder model	τ_y	
10	8.26	5.45	150	45.02	104.98	0.70				0.08	204.40	0.06	0.04	2.866E-07	109.17	
Cylinder geometry : Stainless steel																
Number	Speed (mm.s ⁻¹)	Time	H (mm)	H _r (mm)	h (mm)	s'				τ_y'	τ_y		τ_y'	Cylinder model	τ_y	
10	8.95	5.9	100	52.78	47.22	0.47				0.16	260.85	0.10	0.12	3.333E-07	169.85	
Cone geometry : PVC																
Number	Speed (mm.s ⁻¹)	Time	H (mm)	H _r (mm)	h (mm)	s'				τ_y'	τ_y		τ_y'	Cylinder model	τ_y	
10	8.85	4.95	150	43.79	106.21	0.71				0.08	198.29	0.06	0.04	5.727E-07	105.00	
Cylinder geometry : PVC																
Number	Speed (mm.s ⁻¹)	Time	H (mm)	H _r (mm)	h (mm)	s'				τ_y'	τ_y		τ_y'	Cylinder model	τ_y	
10	10.46	4.74	100	49.58	50.42	0.50				0.14	241.76	0.10	0.10	2.345E-07	153.59	

Table A.36 Slump test for 20 mins 80:20 at relative density of 1.7 Kaolinite tailings and sand using the slump meter

Appendix A- Slump Data

RESULTS ON THE SLUMP TEST: (20mins 80:20 at 1.7)												
Equations: $s' = \frac{h}{H} \quad \tau_y = \rho g H \tau_y$												
Relative density	1.7											
Density (Kg/m ³)	1700											
g (m.s ⁻¹)	9.81											
Without silicone spray :												
Cone geometry : Stainless steel												
Number	Speed (mm.s ⁻¹)	Time	H (mm)	H _r (mm)	h (mm)	s'	τ_y'	Approx.cyl	Calc from vane	τ_y'	Lump Model	τ_y
10	7.21	6.25	150	45.08	104.92	0.70	0.08	τ_y	τ_y'	0.04	0	111.92
Cylinder geometry : Stainless steel												
Number	Speed (mm.s ⁻¹)	Time	H (mm)	H _r (mm)	h (mm)	s'	τ_y'	τ_y	τ_y'	τ_y	Lump model	τ_y
10	7.30	6.32	100	46.12	53.88	0.54	0.13	221.78	0.115	0.09	0	151.25
Cone geometry : PVC												
Number	Speed (mm.s ⁻¹)	Time	H (mm)	H _r (mm)	h (mm)	s'	τ_y'	τ_y	τ_y'	τ_y	Lump model	τ_y
10	7.03	6.72	150	47.24	102.76	0.69	0.09	215.52	0.077	0.05	0	120.25
Cylinder geometry : PVC												
Number	Speed (mm.s ⁻¹)	Time	H (mm)	H _r (mm)	h (mm)	s'	τ_y'	τ_y	τ_y'	τ_y	Lump model	τ_y
10	7.96	5.5	100	43.76	56.24	0.56	0.13	208.52	0.115	0.08	0	137.76
With silicone spray :												
Cone geometry : Stainless steel												
Number	Speed (mm.s ⁻¹)	Time	H (mm)	H _r (mm)	h (mm)	s'	τ_y'	τ_y	τ_y'	τ_y	Lump Model	τ_y
10	8.57	6.21	150	53.2	96.8	0.65	0.10	245.99	0.077	0.06	0	145.07
Cylinder geometry : Stainless steel												
Number	Speed (mm.s ⁻¹)	Time	H (mm)	H _r (mm)	h (mm)	s'	τ_y'	τ_y	τ_y'	τ_y	Lump Model	τ_y
10	8.34	6.4	100	53.4	46.6	0.47	0.16	264.63	0.115	0.12	0	198.65
Cone geometry : PVC												
Number	Speed (mm.s ⁻¹)	Time	H (mm)	H _r (mm)	h (mm)	s'	τ_y'	τ_y	τ_y'	τ_y	Lump Model	τ_y
10	9.37	5.87	150	54.98	95.02	0.63	0.10	255.28	0.077	0.06	0	153.03
Cylinder geometry : PVC												
Number	Speed (mm.s ⁻¹)	Time	H (mm)	H _r (mm)	h (mm)	s'	τ_y'	τ_y	τ_y'	τ_y	Lump Model	τ_y
10	9.82	5.09	100	49.96	50.04	0.50	0.15	243.99	0.115	0.10	0	175.11
Cylinder model												
$S' = 1 - 2\tau_y' (1 - \ln(2\tau_y'))$												

Table A.37 Slump test for 5 mins 80:20 at relative density of 1.8 Kaolinite tailings and sand using the slump meter

Appendix A- Slump Data

RESULTS ON THE SLUMP TEST: (5mins 80:20 at 1.8)										Approximate cylinder	Lump model		Cylinder model
Equations: $s' = \frac{h}{H} \quad \tau_y = \rho g H \tau_y'$										$\tau_y' = \frac{1}{2} - \frac{1}{2} \sqrt{s'}$	$\tau_y' = 0.5(1 - s')e^{\sqrt{3}(-s')}$		$S' = 1 - 2\tau_y'(1 - \ln(2\tau_y'))$
Relative density	1.8												
Density (Kg/m ³)	1800												
g (m.s ⁻¹)	9.81												
Without silicone spray :													
Cone geometry : Stainless steel										Approx.cyl			
Number	Speed (mm.s ⁻¹)	Time	H (mm)	H _r (mm)	h (mm)	s'				τ_y'	τ_y'	τ_y	τ_y
10	8.55	6.95	150	59.44	90.56	0.60				0.11	0.07	184.44	172.84
Cylinder geometry : Stainless steel													
Number	Speed (mm.s ⁻¹)	Time	H (mm)	H _r (mm)	h (mm)	s'				τ_y'	τ_y'	τ_y	τ_y
10	8.87	6.9	100	61.18	38.82	0.39				0.19	0.16	275.75	230.58
Cone geometry : PVC													
Number	Speed (mm.s ⁻¹)	Time	H (mm)	H _r (mm)	h (mm)	s'				τ_y'	τ_y'	τ_y	τ_y
10	8.90	7.13	150	63.44	86.56	0.58				0.12	0.08	206.15	190.62
Cylinder geometry : PVC													
Number	Speed (mm.s ⁻¹)	Time	H (mm)	H _r (mm)	h (mm)	s'				τ_y'	τ_y'	τ_y	τ_y
10	9.66	6.7	100	64.7	35.3	0.35				0.20	0.18	309.94	254.63
With silicone spray :													
Cone geometry : Stainless steel										Approx.cyl			
Number	Speed (mm.s ⁻¹)	Time	H (mm)	H _r (mm)	h (mm)	s'				τ_y'	τ_y'	τ_y	τ_y
10	9.14	6.85	150	62.62	87.38	0.58				0.12	0.08	201.57	186.90
Cylinder geometry : Stainless steel													
Number	Speed (mm.s ⁻¹)	Time	H (mm)	H _r (mm)	h (mm)	s'				τ_y'	τ_y'	τ_y	τ_y
10	10.02	6.4	100	64.15	35.85	0.36				0.20	0.17	304.39	250.75
Cone geometry : PVC													
Number	Speed (mm.s ⁻¹)	Time	H (mm)	H _r (mm)	h (mm)	s'				τ_y'	τ_y'	τ_y	τ_y
10	9.20	6.9	150	63.51	86.49	0.58				0.12	0.08	206.55	190.94
Cylinder geometry : PVC													
Number	Speed (mm.s ⁻¹)	Time	H (mm)	H _r (mm)	h (mm)	s'				τ_y'	τ_y'	τ_y	τ_y
10	10.53	6.3	100	66.36	33.64	0.34				0.21	0.19	327.17	266.64

Table A.38 Slump test for 10 mins 80:20 at relative density of 1.8 Kaolinite tailings and sand using the slump meter

Appendix A- Slump Data

RESULTS ON THE SLUMP TEST: (10mins 80:20 at 1.8)														
Equations: $s' = \frac{1.8}{1800} \frac{h}{H} \tau_y = \rho g H \tau_y$														
Relative density Density (Kg/m ³) g (m.s ⁻¹)														
Without silicone spray :														
Cone geometry : Stainless steel														
Number	Speed (mm.s ⁻¹)	Time	H (mm)	H _r (mm)	h (mm)	s'	Approximate cylinder $\tau_y' = \frac{1}{2} - \frac{1}{2} \sqrt{s'}$							
10	8.69	6.73	150	58.47	91.53	0.61	τ_y'	τ_y	Approx.cyl	Calc. from vane	τ_y'	τ_y	Lump Model	τ_y'
Cylinder geometry : Stainless steel														
Number	Speed (mm.s ⁻¹)	Time	H (mm)	H _r (mm)	h (mm)	s'	τ_y'	τ_y			τ_y'	τ_y		τ_y
10	8.37	6.77	100	56.69	43.31	0.43	0.17	301.86			0.15	236.39	Cylinder model	202.39
Cone geometry : PVC														
Number	Speed (mm.s ⁻¹)	Time	H (mm)	H _r (mm)	h (mm)	s'	τ_y'	τ_y			τ_y'	τ_y	Cylinder model	τ_y
10	9.76	6.04	150	58.95	91.05	0.61	0.11	292.55			0.10	181.89	4.16E-08	170.72
Cylinder geometry : PVC														
Number	Speed (mm.s ⁻¹)	Time	H (mm)	H _r (mm)	h (mm)	s'	τ_y'	τ_y			τ_y'	τ_y	Cylinder model	τ_y
10	8.37	6.38	100	53.42	46.58	0.47	0.16	280.32			0.15	210.49	1.89E-07	183.42
With silicone spray :														
Cone geometry : Stainless steel														
Number	Speed (mm.s ⁻¹)	Time	H (mm)	H _r (mm)	h (mm)	s'	τ_y'	τ_y			τ_y'	τ_y	Lump Model	τ_y
10	8.29	7.31	150	60.61	89.39	0.60	0.11	302.00			0.10	190.63	0	177.95
Cylinder geometry : Stainless steel														
Number	Speed (mm.s ⁻¹)	Time	H (mm)	H _r (mm)	h (mm)	s'	τ_y'	τ_y			τ_y'	τ_y	Lump model	τ_y
10	8.66	6.97	100	60.33	39.67	0.40	0.19	326.81			0.15	267.94	0	225.04
Cone geometry : PVC														
Number	Speed (mm.s ⁻¹)	Time	H (mm)	H _r (mm)	h (mm)	s'	τ_y'	τ_y			τ_y'	τ_y	Lump model	τ_y
10	8.20	7.23	150	59.31	90.69	0.60	0.11	294.59			0.10	183.76	0	172.28
Cylinder geometry : PVC														
Number	Speed (mm.s ⁻¹)	Time	H (mm)	H _r (mm)	h (mm)	s'	τ_y'	τ_y			τ_y'	τ_y	Lump model	τ_y
10	9.79	6.05	100	59.21	40.79	0.41	0.18	319.02			0.15	257.91	0	217.89

Table A. 39 Slump test for 20 mins 80:20 at relative density of 1.8 Kaolinite tailings and sand using the slump meter

Appendix A- Slump Data

RESULTS ON THE SLUMP TEST: (20mins 80:20 at 1.8)															
Relative density Density (Kg/m ³) g (m.s ⁻¹) 1.8 1800 9.81			Equations: $s' = \frac{h}{H}$ $\tau_y = \rho g H \tau_y'$				Approximate cylinder $\tau_y' = \frac{1}{2} - \frac{1}{2} \sqrt{s'}$			Vane τ_y 269.18		Lump model $\tau_y' = 0.5(1 - S')e^{\sqrt{3(1-S')}}$		Cylinder model $S' = 1 - 2\tau_y'(1 - \ln(2\tau_y'))$	
Without silicone spray :															
Cone geometry : Stainless steel															
Number	Speed (mm.s ⁻¹)	Time	H (mm)	H _r (mm)	h (mm)	s'	τ_y'	τ_y	Approx.cyl	τ_y'	Lump Model	τ_y	τ_y'	Cylinder model	τ_y
10	8.22	7.24	150	59.49	90.51	0.60	0.11	295.61	0.10	0.07	0	184.70	0.07	4.19E-07	184.70
Cylinder geometry : Stainless steel															
Number	Speed (mm.s ⁻¹)	Time	H (mm)	H _r (mm)	h (mm)	s'	τ_y'	τ_y		τ_y'	Lump model	τ_y	τ_y'	Cylinder model	τ_y
10	7.99	7.51	100	60.03	39.97	0.40	0.18	324.71	0.15	0.15	0	265.23	0.13	6.73E-07	223.11
Cone geometry : PVC															
Number	Speed (mm.s ⁻¹)	Time	H (mm)	H _r (mm)	h (mm)	s'	τ_y'	τ_y		τ_y'	Lump model	τ_y	τ_y'	Cylinder model	τ_y
10	7.69	7.56	150	58.16	91.84	0.61	0.11	288.08	0.10	0.07	0	177.82	0.06	1.50E-07	167.33
Cylinder geometry : PVC															
Number	Speed (mm.s ⁻¹)	Time	H (mm)	H _r (mm)	h (mm)	s'	τ_y'	τ_y		τ_y'	Lump model	τ_y	τ_y'	Cylinder model	τ_y
10	8.85	6.59	100	58.34	41.66	0.42	0.18	313.04	0.15	0.14	0	250.32	0.12	5.66E-07	212.45
With silicone spray :															
Cone geometry : Stainless steel															
Number	Speed (mm.s ⁻¹)	Time	H (mm)	H _r (mm)	h (mm)	s'	τ_y'	τ_y		τ_y'	Lump Model	τ_y	τ_y'	Cylinder model	τ_y
10	7.79	7.57	150	58.99	91.01	0.61	0.11	292.77	0.10	0.07	0	182.09	0.06	1.49E-07	170.89
Cylinder geometry : Stainless steel															
Number	Speed (mm.s ⁻¹)	Time	H (mm)	H _r (mm)	h (mm)	s'	τ_y'	τ_y		τ_y'	Lump Model	τ_y	τ_y'	Cylinder model	τ_y
10	8.87	7.12	100	63.12	36.88	0.37	0.20	346.72	0.15	0.17	0	294.21	0.14	2.74E-07	243.61
Cone geometry : PVC															
Number	Speed (mm.s ⁻¹)	Time	H (mm)	H _r (mm)	h (mm)	s'	τ_y'	τ_y		τ_y'	Lump Model	τ_y	τ_y'	Cylinder model	τ_y
10	8.58	7.33	150	62.91	87.09	0.58	0.12	315.23	0.10	0.08	0	203.19	0.07	2.14E-07	188.21
Cylinder geometry : PVC															
Number	Speed (mm.s ⁻¹)	Time	H (mm)	H _r (mm)	h (mm)	s'	τ_y'	τ_y		τ_y'	Lump Model	τ_y	τ_y'	Cylinder model	τ_y
10	8.79	6.78	100	59.6	40.4	0.40	0.18	321.72	0.15	0.15	0	261.37	0.12	3.09E-07	220.36

Table A. 40 Slump test for 5 mins 70:30 at relative density of 1.4 Kaolinite tailings and sand using the slump meter

Appendix A- Slump Data

RESULTS ON THE SLUMP TEST: (5mins 70:30 at 1.4)													
Relative density Density (Kg/m ³) g		1.4 1400 9.81		Equations: $s' = \frac{h}{H}$ $\tau_y = \rho g H \tau_y$		Approximate cylinder				Lump model		Cylinder model	
						$\tau_y' = \frac{1}{2} - \frac{1}{2} \sqrt{s'}$		Vane τ_y 38.10		$\tau_y' = 0.5(1-S')e^{\sqrt{3}(1-S')}$			
Without silicone spray :													
Cone geometry : Stainless steel													
Number	Speed (mm.s ⁻¹)	Time	H (mm)	H _r (mm)	h (mm)	s'	τ_y'	Approx.cyl τ_y	Calc.from vane τ_y'	τ_y	τ_y'	Cylinder model 4.23E-07	τ_y
10	5.01	4.12	150	20.64	129.36	0.86	0.04	73.49	0.02	31.82	0.02		31.61
Cylinder geometry : Stainless steel													
Number	Speed (mm.s ⁻¹)	Time	H (mm)	H _r (mm)	h (mm)	s'	τ_y'	τ_y		τ_y	τ_y'	Cylinder model 8.40E-08	τ_y
10	5.68	3.74	100	21.23	78.77	0.79	0.06	77.24	0.03	37.26	0.03		37.24
Cone geometry : PVC													
Number	Speed (mm.s ⁻¹)	Time	H (mm)	H _r (mm)	h (mm)	s'	τ_y'	τ_y		τ_y	τ_y'	Cylinder model 2.08E-08	τ_y
10	5.50	3.89	150	21.38	128.62	0.86	0.04	76.23	0.02	33.25	0.02		33.08
Cylinder geometry : PVC													
Number	Speed (mm.s ⁻¹)	Time	H (mm)	H _r (mm)	h (mm)	s'	τ_y'	τ_y		τ_y	τ_y'	Cylinder model 3.82E-07	τ_y
10	5.82	3.46	100	20.14	79.86	0.80	0.05	73.03	0.03	34.68	0.03		34.71
With silicone spray :													
Cone geometry : Stainless steel													
Number	Speed (mm.s ⁻¹)	Time	H (mm)	H _r (mm)	h (mm)	s'	τ_y'	τ_y		τ_y	τ_y'	Cylinder model 5.47E-07	τ_y
10	5.34	4.08	150	21.78	128.22	0.85	0.04	77.71	0.02	34.03	0.02		33.88
Cylinder geometry : Stainless steel													
Number	Speed (mm.s ⁻¹)	Time	H (mm)	H _r (mm)	h (mm)	s'	τ_y'	τ_y		τ_y	τ_y'	Cylinder model 7.66E-08	τ_y
10	5.17	4.12	100	21.32	78.68	0.79	0.06	77.59	0.03	37.47	0.03		37.46
Cone geometry : PVC													
Number	Speed (mm.s ⁻¹)	Time	H (mm)	H _r (mm)	h (mm)	s'	τ_y'	τ_y		τ_y	τ_y'	Cylinder model 2.47E-07	τ_y
10	5.06	4.18	150	21.17	128.83	0.86	0.04	75.45	0.02	32.84	0.02		32.66
Cylinder geometry : PVC													
Number	Speed (mm.s ⁻¹)	Time	H (mm)	H _r (mm)	h (mm)	s'	τ_y'	τ_y		τ_y	τ_y'	Cylinder model 6.63E-07	τ_y
10	5.25	3.87	100	20.31	79.69	0.80	0.05	73.69	0.03	35.08	0.03		35.10

Table A. 41 Slump test for 10 mins 70:30 at relative density of 1.4 Kaolinite tailings and sand using the slump meter

Appendix A- Slump Data

RESULTS ON THE SLUMP TEST: (10mins 70:30 at 1.4)													
Relative density Density (Kg/m ³) g (m.s ⁻¹)		Equations: $s' = \frac{1.4}{1400} \frac{h}{H} \tau_y = \rho g H \tau_y$		Approximate cylinder $\tau'_y = \frac{1}{2} - \frac{1}{2} \sqrt{s'}$				Vane τ_y 40.03		Lump model $\tau'_y = 0.5(1 - S') e^{\sqrt{3}(-S')}$		Cylinder model $S' = 1 - 2\tau'_y (1 - \ln(2\tau'_y))$	
Without silicone spray :													
Cone geometry : Stainless steel													
Number	Speed (mm.s ⁻¹)	H (mm)	H _r (mm)	h (mm)	s'	τ'_y	τ_y	Calc.from vane τ'_y	τ_y	τ'_y	Cylinder model	τ_y	
10	5.58	150	20.93	129.07	0.86	0.04	74.56	0.02	32.38	0.02	2.48E-07	32.18	
Cylinder geometry : Stainless steel													
Number	Speed (mm.s ⁻¹)	H (mm)	H _r (mm)	h (mm)	s'	τ'_y	τ_y	τ'_y	τ_y	τ'_y	Cylinder model	τ_y	
10	5.15	100	20.84	79.16	0.79	0.06	75.73	0.03	36.33	0.03	1.11E-08	36.33	
Cone geometry : PVC													
Number	Speed (mm.s ⁻¹)	H (mm)	H _r (mm)	h (mm)	s'	τ'_y	τ_y	τ'_y	τ_y	τ'_y	Cylinder model	τ_y	
10	6.35	150	22.34	127.66	0.85	0.04	79.80	0.02	35.13	0.02	2.29E-07	35.01	
Cylinder geometry : PVC													
Number	Speed (mm.s ⁻¹)	H (mm)	H _r (mm)	h (mm)	s'	τ'_y	τ_y	τ'_y	τ_y	τ'_y	Cylinder model	τ_y	
10	5.88	100	20.76	79.24	0.79	0.05	75.42	0.03	36.14	0.03	3.78E-07	36.14	
With silicone spray :													
Cone geometry : Stainless steel													
Number	Speed (mm.s ⁻¹)	H (mm)	H _r (mm)	h (mm)	s'	τ'_y	τ_y	τ'_y	τ_y	τ'_y	Cylinder model	τ_y	
10	5.65	150	21.82	128.18	0.85	0.04	77.86	0.02	34.11	0.02	5.56E-07	33.96	
Cylinder geometry : Stainless steel													
Number	Speed (mm.s ⁻¹)	H (mm)	H _r (mm)	h (mm)	s'	τ'_y	τ_y	τ'_y	τ_y	τ'_y	Cylinder model	τ_y	
10	5.30	100	21.53	78.47	0.78	0.06	78.40	0.03	37.98	0.03	1.87E-07	37.95	
Cone geometry : PVC													
Number	Speed (mm.s ⁻¹)	H (mm)	H _r (mm)	h (mm)	s'	τ'_y	τ_y	τ'_y	τ_y	τ'_y	Cylinder model	τ_y	
10	5.10	150	21.3	128.7	0.86	0.04	75.93	0.02	33.09	0.02	6.89E-07	32.92	
Cylinder geometry : PVC													
Number	Speed (mm.s ⁻¹)	H (mm)	H _r (mm)	h (mm)	s'	τ'_y	τ_y	τ'_y	τ_y	τ'_y	Cylinder model	τ_y	
10	5.76	100	21.13	78.87	0.79	0.06	76.85	0.03	37.02	0.03	6.19E-08	37.01	

Table A. 42 Slump test for 20 mins 70:30 at relative density of 1.4 Kaolinite tailings and sand using the slump meter

Appendix A- Slump Data

RESULTS ON THE SLUMP TEST: (20mins 70:30 at 1.4)										Approximate cylinder		Lump model		Cylinder model	
Equations: $s' = \frac{h}{H} \quad \tau_y = \rho g H \tau_y'$										$\tau_y' = \frac{1}{2} - \frac{1}{2} \sqrt{s'}$		$\tau_y' = 0.5(1 - S')e^{\sqrt{3}(-S')}$		$S' = 1 - 2\tau_y'(1 - \ln(2\tau_y'))$	
Without silicone spray :										Vane τ_y 46.11					
Cone geometry : Stainless steel										Approx.cyl τ_y		Lump Model		Cylinder model	
Number	Speed (mm.s ⁻¹)	Time	H (mm)	H _r (mm)	h (mm)	s'				τ_y'	τ_y	τ_y'	τ_y	τ_y'	τ_y
10	5.33	3.76	150	20.03	129.97	0.87				0.03	71.24	0.02	30.67	0.01	30.41
Cylinder geometry : Stainless steel										τ_y		Lump model		Cylinder model	
Number	Speed (mm.s ⁻¹)	Time	H (mm)	H _r (mm)	h (mm)	s'				τ_y'	τ_y	τ_y'	τ_y	τ_y'	τ_y
10	5.64	3.36	100	18.94	81.06	0.81				0.05	68.44	0.03	31.94	0.02	31.98
Cone geometry : PVC										τ_y		Lump model		Cylinder model	
Number	Speed (mm.s ⁻¹)	Time	H (mm)	H _r (mm)	h (mm)	s'				τ_y'	τ_y	τ_y'	τ_y	τ_y'	τ_y
10	5.20	3.79	150	19.69	130.31	0.87				0.03	69.98	0.02	30.03	0.01	29.75
Cylinder geometry : PVC										τ_y		Lump model		Cylinder model	
Number	Speed (mm.s ⁻¹)	Time	H (mm)	H _r (mm)	h (mm)	s'				τ_y'	τ_y	τ_y'	τ_y	τ_y'	τ_y
10	5.69	3.77	100	21.45	78.55	0.79				0.06	78.09	0.03	37.79	0.03	37.76
With silicone spray :										Approx.cyl τ_y					
Cone geometry : Stainless steel										Calc.from vane		Lump Model		Cylinder model	
Number	Speed (mm.s ⁻¹)	Time	H (mm)	H _r (mm)	h (mm)	s'				τ_y'	τ_y	τ_y'	τ_y	τ_y'	τ_y
10	5.68	3.64	150	20.67	129.33	0.86				0.04	73.60	0.02	31.88	0.02	31.67
Cylinder geometry : Stinless steel										τ_y		Lump Model		Cylinder model	
Number	Speed (mm.s ⁻¹)	Time	H (mm)	H _r (mm)	h (mm)	s'				τ_y'	τ_y	τ_y'	τ_y	τ_y'	τ_y
10	5.32	3.86	100	20.52	79.48	0.79				0.05	74.50	0.03	35.57	0.03	35.58
Cone geometry : PVC										τ_y		Lump Model		Cylinder model	
Number	Speed (mm.s ⁻¹)	Time	H (mm)	H _r (mm)	h (mm)	s'				τ_y'	τ_y	τ_y'	τ_y	τ_y'	τ_y
10	5.25	3.83	150	20.11	129.89	0.87				0.03	71.53	0.02	30.82	0.01	30.57
Cylinder geometry : PVC										τ_y		Lump Model		Cylinder model	
Number	Speed (mm.s ⁻¹)	Time	H (mm)	H _r (mm)	h (mm)	s'				τ_y'	τ_y	τ_y'	τ_y	τ_y'	τ_y
10	5.60	3.86	100	21.63	78.37	0.78				0.06	78.79	0.03	38.22	0.03	38.19

Table A. 43 Slump test for 5 mins 70:30 at relative density of 1.5 Kaolinite tailings and sand using the slump meter

Appendix A- Slump Data

RESULTS ON THE SLUMP TEST: (5mins 70:30 at 1.5)										Approximate cylinder		Lump model		Cylinder model			
Relative density Density (Kg/m ³) g (m.s ⁻³)		Equations: $s' = \frac{1.5}{1500} \frac{h}{H} \tau_y = \rho g H \tau_y$		$\tau_y = \frac{1}{2} - \frac{1}{2} \sqrt{s'}$		Vane τ_y 58.81		$\tau_y' = 0.5(1 - S') e^{\sqrt{3}(-s')}$		$S' = 1 - 2\tau_y' (1 - \ln(2\tau_y'))$							
Without silicone spray :										Approx.cyl				Lump Model		Cylinder model	
Cone geometry : Stainless steel		H (mm)		H _r (mm)		h (mm)		s'		τ_y'				τ_y		τ_y	
10	7.11	5	150	35.57	114.43	0.76	0.06	139.69	0.03	0				69.82		69.51	
Cylinder geometry : Stainless steel		H (mm)		H _r (mm)		h (mm)		s'		τ_y'				τ_y		τ_y	
10	7.78	4.53	100	35.23	64.77	0.65	0.10	143.62	0.04	0				84.42		80.77	
Cone geometry : PVC		H (mm)		H _r (mm)		h (mm)		s'		τ_y'				τ_y		τ_y	
10	7.33	4.93	150	36.16	113.84	0.76	0.06	142.18	0.03	0				71.46		71.09	
Cylinder geometry : PVC		H (mm)		H _r (mm)		h (mm)		s'		τ_y'				τ_y		τ_y	
10	7.35	4.52	100	33.24	66.76	0.67	0.09	134.59	0.04	0				76.95		74.26	
With silicone spray :										Approx.cyl				Lump Model		Cylinder model	
Cone geometry : Stainless steel		H (mm)		H _r (mm)		h (mm)		s'		τ_y'				τ_y		τ_y	
10	7.95	4.57	150	36.32	113.68	0.76	0.06	142.86	0.03	0				71.91		71.52	
Cylinder geometry : Stainless steel		H (mm)		H _r (mm)		h (mm)		s'		τ_y'				τ_y		τ_y	
10	8.13	4.32	100	35.12	64.88	0.65	0.10	143.12	0.04	0				83.99		80.40	
Cone geometry : PVC		H (mm)		H _r (mm)		h (mm)		s'		τ_y'				τ_y		τ_y	
10	7.49	4.79	150	35.86	114.14	0.76	0.06	140.92	0.03	0				70.62		70.29	
Cylinder geometry : PVC		H (mm)		H _r (mm)		h (mm)		s'		τ_y'				τ_y		τ_y	
10	7.34	4.57	100	33.56	66.44	0.66	0.09	136.03	0.04	0				78.12		75.29	

Table A. 44 Slump test for 10 mins 70:30 at relative density of 1.5 Kaolinite tailings and sand using the slump meter

Appendix A- Slump Data

RESULTS ON THE SLUMP TEST: (10mins 70:30 at 1.5)													
Relative density Density ρ (Kg/m^3) (m.s^{-1})		1.5 1500 9.81		Equations: $s' = \frac{h}{H}$ $\tau_y = \rho g H \tau'_y$		Approximate cylinder $\tau'_y = \frac{1}{2} - \frac{1}{2} \sqrt{s'}$			Lump model $\tau'_y = 0.5(1 - S')e^{\sqrt{3}(-s')}$			Cylinder model $S = 1 - 2\tau'_y(1 - \ln(2\tau'_y))$	
Without silicone spray :													
Cone geometry : Stainless steel													
Number	Speed (mm.s ⁻¹)	Time	H (mm)	H _r (mm)	h (mm)	s'	τ'_y	Approx.cyl τ_y	Calc.from vane τ'_y	Lump Model τ_y	τ'_y	Cylinder model τ_y	τ_y
10	9.23	4	150	36.91	113.09	0.75	0.07	145.35	0.03	0	0.03	4.21E-07	73.11
Cylinder geometry : Stainless steel													
Number	Speed (mm.s ⁻¹)	Time	H (mm)	H _r (mm)	h (mm)	s'	τ'_y	τ_y		Lump model τ_y	τ'_y	Cylinder model τ_y	τ_y
10	7.26	4.9	100	35.57	64.43	0.64	0.10	145.18	0.05	0	0.06	4.98E-07	81.90
Cone geometry : PVC													
Number	Speed (mm.s ⁻¹)	Time	H (mm)	H _r (mm)	h (mm)	s'	τ'_y	τ_y		Lump model τ_y	τ'_y	Cylinder model τ_y	τ_y
10	9.44	3.9	150	36.81	113.19	0.75	0.07	144.93	0.03	0	0.03	2.44E-07	72.84
Cylinder geometry : PVC													
Number	Speed (mm.s ⁻¹)	Time	H (mm)	H _r (mm)	h (mm)	s'	τ'_y	τ_y		Lump model τ_y	τ'_y	Cylinder model τ_y	τ_y
10	7.50	4.3	100	32.23	67.77	0.68	0.09	130.06	0.05	0	0.05	7.03E-07	71.05
With silicone spray :													
Cone geometry : Stainless steel													
Number	Speed (mm.s ⁻¹)	Time	H (mm)	H _r (mm)	h (mm)	s'	τ'_y	Approx.cyl τ_y	Calc.from vane τ'_y	Lump Model τ_y	τ'_y	Cylinder model τ_y	τ_y
10	8.47	4.3	150	36.43	113.57	0.76	0.06	143.32	0.03	0	0.03	4.14E-07	71.82
Cylinder geometry : Stainless steel													
Number	Speed (mm.s ⁻¹)	Time	H (mm)	H _r (mm)	h (mm)	s'	τ'_y	τ_y		Lump Model τ_y	τ'_y	Cylinder model τ_y	τ_y
10	7.63	4.6	100	35.11	64.89	0.65	0.10	143.07	0.05	0	0.06	5.36E-07	80.37
Cone geometry : PVC													
Number	Speed (mm.s ⁻¹)	Time	H (mm)	H _r (mm)	h (mm)	s'	τ'_y	τ_y		Lump Model τ_y	τ'_y	Cylinder model τ_y	τ_y
10	8.03	4.52	150	36.29	113.71	0.76	0.06	142.73	0.03	0	0.03	1.25E-07	71.44
Cylinder geometry : PVC													
Number	Speed (mm.s ⁻¹)	Time	H (mm)	H _r (mm)	h (mm)	s'	τ'_y	τ_y		Lump Model τ_y	τ'_y	Cylinder model τ_y	τ_y
10	7.74	4.1	100	31.73	68.27	0.68	0.09	127.83	0.05	0	0.05	2.19E-07	69.48

Table A. 45 Slump test for 20 mins 70:30 at relative density of 1.5 Kaolinite tailings and sand using the slump meter

Appendix A- Slump Data

RESULTS ON THE SLUMP TEST: (20mins 70:30 at 1.5)															
Relative density Density (Kg/m ³) g (m.s ⁻¹)		1.5 1500 9.81		Equations: $s' = \frac{h}{H} \tau_y = \rho g H \tau_y$		Approximate cylinder $\tau_y' = \frac{1}{2} - \frac{1}{2} \sqrt{s'}$				Vane τ_y 87.24		Lump model $\tau_y' = 0.5(1 - S') e^{\sqrt{3}(-s')}$		Cylinder model $S = 1 - 2\tau_y'(1 - \ln(2\tau_y'))$	
Without silicone spray :															
Cone geometry : Stainless steel															
Number	Speed (mm.s ⁻¹)	Time	H (mm)	H _r (mm)	h (mm)	s'	τ_y'	Approx.cyl τ_y	Calc. from vane τ_y'	τ_y'	Lump Model	τ_y	τ_y'	Cylinder model	τ_y
10	7.77	4.76	150	36.98	113.02	0.75	0.07	145.65	0.04	0.03	0	73.78	0.03	2.05E-08	73.30
Cylinder geometry : Stainless steel															
Number	Speed (mm.s ⁻¹)	Time	H (mm)	H _r (mm)	h (mm)	s'	τ_y'	τ_y		τ_y'	Lump model	τ_y	τ_y'	Cylinder model	τ_y
10	7.79	4.71	100	36.71	63.29	0.63	0.10	150.42	0.06	0.06	0	90.25	0.06	4.41E-07	85.76
Cone geometry : PVC															
Number	Speed (mm.s ⁻¹)	Time	H (mm)	H _r (mm)	h (mm)	s'	τ_y'	τ_y		τ_y'	Lump model	τ_y	τ_y'	Cylinder model	τ_y
10	7.88	4.78	150	37.66	112.34	0.75	0.07	148.54	0.04	0.03	0	75.73	0.03	2.01E-07	75.16
Cylinder geometry : PVC															
Number	Speed (mm.s ⁻¹)	Time	H (mm)	H _r (mm)	h (mm)	s'	τ_y'	τ_y		τ_y'	Lump model	τ_y	τ_y'	Cylinder model	τ_y
10	7.22	4.8	100	34.66	65.34	0.65	0.10	141.02	0.06	0.06	0	82.24	0.05	2.60E-07	78.88
With silicone spray :															
Cone geometry : Stainless steel								Approx.cyl	Calc. from vane						
Number	Speed (mm.s ⁻¹)	Time	H (mm)	H _r (mm)	h (mm)	s'	τ_y'	τ_y		τ_y'	Lump Model	τ_y	τ_y'	Cylinder model	τ_y
10	8.36	4.49	150	37.55	112.45	0.75	0.07	148.07	0.04	0.03	0	75.41	0.03	1.67E-07	74.85
Cylinder geometry : Stainless steel															
Number	Speed (mm.s ⁻¹)	Time	H (mm)	H _r (mm)	h (mm)	s'	τ_y'	τ_y		τ_y'	Lump Model	τ_y	τ_y'	Cylinder model	τ_y
10	8.81	4.49	100	39.57	60.43	0.60	0.11	163.80	0.06	0.07	0	102.22	0.07	3.57E-07	95.82
Cone geometry : PVC															
Number	Speed (mm.s ⁻¹)	Time	H (mm)	H _r (mm)	h (mm)	s'	τ_y'	τ_y		τ_y'	Lump Model	τ_y	τ_y'	Cylinder model	τ_y
10	7.99	4.58	150	36.61	113.39	0.76	0.07	144.08	0.04	0.03	0	72.73	0.03	6.88E-07	72.30
Cylinder geometry : PVC															
Number	Speed (mm.s ⁻¹)	Time	H (mm)	H _r (mm)	h (mm)	s'	τ_y'	τ_y		τ_y'	Lump Model	τ_y	τ_y'	Cylinder model	τ_y
10	7.42	4.64	100	34.41	65.59	0.66	0.10	139.88	0.06	0.06	0	81.29	0.05	2.08E-07	78.06

Table A. 46 Slump test for 5 mins 70:30 at relative density of 1.6 Kaolinite tailings and sand using the slump meter

Appendix A- Slump Data

RESULTS ON THE SLUMP TEST: (5mins 70:30 at 1.6)																
Relative density Density (Kg/m ³) g (m.s ⁻²)		1.6 1600 9.81		Equations: $s' = \frac{h}{H}$ $\tau_y = \rho g H \tau'_y$		Approximate cylinder $\tau'_y = \frac{1}{2} - \frac{1}{2} \sqrt{s'}$					Lump model $\tau'_y = 0.5(1 - S')e^{\sqrt{3}(-s')}$		Cylinder model $S' = 1 - 2\tau'_y(1 - \ln(2\tau'_y))$			
						Vane τ_y 144.12										
						Calc. from vane τ'_y 0.06										
<i>Without silicone spray :</i>																
Cone geometry : Stainless steel								Approx.cyl τ_y								
Number	Speed (mm.s ⁻¹)	Time	H (mm)	H _r (mm)	h (mm)	s'	τ'_y	τ_y	τ'_y	Lump Model	τ_y	τ'_y	Cylinder model	τ_y		
10	8.11	6.47	150	52.48	97.52	0.65	0.10	228.01	0.06	0	133.57	0.05	7.99E-07	127.93		
Cylinder geometry : Stainless steel																
Number	Speed (mm.s ⁻¹)	Time	H (mm)	H _r (mm)	h (mm)	s'	τ'_y	τ_y	τ'_y	Lump model	τ_y	τ'_y	Cylinder model	τ_y		
10	8.39	6.23	100	52.29	47.71	0.48	0.15	242.72	0.09	0	179.59	0.10	6.26E-07	157.45		
Cone geometry : PVC																
Number	Speed (mm.s ⁻¹)	Time	H (mm)	H _r (mm)	h (mm)	s'	τ'_y	τ_y	τ'_y	Lump model	τ_y	τ'_y	Cylinder model	τ_y		
10	8.19	6.28	150	51.46	98.54	0.66	0.09	223.06	0.06	0	141.26	0.05	4.85E-07	124.35		
Cylinder geometry : PVC																
Number	Speed (mm.s ⁻¹)	Time	H (mm)	H _r (mm)	h (mm)	s'	τ'_y	τ_y	τ'_y	Lump model	τ_y	τ'_y	Cylinder model	τ_y		
10	8.31	6.04	100	50.17	49.83	0.50	0.15	230.81	0.09	0	166.10	0.09	4.63E-07	147.30		
<i>With silicone spray :</i>																
Cone geometry : Stainless steel								Approx.cyl τ_y								
Number	Speed (mm.s ⁻¹)	Time	H (mm)	H _r (mm)	h (mm)	s'	τ'_y	τ_y	τ'_y	Lump Model	τ_y	τ'_y	Cylinder model	τ_y		
10	8.78	5.96	150	52.34	97.66	0.65	0.10	227.33	0.06	0	133.00	0.05	3.15E-07	127.44		
Cylinder geometry : Stainless steel																
Number	Speed (mm.s ⁻¹)	Time	H (mm)	H _r (mm)	h (mm)	s'	τ'_y	τ_y	τ'_y	Lump Model	τ_y	τ'_y	Cylinder model	τ_y		
10	8.69	6.34	100	55.08	44.92	0.45	0.16	258.81	0.09	0	198.54	0.11	5.93E-07	171.46		
Cone geometry : PVC																
Number	Speed (mm.s ⁻¹)	Time	H (mm)	H _r (mm)	h (mm)	s'	τ'_y	τ_y	τ'_y	Lump Model	τ_y	τ'_y	Cylinder model	τ_y		
10	8.45	6.27	150	52.98	97.02	0.65	0.10	230.45	0.06	0	135.62	0.06	7.40E-07	129.71		
Cylinder geometry : PVC																
Number	Speed (mm.s ⁻¹)	Time	H (mm)	H _r (mm)	h (mm)	s'	τ'_y	τ_y	τ'_y	Lump Model	τ_y	τ'_y	Cylinder model	τ_y		
10	8.78	6.08	100	53.41	46.59	0.47	0.16	249.12	0.09	0	187.03	0.10	7.01E-07	162.99		

Table A. 47 Slump test for 10 mins 70:30 at relative density of 1.6 Kaolinite tailings and sand using the slump meter

Appendix A- Slump Data

RESULTS ON THE SLUMP TEST: (20mins 70:30 at 1.6)									
Equations:									
$S' = \frac{h}{H} \tau_y = \rho g H \tau_y$									
Relative density 1.6 Density (Kg/m ³) 1600 g (m.s ⁻¹) 9.81									
Without silicone spray :									
Cone geometry : Stainless steel									
Number	Speed (mm.s ⁻¹)	Time	H (mm)	H _r (mm)	h (mm)	s'	Approximate cylinder		
10	9.69	5.82	150	56.38	93.62	0.62	$\tau_y' = \frac{1}{2} - \frac{1}{2} \sqrt{s'}$	τ_y	$S' = 1 - 2\tau_y' (1 - \ln(2\tau_y'))$
Cylinder geometry : Stainless steel									
Number	Speed (mm.s ⁻¹)	Time	H (mm)	H _r (mm)	h (mm)	s'	τ_y'	τ_y	τ_y
10	9.85	5.65	100	55.63	44.37	0.44	0.10	247.19	0.06
Cone geometry : PVC									
Number	Speed (mm.s ⁻¹)	Time	H (mm)	H _r (mm)	h (mm)	s'	τ_y'	τ_y	τ_y
10	8.90	6.04	150	53.78	96.22	0.64	0.17	262.04	0.11
Cylinder geometry : PVC									
Number	Speed (mm.s ⁻¹)	Time	H (mm)	H _r (mm)	h (mm)	s'	τ_y'	τ_y	τ_y
10	9.65	5.56	100	53.64	46.36	0.46	0.10	234.36	0.06
With silicone spray :									
Cone geometry : Stainless steel									
Number	Speed (mm.s ⁻¹)	Time	H (mm)	H _r (mm)	h (mm)	s'	τ_y'	τ_y	τ_y
10	9.30	6.21	150	57.73	92.27	0.62	0.16	250.44	0.12
Cylinder geometry : Stainless steel									
Number	Speed (mm.s ⁻¹)	Time	H (mm)	H _r (mm)	h (mm)	s'	τ_y'	τ_y	τ_y
10	9.29	6.11	100	56.76	43.24	0.43	0.11	253.92	0.07
Cone geometry : PVC									
Number	Speed (mm.s ⁻¹)	Time	H (mm)	H _r (mm)	h (mm)	s'	τ_y'	τ_y	τ_y
10	9.27	5.98	150	55.41	94.59	0.63	0.17	268.74	0.13
Cylinder geometry : PVC									
Number	Speed (mm.s ⁻¹)	Time	H (mm)	H _r (mm)	h (mm)	s'	τ_y'	τ_y	τ_y
10	9.44	5.78	100	54.57	45.43	0.45	0.08	242.38	0.06
Cylinder geometry : Stainless steel									
Number	Speed (mm.s ⁻¹)	Time	H (mm)	H _r (mm)	h (mm)	s'	τ_y'	τ_y	τ_y
10	9.44	5.78	100	54.57	45.43	0.45	0.11	194.98	0.11

APPENDIX B – HAND – HELD CYLINDER (DATA)

Table B. 1 Slump test for 14 % and 16 % kaolin using the hand-held cylinder

THE 50 CENTS HAND-HELD SLUMP TEST (14%KAOLIN)									
Relative density Density $\frac{g}{g}$	1.2 1200 9.81 $\frac{(Kg/m^3)}{(m.s^{-3})}$	Equations:		Approximate cylinder		Lump model		Cylinder model	
		$s' = \frac{h}{H}$	$\tau_y = \rho g H \tau'_y$	$\tau'_y = \frac{1}{2} - \frac{1}{2} \sqrt{s'}$		Vane τ_y 33.68	$\tau_y' = 0.5(1 - S')e^{\sqrt{3}(-s')}$	$S' = 1 - 2\tau_y'(1 - \ln(2\tau_y'))$	
				Approx.cyl τ_y	Calc.from vane τ_y'				Lump Model τ_y
Without silicone spray :									
Speed (mm.s ⁻¹)	Time	H _r (mm)	h (mm)	τ_y'	τ_y	τ_y'	τ_y	τ_y'	τ_y
5.29	7.2	75	38.09	0.15	131.76	0.04	0	0.10	84.50
3.07	13.78	75	42.3	0.17	149.96	0.04	0	0.11	100.33
1.77	21.5	75	38.05	0.15	131.60	0.04	0	0.10	84.35
With silicone spray :									
Speed (mm.s ⁻¹)	Time	H _r (mm)	h (mm)	τ_y'	τ_y	τ_y'	τ_y	τ_y'	τ_y
3.71	10.66	75	39.59	0.16	138.12	0.04	0	0.10	89.94
6.60	6.13	75	40.47	0.16	141.91	0.04	0	0.11	93.23
6.79	5.35	75	36.3	0.14	124.34	0.04	0	0.09	78.27

THE 50 CENTS HAND-HELD SLUMP TEST (KAOLIN 16%)									
Relative density Density $\frac{g}{g}$	1.201 1201 9.81 $\frac{(Kg/m^3)}{(m.s^{-3})}$	Equations:		Approximate cylinder		Lump model		Cylinder model	
		$s' = \frac{h}{H}$	$\tau_y = \rho g H \tau'_y$	$\tau'_y = \frac{1}{2} - \frac{1}{2} \sqrt{s'}$		Vane τ_y 48.32	$\tau_y' = 0.5(1 - S')e^{\sqrt{3}(-s')}$	$S' = 1 - 2\tau_y'(1 - \ln(2\tau_y'))$	
				Approx.cyl τ_y	Calc.from vane τ_y'				Lump Model τ_y
Without silicone spray :									
Speed (mm.s ⁻¹)	Time	H _r (mm)	h (mm)	τ_y'	τ_y	τ_y'	τ_y	τ_y'	τ_y
6.70	7.24	75	48.5	0.20	179.04	0.05	0	0.14	127.20
7.62	6.08	75	46.3	0.19	168.37	0.05	0	0.13	117.12
16.93	2.83	75	47.9	0.20	176.09	0.05	0	0.14	124.38
With silicone spray :									
Speed (mm.s ⁻¹)	Time	H _r (mm)	h (mm)	τ_y'	τ_y	τ_y'	τ_y	τ_y'	τ_y
6.66	7.21	75	48	0.20	176.58	0.05	0	0.14	124.85
9.64	4.94	75	47.6	0.20	174.63	0.05	0	0.14	123.00
14.80	3.31	75	49	0.21	181.53	0.05	0	0.15	129.58

Appendix B – Hand-held Cylinder Data

Table B. 2 Slump test for 18 % and 20 % kaolin using the hand-held cylinder

THE 50 CENTS HAND-HELD SLUMP TEST (18%KAOLIN)													
Relative density Density g	1.269 1269 9.81	Equations: $s' = \frac{h}{H} \tau_y = \rho g H \tau_y$											
		Without silicone spray :		H (mm)	H _r (mm)	h (mm)	s'	Approximate cylinder $\tau_y' = \frac{1}{2} - \frac{1}{2} \sqrt{s'}$					
		Speed (mm.s ⁻¹)	Time	75	57.23	17.77	0.24	τ_y'	Approx.cyl				
			8.12	75	58.48	16.52	0.22	0.26	τ_y				
		5.18	75	58.8	16.2	0.22	0.27	τ_y					
With silicone spray :													
		Speed (mm.s ⁻¹)	Time	75	58	17	0.23	τ_y'	τ_y				
			8.89	75	57.46	17.54	0.23	0.26	τ_y				
		5.89	75	56.8	18.2	0.24	0.25	τ_y	τ_y				
Lump model													
		Lump Model	τ_y'	0	243.80	0	243.80	τ_y	Cylinder model				
										Cylinder model	τ_y'	τ_y	Cylinder model
		Lump Model	τ_y'	0	238.53	0	238.53	τ_y	Cylinder model				
										Cylinder model	τ_y'	τ_y	Cylinder model
		Lump Model	τ_y'	0	232.23	0	232.23	τ_y	Cylinder model				
										Cylinder model	τ_y'	τ_y	Cylinder model
		Lump Model	τ_y'	0	4.95E-07	0	4.95E-07	τ_y	Cylinder model				
										Cylinder model	τ_y'	τ_y	Cylinder model
		Lump Model	τ_y'	0	5.91E-07	0	5.91E-07	τ_y	Cylinder model				
										Cylinder model	τ_y'	τ_y	Cylinder model
		Lump Model	τ_y'	0	5.83E-07	0	5.83E-07	τ_y	Cylinder model				
										Cylinder model	τ_y'	τ_y	Cylinder model
		Lump Model	τ_y'	0	4.92E-07	0	4.92E-07	τ_y	Cylinder model				
										Cylinder model	τ_y'	τ_y	Cylinder model
		Lump Model	τ_y'	0	8.42E-07	0	8.42E-07	τ_y	Cylinder model				
										Cylinder model	τ_y'	τ_y	Cylinder model
		Lump Model	τ_y'	0	5.00E-07	0	5.00E-07	τ_y	Cylinder model				
										Cylinder model	τ_y'	τ_y	Cylinder model
		Lump Model	τ_y'	0	251.77	0	251.77	τ_y	Cylinder model				
										Cylinder model	τ_y'	τ_y	Cylinder model
		Lump Model	τ_y'	0	248.55	0	248.55	τ_y	Cylinder model				
										Cylinder model	τ_y'	τ_y	Cylinder model
		Lump Model	τ_y'	0	236.32	0	236.32	τ_y	Cylinder model				
										Cylinder model	τ_y'	τ_y	Cylinder model
		Lump Model	τ_y'	0	5.59E-07	0	5.59E-07	τ_y	Cylinder model				
										Cylinder model	τ_y'	τ_y	Cylinder model
		Lump Model	τ_y'	0	184.99	0	184.99	τ_y	Cylinder model				
										Cylinder model	τ_y'	τ_y	Cylinder model
		Lump Model	τ_y'	0	193.60	0	193.60	τ_y	Cylinder model				
										Cylinder model	τ_y'	τ_y	Cylinder model
		Lump Model	τ_y'	0	195.88	0	195.88	τ_y	Cylinder model				
										Cylinder model	τ_y'	τ_y	Cylinder model
		Lump Model	τ_y'	0	182.12	0	182.12	τ_y	Cylinder model				
										Cylinder model	τ_y'	τ_y	Cylinder model
		Lump Model	τ_y'	0	186.54	0	186.54	τ_y	Cylinder model				
										Cylinder model	τ_y'	τ_y	Cylinder model
		Lump Model	τ_y'	0	181.2	0	181.2	τ_y	Cylinder model				
										Cylinder model	τ_y'	τ_y	Cylinder model
		Lump Model	τ_y'	0	182.12	0	182.12	τ_y	Cylinder model				
										Cylinder model	τ_y'	τ_y	Cylinder model
		Lump Model	τ_y'	0	186.54	0	186.54	τ_y	Cylinder model				
										Cylinder model	τ_y'	τ_y	Cylinder model
		Lump Model	τ_y'	0	181.2	0	181.2	τ_y	Cylinder model				
										Cylinder model	τ_y'	τ_y	Cylinder model
		Lump Model	τ_y'	0	186.54	0	186.54	τ_y	Cylinder model				
										Cylinder model	τ_y'	τ_y	Cylinder model
		Lump Model	τ_y'	0	182.12	0	182.12	τ_y	Cylinder model				
										Cylinder model	τ_y'	τ_y	Cylinder model
		Lump Model	τ_y'	0	186.54	0	186.54	τ_y	Cylinder model				
										Cylinder model	τ_y'	τ_y	Cylinder model
		Lump Model	τ_y'	0	181.2	0	181.2	τ_y	Cylinder model				
										Cylinder model	τ_y'	τ_y	Cylinder model
		Lump Model	τ_y'	0	186.54	0	186.54	τ_y	Cylinder model				
										Cylinder model	τ_y'	τ_y	Cylinder model
		Lump Model	τ_y'	0	182.12	0	182.12	τ_y	Cylinder model				
										Cylinder model	τ_y'	τ_y	Cylinder model
		Lump Model	τ_y'	0	186.54	0	186.54	τ_y	Cylinder model				
										Cylinder model	τ_y'	τ_y	Cylinder model
		Lump Model	τ_y'	0	181.2	0	181.2	τ_y	Cylinder model				
										Cylinder model	τ_y'	τ_y	Cylinder model
		Lump Model	τ_y'	0	186.54	0	186.54	τ_y	Cylinder model				
										Cylinder model	τ_y'	τ_y	Cylinder model
		Lump Model	τ_y'	0	182.12	0	182.12	τ_y	Cylinder model				
										Cylinder model	τ_y'	τ_y	Cylinder model
		Lump Model	τ_y'	0	186.54	0	186.54	τ_y	Cylinder model				
										Cylinder model	τ_y'	τ_y	Cylinder model
		Lump Model	τ_y'	0	181.2	0	181.2	τ_y	Cylinder model				
										Cylinder model	τ_y'	τ_y	Cylinder model
		Lump Model	τ_y'	0	186.54	0	186.54	τ_y	Cylinder model				
										Cylinder model	τ_y'	τ_y	Cylinder model
		Lump Model	τ_y'	0	182.12	0	182.12	τ_y	Cylinder model				
										Cylinder model	τ_y'	τ_y	Cylinder model
		Lump Model	τ_y'	0	186.54	0	186.54	τ_y	Cylinder model				
										Cylinder model	τ_y'	τ_y	Cylinder model
		Lump Model	τ_y'	0	181.2	0	181.2	τ_y	Cylinder model				
										Cylinder model	τ_y'	τ_y	Cylinder model
		Lump Model	τ_y'	0	186.54	0	186.54	τ_y	Cylinder model				
										Cylinder model	τ_y'	τ_y	Cylinder model
		Lump Model	τ_y'	0	182.12	0	182.12	τ_y	Cylinder model				
										Cylinder model	τ_y'	τ_y	Cylinder model
		Lump Model	τ_y'	0	186.54	0	186.54	τ_y	Cylinder model				
										Cylinder model	τ_y'	τ_y	Cylinder model
		Lump Model	τ_y'	0	181.2	0	181.2	τ_y	Cylinder model				
										Cylinder model	τ_y'	τ_y	Cylinder model
		Lump Model	τ_y'	0	186.54	0	186.54	τ_y	Cylinder model				
										Cylinder model	τ_y'	τ_y	Cylinder model
		Lump Model	τ_y'	0	182.12	0	182.12	τ_y	Cylinder model				
										Cylinder model	τ_y'	τ_y	Cylinder model
		Lump Model	τ_y'	0	186.54	0	186.54	τ_y	Cylinder model				
										Cylinder model	τ_y'	τ_y	Cylinder model
		Lump Model	τ_y'	0	181.2	0	181.2	τ_y	Cylinder model				
										Cylinder model	τ_y'	τ_y	Cylinder model
		Lump Model	τ_y'	0	186.54	0	186.54	τ_y	Cylinder model				
										Cylinder model	τ_y'	τ_y	Cylinder model
		Lump Model	τ_y'	0	182.12	0	182.12	τ_y	Cylinder model				
										Cylinder model	τ_y'	τ_y	Cylinder model
		Lump Model	τ_y'	0	186.54	0	186.54	τ_y	Cylinder model				
										Cylinder model	τ_y'	τ_y	Cylinder model
		Lump Model	τ_y'	0	181.2	0	181.2	τ_y	Cylinder model				
										Cylinder model	τ_y'	τ_y	Cylinder model
		Lump Model	τ_y'	0	186.54	0	186.54	τ_y	Cylinder model				
										Cylinder model	τ_y'	τ_y	Cylinder model
		Lump Model	τ_y'	0	182.12	0	182.12	τ_y	Cylinder model				
										Cylinder model	τ_y'	τ_y	Cylinder model
		Lump Model	τ_y'	0	186.54	0	186.54	τ_y	Cylinder model				

Table B. 3 Slump test for 14 % and 16 % kaolinite tailings using the hand-held cylinder

THE 50 CENTS HAND-HELD SLUMP TEST (20%KAOLIN)														
Relative density Density ρ (Kg/m ³) (m.s ⁻¹)	1.31 1310 9.81	Equations: $s' = \frac{h}{H} \tau_y = \rho g H \tau_y$												
		Without silicone spray :		Approx.cyl		Vane		$\tau_y' = 0.5(1 - S') e^{\sqrt{3}(-s')}$						
Speed (mm.s ⁻¹)	Time	H (mm)	H _r (mm)	h (mm)	s'	τ_y'	τ_y	Calc.from vane	$S = 1 - 2\tau_y'(1 - \ln(2\tau_y'))$					
										Cylinder model	τ_y'	Cylinder model	τ_y	
														Cylinder model
3.85	16.6	75	63.94	11.06	0.15	0.31	296.85	0.14	0.33	318.24	0.25	4.36E-07	245.15	
6.14	10.64	75	65.29	9.71	0.13	0.32	308.52	0.14	0.35	0	335.25	0.27	8.07E-07	258.52
9.62	6.5	75	62.52	12.48	0.17	0.30	285.33	0.14	0.31	0	301.13	0.24	3.16E-07	232.17
With silicone spray :														
Speed (mm.s ⁻¹)	Time	H (mm)	H _r (mm)	h (mm)	s'	τ_y'	τ_y	Calc.from vane	$S = 1 - 2\tau_y'(1 - \ln(2\tau_y'))$					
										Cylinder model	τ_y'	Cylinder model	τ_y	
														Cylinder model
3.56	18.2	75	64.71	10.29	0.14	0.31	303.41	0.14	0.34	327.85	0.26	2.59E-07	252.64	
6.25	10.51	75	65.69	9.31	0.12	0.32	312.12	0.14	0.35	0	340.43	0.27	4.15E-07	262.70
10.63	6	75	61.2	11.2	0.15	0.31	295.69	0.14	0.33	0	316.52	0.25	5.89E-07	243.83

Appendix B – Hand-held Cylinder Data

THE 50 CENTS HAND-HELD SLUMP TEST (KAOLINITE TAILING 14%)									
Relative density ρ (Kg/m^3) (m.s^{-3})	1.206 1206 9.81	Equations:		$s' = \frac{h}{H} \tau_y = \rho g H \tau_y$	$\tau_y' = \frac{1}{2} - \frac{1}{2} \sqrt{s'}$	Vane τ_y 50.52	$\tau_y' = 0.5(1 - S') e^{\sqrt{3}(-S')}$		Cylinder model $S = 1 - 2\tau_y'(1 - \ln(2\tau_y'))$
		Without silicone spray :							
Speed (mm.s ⁻¹)	Time	H _r (mm)	h (mm)	s'	τ_y'	Approx.cyl	τ_y'	Lump Model	τ_y
5.68	7.56	42.96	32.04	0.43	0.17	153.68	0.06	0	121.26
8.70	4.99	43.4	31.6	0.42	0.18	155.68	0.06	0	123.75
7.58	5.56	42.16	32.84	0.44	0.17	150.08	0.06	0	116.82
With silicone spray :						Approx.cyl			
Speed (mm.s ⁻¹)	Time	H _r (mm)	h (mm)	s'	τ_y'		τ_y'	Lump Model	τ_y
6.18	6.92	42.75	32.25	0.43	0.17	152.73	0.06	0	120.08
7.98	5.43	43.33	31.67	0.42	0.18	155.36	0.06	0	123.35
16.23	2.43	39.45	35.55	0.47	0.16	138.21	0.06	0	102.68

THE 50 CENTS HAND-HELD SLUMP TEST (KAOLINITE TAILING 16%)									
Relative density ρ (Kg/m^3) (m.s^{-3})	1.338 1338 9.81	Equations:		$s' = \frac{h}{H} \tau_y = \rho g H \tau_y$	$\tau_y' = \frac{1}{2} - \frac{1}{2} \sqrt{s'}$	Vane τ_y 117.61	$\tau_y' = 0.5(1 - S') e^{\sqrt{3}(-S')}$		Cylinder model $S = 1 - 2\tau_y'(1 - \ln(2\tau_y'))$
		Without silicone spray :							
Speed (mm.s ⁻¹)	Time	H _r (mm)	h (mm)	s'	τ_y'	Approx.cyl	τ_y'	Lump Model	τ_y
9.33	5.68	75	53	0.29	0.23	225.63	0.12	0	209.28
4.72	10.81	75	51	0.32	0.22	213.78	0.12	0	192.29
3.50	14.84	75	52	0.31	0.22	219.64	0.12	0	200.64
With silicone spray :						Approx.cyl			
Speed (mm.s ⁻¹)	Time	H _r (mm)	h (mm)	s'	τ_y'		τ_y'	Lump Model	τ_y
7.34	6.68	75	49	0.35	0.21	202.41	0.12	0	176.41
5.94	9.6	75	57	0.24	0.26	251.08	0.12	0	246.85
4.82	11.21	75	54	0.28	0.24	231.76	0.12	0	218.21

Table B. 4 Slump test for 18 % and 20 % kaolinite tailings using the hand-held cylinder

Appendix B – Hand-held Cylinder Data

THE 50 CENTS HAND-HELD SLUMP TEST (KAOLINITE TAILING 18%)												
Relative density Density $\frac{g}{g}$	1.365 1365 9.81	Equations:		$s' = \frac{h}{H}$	$\tau_y = \rho g H \tau_y$	Approximate cylinder		Lump model		Cylinder model		
		$\tau_y' = \frac{1}{2} - \frac{1}{2} \sqrt{s'}$				$\tau_y' = 0.5(1 - S') e^{\sqrt{3}(-s')}$		$S = 1 - 2\tau_y'(1 - \ln(2\tau_y'))$				
		Vane τ_y				Vane τ_y		Cylinder model				
											215.62	
Without silicone spray :												
Speed (mm.s ⁻¹)	H (mm)	H _t (mm)	h (mm)	s'	τ_y'	Approx.cyl τ_y	Calc.from vane τ_y'	Lump Model τ_y	τ_y'	Cylinder model τ_y		
8.72	75	49.98	25.02	0.33	0.21	212.89	0.21	0	188.46	153.39		
5.69	75	49.46	25.54	0.34	0.21	209.88	0.21	0	184.27	150.48		
4.20	75	47.39	27.61	0.37	0.20	198.20	0.21	0	168.32	139.32		
With silicone spray :												
Speed (mm.s ⁻¹)	H (mm)	H _t (mm)	h (mm)	s'	τ_y'	Approx.cyl τ_y	Calc.from vane τ_y'	Lump Model τ_y	τ_y'	Cylinder model τ_y		
7.71	75	48.6	26.4	0.35	0.20	204.97	0.21	0	177.51	145.76		
5.88	75	51.71	23.29	0.31	0.22	223.14	0.21	0	202.93	163.43		
4.64	75	52	23	0.31	0.22	224.89	0.21	0	205.44	165.17		

THE 50 CENTS HAND-HELD SLUMP TEST (KAOLINITE TAILING 20%)												
Relative density Density $\frac{g}{g}$	1.37 1370 9.81	Equations:		$s' = \frac{h}{H}$	$\tau_y = \rho g H \tau_y$	Approximate cylinder		Lump model		Cylinder model		
		$\tau_y' = \frac{1}{2} - \frac{1}{2} \sqrt{s'}$				$\tau_y' = 0.5(1 - S') e^{\sqrt{3}(-s')}$		$S = 1 - 2\tau_y'(1 - \ln(2\tau_y'))$				
		Vane τ_y				Vane τ_y		Cylinder model				
											300.93	
Without silicone spray :												
Speed (mm.s ⁻¹)	H (mm)	H _t (mm)	h (mm)	s'	τ_y'	Approx.cyl τ_y	Calc.from vane τ_y'	Lump Model τ_y	τ_y'	Cylinder model τ_y		
5.68	75	42.96	32.04	0.43	0.17	174.58	0.30	0	137.74	117.56		
8.70	75	43.4	31.6	0.42	0.18	176.85	0.30	0	140.58	119.61		
16.47	75	42.16	32.84	0.44	0.17	170.49	0.30	0	132.71	113.91		
With silicone spray :												
Speed (mm.s ⁻¹)	H (mm)	H _t (mm)	h (mm)	s'	τ_y'	Approx.cyl τ_y	Calc.from vane τ_y'	Lump Model τ_y	τ_y'	Cylinder model τ_y		
6.18	75	42.75	32.25	0.43	0.17	173.50	0.30	0	136.41	116.60		
7.98	75	43.33	31.67	0.42	0.18	176.49	0.30	0	140.12	119.28		
16.23	75	39.45	35.55	0.47	0.16	157.00	0.30	0	116.64	102.09		

Table B. 5 Slump test for 4 % and 5 % laponite using the hand-held cylinder

Appendix B – Hand-held Cylinder Data

THE HAND-HELD SLUMP TEST (4% LAPTONITE)										Approximate cyl. Model		Lump model		Cylinder model	
Relative Density $\frac{g}{g}$		1.028 (Kg/m ³) 1028 (m.s ⁻¹) 9.81		Equations: $s' = \frac{h}{H}$ $\tau_y = \rho g H \tau'_y$		$\tau'_y = \frac{1}{2} - \frac{1}{2} \sqrt{s'}$		Vane τ_y 100.08		$\tau'_y = 0.5(1 - S') e^{\sqrt{3}(-s')}$		$S = 1 - 2\tau'_y(1 - \ln(2\tau'_y))$			
Without silicon spray		Speed (mm.s ⁻¹)	H (mm)	H _r (mm)	h (mm)	s'	Approx cyl		Calc. from vane	Lump Model		Cylinder model			
		2.90	13.44	75	39	0.48	τ'_y	τ_y	τ'_y	τ_y	τ'_y	τ_y	τ'_y	τ_y	τ'_y
		4.33	8.55	75	37	0.51	0.15	116.17	0.13	0	85.63	0.10	3.24E-07	75.19	
		11.71	2.99	75	35	0.53	0.14	108.99	0.13	0	81.77	0.11	4.00E-02	78.35	
With silicon spray		Speed (mm.s ⁻¹)	H (mm)	H _r (mm)	h (mm)	s'	Approx cyl		Calc. from vane						
		2.35	14.88	75	35	0.53	τ'_y	τ_y	τ'_y	τ_y	τ'_y	τ_y	τ'_y	τ_y	τ'_y
		3.60	9.45	75	34	0.55	0.13	102.00	0.13	0	85.63	0.08	2.65E-07	63.32	
		5.77	5.89	75	34	0.55	0.13	98.56	0.13	0	66.51	0.08	1.42E-07	60.53	
							0.13	98.56	0.13	0	66.51	0.08	1.42E-07	60.53	

THE HAND-HELD SLUMP TEST (5% LAPTONITE)										Approximate cyl. Model		Lump model		Cylinder model	
Relative Density $\frac{g}{g}$		1.0409 (Kg/m ³) 1040.9 (m.s ⁻¹) 9.81		Equations: $s' = \frac{h}{H}$ $\tau_y = \rho g H \tau'_y$		$\tau'_y = \frac{1}{2} - \frac{1}{2} \sqrt{s'}$		Vane τ_y 174.88		$\tau'_y = 0.5(1 - S') e^{\sqrt{3}(-s')}$		$S = 1 - 2\tau'_y(1 - \ln(2\tau'_y))$			
Without silicon spray		Speed (mm.s ⁻¹)	H (mm)	H _r (mm)	h (mm)	s'	Approx cyl		Calc. from vane	Lump Model		Cylinder model			
		3.47	14.12	75	49	0.35	τ'_y	τ_y	τ'_y	τ_y	τ'_y	τ_y	τ'_y	τ_y	τ'_y
		6.03	8.12	75	49	0.35	0.21	157.46	0.23	0	137.24	0.15	7.86E-03	114.88	
		9.46	5.18	75	49	0.35	0.21	157.46	0.23	0	137.24	0.15	7.86E-03	114.88	
With silicon spray		Speed (mm.s ⁻¹)	H (mm)	H _r (mm)	h (mm)	s'	Approx cyl		Calc. from vane						
		3.62	13.52	75	49	0.35	τ'_y	τ_y	τ'_y	τ_y	τ'_y	τ_y	τ'_y	τ_y	τ'_y
		5.94	8.59	75	51	0.32	0.22	166.31	0.23	0	149.59	0.16	4.62E-03	122.53	
		8.49	5.89	75	50	0.33	0.21	161.84	0.23	0	143.31	0.15	5.47E-03	114.88	

Table B. 6 Slump test for 6 % and 7 % laponite using the hand-held cylinder

Appendix B – Hand-held Cylinder Data

THE HAND-HELD SLUMP TEST (5% LAPTONITE)										Approximate cyl. Model		Lump model		Cylinder model		
Relative density Density g		1.052 1052 9.81		Equations: $s' = \frac{h}{H} \quad \tau_y = \rho g H \tau_y'$		$\tau_y' = \frac{1}{2} - \frac{1}{2} \sqrt{s'}$				Vane		$\tau_y' = 0.5(1 - S')e^{\sqrt{3}(-s')}$		$S = 1 - 2\tau_y'(1 - \ln(2\tau_y'))$		
										τ_y						
										243.03						
Without silicone spray :										Calc. from vane						
Speed (mm.s ⁻¹)	Time	H (mm)	H _r (mm)	h (mm)	s'	τ_y'	τ_y	Approx cyl		τ_y'	Lump Model	τ_y	τ_y'	Cylinder model	τ_y	
9.25	7.24	75	67	8.00	0.11	0.34	260.61			0.31	0	287.40	0.30	1.32E-02	222.62	
10.69	6.08	75	65	10.00	0.13	0.32	245.69			0.31	0	274.43	0.30	3.98E-02	205.22	
21.91	2.83	75	62	13.00	0.17	0.29	225.88			0.31	0	236.95	0.24	5.64E-03	182.82	
With silicone spray :										Calc. from vane						
Speed (mm.s ⁻¹)	Time	H (mm)	H _r (mm)	h (mm)	s'	τ_y'	τ_y	Approx cyl		τ_y'	Lump Model	τ_y	τ_y'	Cylinder model	τ_y	
9.02	7.21	75	65	10.00	0.13	0.32	245.69			0.31	0	266.00	0.20	-1.00E-01	205.00	
12.55	4.94	75	62	13.00	0.17	0.29	225.88			0.31	0	237.00	0.24	5.64E-03	182.82	
19.64	3.31	75	65	10.00	0.13	0.32	245.69			0.31	0	202.00	0.30	3.98E-02	157.00	

THE HAND-HELD SLUMP TEST (6% LAPTONITE)										Approximate cyl. Model		Lump model		Cylinder model		
Relative density Density g		1.061 1061 9.81		Equations: $s' = \frac{h}{H} \quad \tau_y = \rho g H \tau_y'$		$\tau_y' = \frac{1}{2} - \frac{1}{2} \sqrt{s'}$				Vane		$\tau_y' = 0.5(1 - S')e^{\sqrt{3}(-s')}$		$S = 1 - 2\tau_y'(1 - \ln(2\tau_y'))$		
										τ_y						
										482.48						
Without silicone spray :										Calc. from vane						
Speed (mm.s ⁻¹)	Time	H (mm)	H _r (mm)	h (mm)	s'	τ_y'	τ_y	Approx cyl		τ_y'	Lump Model	τ_y	τ_y'	Cylinder model	τ_y	
14.18	5.29	75	75	0.00	0.00	0.50	350.15			0.50	0	381.52	0.50	0.00E+00	333.12	
23.05	3.21	75	74	1.00	0.01	0.50	331.36			0.50	0	367.95	0.50	1.33E-02	308.32	
43.27	1.71	75	74	1.00	0.01	0.50	331.36			0.50	0	367.95	0.08	-5.45E-01	308.32	
With silicone spray :										Calc. from vane						
Speed (mm.s ⁻¹)	Time	H (mm)	H _r (mm)	h (mm)	s'	τ_y'	τ_y	Approx cyl		τ_y'	Lump Model	τ_y	τ_y'	Cylinder model	τ_y	
11.14	6.64	75	74	1.00	0.01	0.44	331.36			0.50	0	367.95	0.39	3.16E-07	308.32	
24.74	2.87	75	71	4.00	0.05	0.38	294.07			0.62	0	329.70	0.33	5.28E-07	261.02	
35.15	2.02	75	71	4.00	0.05	0.38	331.36			0.62	1.00E-06	367.95	0.39	2.77E-07	308.32	

Table B. 7 Slump test for 5 mins 90:10 relative density at 1.75 Kaolinite tailings and sand using the hand-held cylinder

Appendix B – Hand-held Cylinder Data

RESULTS ON THE 50CENTS: (5mins 90:10 at 1.75)									
Equations:									
Relative density	1.75								
Density (Kg/m ³)	1750								
g (m.s ⁻¹)	9.81								
Without silicone spray :									
Speed	Time	H (mm)	H _r (mm)	h (mm)	s'				
17.67	1.23	75	21.73	53.27	0.71				
With silicone spray :									
Speed	Time	H (mm)	H _r (mm)	h (mm)	s'				
13.09	1.86	75	24.35	50.65	0.68				
Approximate cylinder						vane		Lump model	
$\tau_y' = \frac{1}{2} - \frac{1}{2} \sqrt{s'}$						τ_y'		$\tau_y' = 0.5(1 - S')e^{\sqrt[3]{3(-S')}}$	
Approx.cyl						Calc. from vane			
τ_y'						τ_y'		τ_y'	
0.08						0.06		54.51	
Approx.cyl						Calc. from vane			
τ_y'						τ_y'		τ_y'	
0.09						0.06		64.89	
Cylinder model								Cylinder model	
								$S' = 1 - 2\tau_y' (1 - \ln(2\tau_y'))$	

Appendix B – Hand-held Cylinder Data

RESULTS ON THE 50CENTS: (20mins 90:10 at 1.75)									
Equations:									
Relative density	1.75	$\tau_y = \frac{h}{H} \tau_y = \rho g H \tau_y$							
Density (Kg/m ³)	1750	$s' = \frac{h}{H}$							
g (m.s ⁻¹)	9.81	$\tau_y = \frac{1}{2} - \frac{1}{2} \sqrt{s'}$							
Without silicone spray :									
Speed	Time	H (mm)	H _r (mm)	h (mm)	s'	Approx. cyl			
17.16	3.07	75	52.69	22.31	0.30	τ_y'	τ_y		
With silicone spray :									
Speed	Time	H (mm)	H _r (mm)	h (mm)	s'	τ_y'	τ_y		
16.74	3.23	75	54.08	20.92	0.28	τ_y'	τ_y		
						Approximate cylinder			
						$\tau_y' = \frac{1}{2} - \frac{1}{2} \sqrt{s'}$			
						vane			
						τ_y			
						356.15			
						Approx. cyl			
						τ_y'			
						Calc. from vane			
						τ_y'			
						292.66			
						0.23			
						Lump Model			
						τ_y'			
						0.21			
						270.17			
						0.17			
						Cylinder model			
						τ_y			
						216.36			
						Cylinder model			
						τ_y'			
						0.18			
						286.35			
						0.22			
						Lump Model			
						0			
						τ_y'			
						0.22			
						286.35			
						0.18			
						Cylinder model			
						τ_y			
						227.56			
						Cylinder model			
						τ_y'			
						0.18			
						3.54E-07			
						Cylinder model			
						τ_y			
						227.56			
						Cylinder model			
						τ_y'			
						0.18			
						3.54E-07			
						Cylinder model			
						τ_y			
						227.56			
						Cylinder model			
						τ_y'			
						0.18			
						3.54E-07			
						Cylinder model			
						τ_y			
						227.56			
						Cylinder model			
						τ_y'			
						0.18			
						3.54E-07			
						Cylinder model			
						τ_y			
						227.56			
						Cylinder model			
						τ_y'			
						0.18			
						3.54E-07			
						Cylinder model			
						τ_y			
						227.56			
						Cylinder model			
						τ_y'			
						0.18			
						3.54E-07			
						Cylinder model			
						τ_y			
						227.56			
						Cylinder model			
						τ_y'			
						0.18			
						3.54E-07			
						Cylinder model			
						τ_y			
						227.56			
						Cylinder model			
						τ_y'			
						0.18			
						3.54E-07			
						Cylinder model			
						τ_y			
						227.56			
						Cylinder model			
						τ_y'			
						0.18			
						3.54E-07			
						Cylinder model			
						τ_y			
						227.56			
						Cylinder model			
						τ_y'			
						0.18			
						3.54E-07			
						Cylinder model			
						τ_y			
						227.56			
						Cylinder model			
						τ_y'			
						0.18			
						3.54E-07			
						Cylinder model			
						τ_y			
						227.56			
						Cylinder model			
						τ_y'			
						0.18			
						3.54E-07			
						Cylinder model			
						τ_y			
						227.56			
						Cylinder model			
						τ_y'			
						0.18			
						3.54E-07			
						Cylinder model			
						τ_y			
						227.56			
						Cylinder model			
						τ_y'			
						0.18			
						3.54E-07			
						Cylinder model			
						τ_y			
						227.56			
						Cylinder model			
						τ_y'			
						0.18			
						3.54E-07			
						Cylinder model			
						τ_y			
						227.56			
						Cylinder model			
						τ_y'			
						0.18			
						3.54E-07			
						Cylinder model			
						τ_y			
						227.56			
						Cylinder model			
						τ_y'			
						0.18			
						3.54E-07			
						Cylinder model			
						τ_y			
						227.56			
						Cylinder model			
						τ_y'			
						0.18			
						3.54E-07			
						Cylinder model			
						τ_y			
						227.56			
						Cylinder model			
						τ_y'			
						0.18			
						3.54E-07			
						Cylinder model			
						τ_y			
						227.56			
						Cylinder model			
						τ_y'			
						0.18			
						3.54E-07			
						Cylinder model			
						τ_y			
						227.56			
						Cylinder model			
						τ_y'			
						0.18			
						3.54E-07			
						Cylinder model			
						τ_y			
						227.56			
						Cylinder model			
						τ_y'			
						0.18			
						3.54E-07			
						Cylinder model			
						τ_y			
						227.56			
						Cylinder model			
						τ_y'			
						0.18			
						3.54E-07			
						Cylinder model			
						τ_y			
						227.56			
						Cylinder model			
						τ_y'			
						0.18			
						3.54E-07			
						Cylinder model			
						τ_y			
						227.56			
						Cylinder model			
						τ_y'			
						0.18			
						3.54E-07			
						Cylinder model			
						τ_y			
						227.56			
						Cylinder model			
						τ_y'			
						0.18			
						3.54E-07			
						Cylinder model			
						τ_y			
						227.56			
						Cylinder model			
						τ_y'			
						0.18			
						3.54E-07			
						Cylinder model			
						τ_y			
						227.56			
						Cylinder model			
						τ_y'			
						0.18			
						3.54E-07			
						Cylinder model			
						τ_y			
						227.56			
						Cylinder model			
						τ_y'			
						0.18			
						3.54E-07			
						Cylinder model			
						τ_y			
						227.56			
						Cylinder model			
						τ_y'			
						0.18			
						3.54E-07			
						Cylinder model			
						τ_y			
						227.56			
						Cylinder model			
						τ_y'			
						0.18			
						3.54E-07			
						Cylinder model			
						τ_y			
						227.56			
						Cylinder model			
						τ_y'			
						0.18			
						3.54E-07			
						Cylinder model			
						τ_y			
						227.56			
						Cylinder model			
						τ_y'			
						0.18			
						3.54E-07			
						Cylinder model			
						τ_y			
						227.56			
						Cylinder model			
						τ_y'			
						0.18			
						3.54E-07			
						Cylinder model			
						τ_y			
						227.56			
						Cylinder model			
						τ_y'			
						0.18			
						3.54E-07			
						Cylinder model			
						τ_y			
						227.56			
						Cylinder model			
						τ_y'			
						0.18			
						3.54E-07			
						Cylinder model			
						τ_y			
						227.56			
						Cylinder model			
						τ_y'			
						0.18			
						3.54E-07			
						Cylinder model			
						τ_y			
						227.56			
						Cylinder model			
						τ_y'			
						0.18			
						3.54E-07			
						Cylinder model			
						τ_y			
						227.56			
						Cylinder model			
						τ_y'			
						0.18			
						3.54E-07			
						Cylinder model			
						τ_y			
						227.56			
						Cylinder model			
						τ_y'			
						0.18			
						3.54E-07			
						Cylinder model			
						τ_y			
						227.56			
						Cylinder model			
						τ_y'			
						0.18			
						3.54E-07			
						Cylinder model			
						τ_y			
						227.56			
						Cylinder model			
						τ_y'			
						0.18			
						3.54E-07			
						Cylinder model			
						τ_y			
						227.56			
						Cylinder model			
						τ_y'			
						0.18			
						3.54E-07			
						Cylinder model			
						τ_y			
						227.56			
						Cylinder model			
						τ_y'			
						0.18			
						3.54E-07			
						Cylinder model			
						τ_y			
						227.56			
						Cylinder model			
						τ_y'			
						0.18			
						3.54E-07			
						Cylinder model			
						τ_y			
						227.56			
						Cylinder model			
						τ_y'			
						0.18			
						3.54E-07			
						Cylinder model			
						τ_y			
						227.56			
						Cylinder model			
						τ_y'			
						0.18			
						3.54E-07			
						Cylinder model			
						τ_y			
						227.56			
						Cylinder model			
						τ_y'			
						0.18			
						3.54E-07			
						Cylinder model			
						τ_y			
						227.56			
						Cylinder model			
						τ_y'			
						0.18			
						3.54E-07			
						Cylinder model			
						τ_y			
						227.56			
						Cylinder model			
						τ_y'			
						0.18			
						3.54E-07			
						Cylinder model			
						τ_y			
						227.56			
						Cylinder model			
						τ_y'			
						0.18			
						3.54E-07			
						Cylinder model			
						τ_y			
						227.56			
						Cylinder model			
						τ_y'			
						0.18			
						3.54E-07			
						Cylinder model			
						τ_y			
						227.56			
						Cylinder model			
						τ_y'			
						0.18			
						3.54E-07			
						Cylinder model			
						τ_y			
						227.56			
						Cylinder model			
						τ_y'			
						0.18			
						3.54E-07			
						Cylinder model			
						τ_y			
						227.56			
						Cylinder model			
						τ_y'			
						0.18			
						3.54E-07			
						Cylinder model			
						τ_y			
						227.56			
						Cylinder model			
						τ_y'			
						0.18			
						3.54E-07			
						Cylinder model			
						τ_y			
						227.56			
						Cylinder model			
						τ_y'			
						0.18			
						3.54E-07			
						Cylinder model			
						τ_y			
						227.56			
						Cylinder model			
						τ_y'			
						0.18			
						3.54E-07			
						Cylinder model			
						τ_y			
						227.56			
						Cylinder model			
						τ_y'			
						0.18			
						3.54E-07			
						Cylinder model			
						τ_y			
						227.56			
						Cylinder model			
						τ_y'			
						0.18			
						3.54E-07			
						Cylinder model			
						τ_y			
						227.56			
						Cylinder model			
						τ_y'			
						0.18			
						3.54E-07			
						Cylinder model			
						τ_y			
						227.56			
						Cylinder model			
						τ_y'			
						0.18			
						3.54E-07			
						Cylinder model			
						τ_y			
						227.56			
						Cylinder model			
						τ_y'			
						0.18			
						3.54E-07			
						Cylinder model			
						τ_y			
						227.56			
						Cylinder model			
						τ_y'			
						0.18			
						3.54E-07			
						Cylinder model			
						τ_y			
						227.56			
						Cylinder model			
						τ_y'			
						0.18			
						3.54E-07			
						Cylinder model			
						τ_y			
						227.56			
						Cylinder model			

Appendix B – Hand-held Cylinder Data

RESULTS ON THE 50CENTS: (10mins 90:10 at 1.8)									
Equations:									
Relative density Density (Kg/m ³) g (m.s ⁻¹)	1.8 1800 9.81	$s' = \frac{h}{H} \quad \tau_y = \rho g H \tau_y'$							
Without silicone spray :									
Speed	Time	H (mm)	H _r (mm)	h (mm)	s'	Approx.cyl			
24.78	1.71	75	42.38	32.62	0.43	τ_y'	τ_y	τ_y'	τ_y
With silicone spray :									
Speed	Time	H (mm)	H _r (mm)	h (mm)	s'	Approx.cyl			
26.17	1.69	75	44.23	30.77	0.41	τ_y'	τ_y	τ_y'	τ_y
						Lump model			
						τ_y'	τ_y	τ_y'	τ_y
						0	176.16	0.11	4.27E-07
						Cylinder model			
						$S' = 1 - 2\tau_y'(1 - \ln(2\tau_y'))$			
						vane			
						τ_y			
						309.21			
						Calc.from.vane			
						τ_y'	τ_y	τ_y'	τ_y
						0.23	176.16	0.11	150.97
						Cylinder model			
						$S' = 1 - 2\tau_y'(1 - \ln(2\tau_y'))$			
						vane			
						τ_y			
						309.21			
						Calc.from.vane			
						τ_y'	τ_y	τ_y'	τ_y
						0.23	191.87	0.12	7.75E-07
						Cylinder model			
						$S' = 1 - 2\tau_y'(1 - \ln(2\tau_y'))$			
						vane			
						τ_y			
						162.30			
						Calc.from.vane			
						τ_y'	τ_y	τ_y'	τ_y
						0.23	191.87	0.12	162.30
						Cylinder model			
						$S' = 1 - 2\tau_y'(1 - \ln(2\tau_y'))$			
						vane			
						τ_y			
						162.30			
						Calc.from.vane			
						τ_y'	τ_y	τ_y'	τ_y
						0.23	191.87	0.12	162.30
						Cylinder model			
						$S' = 1 - 2\tau_y'(1 - \ln(2\tau_y'))$			
						vane			
						τ_y			
						162.30			
						Calc.from.vane			
						τ_y'	τ_y	τ_y'	τ_y
						0.23	191.87	0.12	162.30
						Cylinder model			
						$S' = 1 - 2\tau_y'(1 - \ln(2\tau_y'))$			
						vane			
						τ_y			
						162.30			
						Calc.from.vane			
						τ_y'	τ_y	τ_y'	τ_y
						0.23	191.87	0.12	162.30
						Cylinder model			
						$S' = 1 - 2\tau_y'(1 - \ln(2\tau_y'))$			
						vane			
						τ_y			
						162.30			
						Calc.from.vane			
						τ_y'	τ_y	τ_y'	τ_y
						0.23	191.87	0.12	162.30
						Cylinder model			
						$S' = 1 - 2\tau_y'(1 - \ln(2\tau_y'))$			
						vane			
						τ_y			
						162.30			
						Calc.from.vane			
						τ_y'	τ_y	τ_y'	τ_y
						0.23	191.87	0.12	162.30
						Cylinder model			
						$S' = 1 - 2\tau_y'(1 - \ln(2\tau_y'))$			
						vane			
						τ_y			
						162.30			
						Calc.from.vane			
						τ_y'	τ_y	τ_y'	τ_y
						0.23	191.87	0.12	162.30
						Cylinder model			
						$S' = 1 - 2\tau_y'(1 - \ln(2\tau_y'))$			
						vane			
						τ_y			
						162.30			
						Calc.from.vane			
						τ_y'	τ_y	τ_y'	τ_y
						0.23	191.87	0.12	162.30
						Cylinder model			
						$S' = 1 - 2\tau_y'(1 - \ln(2\tau_y'))$			
						vane			
						τ_y			
						162.30			
						Calc.from.vane			
						τ_y'	τ_y	τ_y'	τ_y
						0.23	191.87	0.12	162.30
						Cylinder model			
						$S' = 1 - 2\tau_y'(1 - \ln(2\tau_y'))$			
						vane			
						τ_y			
						162.30			
						Calc.from.vane			
						τ_y'	τ_y	τ_y'	τ_y
						0.23	191.87	0.12	162.30
						Cylinder model			
						$S' = 1 - 2\tau_y'(1 - \ln(2\tau_y'))$			
						vane			
						τ_y			
						162.30			
						Calc.from.vane			
						τ_y'	τ_y	τ_y'	τ_y
						0.23	191.87	0.12	162.30
						Cylinder model			
						$S' = 1 - 2\tau_y'(1 - \ln(2\tau_y'))$			
						vane			
						τ_y			
						162.30			
						Calc.from.vane			
						τ_y'	τ_y	τ_y'	τ_y
						0.23	191.87	0.12	162.30
						Cylinder model			
						$S' = 1 - 2\tau_y'(1 - \ln(2\tau_y'))$			
						vane			
						τ_y			
						162.30			
						Calc.from.vane			
						τ_y'	τ_y	τ_y'	τ_y
						0.23	191.87	0.12	162.30
						Cylinder model			
						$S' = 1 - 2\tau_y'(1 - \ln(2\tau_y'))$			
						vane			
						τ_y			
						162.30			
						Calc.from.vane			
						τ_y'	τ_y	τ_y'	τ_y
						0.23	191.87	0.12	162.30
						Cylinder model			
						$S' = 1 - 2\tau_y'(1 - \ln(2\tau_y'))$			
						vane			
						τ_y			
						162.30			
						Calc.from.vane			
						τ_y'	τ_y	τ_y'	τ_y
						0.23	191.87	0.12	162.30
						Cylinder model			
						$S' = 1 - 2\tau_y'(1 - \ln(2\tau_y'))$			
						vane			
						τ_y			
						162.30			
						Calc.from.vane			
						τ_y'	τ_y	τ_y'	τ_y
						0.23	191.87	0.12	162.30
						Cylinder model			
						$S' = 1 - 2\tau_y'(1 - \ln(2\tau_y'))$			
						vane			
						τ_y			
						162.30			
						Calc.from.vane			
						τ_y'	τ_y	τ_y'	τ_y
						0.23	191.87	0.12	162.30
						Cylinder model			
						$S' = 1 - 2\tau_y'(1 - \ln(2\tau_y'))$			
						vane			
						τ_y			
						162.30			
						Calc.from.vane			
						τ_y'	τ_y	τ_y'	τ_y
						0.23	191.87	0.12	162.30
						Cylinder model			
						$S' = 1 - 2\tau_y'(1 - \ln(2\tau_y'))$			
						vane			
						τ_y			
						162.30			
						Calc.from.vane			
						τ_y'	τ_y	τ_y'	τ_y
						0.23	191.87	0.12	162.30
						Cylinder model			
						$S' = 1 - 2\tau_y'(1 - \ln(2\tau_y'))$			
						vane			
						τ_y			
						162.30			
						Calc.from.vane			
						τ_y'	τ_y	τ_y'	τ_y
						0.23	191.87	0.12	162.30
						Cylinder model			
						$S' = 1 - 2\tau_y'(1 - \ln(2\tau_y'))$			
						vane			
						τ_y			
						162.30			
						Calc.from.vane			
						τ_y'	τ_y	τ_y'	τ_y
						0.23	191.87	0.12	162.30
						Cylinder model			
						$S' = 1 - 2\tau_y'(1 - \ln(2\tau_y'))$			
						vane			
						τ_y			
						162.30			
						Calc.from.vane			
						τ_y'	τ_y	τ_y'	τ_y
						0.23	191.87	0.12	162.30
						Cylinder model			
						$S' = 1 - 2\tau_y'(1 - \ln(2\tau_y'))$			
						vane			
						τ_y			
						162.30			
						Calc.from.vane			
						τ_y'	τ_y	τ_y'	τ_y
						0.23	191.87	0.12	162.30
						Cylinder model			
						$S' = 1 - 2\tau_y'(1 - \ln(2\tau_y'))$			
						vane			
						τ_y			
						162.30			
						Calc.from.vane			
						τ_y'	τ_y	τ_y'	τ_y
						0.23	191.87	0.12	162.30
						Cylinder model			
						$S' = 1 - 2\tau_y'(1 - \ln(2\tau_y'))$			
						vane			
						τ_y			
						162.30			
						Calc.from.vane			
						τ_y'	τ_y	τ_y'	τ_y
						0.23	191.87	0.12	162.30
						Cylinder model			
						$S' = 1 - 2\tau_y'(1 - \ln(2\tau_y'))$			
						vane			
						τ_y			
						162.30			
						Calc.from.vane			
						τ_y'	τ_y	τ_y'	τ_y
						0.23	191.87	0.12	162.30
						Cylinder model			
						$S' = 1 - 2\tau_y'(1 - \ln(2\tau_y'))$			
						vane			
						τ_y			
						162.30			
						Calc.from.vane			
						τ_y'	τ_y	τ_y'	τ_y
						0.23	191.87	0.12	162.30
						Cylinder model			
						$S' = 1 - 2\tau_y'(1 - \ln(2\tau_y'))$			
						vane			
						τ_y			
						162.30			
						Calc.from.vane			
						τ_y'	τ_y	τ_y'	τ_y
						0.23	191.87	0.12	162.30
						Cylinder model			
						$S' = 1 - 2\tau_y'(1 - \ln(2\tau_y'))$			
						vane			
						τ_y			
						162.30			
						Calc.from.vane			
						τ_y'	τ_y	τ_y'	τ_y
						0.23	191.87	0.12	162.30
						Cylinder model			
						$S' = 1 - 2\tau_y'(1 - \ln(2\tau_y'))$			
						vane			
						τ_y			
						162.30			
						Calc.from.vane			
						τ_y'	τ_y	τ_y'	τ_y
						0.23	191.87	0.12	162.30
						Cylinder model			
						$S' = 1 - 2\tau_y'(1 - \ln(2\tau_y'))$			
						vane			
						τ_y			
						162.30			
						Calc.from.vane			
						τ_y'	τ_y	τ_y'	τ_y
						0.23	191.87	0.12	162.30
						Cylinder model			
						$S' = 1 - 2\tau_y'(1 - \ln(2\tau_y'))$			
						vane			
						τ_y			
						162.30			
						Calc.from.vane			
						τ_y'	τ_y	τ_y'	τ_y
						0.23	191.87	0.12	162.30
						Cylinder model			
						$S' = 1 - 2\tau_y'(1 - \ln(2\tau_y'))$			
						vane			
						τ_y			
						162.30			
						Calc.from.vane			
						τ_y'	τ_y	τ_y'	τ_y
						0.23	191.87	0.12	162.30
						Cylinder model			
						$S' = 1 - 2\tau_y'(1 - \ln(2\tau_y'))$			
						vane			
						τ_y			
						162.30			
						Calc.from.vane			
						τ_y'	τ_y	τ_y'	τ_y
						0.23	191.87	0.12	162.30
						Cylinder model			
						$S' = 1 - 2\tau_y'(1 - \ln(2\tau_y'))$			
						vane			
						τ_y			
						162.30			
						Calc.from.vane			
						τ_y'	τ_y	τ_y'	τ_y
						0.23	191.87	0.12	162.30
						Cylinder model			
						$S' = 1 - 2\tau_y'(1 - \ln(2\tau_y'))$			
						vane			
						τ_y			
						162.30			
						Calc.from.vane			
						τ_y'	τ_y	τ_y'	τ_y
						0.23	191.87	0.12	162.30
						Cylinder model			
						$S' = 1 - 2\tau_y'(1 - \ln(2\tau_y'))$			
						vane			
						τ_y			
						162.30			
						Calc.from.vane			
						τ_y'	τ_y	τ_y'	τ_y
						0.23	191.87	0.12	162.30
						Cylinder model			
						$S' = 1 - 2\tau_y'(1 - \ln(2\tau_y'))$			
						vane			
						τ_y			
						162.30			
						Calc.from.vane			
						τ_y'	τ_y	τ_y'	τ_y
						0.23	191.87	0.12	162.30
						Cylinder model			
						$S' = 1 - 2\tau_y'(1 - \ln(2\tau_y'))$			
						vane			
						τ_y			
						162.30			
						Calc.from.vane			
						τ_y'	τ_y	τ_y'	τ_y
						0.23	191.87	0.12	162.30
						Cylinder model			
						$S' = 1 - 2\tau_y'(1 - \ln(2\tau_y'))$			
						vane			
						τ_y			
						162.30			
						Calc.from.vane			
						τ_y'	τ_y	τ_y'	τ_y
						0.23	191.87	0.12	162.30
						Cylinder model			
						$S' = 1 - 2\tau_y'(1 - \ln(2\tau_y'))$			

Appendix B – Hand-held Cylinder Data

RESULTS ON THE 50CENTS: (5mins 80:20 at 1.6)													
Relative density Density g (Kg/m ³) (m.s ⁻¹)		1.6 1600 9.81		Equations: $s' = \frac{h}{H} \tau_y = \rho g H \tau_y$		Approximate cylinder $\tau_y' = \frac{1}{2} \frac{1}{2} \sqrt{s'}$		Vane τ_y 66.54		Lump model $\tau_y' = 0.5(1 - S') e^{\sqrt{3}(-S')}$		Cylinder model $S' = 1 - 2\tau_y'(1 - \ln(2\tau_y'))$	
Without silicone spray :													
Speed	Time	H (mm)	H _r (mm)	h (mm)	s'	τ_y'	Approx.cyl τ_y	Calc.from vane τ_y'	Lump Model τ_y'	τ_y	τ_y'	Cylinder model τ_y	
17.7	1.19	75	21.05	53.95	0.72	0.08	89.39	0.06	0	47.52	0.04	2.85582E-07	
With silicone spray :													
Speed	Time	H (mm)	H _r (mm)	h (mm)	s'	τ_y'	Approx.cyl τ_y	Calc. from vane τ_y'	Lump Model τ_y'	τ_y	τ_y'	Cylinder model τ_y	
14.10	1.54	75	21.63	53.37	0.71	0.08	92.08	0.06	0	49.49	0.4	3.77188E-07	

Table B. 12 Slump test for 10 mins 80:20 relative density at 1.6 Kaolinite tailings and sand using the hand-held cylinder

RESULTS ON THE 50CENTS: (10mins 80:20 at 1.6)										Approximate cylinder		Lump model		Cylinder model	
Relative density Density g (Kg/m ³) (m.s ⁻¹)		1.7 1700 9.81		Equations: $s' = \frac{h}{H} \tau_y = \rho g H \tau_y$		$\tau_y' = \frac{1}{2} \frac{1}{2} \sqrt{s'}$		$\tau_y' = 0.5(1 - S') e^{\sqrt{3}(-s')}$		$S' = 1 - 2\tau_y'(1 - \ln(2\tau_y'))$					
Without silicone spray :															
Speed	Time	H (mm)	H _r (mm)	h (mm)	s'	τ_y'	Approx.cyl τ_y	Calc.from vane τ_y'	τ_y'	Lump Model	τ_y	τ_y'	Cylinder model	τ_y	
17.67	1.20	75	21.2	53.8	0.72	0.08	90.08	0.07	0.04	0	48.03	0.04	3.21284E-07	47.23	
With silicone spray :															
Speed	Time	H (mm)	H _r (mm)	h (mm)	s'	τ_y'	Approx.cyl τ_y	Calc.from vane τ_y'	τ_y'	Lump Model	τ_y	τ_y'	Cylinder model	τ_y	
20.59	1.13	75	23.27	51.73	0.69	0.08	99.77	0.07	0.05	0	55.30	0.05	1.09165E-07	53.85	

Table B. 13 Slump test for 20 mins 80:20 relative density at 1.6 Kaolinite tailings and sand using the hand-held cylinder

Appendix B – Hand-held Cylinder Data

RESULTS ON THE 50CENTS: (20mins 80:20 at 1.6)													
Relative density Density (Kg/m ³) (m.s ⁻¹)		Equations: $s' = \frac{1.6}{1600} \tau_y = \frac{\rho g H \tau_y}{H}$		Approximate cylinder $\tau_y' = \frac{1}{2} - \frac{1}{2} \sqrt{s'}$		Vane τ_y 82.27		Lump model $\tau_y' = 0.5(1 - s') e^{\sqrt{s'}(-s')}$		Cylinder model $S = 1 - 2\tau_y'(1 - \ln(2\tau_y'))$			
Without silicone spray :													
Speed	Time	H (mm)	H _r (mm)	h (mm)	s'	τ_y'	Approx.cyl τ_y	Calc.from vane τ_y'	Lump Model τ_y'	τ_y	Cylinder model τ_y		
30.52	0.77	75	23.5	51.5	0.69	0.09	100.85	0.07	0.05	56.14	0.05	3.66E-07	54.60
With silicone spray :													
Speed	Time	H (mm)	H _r (mm)	h (mm)	s'	τ_y'	Approx.cyl τ_y	Calc.from vane τ_y'	Lump Model τ_y'	τ_y	Cylinder model τ_y		
21.75	1.18	75	25.67	49.33	0.66	0.09	111.24	0.07	0.06	70.63	0.05	1.76E-07	61.97

Appendix B – Hand-held Cylinder Data

RESULTS ON THE SOCENTS: (10mins 80:20 at 1.7)											
Relative density Density (Kg/m ³) g (m.s ⁻¹)		1.7 1700 9.81		Equations: $s' = \frac{h}{H}$ $\tau_y = \rho g H \tau'_y$		Approximate cylinder					
						Vane τ_y 191.23		Lump model $\tau_y' = 0.5(1-S')e^{\sqrt{3}(-s')}$		Cylinder model $S'' = 1 - 2\tau_y'(1 - \ln(2\tau_y'))$	
Without silicone spray :											
Speed	Time	H (mm)	H _r (mm)	h (mm)	s'	Approx.cyl τ_y		Lump Model τ_y'		Cylinder model τ_y	
18.14	2.07	75	37.54	37.46	0.50	τ_y' 0.15		0.11		131.79	
With silicone spray :											
Speed	Time	H (mm)	H _r (mm)	h (mm)	s'	Approx.cyl τ_y		Lump Model τ_y'		Cylinder model τ_y	
13.62	3.03	75	41.27	33.73	0.45	τ_y' 0.16		0.13		157.92	

Appendix B – Hand-held Cylinder Data

RESULTS ON THE 50CENTS: (10mins 70:30 at 1.4)						Approximate cylinder		vane		Lump model		Cylinder model	
Relative density		1.4		Equations:		$\tau_y = \frac{1}{2} - \frac{1}{2} \sqrt{s'}$		vane		$\tau_y = 0.5(1 - S')e^{\sqrt{3}(-S')}$		$S = 1 - 2\tau_y(1 - \ln(2\tau_y))$	
Density (Kg/m ³)		1400		$s' = \frac{h}{H} \tau_y = \frac{\rho g H \tau_y}{g}$				τ_y		τ_y		τ_y	
g (m.s ⁻¹)		9.81						40.03					
Without silicone spray :						Approx.cyl		Calc.from vane					
Speed	Time	H (mm)	H _r (mm)	h (mm)	s'	τ_y	τ_y	τ_y	τ_y	τ_y	τ_y	τ_y	τ_y
18.13	0.94	75	17.04	57.96	0.77	0.06	62.27	0.04	0.03	0.03	30.68	0.03	30.61
With silicone spray :						Approx.cyl		Calc.from vane					
Speed	Time	H (mm)	H _r (mm)	h (mm)	s'	τ_y	τ_y	τ_y	τ_y	τ_y	τ_y	τ_y	τ_y
18.67	1.03	75	19.23	55.77	0.74	0.07	70.91	0.04	0.04	0.04	36.42	0.04	36.10

Table B. 22 Slump test for 20 mins 70:30 relative density at 1.4 Kaolinite tailings and sand using the hand-held cylinder

RESULTS ON THE 50CENTS: (20mins 70:30 at 1.4)										Approximate cylinder		Lump model		Cylinder model	
Relative density Density (Kg/m ³) g (m.s ⁻¹)		1.4 1400 9.81		Equations: $s' = \frac{h}{H} \tau_y = \rho g H \tau_y$		$\tau_y = \frac{1}{2} - \frac{1}{2} \sqrt{s'}$		vane		$\tau_y' = 0.5(1 - S') e^{\sqrt{3}(-S')}$		$S' = 1 - 2\tau_y'(1 - \ln(2\tau_y'))$			
								τ_y							
								46.11							
Without silicone spray :															
Speed	Time	H (mm)	H _r (mm)	h (mm)	s'	τ_y'	Approx.cyl τ_y	Calc.from.vane τ_y'	τ_y'	Lump Model τ_y	τ_y	τ_y'	Cylinder model τ_y		
17.91	0.7	75	12.54	62.46	0.83	0.04	48.24	0.04	0.02	0	21.81	0.02	2.78E-07		
With silicone spray :															
Speed	Time	H (mm)	H _r (mm)	h (mm)	s'	τ_y'	Approx.cyl τ_y	Calc.from.vane τ_y'	τ_y'	Lump Model τ_y	τ_y	τ_y'	Cylinder model τ_y		
15.41	0.9	75	13.87	61.13	0.82	0.05	53.63	0.04	0.02	0	24.87	0.02	2.94E-07		

Table B. 23 Slump test for 5 mins 70:30 relative density at 1.5 Kaolinite tailings and sand using the hand-held cylinder

Appendix B – Hand-held Cylinder Data

RESULTS ON THE 50CENTS: (20mins 70:30 at 1.5)									
Relative density Density (Kg/m ³) g (m.s ⁻¹)		1.5 1500 9.81		Equations: $s' = \frac{h}{H} \tau_y = \rho g H \tau_y$					
Without silicone spray :									
Speed	Time	H (mm)	H _r (mm)	h (mm)	s'	Approx.cyl		Vane	Cylinder model $S' = 1 - 2\tau_y (1 - \ln(2\tau_y))$
10.55	2.9	75	30.59	44.41	0.59	τ_y'	τ_y	τ_y'	
						0.12	127.19	0.08	
With silicone spray :									
Speed	Time	H (mm)	H _r (mm)	h (mm)	s'	Approx.cyl		Calc. from vane	Cylinder model $S' = 1 - 2\tau_y (1 - \ln(2\tau_y))$
7.66	4	75	30.65	44.35	0.59	τ_y'	τ_y	τ_y'	
						0.12	127.48	0.08	

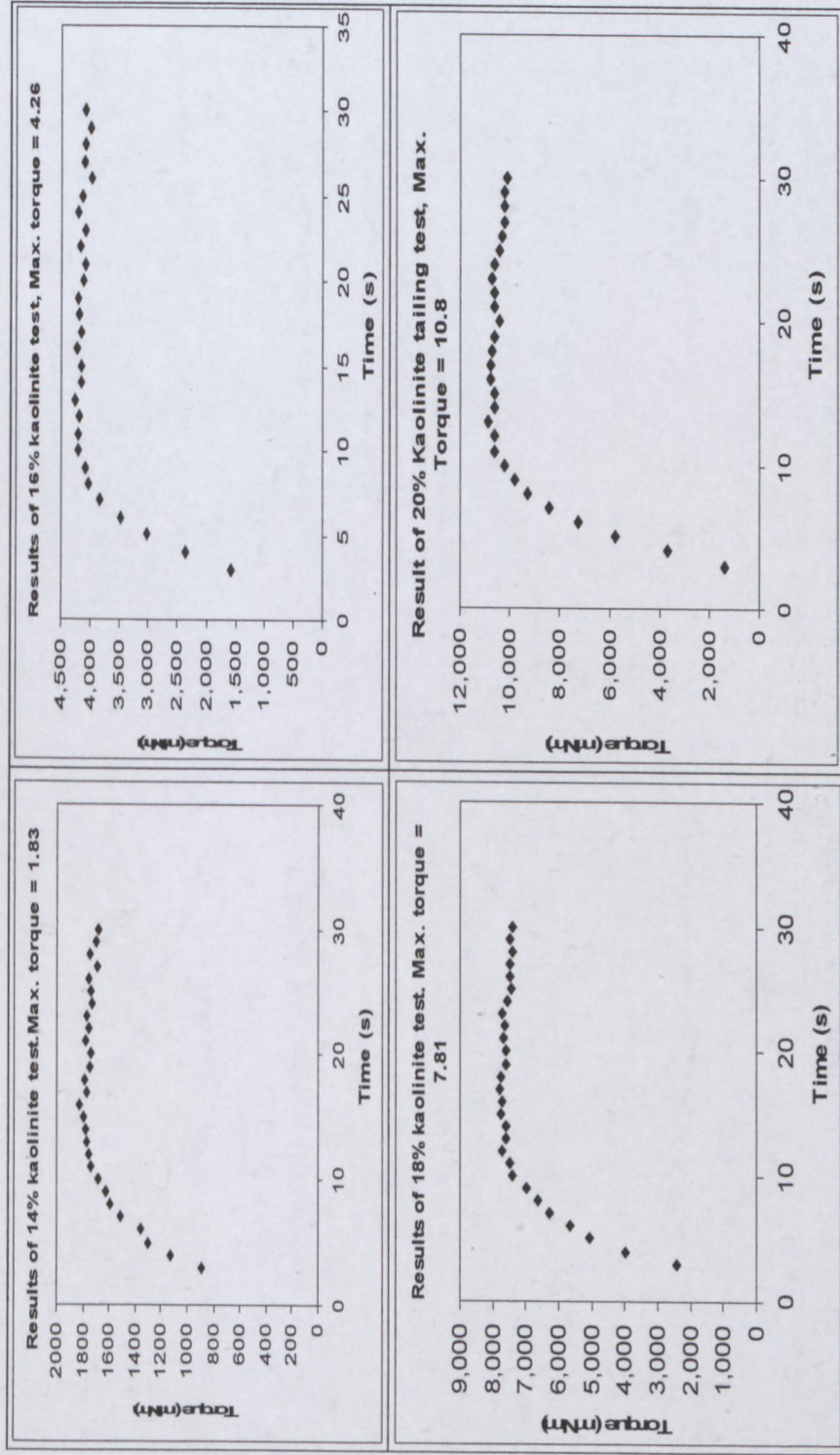
Table B. 27 Slump test for 5 mins 70:30 relative density at 1.6 Kaolinite tailings and sand using the hand-held cylinder

RESULTS ON THE 50 CENTS: (5mins 70:30 at 1.6)						Approximate cylinder		Lump model		Cylinder model								
Relative density Density (Kg/m ³) g (m.s ⁻¹)		1.6 1600 9.81		Equations: $s' = \frac{h}{H} \tau_y = \rho g H \tau_y$		$\tau_y' = \frac{1}{2} - \frac{1}{2} \sqrt{s'}$		Vane		$\tau_y' = 0.5(1 - S') e^{\sqrt{3}(-s')}$ $S' = 1 - 2\tau_y'(1 - \ln(2\tau_y'))$								
								τ_y 144.1155										
Without silicone spray :																		
						Speed	Time	H (mm)	H _r (mm)	h (mm)	s'	τ_y'	Approx.cyl τ_y	Calc. from vane τ_y	τ_y'	Lump Model 0	τ_y	τ_y'
With silicone spray :						24.44	1.82	75	44.48	30.52	0.41	0.18	206.46	0.13	0.15	167.12	0.12	141.11

Table B. 28 Slump test for 10 mins 70:30 relative density at 1.6 Kaolinite tailings and sand using the hand-held cylinder

APPENDIX C – VANE DATA

Table C. 1 Torque as a function of time for kaolinite tailings



Appendix C – Vane Data

Table C. 2 Torque as a function of time for kaolin tailings

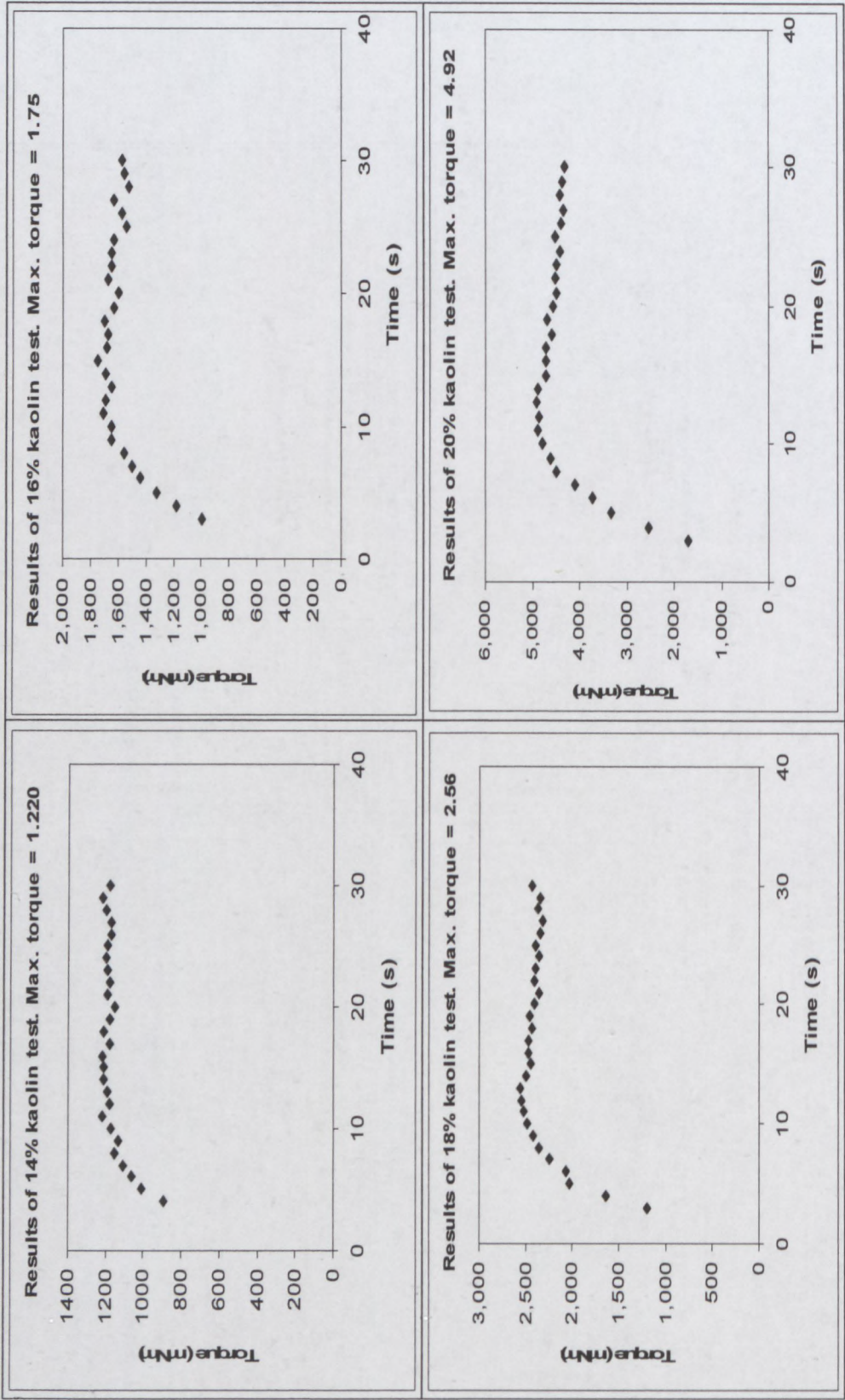


Table C. 3 Torque as a function of time for 90:10 kaolinite tailings and sand for each relative density and shear period

Appendix C – Vane Data

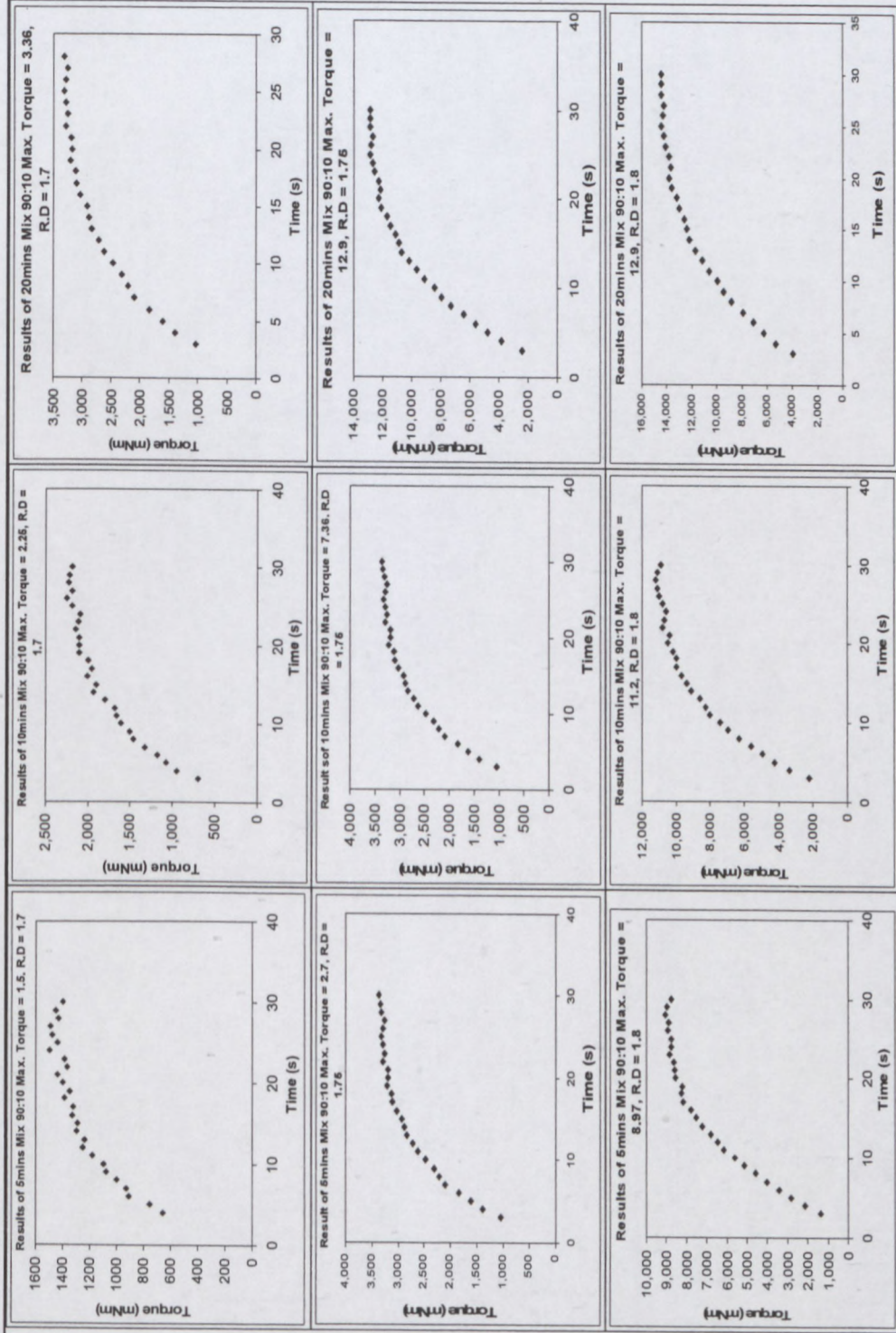


Table C. 4 Torque as a function of time for 80:20 kaolinite tailings and sand for each relative density and shear period

Appendix C – Vane Data

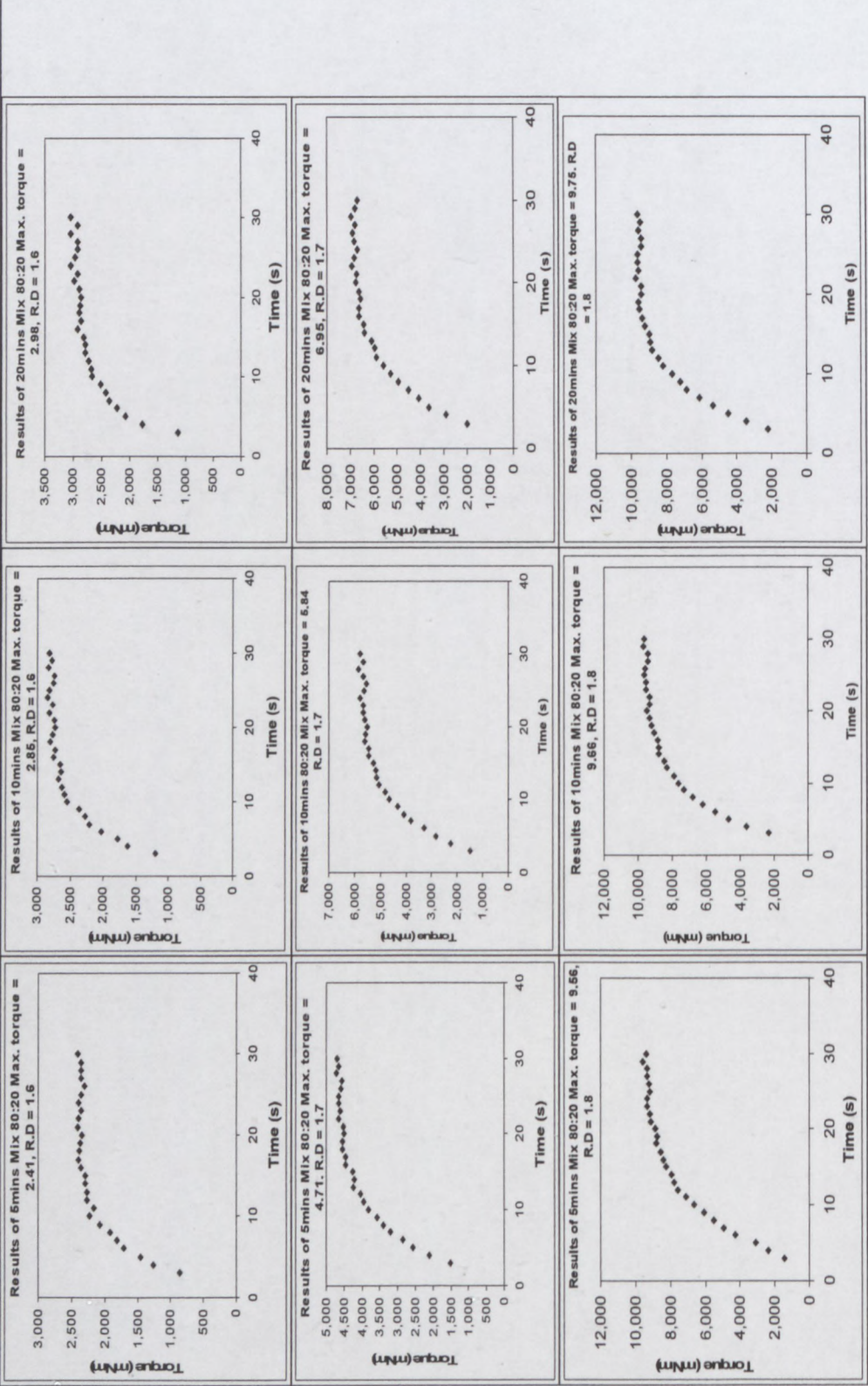
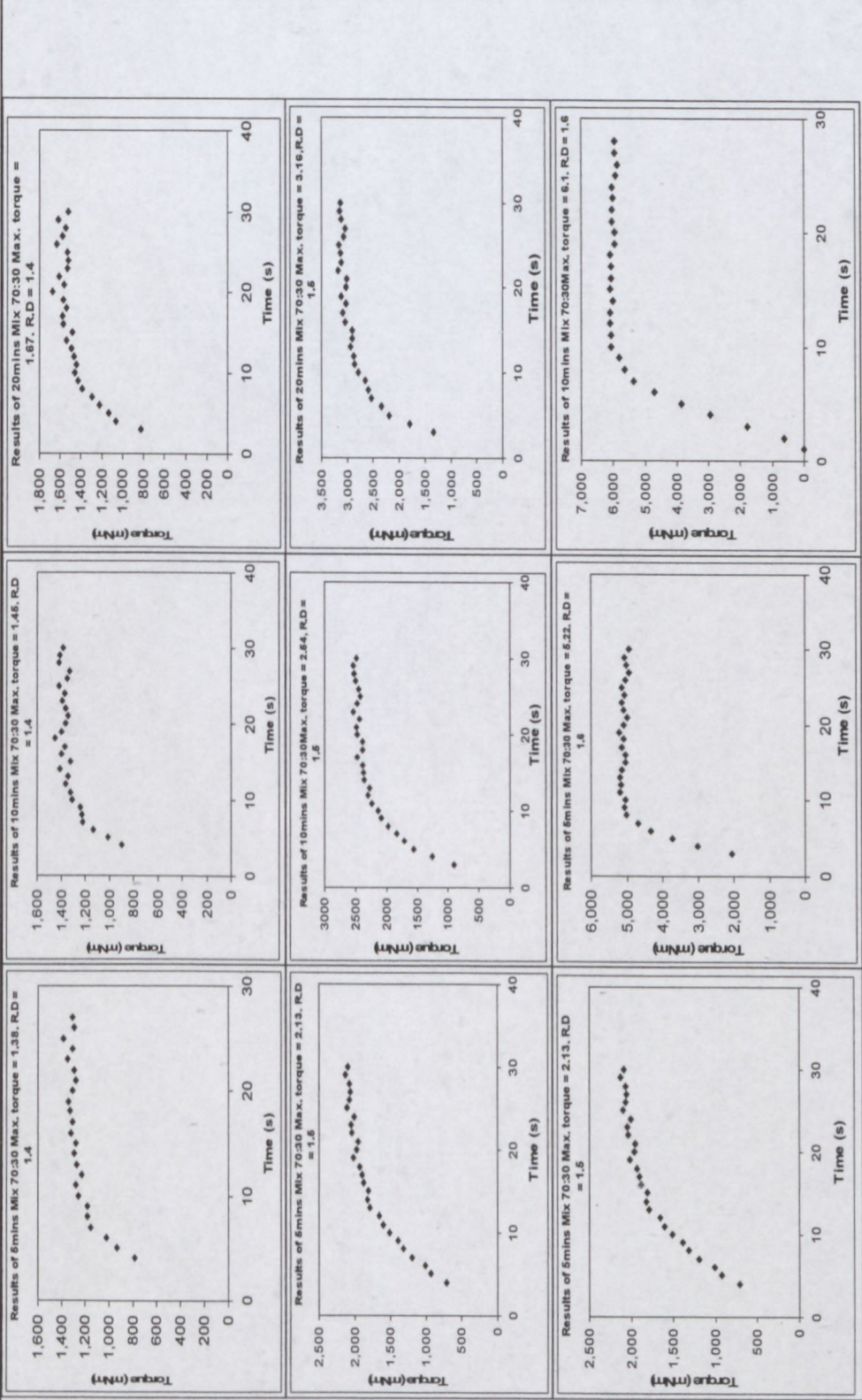


Table C. 5 Torque as a function of time for 70:30 kaolinite tailings and sand for each relative density and shear period

Appendix C – Vane Data



APPENDIX D – ANALYSIS OF RESULTS

Table D: 1 Validation of yield stress models on yield stress

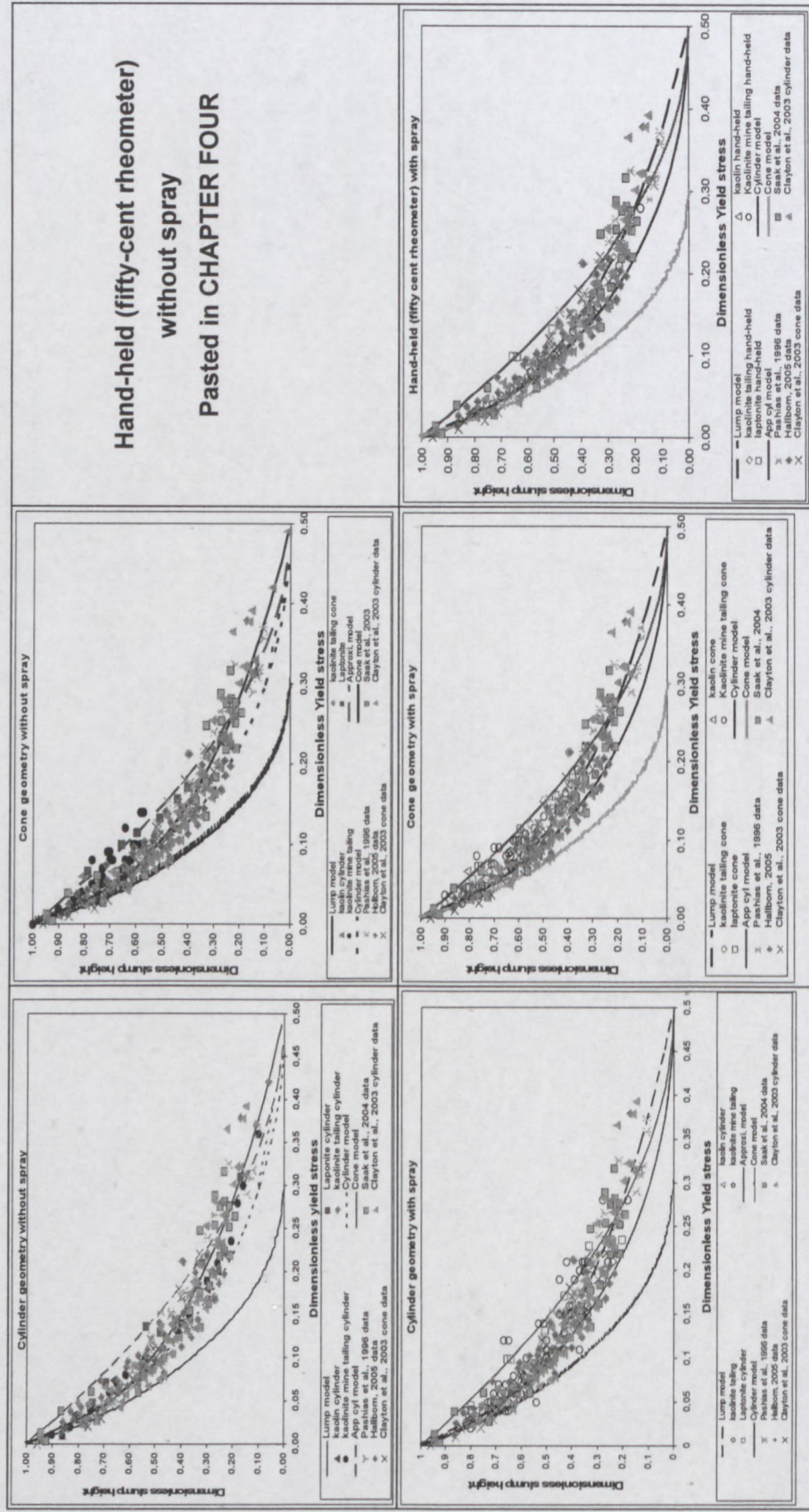


Table D: 2 Validation of yield stress models on yield stress

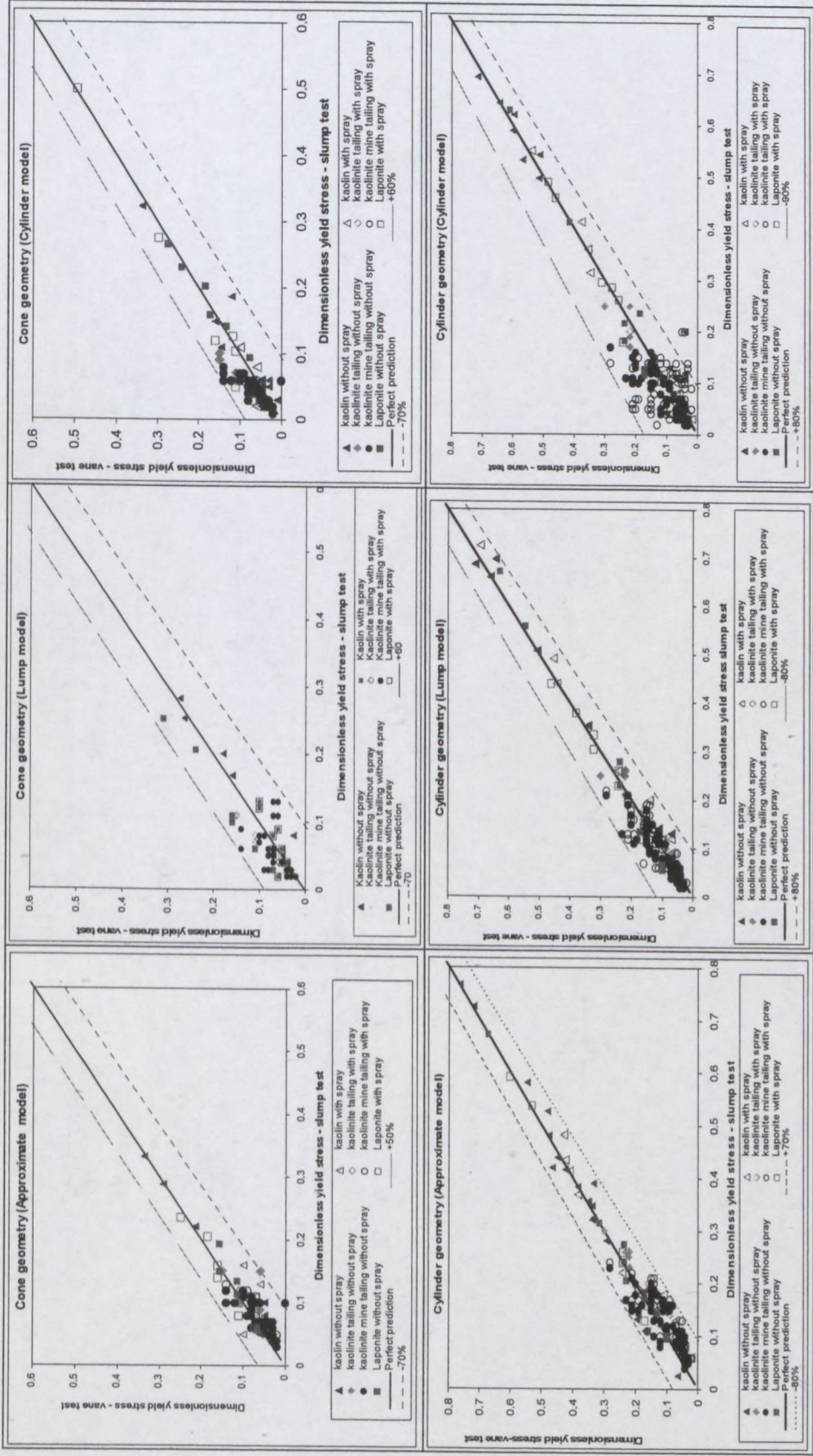


Table D: 3 Summary for validation of yield stress models

Cylinder geometry

Models	Ave. τ_v' slump	Min. τ_v' slump	Max. τ_v' slump	St.dev. τ_v' slump
Approximate cylinder	40	0.04	0.83	80
Lump	0.12	0.02	0.49	80
Cylinder	0.12	0.02	0.49	80

Cone geometry

Models	Ave. τ_v' slump	Min. τ_v' slump	Max. τ_v' slump	St.dev.% τ_v' slump
Approximate cylinder	0.09	0.03	0.33	70
Lump	0.06	0.02	0.25	67
Cylinder	0.06	0.02	0.5	70

Table D: 4 Effect of slip on yield stress for materials with approximate model

Appendix D – Analysis of Results

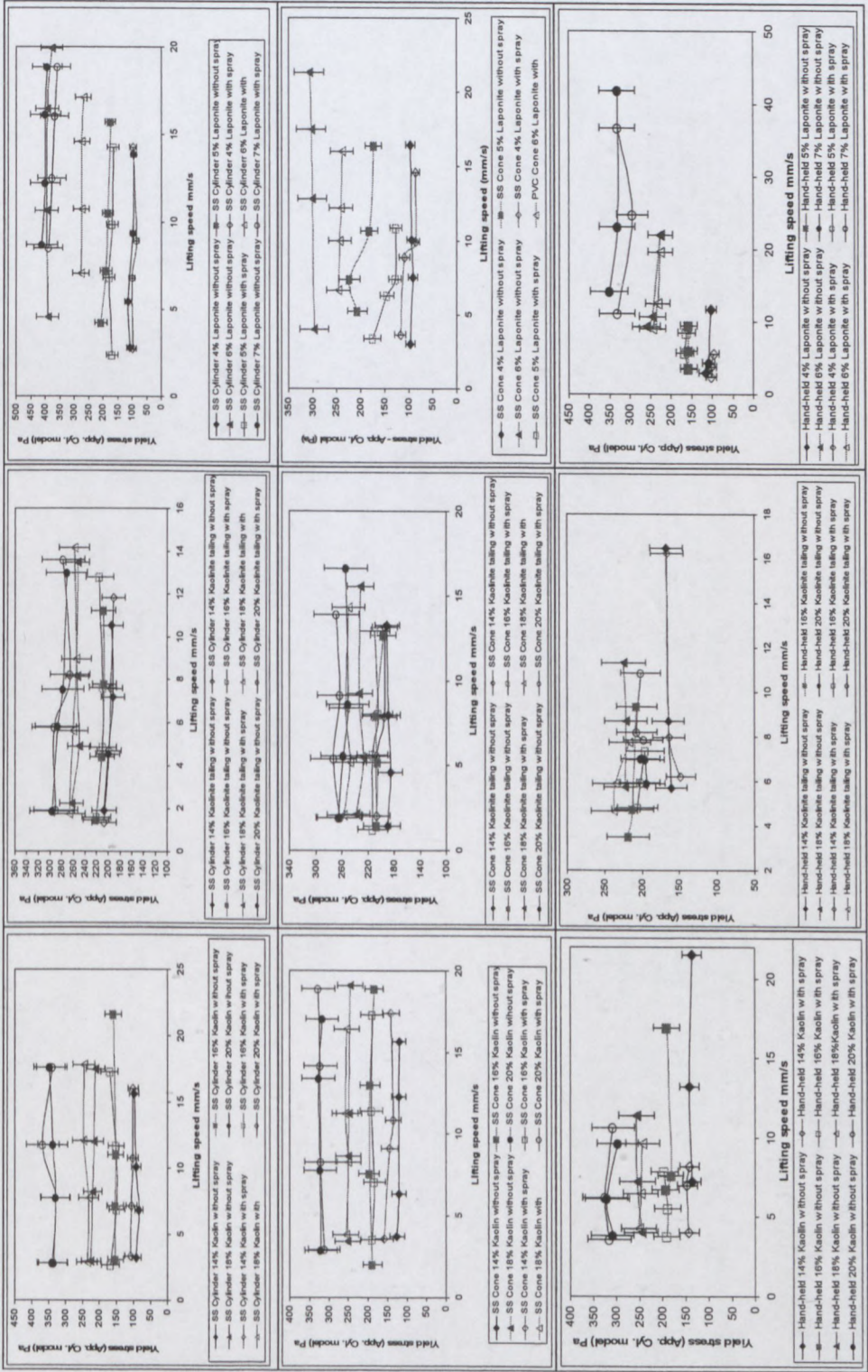


Table D: 5 Effect of slip on yield stress for materials with lump model



Table D: 6 Effect of slip on yield stress for materials with cylinder model

Appendix D – Analysis of Results

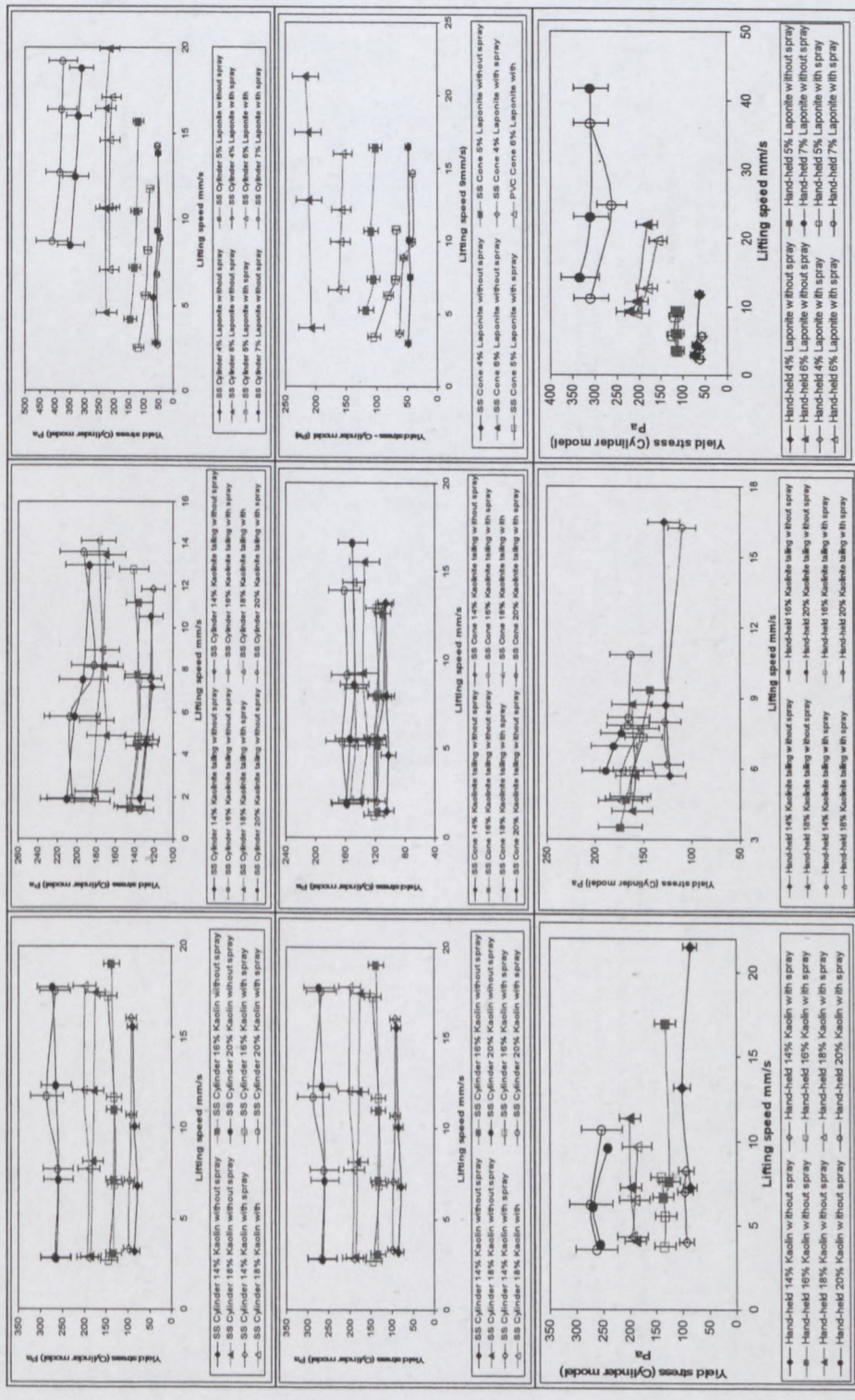


Table D: 7 Effect of slip on yield stress for materials with lump model

Appendix D – Analysis of Results

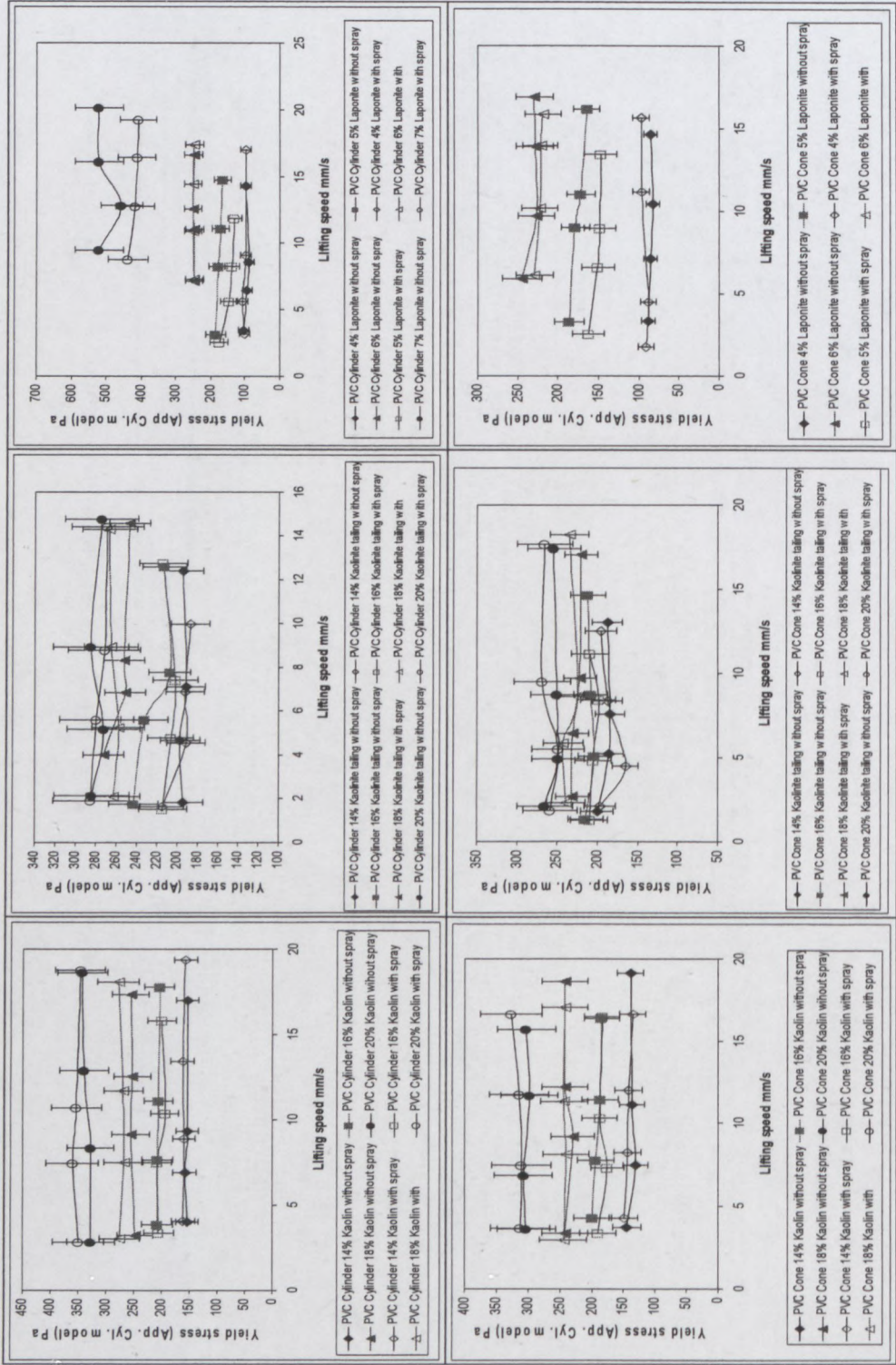


Table D: 8 Effect of slip on yield stress for materials with lump model

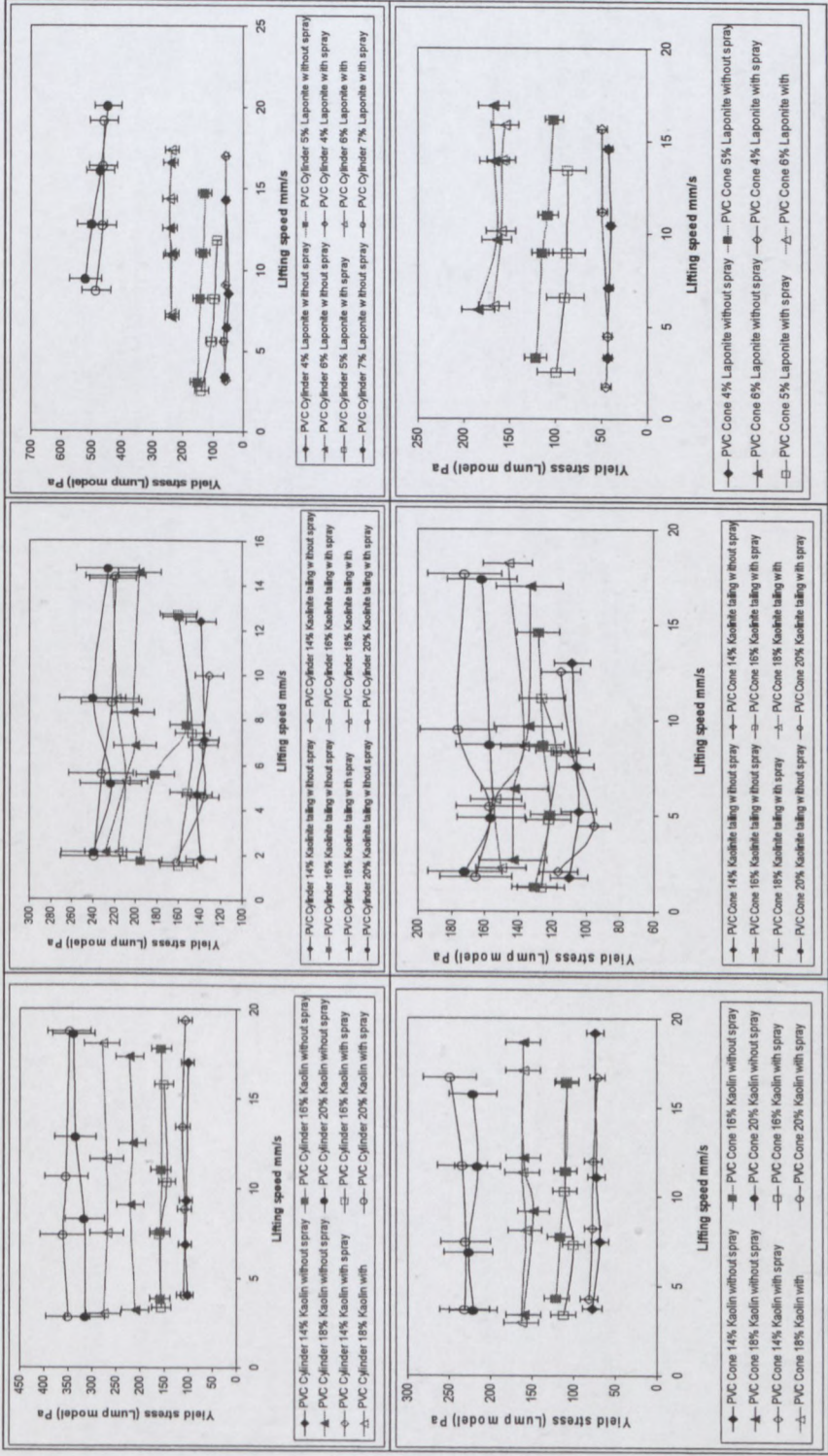
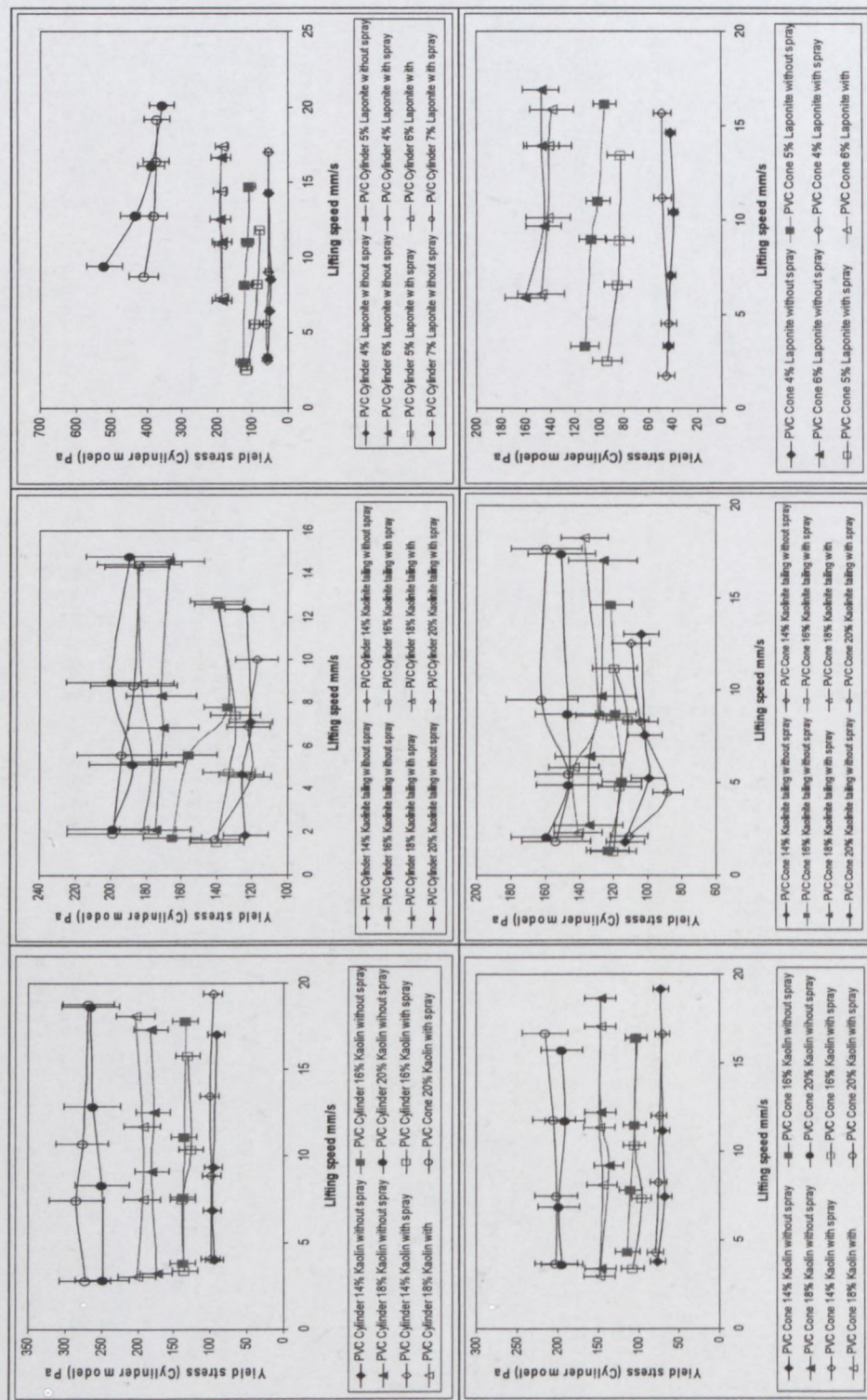


Table D: 9 Effect of slip on yield stress for materials with lump model



Appendix D – Analysis of Results

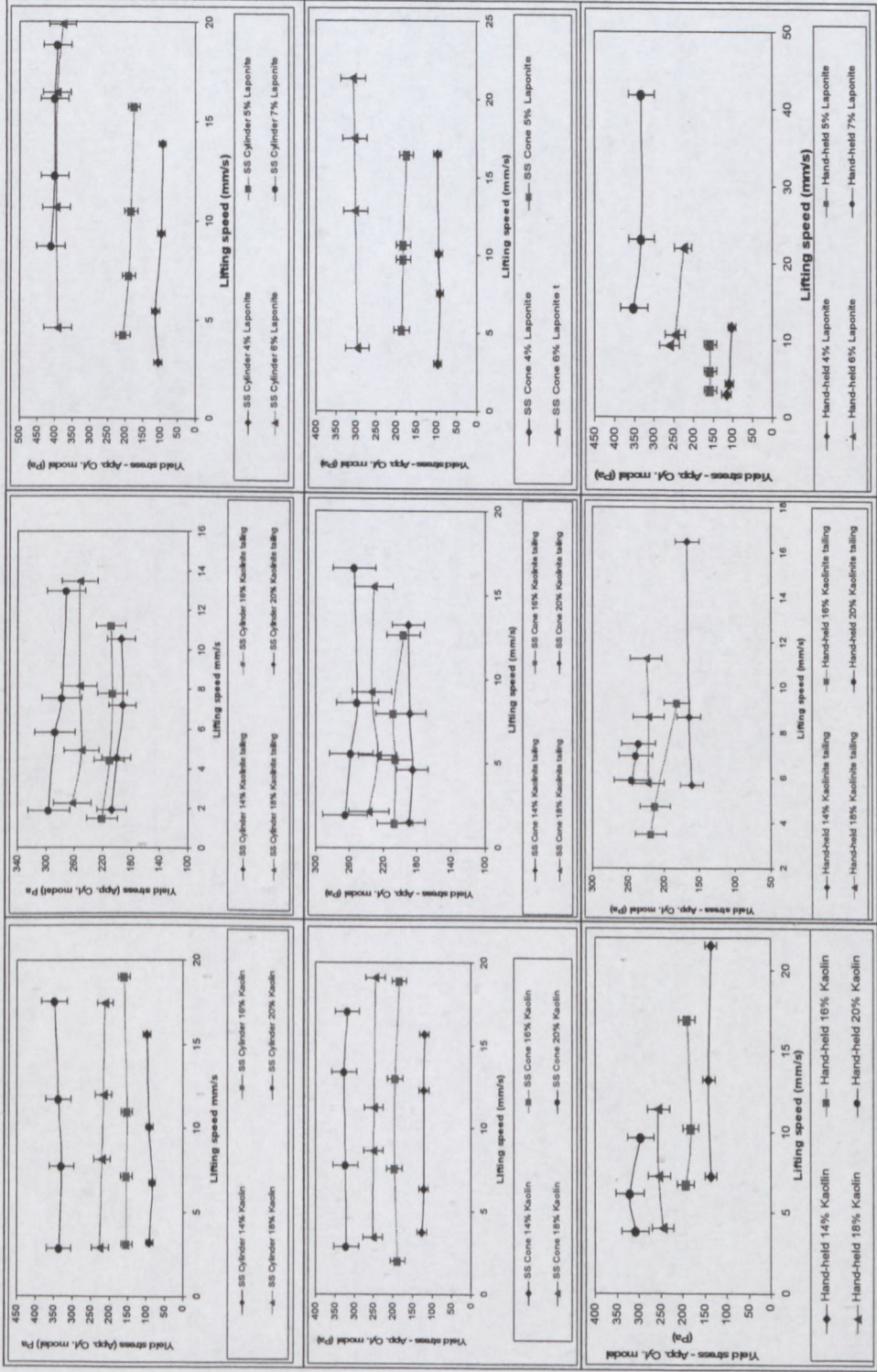


Table D: 11 Effect of lift speed on yield stress for materials with lump model

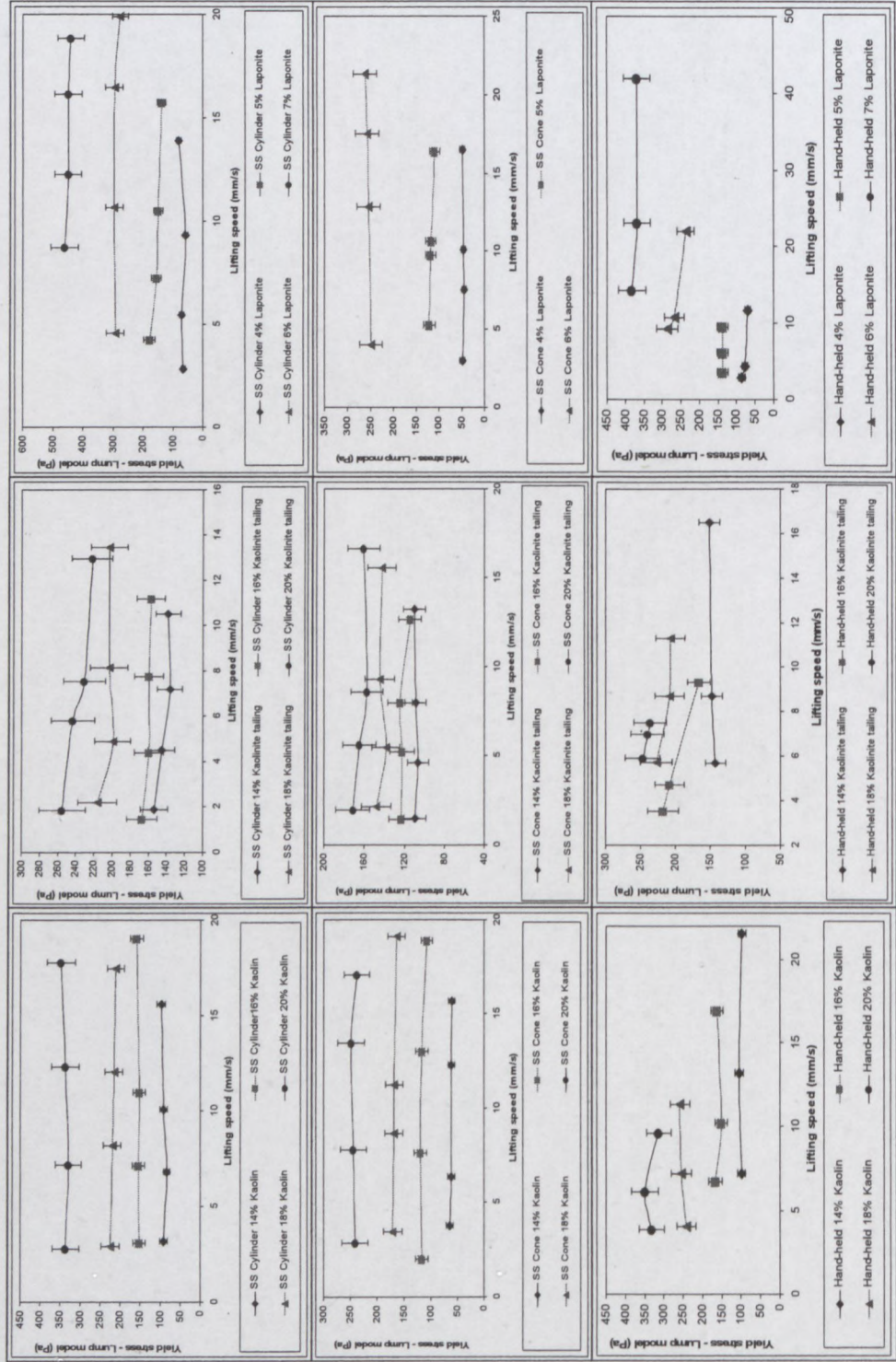


Table D: 12 Effect of lift speed on yield stress for materials with cylinder model

Appendix D – Analysis of Results

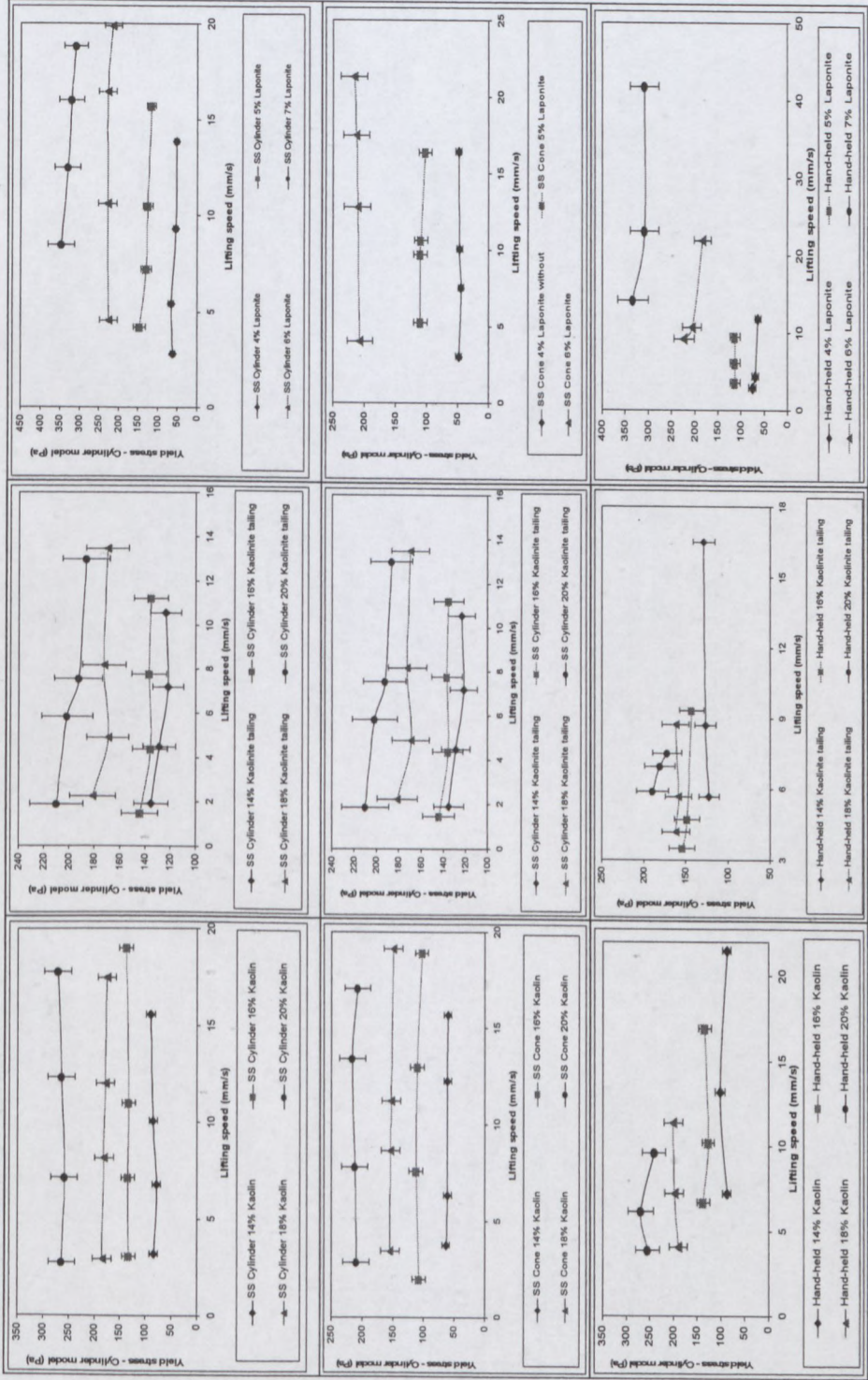


Table D: 13 Effect of lift speed on yield stress for materials with approximate model

Appendix D – Analysis of Results

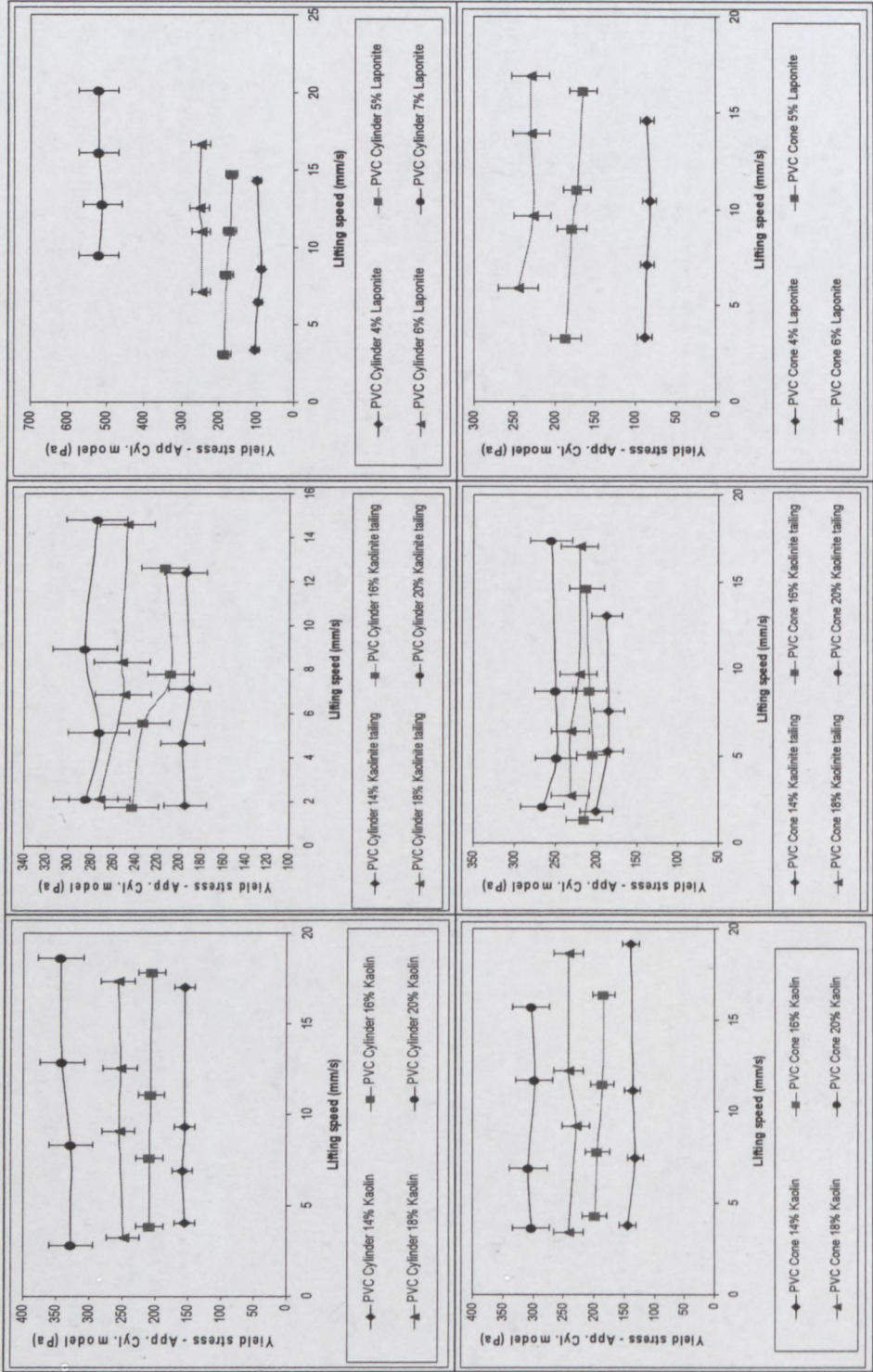


Table D: 14 Effect of lift speed on yield stress for materials with lump model

Appendix D – Analysis of Results

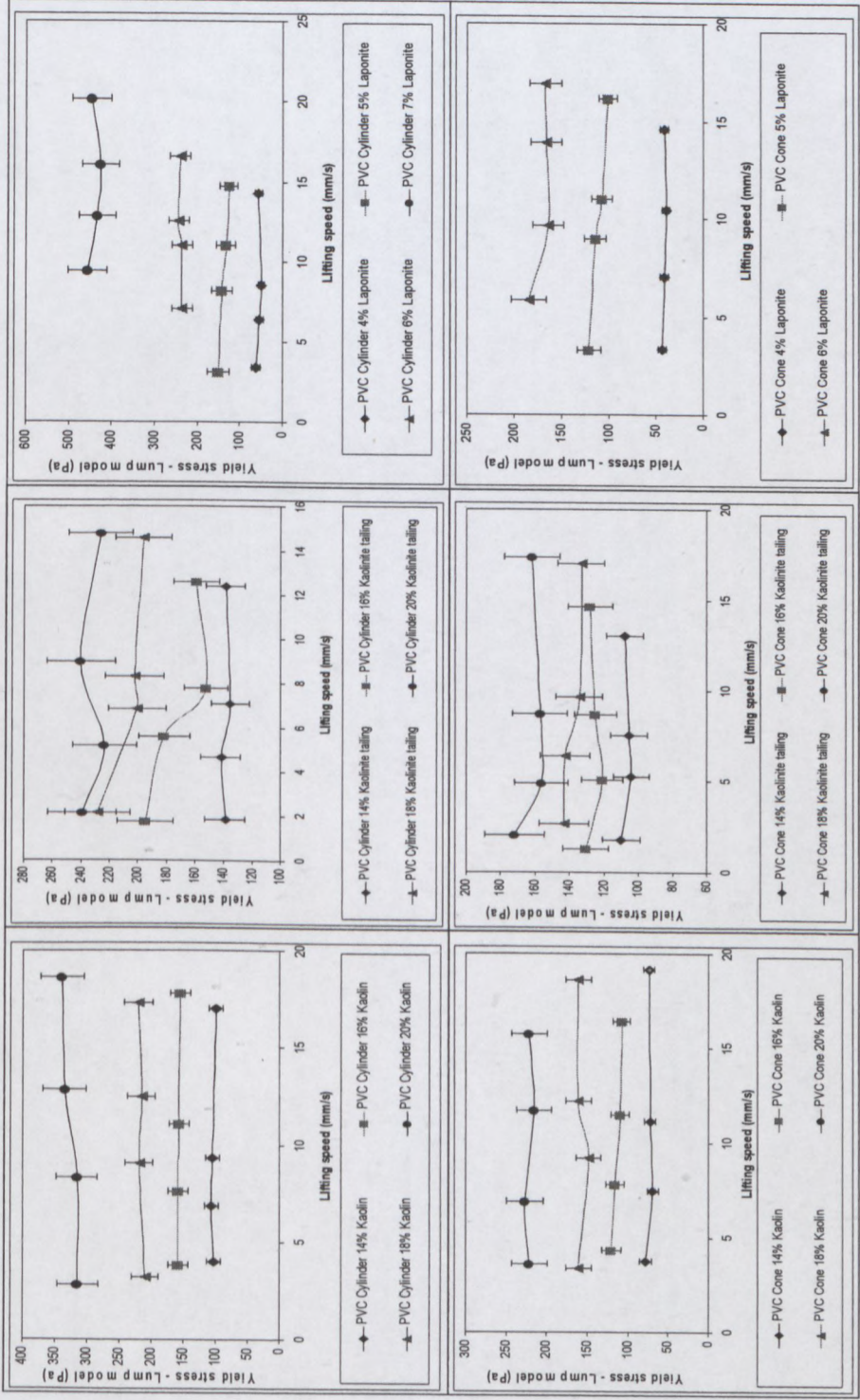


Table D: 15 Effect of lift speed on yield stress for materials with cylinder model

Appendix D – Analysis of Results

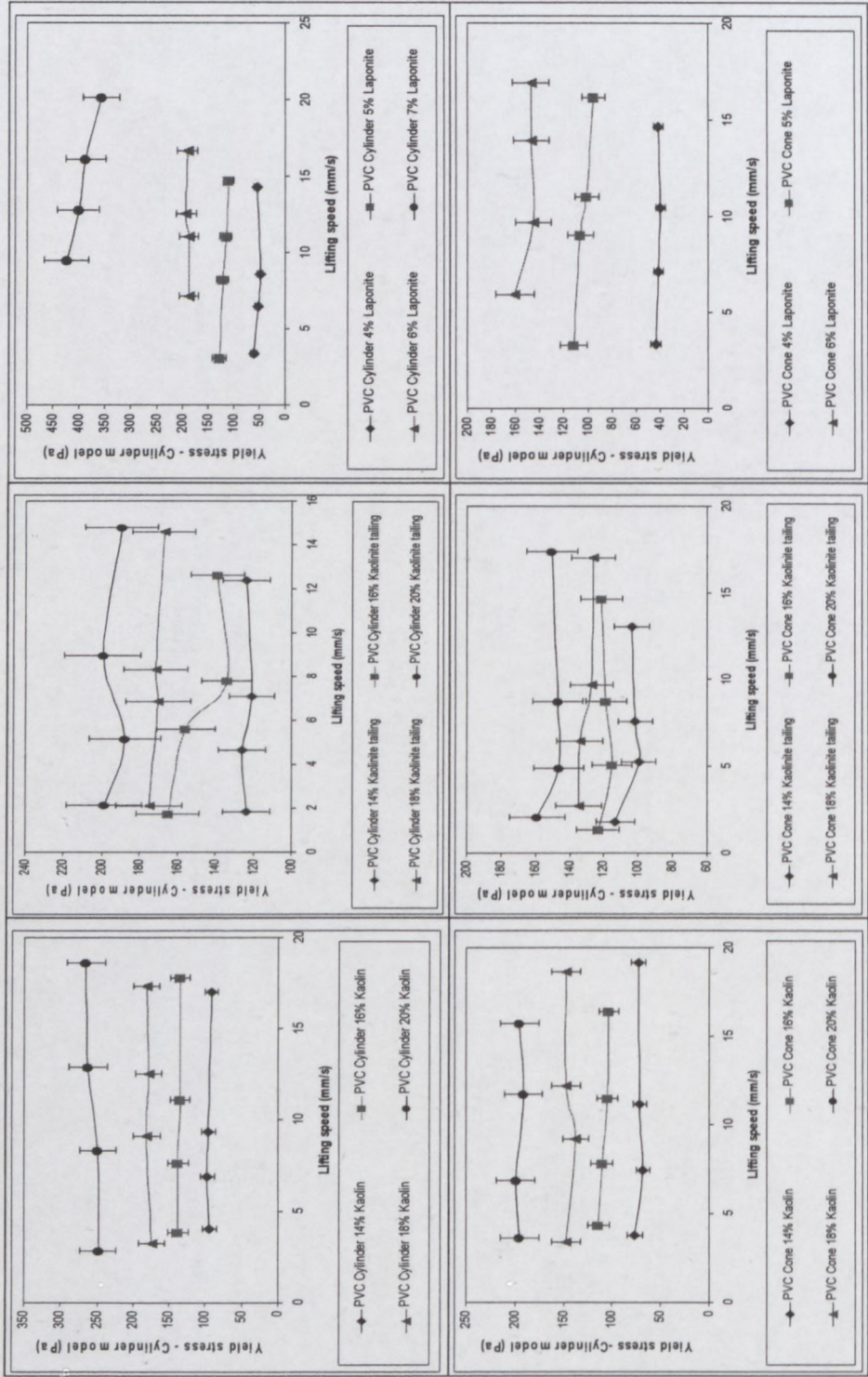


Table D: 16a Effect of stability on yield stress for three materials.

Appendix D – Analysis of Results

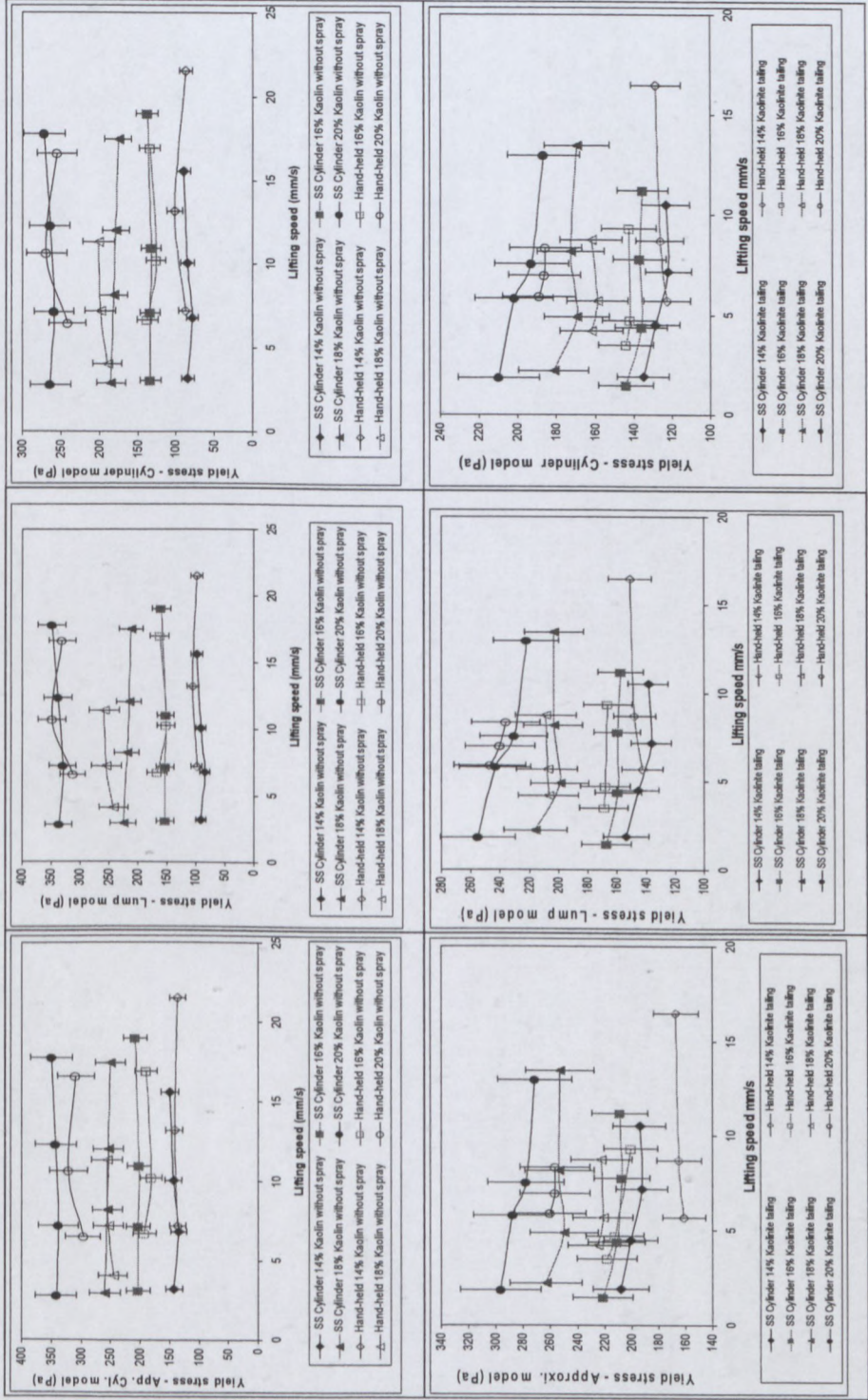


Table D: 16b Effect of stability on yield stress for three materials.

Appendix D – Analysis of Results

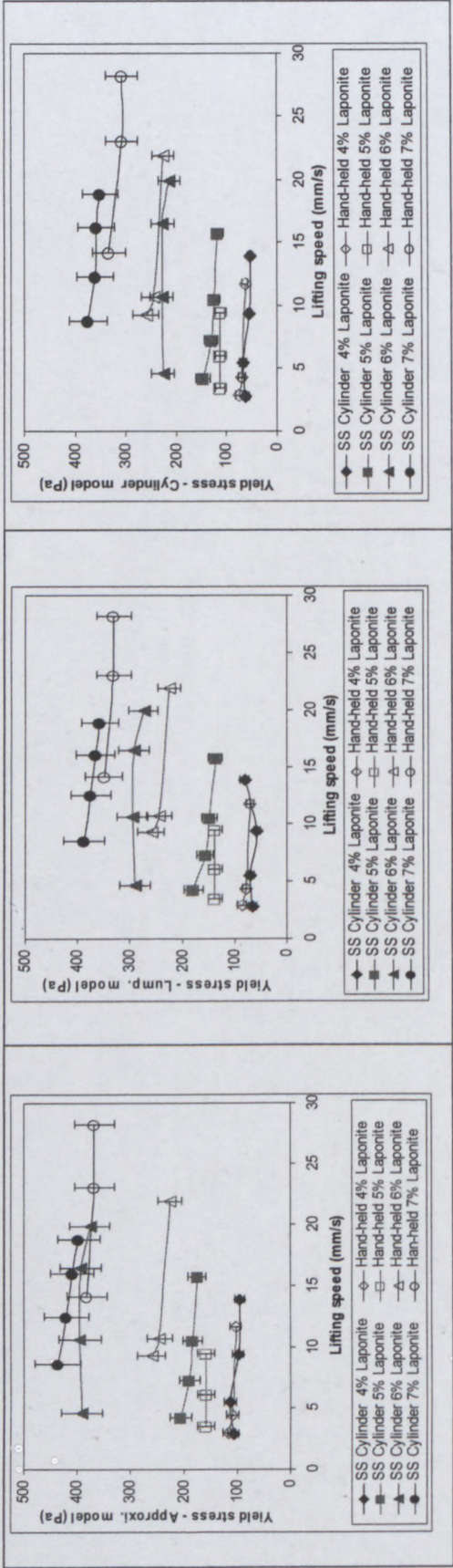


Table D: 17 Effect of stability on yield stress for three materials.

Appendix D – Analysis of Results

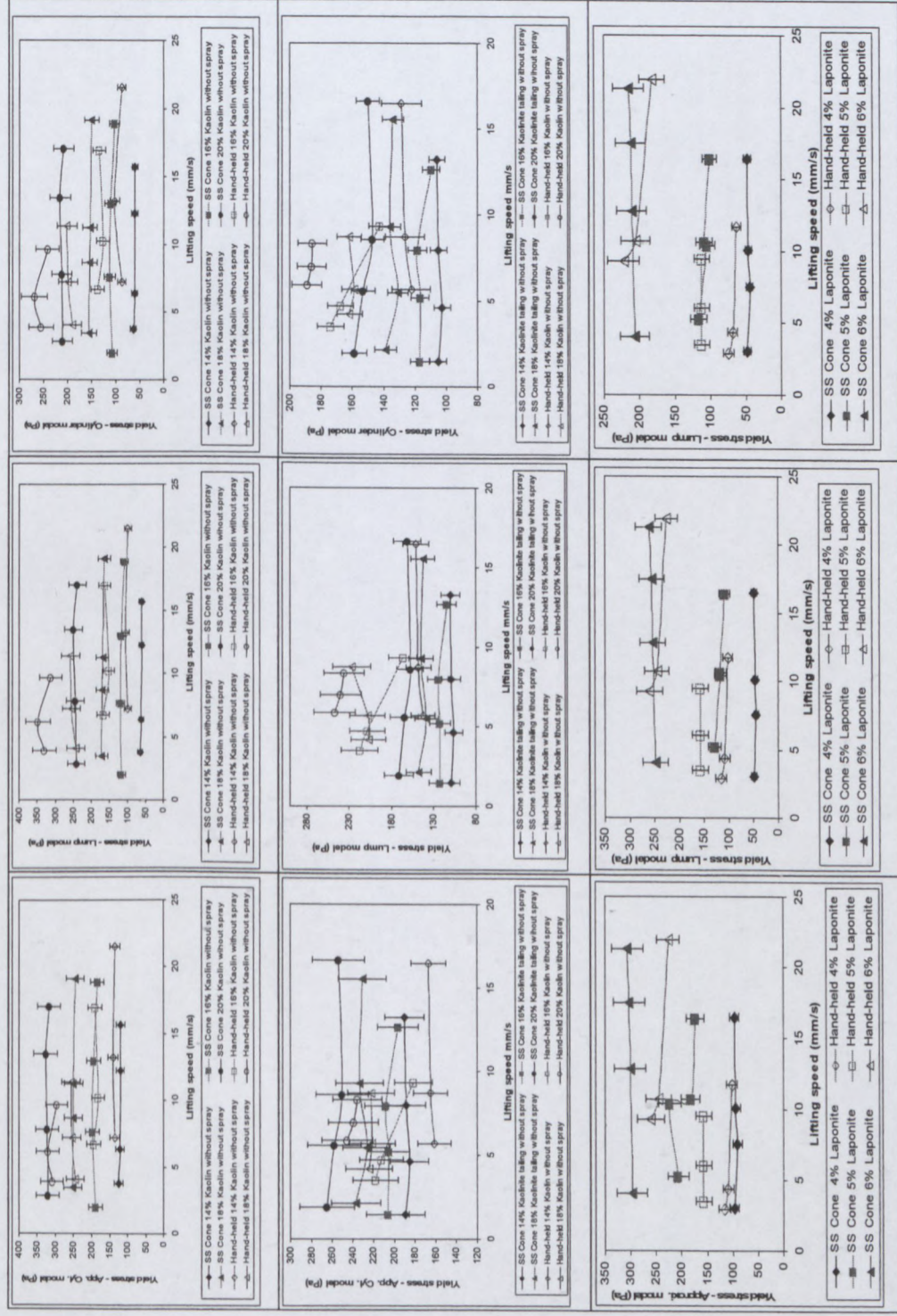


Table D: 18 Effect of stability on yield stress for materials.

Maxwell Nyekwe Icheigbo: Investigation of factors effecting yield stress determinations using the slump test.

Appendix D – Analysis of Results

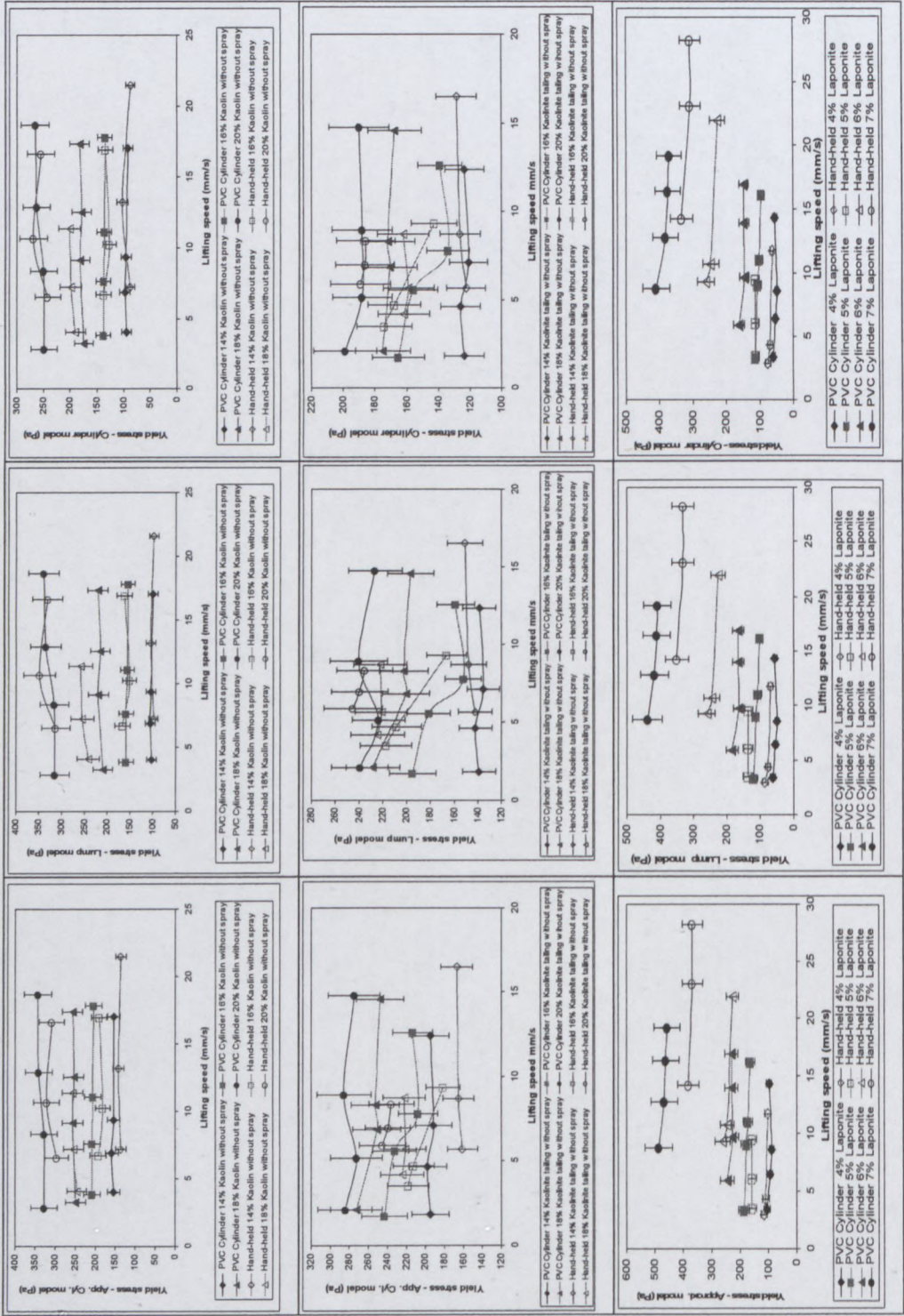


Table D: 19 Effect of stability on yield stress for materials.

Appendix D – Analysis of Results

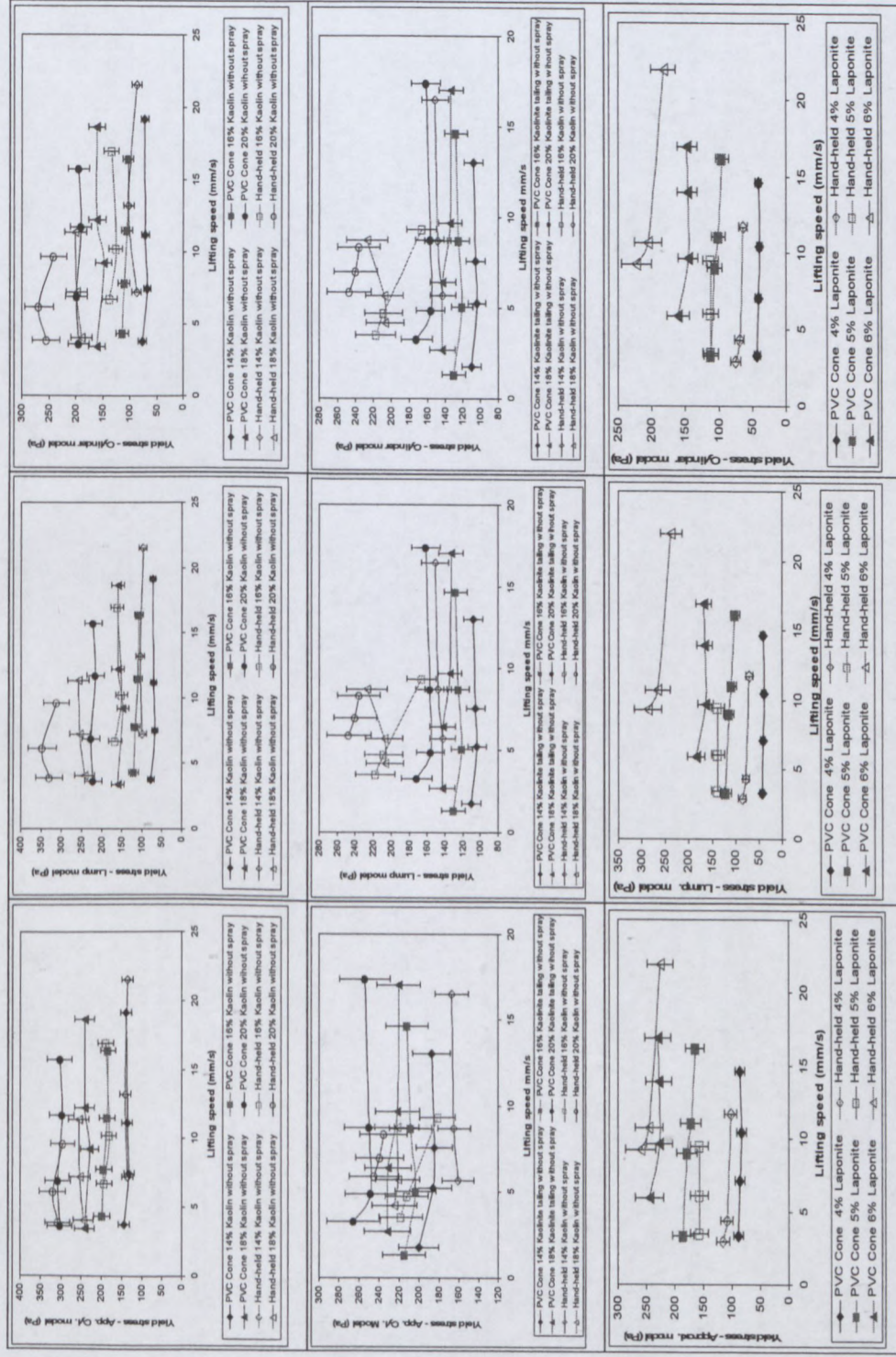


Table D: 20 Effect of geometry surface materials on yield stress for three materials.

Appendix D – Analysis of Results

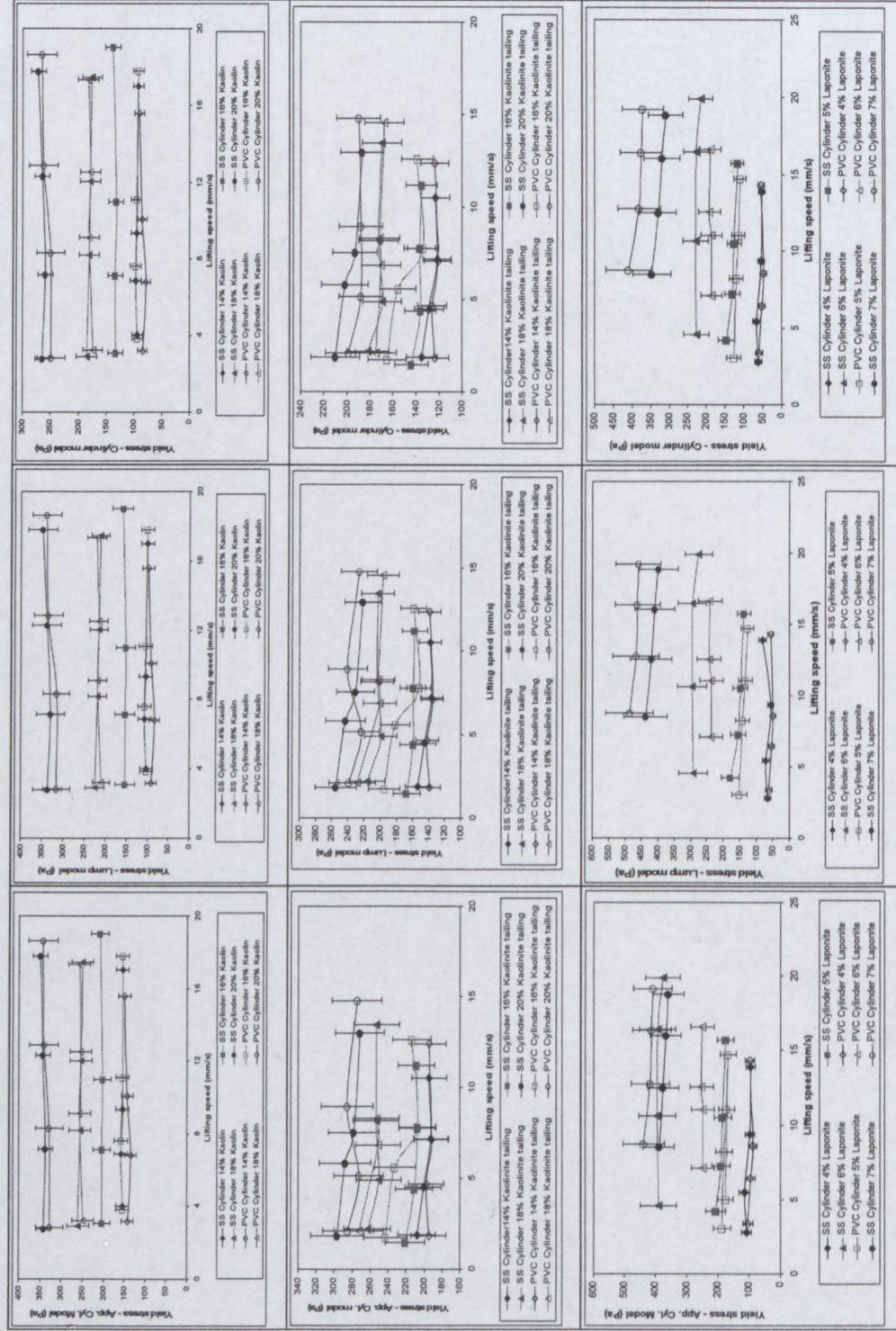


Table D: 21 Effect of geometry surface materials on yield stress for three materials.

Appendix D – Analysis of Results

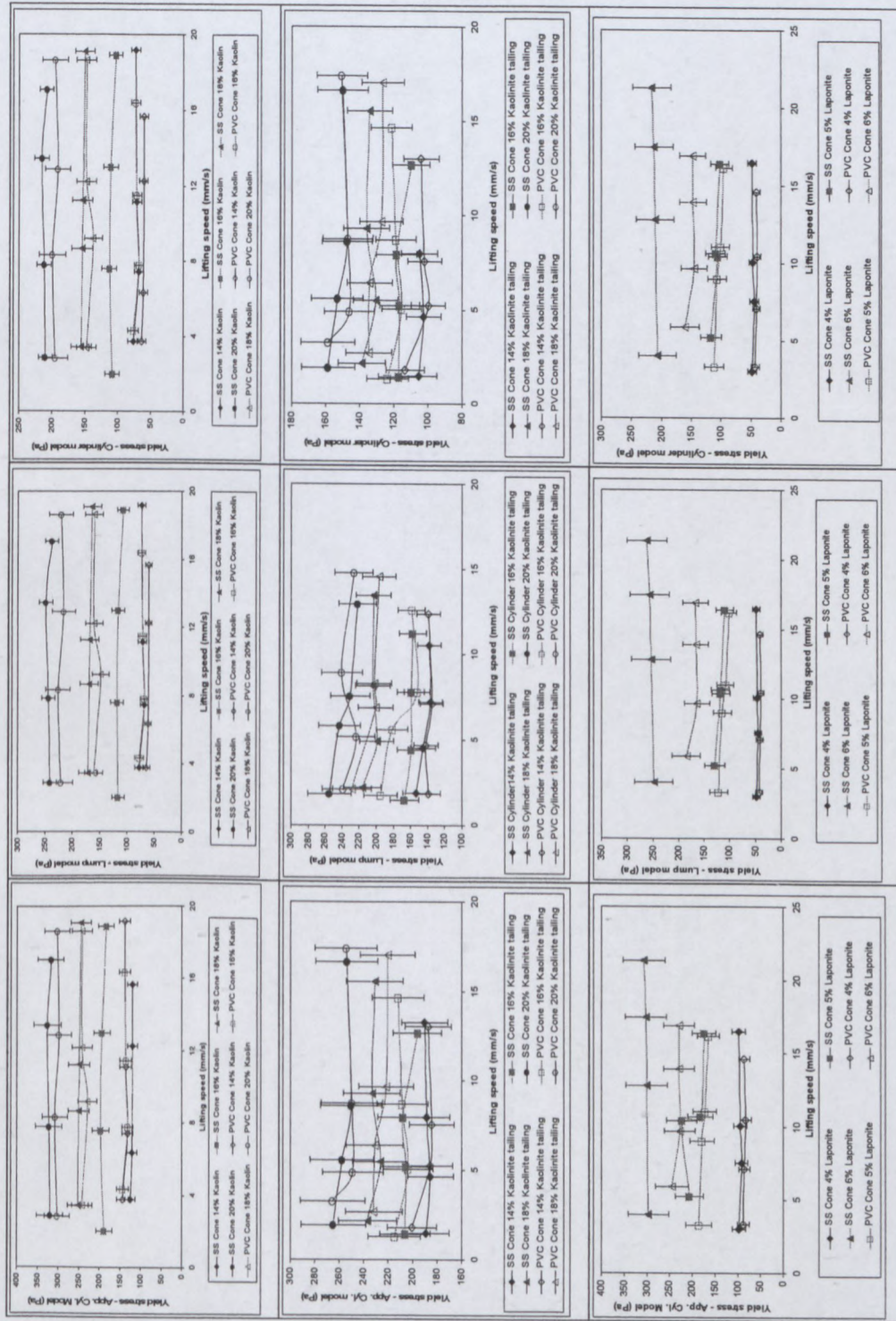
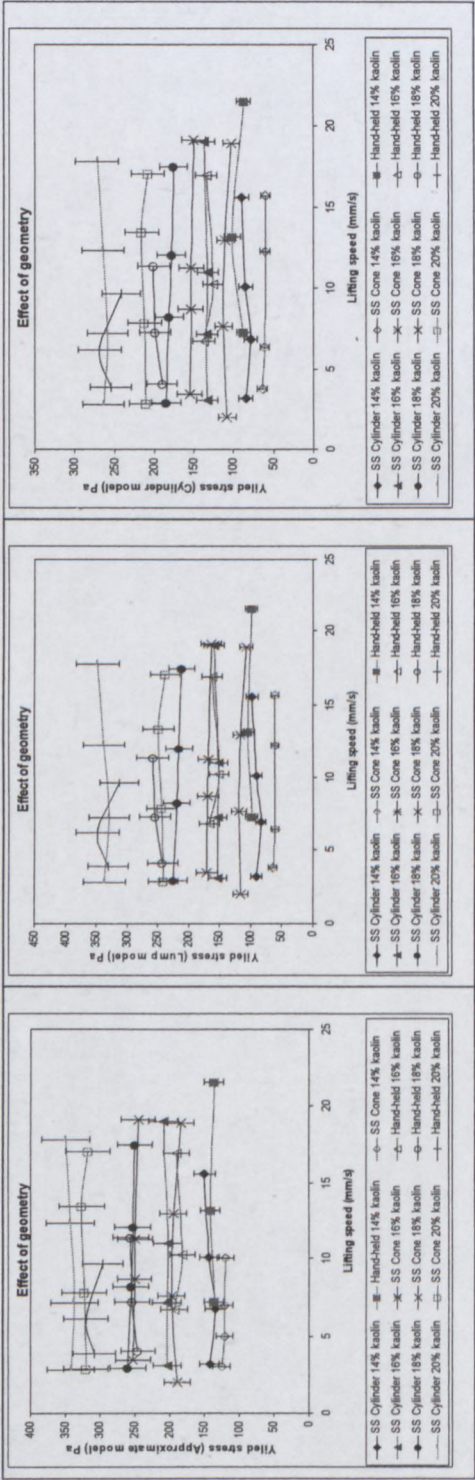


Table D: 22 Effect of geometry on yield stress for three materials.



Appendix D – Analysis of Results

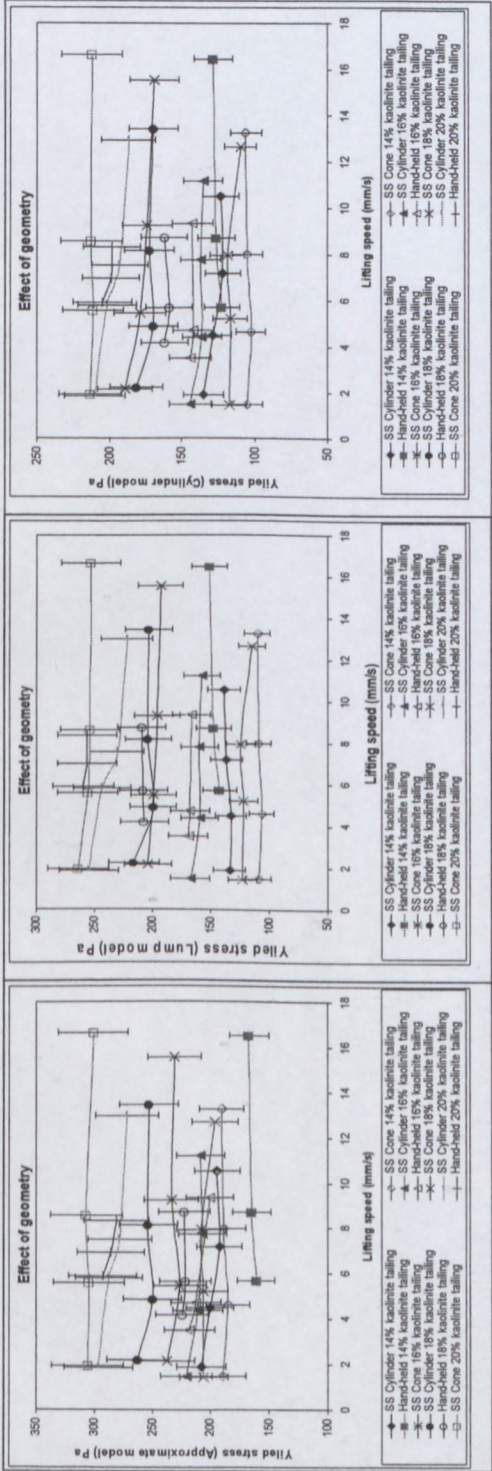


Table D: 22b Effect of geometry on yield stress for three materials.

Appendix D – Analysis of Results

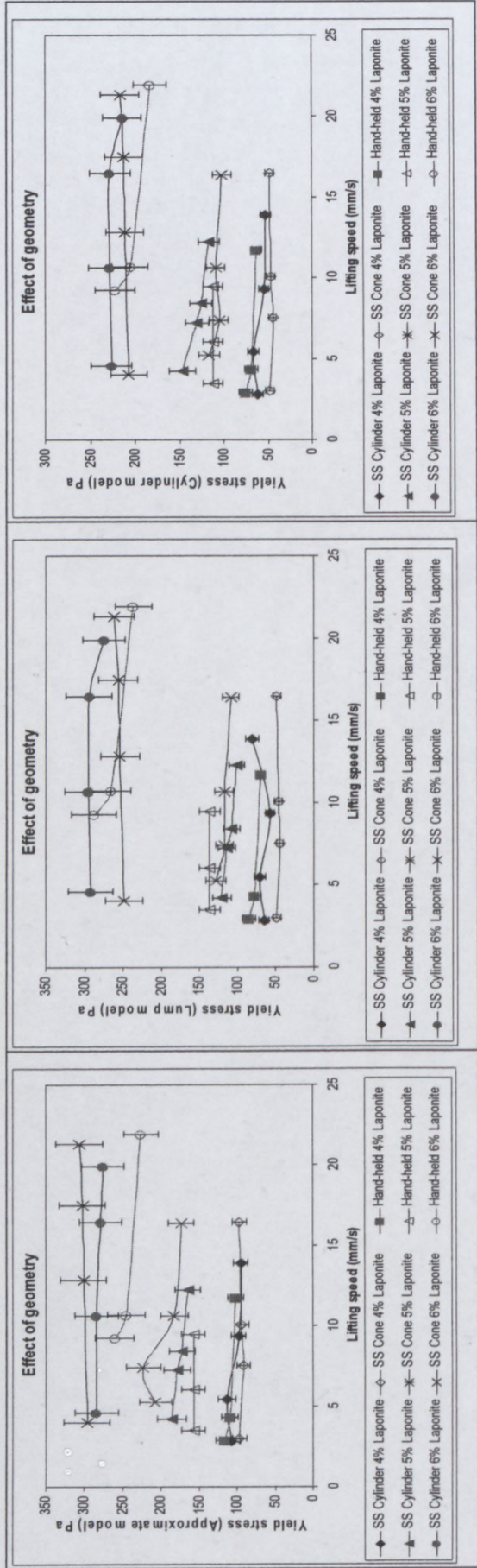


Table D: 23a Effect of geometry on yield stress for three materials.

Appendix D – Analysis of Results

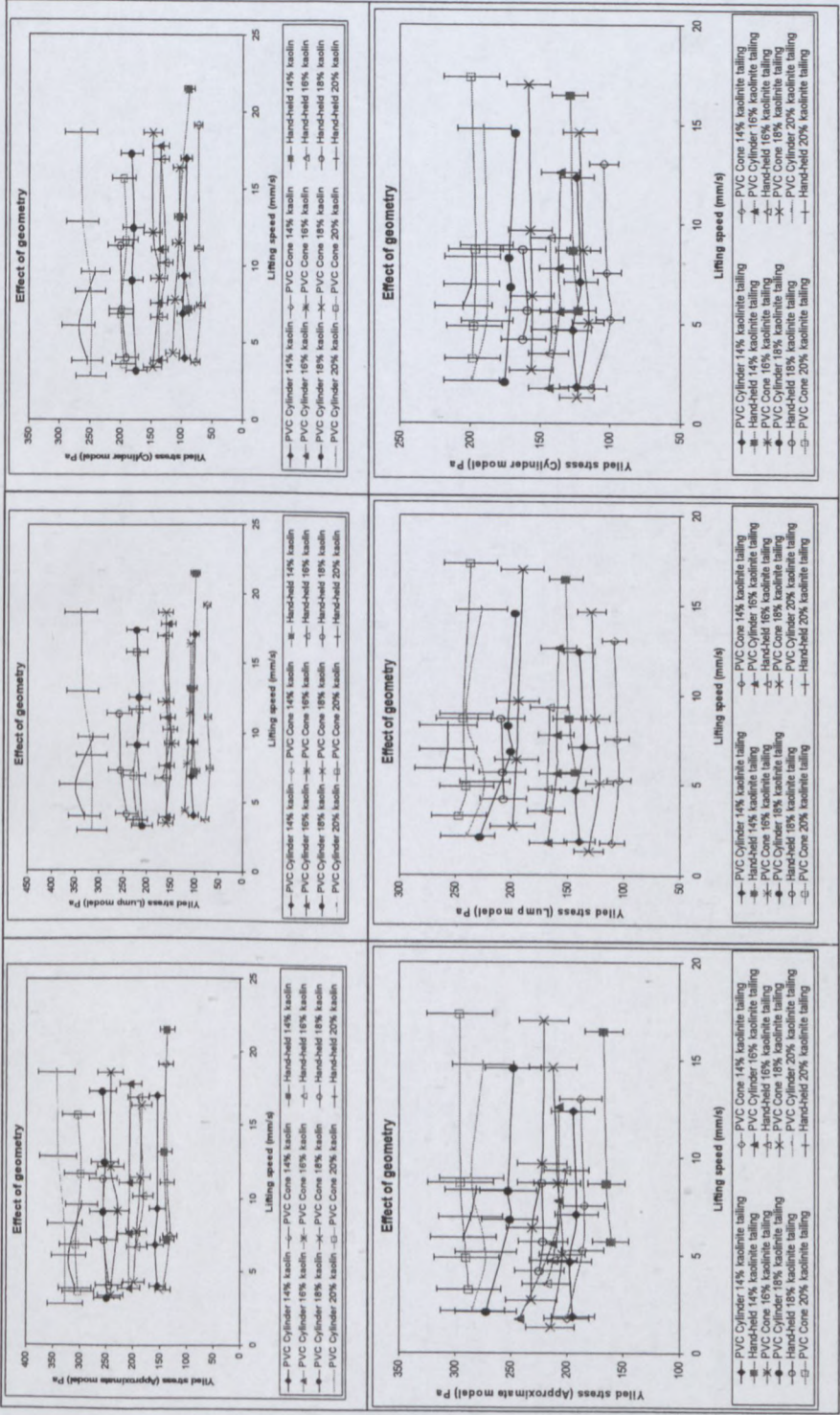
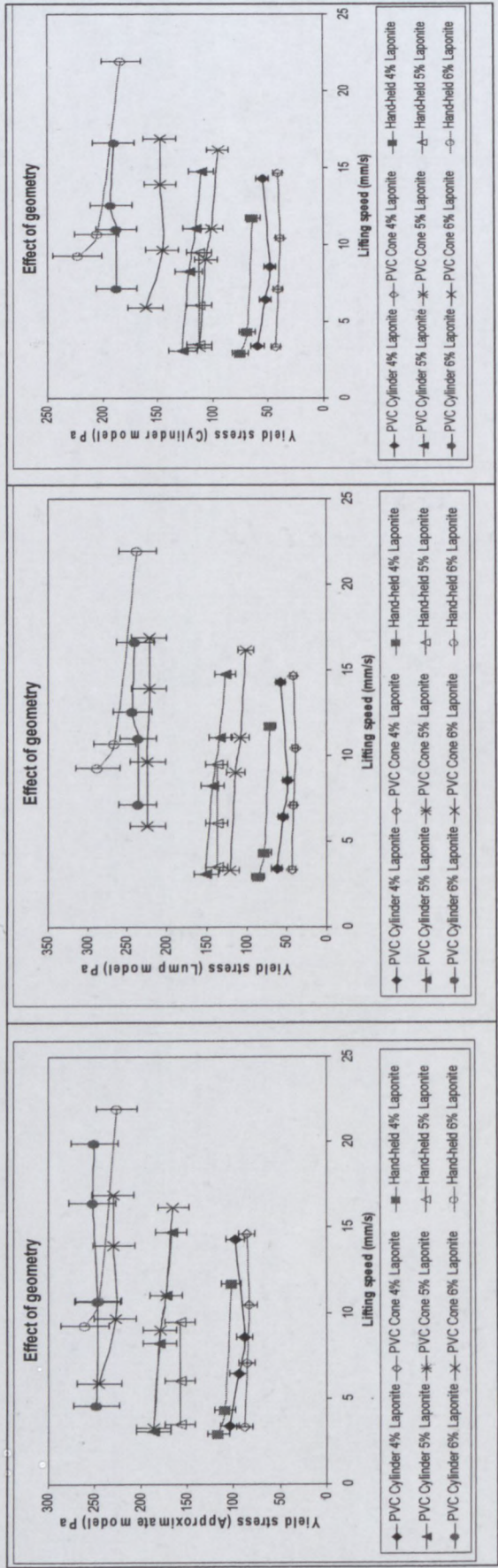


Table D: 23b Effect of geometry on yield stress for three materials.

Appendix D – Analysis of Results



APPENDIX E - PHOTOS

Table E: 1 Slump height of kaolinite tailings material using cone (stainless steel and PVC) for all concentrations

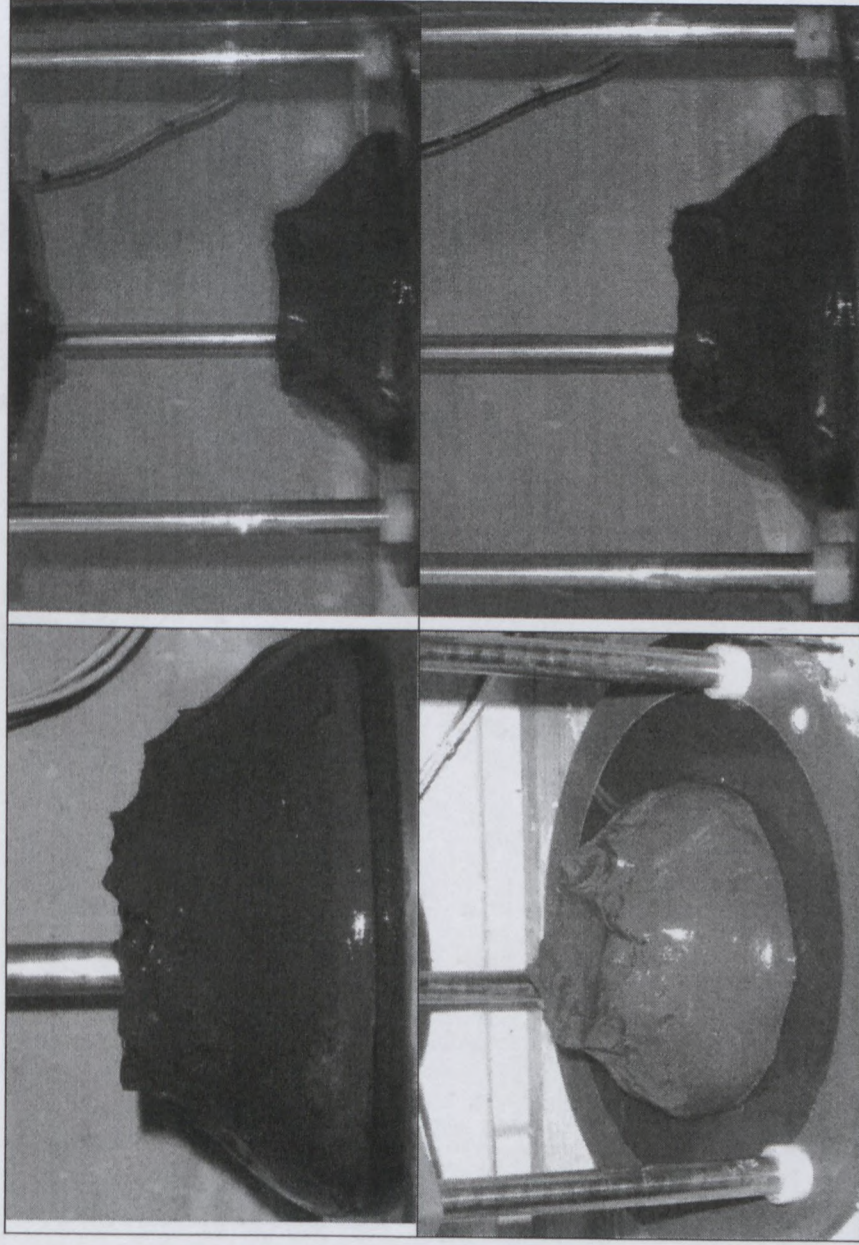


Table E: 2 Slump height of kaolinite tailings material using hand-held cylinder

E - Photos

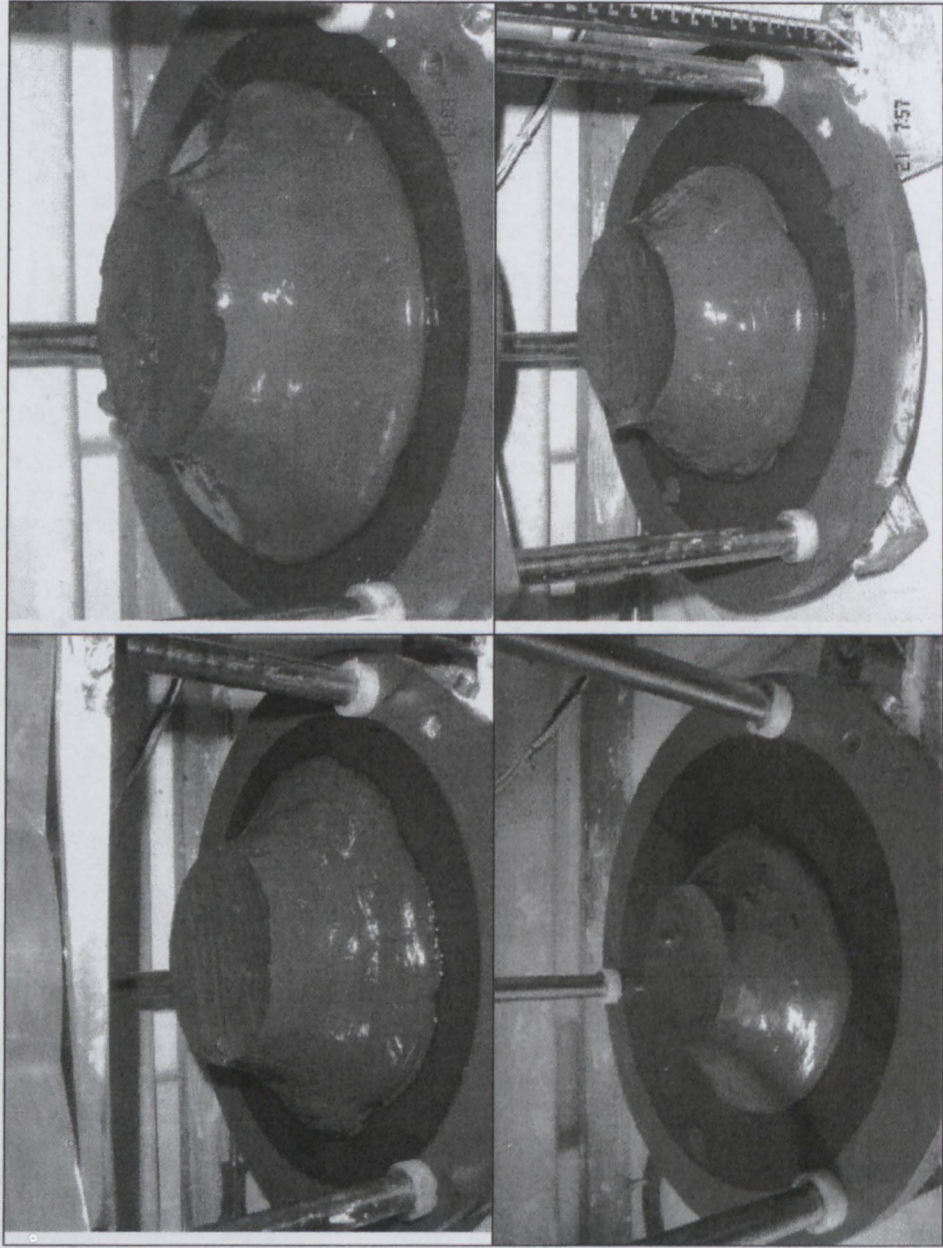


Table E: 3 Geometries (cone and cylinder) and hand-held cylinder used for the test work

E - Photos

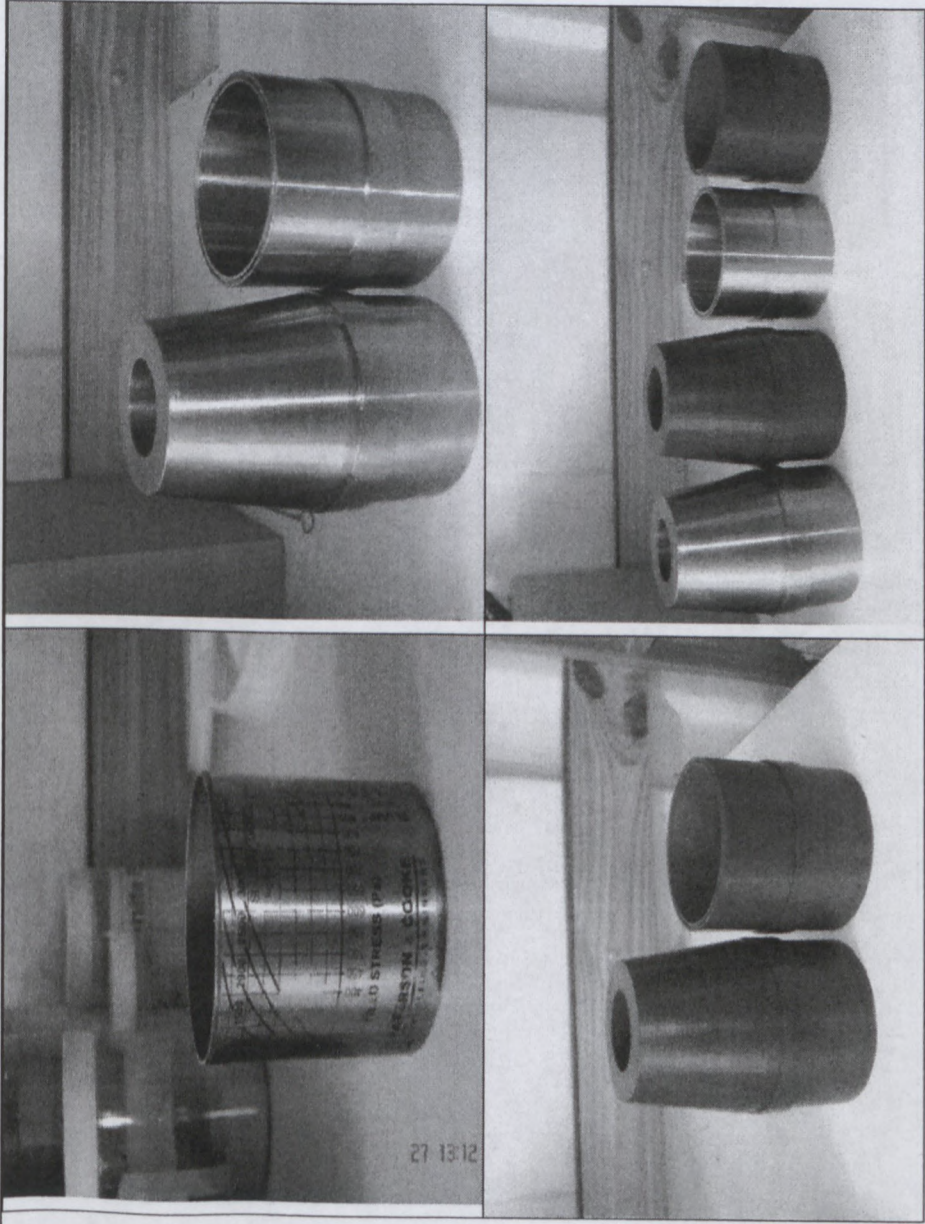
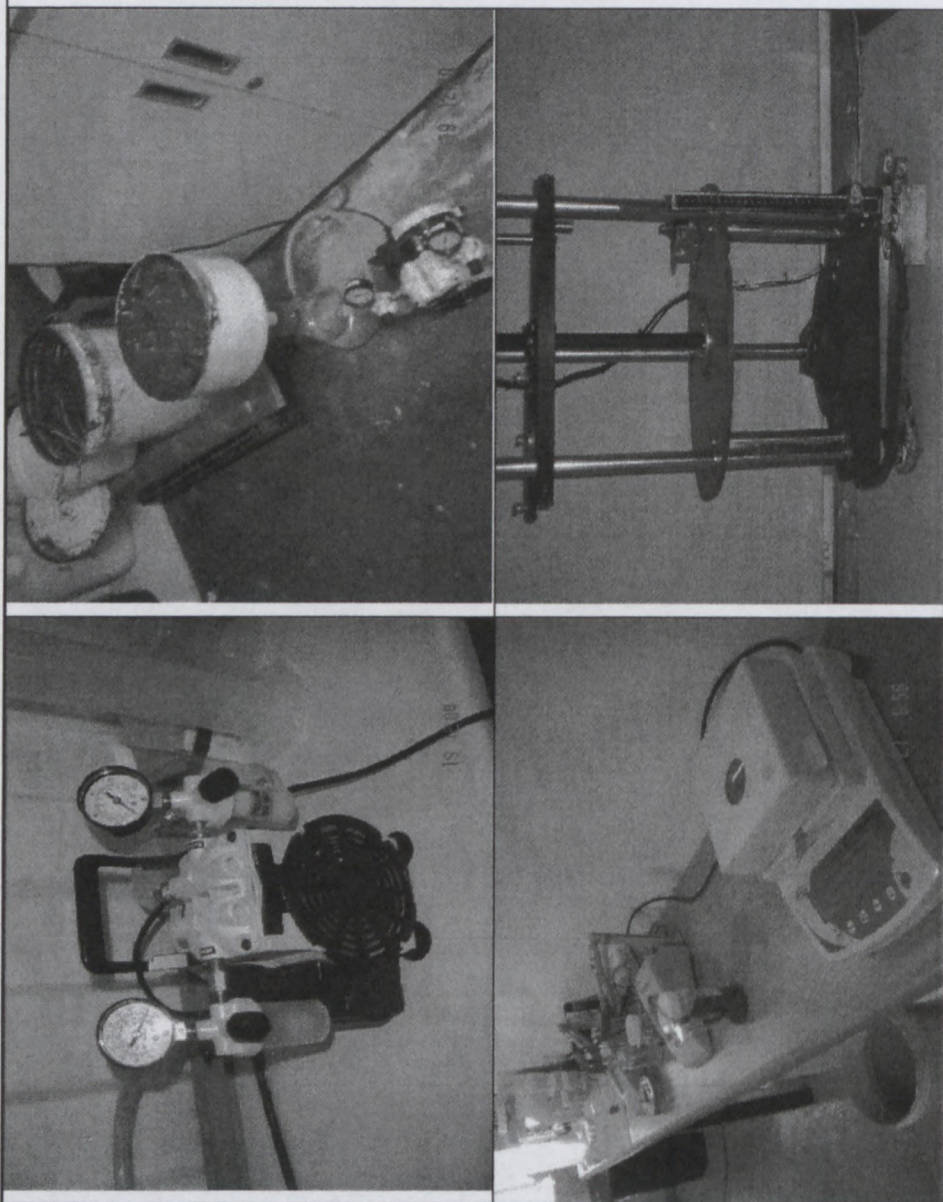


Table E: 4 Equipments used for the test work

E - Photos



Maxwell Nyekwe Ichegbo: Investigation of factors effecting yield stress determinations using the slump test.

E - Photos

